Facultat de Química

VNIVERSITAT DE VALÈNCIA

Departament de Química Analítica

Emerging hierarchical porous silica-based nanomaterials as sorbents for the analytical determination of organic hazardous compounds

Tesi Doctoral

Enric Pellicer Castell

Març 2022

Directors:
Dra. Adela R. Mauri Aucejo
Dr. José Manuel Herrero Martínez
Dr. Pedro J. Amorós del Toro

VNIVERSITAT DE VALÈNCIA

Facultat de Química

TESI DOCTORAL

Emerging hierarchical porous silica-based nanomaterials as sorbents for the analytical determination of organic hazardous compounds

Memòria per assolir el Grau de Doctor en Química dins del Programa de Doctorat en Química (RD 1999/2011) presentada per:

Enric Pellicer Castell

Directors:

Dra. Adela R. Mauri Aucejo

Dr. José Manuel Herrero Martínez

Dr. Pedro J. Amorós del Toro

València, març de 2022

Universitat de València
Departament de Química Analítica
Campus de Burjassot-Paterna
46100 Burjassot, Espanya

La Dra. Adela R. Mauri Aucejo, Professora Titular d'Universitat, el Dr. José Manuel Herrero Martínez, Catedràtic d'Universitat, ambdós del Departament de Química Analítica de la Universitat de València, i el Dr. Pedro J. Amorós del Toro, Catedràtic d'Universitat de l'Institut de Ciència dels Materials de la Universitat de València,

CERTFIQUEN

Que Enric Pellicer Castell ha realitzat la present Tesi Doctoral titulada "*Emerging hierarchical porous silica-based nanomaterials as sorbents for the analytical determination of organic hazardous compounds*" baix la seua direcció i supervisió en el Departament de Química Analítica de la Universitat de València i autoritzen la seua presentació per a optar al Grau de Doctor en Química.

I perquè conste, als efectes oportuns, signen la present a Burjassot, abril de 2022.

ADELA REYES| MAURI| AUCEJO

Firmado digitalmente por ADELA REYES| MAURI|AUCEJO
Fecha: 2022.04.29 10:20:19 +02'00'

Dra. Adela R. Mauri Aucejo

JOSE MANUEL| HERRERO| MARTINEZ

Firmado digitalmente por JOSE MANUEL| HERRERO| MARTINEZ
Fecha: 2022.04.28 11:03:55 +02'00'

Dr. José Manuel Herrero Martínez

PEDRO JOSE| AMOROS| DEL TORO

Firmado digitalmente por PEDRO JOSE| AMOROS|DEL TORO
Fecha: 2022.04.28 15:21:17 +02'00'

Dr. Pedro J. Amorós del Toro

Aquesta Tesi Doctoral ha estat realitzada gràcies a una beca predoctoral de Formació de Professorat Universitari (FPU16/02358) concedida per el Ministeri d'Educació, Cultura i Esports d'Espanya, així com una beca per a la realització de l'estada a l'estranger (EST18/00657) que ha permès optar a la menció internacional del títol

Agraïments

En primer lloc, voldria agrair als meus directors tota l'ajuda i dedicació, que han fet realitat aquesta tesi doctoral. Moltes gràcies a Adela per haver-me acompanyat durant tots aquestos anys i haver convertit en investigador a un estudiant de TFG que a penes sabia de què anava tot açò; a José Manuel per transmetre'm la passió per la química i el treball; i a Pedro per saber fer sempre les coses tan senzilles. Sense la guia, coneixements, dedicació, hores extra i paciència de tots tres, aquesta tesi no hagués estat possible.

Tanmateix, voldria agrair també l'ajuda de totes les persones amb qui he compartit el treball de laboratori durant aquestos anys, en especial a Carol que ha estat un recolzament inestimable, tant per a aquesta investigació, amb totes les discussions, consells i ajuda en el treball experimental, com també a nivell personal a l'hora de compartir moments bons i dolents. El seu acompanyament en la feina del dia a dia i totes les hores que hem passat junts han estat una sort per a mi i per al desenvolupament d'aquesta tesi doctoral. Igualment moltes gràcies també a tots aquells qui han participat en la seua realització, com Jamal, Alaina, Sole, Vicent o Noèlia que han prestat el seu temps i coneixements sempre que ha sigut necessari, així com a tots els membres del grup CLECEM per acollir-me i prestar la seua ajuda sempre que ha fet falta.

Una menció especial també per a tot l'equip de Departament de Química Ambiental del Helmholtz-Zentrum de Geesthacht per haver-me acollit durant tres mesos, en especial al Dr. Ralf Ebinghaus per haver posat tantes facilitats perquè la meua estada fora agradable i instructiva. Estic molt agraït de tot el que vaig aprendre d'ells i de la seua forma de treballar, tant a nivell acadèmic com personal.

I, no podria oblidar-me de totes les persones que m'han acompanyat des de que vaig començar a conèixer que significava açò de ser químic, de tots els companys tant de la carrera com del màster. En especial Aitor, Lorenzo, Sonia i Pepe, amb ells he compartit, no només hores de dinars a la cafeteria, sinó també totes les preocupacions, alegries, decepcions, il · lusions i frustracions que comporta un doctorat. Sense el seu recolzament hagués estat molt més difícil tot el treball d'aquestos anys.

També m'agradaria enrecordar-me de totes les persones que m'han envoltat durant aquest temps, en especial els amics de l'Hort de Romero, que en els moments més difícils sempre han aconseguit que desconnectara i agafara un poc de distància per veure les coses amb més claredat. I, sobretot, moltes gràcies a Isabel per haver estat al meu costat durant aquestos més de quatre anys. Gràcies per ser la persona en qui recolzar-me en els moments més difícils, i també amb qui compartir les alegries. Gràcies per aconsellar-me i fer-me ser millor persona. Gràcies per ser el meu suport fonamental en aquest repte.

Finalment, un agraïment immens a la meua família, que ha estat sempre al meu costat de forma incondicional, i d'una manera especial els meus pares Esther i Vicent. Moltes gràcies pels esforços que heu fet per fer possible la meua educació universitària, i per haver facilitat que no m'haguera de preocupar de res més que la meua formació. Però sobretot, moltes gràcies per haver-me transmés els valors de treball, esforç, paciència i constància que m'han permés arribar fins ací i ser la persona que sóc.

Abbreviations

acac	Acetylacetonate
ACN	Acetonitrile
AF	Aflatoxin
AOAC	Association of Official Agricultural Chemists
APCI	Atmospheric pressure chemical ionization
API	Atmospheric pressure ionization
APPI	Atmospheric pressure photoionization
ASE	Accelerated solvent extraction
BET	Brunauer-Emmett-Teller
BFR	Brominated flame retardant
BJH	Barrett-Joyner-Halenda
Bodipy-Me	difluoro{2-[1-(3,5-dimethyl-2H-pyrrol-2-ylidene-N)ethyl]3,5-dimethyl-1H-pyrrolato-N}boron
BPA	Bisphenol A
BTEX	Benzene, toluene, ethylbenzene, and xylenes
CD	Cyclodextrin
CE	Capillary electrophoresis
cmc	Critical micellar concentration
CNT	Carbon nanotube
C_{16}TAB	Cetyl trimethylammonium bromide
C_{12}TAB	Dodecyl trimethylammonium bromide
C_{10}TAB	Decyl trimethylammonium bromide
CXP	Collision cell exit potential
CZE	Capillary zone electrophoresis
DAD	Diode array detector
DCM	Dichloromethane
DLLME	Dispersive liquid-liquid microextraction
DMF	Dimethylformamide
DP	Declustering potential
dSPE	Dispersive solid-phase extraction
D-μ-SPE	Dispersive micro-solid-phase extraction

ECD	Electron capture detector
EDC	Endocrine-disrupting chemical
EDTA	Ethylenediamine tetraacetic acid
EDX	Energy-dispersive X-ray spectroscopy
EF	Enrichment factor
EI	Electron ionization
ELISA	Enzyme-linked immunosorbent assay
ESI	Electrospray ionization
EtOAc	Ethyl acetate
EtOH	Ethanol
FAO	Food and Agriculture Organization (United Nations)
FID	Flame-ionization detector
FLD	Fluorescence detector
FPD	Flame photometric detector
FR	Flame retardant
FTIR	Fourier-transform infrared spectroscopy
G	Graphene
GC	Gas chromatography
GO	Graphene oxide
HAADF	High-angle annular dark-field
HAcO	Acetic acid
HLB	Hydrophilic/lipophilic balanced
HPLC	High-resolution liquid chromatography
HRMS	High-resolution mass spectrometry
HRTEM	High-resolution transmission electron microscopy
IAC	Immunoaffinity column
IARC	International Agency for Research on Cancer
IASPE	Immunoaffinity solid-phase extraction
IPA	Isopropyl alcohol
IT	Ion trap
IUPAC	International Union of Pure and Applied Chemistry
LCT	Liquid-crystal templating mechanism
LDH	Layered double hydroxide
LFIA	Lateral flow immunoassay
LLE	Liquid-liquid extraction

SPE	Solid-phase extraction
LLME	Liquid-liquid microextraction
LOD	Limit of detection
LOQ	Limit of quantification
LPME	Liquid-phase microextraction
LRMS	Low-resolution mass spectrometry
MAE	Microwave-assisted extraction
MAS	Magic angle spinning
MeOH	Methanol
MIP	Molecularly imprinted polymer
MOF	Metal-organic framework
MRL	Maximum residue level
MS	Mass spectrometry
MSPE	Magnetic solid-phase extraction
MTBE	Methyl *tert*-butyl ether
MWCNT	Multi-wall carbon nanotube
NICI	Negative-ion chemical ionization
NIOSH	National Institute for Occupational Safety and Health (USA)
NMR	Nuclear magnetic resonance
NPD	Nitrogen-phosphorus detector
OCP	Organochlorine pesticide
OEL	Occupational exposure limit
ONP	Organonitrogen pesticide
OPP	Organophosphorus pesticides
PAH	Polycyclic aromatic hydrocarbon
PBDE	Polybrominated diphenyl ether
PCB	Polychlorinated biphenyl
PCDD	Polychlorinated dibenzo dioxin
PCDF	Polychlorinated dibenzofuran
PDA	Photodiode array
PDMS	Polydimethylsiloxane
PFAS	Per- and polyfluoroalkyl substance
PFCA	Perfluoroalkyl carboxylate
PFR	Phosphorus flame retardant
PFSA	Perfluoroalkyl sulfonate

PLE	Pressurized liquid extraction
POP	Persistent organic pollutant
PPCP	Pharmaceutical and personal care product
PS-DVB	Polystyrene-divinylbenzene
pSFC	Packed column supercritical fluid chromatography
PUF	Polyurethane foam
Q	Quadrupole
QqQ	Triple quadrupole
QToF	Quadrupole-time-of-flight
QuEChERS	Quick, easy, cheap, efficient, rugged, safe
RAM	Restricted access material
RSD	Relative standard deviation
SAX	Strong anionic exchange
SBSE	Stir-bar sorptive extraction
SCX	Strong cationic exchange
SDME	Single-drop microextraction
SPDE	Solid-phase dynamic extraction
SPME	Solid-phase microextraction
STEM	Scanning-transmission electron microscopy
STP	Standard temperature and pressure
SWCNT	Single-wall carbon nanotube
TBOT	Tetrabutyl orthotitanate
TEA	Triethanolamine
TEM	Transmission electron microscopy
TEOS	Tetraethyl orthosilicate
TGA	Thermogravimetric analysis
TLC	Thin-layer chromatography
TMOS	Tetramethyl orthosilicate
ToF	Time-of-flight
UHPLC	Ultra-high-resolution liquid chromatography
US FDA	United States Food and Drug Administration
USEPA	United States Environmental Protection Agency
µ-SPE	Micro-solid-phase extraction
UV	Ultraviolet
UV-Vis	Ultraviolet-visible

VOC	Volatile organic compound
WAX	Weak anionic exchange
WCX	Weak cationic exchange
WHO	World Health Organization
WWTP	Wastewater treatment plant
XRD	X-ray diffraction

Organochlorine pesticides

DDD	Dichlorodiphenyl dichloroethane
DDE	Dichlorodiphenyl dichloroethylene
DDT	Dichlorodiphenyl trichloroethane
HCH	Hexachloro cyclohexane

Phosphorus flame retardants

TCEP	Tris(2-chloroethyl) phosphate
TCIPP	Tris(2-chloroisopropyl) phosphate
TDCIPP	Tris(1,3-dichloro-2-propyl) phosphate
TEP	Triethyl phosphate
TnBP	Tri-n-butyl phosphate
TPhP	Triphenyl phosphate
TPP	Tripropyl phosphate

Perfluoroalkyl substances

PFBA	Perfluoro-n-butanoic acid
PFBS	Perfluoro-1-butanesulfonic acid
PFDA	Perfluoro-n-decanoic acid
PFDoDA	Perfluoro-n-dodecanoic acid
PFDS	Perfluoro-1-decanesulfonic acid
PFHpA	Perfluoro-n-heptanoic acid
PFHxA	Perfluoro-n-hexanoic acid
PFHxS	Perfluoro-1-hexanesulfonic acid
PFNA	Perfluoro-n-nonanoic acid
PFOA	Perfluoro-n-octanoic acid
PFOS	Perfluoro-1-octanesulfonic acid

PFPA	Perfluoro-n-pentanoic acid
PFTeDA	Perfluoro-n-tetradecanoic acid
PFTrDA	Perfluoro-n-tridecanoic acid
PFUnDA	Perfluoro-n-undecanoic acid

Parabens

BuP	Butylparaben
EtP	Ethylparaben
MeP	Methylparaben
PrP	Propylparaben

Resum

Introducció

Actualment, l'estil i la qualitat de vida de què disposem han comportat un notable augment de les emissions de substàncies potencialment nocives al medi ambient. Açò ha anat de la mà d'una creixent preocupació per la seua presència en aire, aigües, biota o aliments, així com pels seus efectes nocius, fet que ha propiciat la seua regulació a nivell legislatiu, i també a través de convenis com la Convenció d'Estocolm. Amb tot açò, el control i monitorització de substàncies orgàniques nocives ha esdevingut un gran repte per a la química analítica actual, no sols a nivell mediambiental amb el control de contaminants orgànics persistents, sinó també pel que fa al control alimentari de tot tipus de substàncies contaminants, o al biomonitoratge.

Per tal de respondre a aquest gran repte, el desenvolupament de tècniques instrumentals avançades com són la cromatografia líquida o de gasos acoblades a detectors d'espectrometria de masses, ha estat crucial en la detecció i quantificació de quantitats molt menudes de contaminants. No obstant això, les baixes concentracions dels anàlits, així com la complexitat de les matrius, fan necessària una etapa de preconcentració i neteja (*clean-up*). En aquesta etapa és on les fases adsorbents juguen un paper clau, principalment en el disseny de metodologies basades en l'extracció en fase sòlida, àmpliament utilitzades per a l'extracció i preconcentració de contaminants orgànics en tot tipus de matrius, gràcies als seus avantatges com la rapidesa, simplicitat, menor ús de dissolvents o la possibilitat d'automatització.

Al llarg de les últimes dècades són molts els estudis que s'han centrat en el desenvolupament de materials amb l'objectiu de ser utilitzats com a fases adsorbents, començant per les fases clàssiques de sílice enllaçada, les fases polimèriques o els cartutxos de bescanvi iònic. No obstant això, la recerca de millors rendiments d'extracció així com d'una major selectivitat, han comportat el desenvolupament de molts materials nous, entre els quals destaquen les xarxes organometàl·liques, els materials basats en carboni, els materials d'accés restringit, o els materials de reconeixement molecular com els immunosorbents o els polímers de reconeixement molecular.

En aquest punt, emergeixen també els materials de sílice mesoporosa que, en els últims anys, han rebut una gran atenció per a una gran varietat d'aplicacions en què es fa necessària la retenció de tot tipus de compostos. L'aparició dels sòlids M41S de la corporació Mobil va revolucionar aquest camp, ja que va modificar els clàssics processos sol-gel amb la introducció de surfactants com agents directors de l'estructura porosa. Aquesta tecnologia ha donat lloc a una gran quantitat de materials, entre els quals podem destacar l'UVM-7. Aquest material presenta una estructura porosa molt característica, amb una xarxa de porus

bimodal formada per la unió de nanopartícules mesoporoses, que dona lloc a un material amb una alta àrea superficial que disposa tant de macroporus com de mesoporus parcialment ordenats. Així, els materials basats en UVM-7, tant en la seua forma pura com modificats mitjançant l'addició de metalls o de lligands orgànics, s'han utilitzat en diverses aplicacions, principalment en catàlisi, com a nano-contenidors, o en el desenvolupament de sensors. Així i tot, la seua aplicació per a la retenció, extracció i determinació de contaminants orgànics en química analítica no ha estat estudiada.

Objectius i pla de treball

Aquesta Tesi Doctoral, per tant, té com a principal objectiu estudiar el potencial dels materials de tipus UVM-7 com a fases adsorbents en la determinació de contaminants orgànics, per tal de desenvolupar noves metodologies analítiques. Amb aquest objectiu, s'han aplicat diverses estratègies de síntesi per tal d'obtenir materials derivats de l'UVM-7, amb l'addició de metalls com titani, ferro o or, la modificació de la grandària dels mesoporus, o l'ancoratge de ciclodextrines com a centres actius per a la retenció. A partir d'aquestos materials, l'objectiu general consisteix a desenvolupar diverses metodologies analítiques per al mostreig i tractament de mostra, i donar així resposta al repte que suposa la determinació de contaminants orgànics a nivell d'anàlisi d'aliments, mediambiental o clínic.

A partir d'aquestos objectius, el pla de treball plantejat consta de dos grans etapes:

a) Síntesi i caracterització de materials de sílice mesoporosa tipus UVM-7, modificats adequadament per a la retenció selectiva dels compostos objectiu. L'estructura dels materials sintetitzats es caracteritza mitjançant diverses tècniques com la microscòpia electrònica, difracció de raig X, porosiometria, ressonància magnètica nuclear, o espectroscòpia UV-Visible i Raman.

b) Desenvolupament de metodologies analítiques per al mostreig o extracció dels compostos orgànics objectiu. Els paràmetres analítics més importats del mètode s'optimitzen experimentalment, i s'avalua el mètode desenvolupat, tant en funció de la seua sensibilitat, eficiència, repetibilitat o linealitat, en comparació als mètodes prèviament publicats, com mitjançant la seua aplicació a mostres reals en comparació amb un mètode de referència.

Metodologia, resultats i discussió

A continuació s'exposa un resum dels principals resultats obtinguts en la realització de la present Tesi Doctoral, així com de la metodologia utilitzada. Els resultats es troben subdividits en funció dels capítols i seccions en què es divideix la Tesi, fent referència a cadascuna de les parts corresponents.

Secció A. Síntesi de materials de sílice mesoporosa

En la primera secció de la tesi, que consta del *Capítol 1*, es fa una exposició de tots els materials que s'han sintetitzat durant la realització de la Tesi Doctoral. En aquet capítol es presenta el procediment de síntesi que es va seguir per a cadascun d'aquestos materials, incloent els materials d'UVM-7 pura (calcinada i extreta) i els modificats amb metalls (titani, ferro i or, bé siga per cohidròlisi o impregnació), o amb l'addició de ciclodextrines. A més a més, també s'exposa la síntesi d'altres materials de sílice que es van sintetitzar per poder comparar les seues propietats. Finalment, es fa una recopilació de totes les tècniques que s'han utilitzat per a caracteritzar l'estructura d'aquestos materials, així com dels paràmetres experimentals més importants.

Secció B. Aplicació de sílice mesoporosa tipus UVM-7 a l'extracció d'aflatoxines en mostres alimentàries

En aquesta part de la tesi, es va sintetitzar el material UVM-7 mitjançant el procediment descrit que utilitza la trietanolamina com agent tamponant del pH i de la reactivitat, així com el bromur de cetil trimetilamoni com a surfactant per a la configuració dels mesoporus. En aquest sentit, es van explorar dues vies per a l'eliminació del surfactant: mitjançant extracció en medi àcid, o per calcinació. Tal i com s'exposa a l'inici d'aquesta secció (*Capítol 2*), els materials sintetitzats van ser caracteritzats utilitzant diverses tècniques com la microscòpia electrònica, difracció de raigs X, porosimetria o ressonància magnètica nuclear, tot comprovant la seua estructura característica formada per un sistema de porus bimodals, amb la presència de macroporus d'una grandària d'uns 44-46 nm, i de mesoporous hexagonalment pseudoordenats d'uns 2,6-2,9 nm. Tot i això, sí que es va observar una important diferència en quant a la presència de grups silanol a la superfície del material, molt més alta en el cas de l'UVM-7 extreta, aspecte que resulta important en quant a la retenció dels anàlits.

Així doncs, les característiques de la xarxa porosa d'aquestos materials van donar lloc a la seua aplicació com a fases adsorbents en la retenció d'aflatoxines, estudi que es troba exposat al *Capítol 3*. Les aflatoxines són una de les famílies més importants de micotoxines, uns metabòlits produïts per diverses espècies de fongs que poden contaminar tot tipus d'aliments, i que suposen un important risc per a la salut pública. Entre les aflatoxines, les més importants són la B_1, B_2, G_1, G_2 i M_1, no sols per la seua major incidència, sinó també per la seua alta toxicitat i la seua classificació com a agents cancerígens. Així, el seu control i vigilància en aliments està actualment molt estés, i ha donat lloc a diverses legislacions que regulen la seua presència, principalment en aliments com els fruits secs, cereals o llet. A més a més, malgrat la gran quantitat de mètodes disponibles per a la seua determinació, la major part es basen en l'extracció en fase sòlida d'immunoafinitat que, si bé presenta una alta selectivitat per a aquestos anàlits, suposa la utilització de cartutxos d'un alt cost i no reutilitzables.

Per tant, els materials tipus UVM-7 sintetitzats es van proposar com a possible alternativa per a la determinació d'aflatoxines en mostres d'aliments, començant pel disseny d'un mètode analític per a la seua extracció de mostres de té, i la seua posterior quantificació per UHPLC-MS/MS. En primer lloc es va constatar la idoneïtat de l'UVM-7 extreta front a la calcinada, atesa la seua major densitat de grups silanol disponibles, tal i com s'ha comentat. Amb aquesta fase es van optimitzar els corresponents aspectes del procediment d'extracció en fase sòlida, i es van determinar els paràmetres analítics del mètode desenvolupat. D'aquesta forma, amb el mètode optimitzat es van assolir recuperacions satisfactòries en el rang de 96,0-98,2% per a les aflatoxines B_1, B_2, G_1 i G_2, amb coeficients de variació inferiors al 5,1% en tots els casos, així com límits de detecció entre 0,14 i 0,7 µg kg^{-1}. A més a més, el mètode es va aplicar a la determinació d'aflatoxines en mostres de té reals, encara que només es van quantificar concentracions baixes d'aflatoxina G_2 en una mostra. No obstant això, aquestos resultats van ser comparats amb els obtinguts mitjançant un mètode de referència fent servir cartutxos d'immunoafinitat, i es va provar que eren estadísticament comparables. Per tant, els cartutxos desenvolupats han demostrat ser una alternativa fiable i més econòmica, a més de reutilitzable, per a la determinació d'aflatoxines en mostres de té, i ofereixen bons paràmetres analítics en comparació a altres mètodes publicats a la bibliografia.

En segon lloc, aquestos cartutxos contenint la fase d'UVM-7 extreta es van aplicar també a l'extracció d'aflatoxina M_1 en mostres de llet, tot desenvolupant un mètode analític per a la neteja de la matriu o *clean-up*, amb una prèvia extracció amb acetonitril. En aquest cas, també es van obtenir recuperacions satisfactòries superiors al 94% per a diversos tipus de llet, i del 85 ± 7% en el cas de mostres de iogurt. Igualment, mitjançant la quantificació amb instrumentació convencional com HPLC-FLD, es va obtenir un límit de quantificació de 0,015 µg kg^{-1}. Per tant, la sensibilitat obtinguda per a ambdós mètodes va resultar satisfactòria, tenint en compte els límits legals establerts tant per la Unió Europea com per l'Estat Espanyol. Aquest mètode també va ser aplicat a l'anàlisi de mostres reals. Encara que no es van detectar mostres positives, l'anàlisi de mostres fortificades en comparació amb un mètode de referència va oferir resultats estadísticament comparables.

Finalment, i, atesos els bons resultats oferts per part dels dos mètodes dissenyats, es va estudiar la interacció dels anàlits amb la fase sòlida sintetitzada, i el paper de l'estructura porosa del material en la seua retenció. En primer lloc, mitjançant la comparació de l'UVM-7 amb altres materials de sílice d'estructures diferents, es va establir el paper clau que juguen els mesoporus en la retenció de les aflatoxines. Si bé la presència dels macroporus també es va constatar que tenia un paper important, els mesoporus van mostrar ser més determinants en la retenció. Així, l'estructura de porus bimodals que presenta l'UVM-7 esdevé idònia per a la retenció de compostos de la grandària i característiques de les aflatoxines, donant lloc a una retenció quantitativa i homogènia, com també es va comprovar mitjançant microscòpia confocal.

Secció C. Avaluació de materials UVM-7 dopats amb metalls per a la determinació de pesticides i contaminants emergents en anàlisi mediambiental

Una vegada determinada l'estructura dels materials UVM-7 i els seus beneficis, es van estudiar diverses modificacions mitjançant l'addició de metalls. L'estructura de tots els materials que contenen metalls es troba caracteritzada al *Capítol 4* com a inici d'aquesta secció. En primer lloc, atés que es requeria una fase per a la retenció de compostos organofosforats, es va modificar el material amb l'addició de Ti i de Fe. Per tal de realitzar aquesta addició, es van estudiar dos rutes de síntesi diferents: mitjançant cohidròlisi amb l'addició del corresponent precursor metàl·lic a la mescla inicial, o mitjançant impregnació en una etapa posterior quan l'estructura de sílice ja està formada. També es van sintetitzar materials similars però amb una estructura microporosa unimodal (de tipus xerogel) per tal de poder comparar-los i obtenir més informació al voltant de la retenció dels anàlits. De nou, els sòlids preparats foren caracteritzats, tant la seua estructura de sílice porosa mitjançant les tècniques abans esmentades, com també la incorporació dels metalls utilitzant tècniques com l'energia dispersiva de raigs X, o l'espectroscòpia ultravioleta-visible i Raman.

Tots aquestos materials foren posats a prova per a la retenció de pesticides (*Capítol 5*), començant pels pesticides organofosforats. Aquestos pesticides són àmpliament utilitzats actualment com a substitutius dels pesticides clorats, i presenten una estructura comuna caracteritzada per la presència de grups fosfat o tiofosfat. A pesar de la seua menor persistència en comparació d'altres pesticides, la seua alta toxicitat ha provocat que en les darreres dècades la seua vigilància haja anat en augment, així com els estudis enfocats a constatar els seus efectes toxicològics. A més a més, cal tenir en compte que, durant l'aplicació d'aquestos pesticides, una quantitat significativa s'allibera al medi ambient, comportant la seua presència en aire, i també en aigües o sòls. Per aquest motiu, la legislació ha anat evolucionant cap a la seua regulació o restricció, fet que requereix el desenvolupament de tècniques analítiques fiables per a la seua determinació a diversos nivells.

En un primer estudi, es van aplicar els materials sintetitzats a la retenció de pesticides organofosforats en aire. Així, es va observar com l'addició de titani per cohidròlisi dona lloc a una incorporació homogènia del metall substituint els àtoms de silici, que dota d'una especial selectivitat al material front a aquestos compostos. També es va observar que, en el cas de la seua addició per impregnació, la formació de nanodominis de TiO_2 obstruïa els porus del material i, en conseqüència, disminuïa considerablement la seua capacitat per adsorbir els anàlits. Es va destacar també la major capacitat del titani front al ferro en el disseny d'aquestos mostrejadors, probablement a causa de la pitjor distribució del Fe en la xarxa porosa del material. Finalment, també es va constatar l'avantatge dels materials de tipus UVM-7 front als materials microporosos com els xerogels gràcies a la seua estructura porosa ja descrita.

Per tant, es van dissenyar mostrejadors contenint el material Ti25-UVM-7, amb els quals es van optimitzar les diferents etapes i paràmetres del mostreig, desorció i determinació mitjançant GC-NPD i GC-MS. Amb aquestos mostrejadors es van obtenir bons paràmetres analítics, com per exemple recuperacions en el rang 93-107% per a tots els anàlits excepte per al diazinon. Igualment, en tots els casos es van obtenir coeficients de variació inferiors al 13%, així com límits de detecció per sota de 0,5 µg m^{-3}. Una vegada establerts els paràmetres analítics del mètode i comprovada, a més a més, la possibilitat de reutilitzar el material, es van aplicar els dispositius dissenyats a la determinació de pesticides en mostres d'aire reals per a l'avaluació de riscos laborals, mitjançant el mostreig durant l'aplicació d'un producte fitosanitari contenint metil clorpirifós. Així, es va mostrejar l'aire durant i després de l'aplicació del pesticida, en comparació també amb mostrejadors comercials contenint XAD-2. Els resultats obtinguts van mostrar, en primer lloc, les altes concentracions presents a l'aire durant i després de l'aplicació, fet que fa necessària la utilització d'equips de protecció personal. En segon lloc, els resultats obtinguts amb ambdós mètodes van resultar ser estadísticament comparables, i es va demostrar així la fiabilitat dels mostrejadors desenvolupats per a la determinació de pesticides organofosforats en aire.

Atesos aquestos bons resultats, el material Ti25-UVM-7 es va aplicar també a la determinació dels pesticides organofosforats en mostres d'aigua mediambientals. En quest cas, el material es va comparar amb materials microporosos amb ciclodextrines ancorades. Encara que aquestos últims van oferir bones retencions per als pesticides amb grups clorats o grups aromàtics a l'estructura, van resultar ser ineficaços per a la resta de compostos. Així, en termes generals, el material de Ti25-UVM-7 va oferir millors resultats. Després de l'optimització de diversos paràmetres analítics, es va desenvolupar un mètode per a la determinació de pesticides organofosforats per GC-NPD, gràcies a la prèvia preconcentració amb cartutxos d'extracció en fase sòlida que contenen aquest material. Amb aquest mètode es van obtenir recuperacions d'entre 81 i 104,5%, encara que, en aquest cas, es va constatar un efecte matriu important en diverses mostres analitzades. També, es van obtenir límits de detecció en el rang 0,5-4,4 µg L^{-1} per a tots els anàlits estudiats, així com coeficients de variació per sota de 7,8 i 12% per a la repetibilitat intra-dia i inter-dia respectivament, i una bona reutilització. El mètode va ser aplicat a l'anàlisi de mostres d'aigua reals i, si bé no es van detectar mostres positives, l'anàlisi de mostres fortificades va oferir bons resultats, comparables als obtinguts mitjançant un mètode de referència amb cartutxos de C18.

Seguint amb la determinació de pesticides, es va introduir una nova modificació en els materials sintetitzats, incorporant nanopartícules d'or per tal d'afavorir la retenció selectiva de pesticides clorats. Com ja s'ha comentat, l'ús d'aquestos pesticides als països desenvolupats ha anat decreixent en les darreres dècades, atesa la prohibició de molts d'ells per part de diversos organismes, i també per la seua inclusió a la Convenció d'Estocolm. No obstant, el seu ús en països d'altres continents com Àsia o Àfrica, junt amb la seua gran persistència,

toxicitat i transport de llarg abast, fa necessària encara la seua vigilància a nivell mediambiental.

En aquest cas, atesa la impossibilitat d'addicionar l'or per cohidròlisi com en els casos anteriors, es va procedir a la seua incorporació per impregnació en una etapa posterior, utilitzant la presència de titani a l'estructura de sílice per tal d'afavorir el seu ancoratge, tal i com ja s'havia observat en estudis anteriors.

Així, es van sintetitzar materials amb distintes quantitats d'or (a partir de materials amb distintes quantitats de titani), que van ser avaluats com a fases adsorbents per a l'extracció en fase sòlida de pesticides clorats en mostres d'aigua, per a la seua posterior determinació per GC-ECD. Després d'optimitzar diversos paràmetres de l'extracció, es va optar per cartutxos en mode *sandwich* contenint tant UVM-7 pura com el material Au/Ti50-UVM-7, ja que van oferir els millors resultats per a la retenció dels 20 anàlits estudiats. Amb aquestos cartutxos es va desenvolupar també un mètode analític que va donar lloc a rendiments d'extracció d'entre 80 i 100% per a la majoria dels anàlits en diverses matrius reals i a distints nivells de concentració, encara que alguns d'ells oferiren recuperacions un poc menors, sempre per sobre del 60%. A més a més, es van obtenir factors de preconcentració d'entre 275 i 430, així com límits de quantificació en el rang 0.3-20 ng L^{-1}, que permeten la determinació d'aquestos pesticides clorats per sota dels límits marcats per la legislació europea. El mètode va ser també aplicat a la determinació de pesticides clorats en mostres d'aigua, encara que, de nou, no es va detectar cap mostra positiva. Tot i això, un estudi similar a l'anterior, amb la comparació dels resultats de mostres fortificades amb un mètode de referència (amb cartutxos C18) va oferir resultats estadísticament comparables.

Amb els materials prèviament descrits, en els quals es van introduir metalls en la xarxa de sílice característica de l'UVM-7, es van dissenyar també dos nous mètodes per a l'anàlisi d'aigües, centrant el focus en els contaminants emergents (*Capítol 6*). Els contaminants emergents són compostos que, si bé molts d'ells han estat presents al medi ambient des de fa temps, la seua presència no s'ha constatat fins al desenvolupament de tècniques analítiques més sensibles, fet que ha provocat que molts d'ells no estiguen adequadament regulats per la legislació actual, i que els seus efectes toxicològics no estiguen completament estudiats. No obstant això, la seua potencial toxicitat ha provocat un gran interés per aquestes substàncies, i ha fet necessari el seu monitoratge a nivell mediambiental. Entre ells, els retardants de flama han rebut una gran atenció en els últims anys, atés el seu ús com additius per previndre la propagació del foc, ja que molts d'ells poden ser alliberats al medi ambient per volatilització, abrasió o dissolució. Això ha provocat la regulació dels retardants de flama bromats, altament tòxics i persistents, i la seu substitució pels retardants de flama organofosforats. Així i tot, aquestos últims també presenten una gran toxicitat en tractar-se també de compostos organofosforats, per la qual cosa actualment hi ha un gran interés en desenvolupar mètodes analítics fiables per a la seua determinació i control a nivell mediambiental.

Així, en primer lloc es va desenvolupar un mètode per a l'extracció de retardants de flama organofosforats. En aquest cas, es van sintetitzar materials

de tipus UVM-7 que contenien diverses quantitats de titani, per tal d'estudiar la seua estructura i determinar la influència del titani en la capacitat del material com a fase adsorbent. Mitjançant les tècniques anteriorment descrites, es va comprovar l'estructura d'UVM-7 de tots els materials. No obstant això, també s'observaren diferències significatives en quant a l'entorn químic dels centres de titani addicionats, ja que en els materials on la quantitat introduïda va ser menor, el titani es trobava envoltat d'oxígens en entorns tetraèdrics (substituint isomòrficament al silici), mentre que un augment en la quantitat d'heteroelement, provocava un major predomini d'entorns octaèdrics. Fins, i tot, en el material amb la major quantitat de titani (Ti5-UVM-7) es van detectar xicotets *clústers* de TiO_2 en forma d'anatasa. Açò és un aspecte important en quant a l'ús dels materials com a fases adsorbents, ja que el titani en entorns tetraèdrics tindrà una major disponibilitat per interaccionar amb els anàlits, que no pas els que estiguen coordinats octaèdricament. Per tant, el millor material serà aquell amb una quantitat de titani suficient per interaccionar amb els grups fosfat dels anàlits, però no excessivament gran com per alterar l'entorn de coordinació del titani o l'estructura del material UVM-7.

Després de provar els diversos materials, aquest compromís es va observar en el cas del material Ti50-UVM-7, que va oferir els millors resultats per a l'extracció dels retardants de flama organofosforats seleccionats. Per tant, amb aquest material es va posar a punt un mètode per a la seua extracció, preconcentració i posterior determinació per GC-MS. El mètode optimitzat va mostrar una bona sensibilitat (límits de detecció en el rang 0,019-0,21 µg L^{-1}), i rendiments d'extracció per sobre del 80% per a tots els anàlits en el cas de mostres d'aigües, encara que aquestes recuperacions foren menors en el cas de mostres més complexes com les aigües residuals (superiors al 65%). També es va obtenir una bona repetibilitat, amb coeficients de variació inferiors a l'11% en el cas de la repetibilitat intra-dia, i es va comprovar la possibilitat de reutilitzar els cartutxos. L'aplicació del mètode a l'anàlisi de mostres reals va oferir concentracions quantificables en el cas de les mostres corresponents als canals influents d'estacions de depuració d'aigües residuals. Així, concentracions en el rang de 0,38-1,8 µg L^{-1} es van detectar per al TCIPP, TDCIPP i TPhP. Mitjançant l'anàlisi d'aquestes mostres per un mètode de referència utilitzant cartutxos de C18, es van obtenir també concentracions similars i estadísticament comparables. Per tant, el mètode desenvolupat va ser validat com un mètode fiable per a l'extracció i determinació de retardants de flama organofosforats en aigües mediambientals, amb la millora de diverses de les característiques i paràmetres dels mètodes presentats anteriorment.

Per altra banda, una altra família de contaminants emergents que ha rebut una gran atenció han estat els compostos per- i polifluoroalquilats, unes substàncies químiques d'origen industrial que han estat utilitzades per a diverses aplicacions com la producció de polímers, o com a surfactants. Atesa la seua persistència al medi ambient, ubiqüitat, i el seu transport de llarg abast han estat detectats en aire, aigües i altres matrius mediambientals, i la seua presència ha esdevingut una important problemàtica. Entre ells, els més comuns són els àcids perfluorocarboxílics i els àcids perfluorosulfònics.

Així, atesa la possible interacció entre els grups fluorurs presents en les estructures d'aquestos compostos i el ferro, es va pensar en l'aplicació dels materials de tipus Fe-UVM-7 ja sintetitzats per a la retenció d'aquestos compostos. En aquest cas, es van provar materials amb diverses quantitats de ferro, que foren també caracteritzats mitjançant les tècniques anteriorment descrites. Cal destacar també que, en aquest cas, si bé no es pot descartar la presència de nanodominis de Fe_2O_3 en l'estructura dels materials tal i com s'ha comentat prèviament (fet que no s'observava en la incorporació del titani), l'addició del ferro es pot considerar homogènia en quasi tots els materials sintetitzats, llevat del material amb una quantitat de ferro molt elevada, on sí que es va observar una important presència de nanodominis d'hematites.

No obstant, després d'aplicar aquestos materials, i malgrat l'augment de la capacitat de retenció que es va observar gràcies a la presència del ferro, les recuperacions obtingudes foren molt dispars entres els anàlits estudiats, i alguns d'ells presentaren recuperacions molt baixes amb tots els materials. Com que els compostos perfluoroalquilats presenten una gran varietat en la seua grandària, es va proposar la modificació de la grandària dels mesoporus de l'UVM-7 com a possible solució a aquesta problemàtica. Així, mitjançant l'ús de surfactants de cadena més curta (12 i 10 carbonis), es van sintetitzar materials de tipus Fe-UVM-7 amb els mesoporus més menuts. Cal destacar que la modificació simultània amb la incorporació d'un metall i la modificació de la grandària del mesoporus va ser estudiada per primera vegada, amb resultats satisfactoris tal i com van mostrar els resultats de la caracterització dels materials.

Finalment, els millors resultats es van obtenir amb la fase sòlida Fe50-UVM--C_{12} (amb una grandària de porus de 2,26 nm), amb la qual es va desenvolupar un mètode per a l'extracció en fase sòlida i determinació de compostos perfluoroalquitas amb cadenes d'entre 8 i 14 carbonis en mostres d'aigua, amb la posterior determinació mitjançant UHPLC-MS/MS. No obstant això, el mètode no es va poder aplicar als compostos de cadena més curta (C_4-C_7), ateses les baixes recuperacions obtingudes. Amb el material seleccionat es van optimitzar els diversos paràmetres del mètode, en relació a les condicions de retenció i elució, i es van obtenir eficiències d'extracció en el rang 61-110% per als anàlits seleccionats (C_8-C_{14}), tant perfluoroalquil carboxilats com perfluoroalquil sulfonats, en mostres reals d'aigües. Així mateix, es van obtenir límits de detecció entre 3,0 i 8,1 ng L^{-1} per a tots ells. Encara que l'anàlisi de diverses mostres reals no va donar lloc a cap mostra positiva, l'anàlisi de mostres fortificades en comparació amb un mètode de referència utilitzant cartutxos de bescanvi iònic (Oasis WAX) va conduir a resultats estadísticament comparables, fet que posa de manifest la fiabilitat del mètode per a la determinació d'aquestos contaminants en mostres mediambientals.

Secció D. Funcionalització de l'UVM-7 amb ciclodextrines per a l'extracció de disruptors endocrins en anàlisi clínic

En darrer lloc, es va estudiar la possibilitat d'incorporar ciclodextrines a l'estructura de sílice de l'UVM-7 com a centres actius per a la retenció. Les ciclodextrines són una família d'oligosacàrids cíclics formats per la unió de monòmers de glucosa que, gràcies a la seua forma de con truncat i al seu equilibri hidròfil/hidròfob, són capaces de formar complexos d'inclusió amb determinats compostos orgànics. Per tant, el seu ancoratge al suport de sílice pot oferir una alta selectivitat i eficiència en la retenció d'alguns contaminants, com puguen ser els parabens o els bisfenols. Aquest ancoratge es va dur a terme mitjançant una modificació del procediment de síntesi *one-pot* de l'UVM-7, addicionant la β-ciclodextrina, prèviament funcionalitzada amb grups silans, a la mescla inicial. El material resultant es va caracteritzar per primera vegada (*Capítol 7*), ja que no havia estat prèviament sintetitzat, per diverses de les tècniques anteriorment esmentades, a més de l'anàlisi elemental CNH i l'anàlisi termogravimètrica. Amb tot açò, es va comprovar que el material resultant mantenia l'estructura porosa bimodal característica de l'UVM-7, amb una xicoteta disminució de l'àrea superficial, i una reducció molt menuda en el cas de la grandària dels mesoporus a causa de la presència de les ciclodextrines. A més a més, es va comprovar l'ancoratge de la ciclodextrina al suport de sílice, així com la quantitat de ciclodextrina present al material, que es va estimar en uns 0,117-0,119 mmol β-CD g^{-1}.

El material obtingut es va aplicar a l'extracció de disruptors endocrins en mostres biològiques, concretament en mostres d'orina (*Capítol 8*). Els disruptors endocrins són un grup de compostos sintètics o naturals que poden alterar el funcionament normal del sistema endocrí dels humans, fet que comporta nombrosos efectes adversos sobre la salut. Entre ells, el bisfenol A ha rebut una gran atenció en els últims anys atés el seu ús com a antioxidant o estabilitzador, i nombrosos estudis han destacat els seus efectes nocius i el seu potencial risc per a la salut de les persones. Per altra banda, els alquil ésters de l'àcid p-hidroxibenzoic, també coneguts com parabens, són àmpliament utilitzats com a conservants, a pesar de la creixent evidència dels seus efectes toxicològics sobre la salut. Per això, tots aquestos compostos han començat a estar regulats per part de diversos organismes, i són molts els estudis de biomonitoratge que han posat de manifest la seua presència en els nostres organismes. Per tant, el desenvolupament de metodologies analítiques fiables per a la seua determinació és de gran interés en l'actualitat, fet que ha propiciat el disseny d'aquest material d'UVM-7 amb ciclodextrines per a la seua extracció en mostres d'orina.

Així, després de desconjugar els anàlits mitjançant una hidròlisi enzimàtica, es va posar a punt un mètode d'extracció en fase sòlida per tal de purificar la mostra i extraure el anàlits, que van ser posteriorment quantificats per UHPLC-MS/MS. Després d'optimitzar diversos paràmetres del mètode, es van obtenir recuperacions molt bones comparant-les amb les aportades per altres mètodes, dins del rang 96-109% per a tots els anàlits estudiats. També, es van obtenir

límits de quantificació per sota de 0,2 µg L^{-1} en tots els casos, així com repetibilitats entre el 8 i el 24%. El mètode desenvolupat es va aplicar a l'anàlisi de diverses mostres reals d'orina, i totes elles van donar positiu en un o més dels anàlits estudiats. Per tal de comptabilitzar les possibles diferències en la dilució de les mostres d'orina, també es va determinar el contingut en creatinina de totes elles mitjançant el mètode de Jaffé, per tal d'estandarditzar els resultats. Cal destacar també que, de tots ells, el bisfenol A va ser detectat amb la major freqüència i en les majors concentracions. Les mostres, a més a més, es van analitzar també mitjançant un mètode de referència prèviament publicat, i es van obtenir concentracions estadísticament comparables. Per tant, el mètode desenvolupat a partir del material β-CD-UVM-7 va ser aplicat amb èxit, fet que demostra el seu potencial com a alternativa a les fases adsorbents comunament utilitzades.

A més a més, es va estudiar també el procés d'adsorció del material sintetitzat envers el bisfenol A com anàlit model, i es va observar que tant la cinètica d'adsorció (que s'ajustava a una cinètica de segon pseudo-ordre), com les isotermes d'adsorció (que s'ajustaven al model d'adsorció de Langmuir), concordaven amb un mecanisme d'adsorció basat en la formació de complexos d'inclusió de l'anàlit amb la ciclodextrina, tal i com s'esperava, i es va estimar així una capacitat d'adsorció màxima de 24,4 mg g^{-1}.

Conclusions

Com a conclusió general de la present tesi doctoral es pot destacar l'èxit en l'aplicació dels materials de tipus UVM-7 com a fases adsorbents per a la determinació de contaminants orgànics. Aquestos materials han demostrat tenir unes propietats altament favorables per al seu ús analític, tant en el mostreig d'aire com en el tractament de mostres mediambientals, d'aliments o clíniques.

Els avantatges de la seua xarxa porosa bimodal s'han posat de manifest en els estudis de determinació d'aflatoxines, on s'ha comprovat el paper clau dels mesoporus en la retenció d'aquestes toxines mitjançant mecanismes d'exclusió. Gràcies a aquestes característiques s'han desenvolupat dos mètodes per a la determinació d'aflatoxines en mostres d'aliments, que han ofert grans resultats com a alternativa als costosos cartutxos d'immunoafinitat.

A més a més, la modificació de l'UVM-7 mitjançant l'addició de metalls com Ti, Fe o Au, ha donat lloc també a una gran versatilitat en quant a la retenció selectiva de diverses famílies de contaminants. Així, s'ha comprovat la influència de l'addició dels metalls en la retenció dels anàlits objectiu, ja siga la de compostos organofosforats per part del Ti, de compostos clorats per part de l'Au, o compostos fluorats amb el Fe. A més a més, la incorporació del metall de forma simultània a la modificació de la grandària de porus de l'UVM-7 amb surfactants de cadena curta s'ha dut a terme també de forma exitosa per primera vegada.

Gràcies a aquestes modificacions s'han desenvolupat metodologies analítiques per a l'anàlisi mediambiental, com són el mostreig de pesticides organofosforats

en aire, l'extracció d'aquestos pesticides i els organoclorats de mostres d'aigua, i mètodes d'extracció en fase sòlida per a la determinació de retardants de flama organofosforats i compostos perfluoroalquilats. Tots aquestos mètodes han presentat paràmetres analítics molt bons en comparació als mètodes prèviament publicats, amb l'excepció dels compostos perfluorolquilats de cadena curta (C_4-C_8), per als quals els materials estudiats no han ofert bons resultats.

Per últim, s'ha desenvolupat per primera vegada un nou material mitjançant la funcionalització de l'UVM-7 amb β-ciclodextrina, l'estructura del qual ha sigut correctament caracteritzada. Aquesta modificació li ha dotat d'una selectivitat que ha permés el desenvolupament d'un mètode analític per la determinació de disruptors endocrins (parabens i bisfenol A) en mostres d'orina, amb resultats molt bons pel que fa als seus paràmetres analítics.

Amb tot açò, s'ha comprovat el potencial dels materials amb porositat bimodal, i concretament dels materials UVM-7, per a la seua aplicació en la retenció i extracció de compostos orgànics nocius i en la química analítica en general.

Table of contents

INTRODUCCIÓ

1. La problemàtica dels contaminants orgànics

L'estil i la qualitat de vida de què disposem des de les últimes dècades han comportat un creixement exponencial no sols econòmic sinó també industrial, fet que ha resultat en un notable augment de les emissions de substàncies potencialment nocives al medi ambient. L'alliberament de tots aquestos contaminants, com són els pesticides, metalls pesants o fàrmacs, i el seu contacte amb els ecosistemes, ha comportant un augment dels seus efectes mediambientals, així com dels potencials problemes de salut per a l'ésser humà. Entre ells, la presència de contaminants orgànics s'ha vist incrementada especialment, atés el seu ús per a múltiples aplicacions, ja siguen industrials o d'ús quotidià. Així, l'augment en els últims anys dels coneixements que tenim sobre la potencial toxicitat dels productes químics, ha anat de la mà d'una creixent preocupació per la seua presència en aire, aigües, biota o aliments, així com pels seus efectes nocius. A més a més, la diversitat d'estructures químiques dels contaminants i, en conseqüència, la varietat de les seues propietats fisicoquímiques, així com les baixes concentracions en què es troben, han provocat que el seu control i monitorització esdevinga un gran repte per a la química analítica [1–3].

Aquesta preocupació s'ha traduït, no sols en un major estudi dels contaminants orgànics, sinó també en una voluntat per part de diversos organismes d'identificar-los i classificar-los per tal d'afavorir la seua regulació. En aquest sentit, destaca de manera especial la Convenció d'Estocolm, un acord impulsat per les Nacions Unides que va entrar en vigor en 2004, i que actualment ha estat signat per més de 150 països. En aquest document s'acorda la regulació d'un gran nombre de compostos considerats com a contaminants orgànics persistents (*persistent organic pollutants, POPs*), i s'estableixen les principals línies de vigilància dels seus efectes, amb l'objectiu de buscar substàncies alternatives i migrar cap a un futur més saludable i sostenible. D'ençà la seua signatura, la fabricació de diversos compostos ha estat prohibida o limitada, donant lloc a un llistat de substàncies vigilades que està en constant revisió per tal d'adaptar-se a l'aparició de nous contaminants [4], anomenats contaminants emergents. Cal destacar que, tot i que els contaminants emergents poden haver estat presents al medi des de fa temps, no han estat identificats fins al desenvolupament de tècniques analítiques més sensibles i, per tant, molts d'ells no estan regulats o no es coneixen amb exactitud els seues efectes sobre la salut [5].

La Convenció d'Estocolm defineix els POPs com aquells contaminants que presenten un toxicitat per als humans o la fauna, que persisteixen durant anys provocant la seua bioacumulació, i que, degut a açò, són distribuïts arreu de tot el planeta. Aquesta definició tan àmplia ha anat acotant-se a través de la classificació dels compostos considerats com POPs, que es va iniciar amb l'enumeració dels 12 primers compostos o grups de compostos que es van prohibir amb aquesta convenció. Les 12 substàncies inicials comprenien principalment compostos halogenats, que es podien classificar en 3 categories [4]:

- Pesticides: aldrin, dieldrina, clordà, DDT, endrina, heptaclor, mirex, toxafè i hexaclorobenzè.
- Compostos industrials de producció intencionada: bifenils policlorats (*polychlorinated biphenyls, PCBs*).
- Compostos de producció no intencionada: dibenzodioxines policlorades (*polychlorinated dibenzo dioxins, PCDDs*), també conegudes com dioxines, i dibenzofurans policlorats (*polychlorinated dibenzofurans, PCDFs*) [6].

El llistat inicial s'ha anat ampliant al llarg dels anys, fins a uns 30 compostos o grups de compostos, que actualment es troben enregistrats per a la seua eliminació o limitació per part dels països signants. No obstant, i a pesar del gran avanç que ha suposat la regulació dels contaminants amb la Convenció d'Estocolm, els contaminants orgànics ambientals comprenen un conjunt de compostos molt més ampli, i són molt nombrosos els estudis que n'han identificat centenars d'ells com a contaminants persistents o semipersistents, que poden resultar nocius per al medi ambient i les persones. Per això, altres organismes han posat el focus d'atenció també en ells, com és el cas del llistat de contaminants prioritaris de l'agència de protecció mediambiental dels Estats Units (*United States Environmental Protection Agency, USEPA)* [7]. A més a més, cal tenir en compte que la prohibició o limitació dels compostos enumerats a la Convenció d'Estocolm o altres regulacions ha propiciat l'aparició de noves substàncies que s'utilitzen com a substitutius, i que poden esdevenir nous contaminants orgànics. A la Taula 1 es troben resumits alguns dels grups més importants de compostos orgànics que són àmpliament reconeguts com a contaminants ambientals d'interés, per la qual cosa molts d'ells han estat inclosos en diverses regulacions.

D'una banda, el llistat de pesticides regulats per la Convenció d'Estocolm s'ha vist augmentat amb la inclusió de nous plaguicides halogenats com són l'α-hexaclorociclohexà, β-hexaclorociclohexà, clordecona, dicofol, lindà o endoslufan, i altres pesticides similars com el metoxiclor es troben en revisió com a candidats proposats per a formar-ne part. Tots aquestos pesticides es coneixen com pesticides organoclorats (*organochlorine pesticides, OCPs*) a causa de la presència de grups clorats en la seua estructura. No obstant, la seua regulació des de ja fa dècades ha propiciat la seua substitució per nous compostos com són els pesticides organonitrogenats (*organonitrogen pesticides, ONP*) que comprenen principalment els carbamats i triazines, o els pesticides organofosforats (*organophosphorous pesticides, OPPs*), fet que ha causat que actualment siguen els pesticides més àmpliament utilitzats. Els OPPs, es caracteritzen per tenir grups fosfat o tiofosfat a l'estructura molecular i, encara que són menys persistents que els OCPs, presenten una alta toxicitat, per la qual cosa han estat també considerats com a contaminants perillosos des de fa molt de temps, i s'han establert un gran nombre de regulacions per limitar-los i controlar-los [8]. De fet, el clorpirifós, un dels OPPs més comuns, es troba actualment en revisió per part de les Nacions Unides per ser inclòs en el llistat de la Convenció d'Estocolm [9].

En segon lloc, i per la part dels compostos industrials de producció intencionada, a més dels PCBs que comprenen una família molt àmplia de compostos clorats [10], la creixent industrialització ha provocat l'aparició de moltes substàncies orgàniques potencialment nocives per al medi ambient. Entre elles destaquen els retardants de flama que van prendre importància, en primer lloc, amb l'aparició dels retardants de flama bromats (*brominated flame retardants, BFRs*), un conjunt de compostos amb grups bromats a la seua estructura que s'addicionen en la fabricació d'una gran varietat de productes com tèxtils, mobiliari, materials de construcció o productes electrònics per tal de retardar la seua combustió. No obstant, l'augment del seu ús, juntament a la seua toxicitat i persistència, va donar lloc a la seua regulació, i actualment molts d'ells es troben ja inclosos a la Convenció d'Estocolm, com són els difenil éters polibromats, l'hexabromociclododecà o l'hexabromodifenil, o també el declorà plus que es torba actualment en revisió. Anàlogament al cas dels pesticides, la seua prohibició ha provocat l'aparició de compostos alternatius, principalment els retardants de flama organofosforats (*phosphorous flame retardants, PFRs*) que, atés que també contenen grups fosfats a l'estructura, presenten una alta toxicitat i nombrosos estudis han mostrat els potencials efectes nocius de l'exposició per part dels humans i del medi ambient, fet que ha generat que actualment siguen considerats com a contaminants emergents [4,9,11].

En aquest sentit destaca també la preocupació en els últims anys pels compostos per- i polifluoroalquilats (*per- and polyfluoroalkyl substances, PFASs*), que són compostos amb un gran nombre de grups fluorats en l'estructura, que s'han utilitzat àmpliament des dels anys 50 com a surfactants o en la producció de polímers. A causa de la seua persistència i toxicitat, han rebut una gran atenció en les últimes dècades com a contaminants emergents. De fet, l'àcid perfluorooctanoic (*perfluorooctanoic acid, PFOA*) i l'àcid perfluorooctanosulfònic (*perfluorooctanesulfònic acid, PFOS*), que són els més coneguts, ja es troben inclosos al llistat de POPs, i altres compostos similars es troben actualment en revisió per a ser inclosos també en la Convenció d'Estocolm [4,9,12]. A més d'aquestes, altres substàncies produïdes industrialment també han estat incloses com a POPs, com puguen ser el pentaclorobenzè, el pentaclorofenol, l'hexaclorobutadiè, o les parafines policlorades [4].

Per altra banda, en els últims anys han rebut una gran atenció també els productes farmacèutics i de cura personal (*pharmaceuticals and personal care products, PPCPs*), definits per l'USEPA com "qualsevol producte utilitzat per persones per motius de salut personal o cosmètics, o utilitzat per la indústria agrícola i ramadera per millorar el creixement o la salut del bestiar". Aquestos productes inclouen tot tipus de fàrmacs com puguen ser els antibiòtics, els antiinflamatoris no esteroides, hormones o reguladors lipídics, i també productes utilitzats per a la higiene o cura personal com per exemple filtres UV, desinfectants, fragàncies o conservants.

Taula 1. Grups de contaminants ambientals més importants amb els seus usos o precedència i alguns exemples.

Contaminants		Usos, aplicacions o producció	Exemples d'estructura		
Pesticides	**Pesticides organoclorats (OCPs)**	Control de plagues a nivell agrícola o domèstic	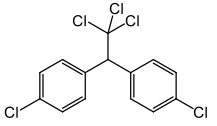 DDT (OCP)	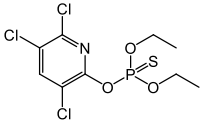 Clorpirifós (OPP)	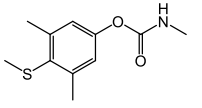 Metiocarb (ONP)
	Pesticides organofosforats (OPPs)				
	Pesticides organonitrogenats (ONPs)				
Bifenils policlorats (PCBs)		Additius en materials aïllants, equipament electrònic o segelladors	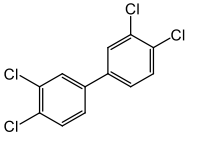 PCB 77		
Retardants de flama	**Retardants de flama bromats (BFRs)**	Additius per retardar la combustió de productes tèxtils, mobiliari, materials de construcció o productes electrònics	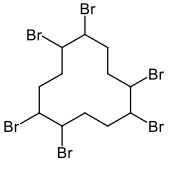 Hexabromociclododecà (BFR)	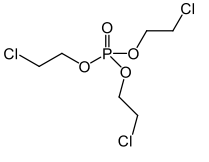 TCEP (PFR)	
	Retardants de flama organofosforats (PFRs)				
Compostos per- i polifluoroalquilats (PFASs)		Utilitzats com a surfactants i en la producció de polímers	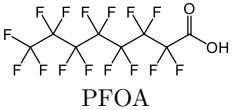 PFOA		

Taula 1. (*continuació*)

Contaminants		Usos, aplicacions o producció	Exemples d'estructura
Fàrmacs i productes de cura personal (PPCPs)	**Fàrmacs**	Prevenir o tractar malalties humanes i animals	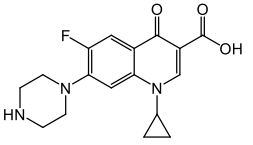 Ciprofloxacina
	Productes cosmètics i de cura personal	Millorar la higiene i altres aspectes de la nostra qualitat de vida	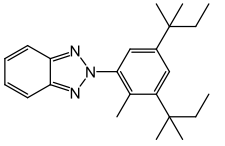 UV-328
Disruptors endocrins més comuns (EDCs)	**Parabens**	Conservants	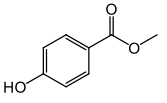 Metilparabé
	Ftalats	Conservants i fabricació de plàstics	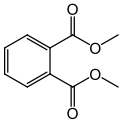 Dimetilftalat
	Bisfenols	Additius en la fabricació de plàstics	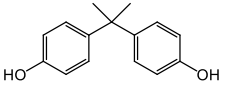 Bisfenol A
Dibenzodioxines policlorades (PCDDs)		Productes secundaris en la combustió de residus, fosa de metalls o fabricació de compostos clorats, també poden tenir orígens naturals	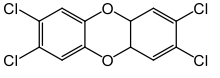 2,3,7,8-tetracloro dibenzodioxina
Dibenzofurans policlorats (PCDFs)			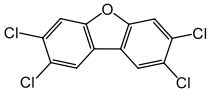 2,3,7,8-tetracloro dibenzofurà
Hidrocarburs policíclics aromàtics (PAHs)		Combustions incompletes en processos industrials o de transport, incineració de residus, o tractament de metalls, també poden tenir orígens naturals	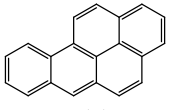 Benzo(a)piré
Compostos orgànics volàtils (VOCs)		Combustió de combustibles fòssils, refineria de petroli, ús com a dissolvents o producció de materials sintètics	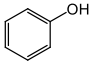 Fenol

Encara que els PPCPs són utilitzats personalment per la població, a través de la seua excreció poden alliberar-se al medi ambient, i s'han detectat en aigües en concentracions fins i tot de l'ordre de μg L^{-1}, per la qual cosa alguns d'ells es consideren contaminants emergents (actualment els més importants són de procedència urbana). Així, el seu ús cada vegada més gran ha anat provocant la seua acumulació, fins a esdevenir un problema a nivell global per al medi ambient i els ecosistemes aquàtics, principalment pel que fa al seu impacte en quant a desordres reproductius i endocrins [13–15]. De fet, malgrat que els seus efectes i toxicitat encara estan en estudi, molts d'ells ja han començat a estar vigilats i regulats, com és el cas del compost UV-328, un filtre ultraviolat que actualment també es troba en revisió com a possible candidat en la Convenció d'Estocolm [9]. A més a més, entre aquestos productes destaquen també els èsters de l'àcid parahidroxibenzoic, també coneguts com parabens, que s'utilitzen com a conservants en una gran varietat de productes, i han rebut una gran atenció en els últims anys. De fet, tant els filtres UV com els parabens han estat identificats com a compostos que alteren el sistema endocrí, fet que ha propiciat la seua classificació com a disruptors endocrins (*endocrine-disrupting chemicals, EDCs*). Dins d'aquest grup d'EDCs podem trobar també altres compostos utilitzats en la fabricació de plàstics com són els diésters de l'àcid ftàlic o ftalats, que s'utilitzen també com a conservants. També els bisfenols, principalment el bisfenol A (BPA), un compost que ha estat utilitzat des de fa temps per a la fabricació de plàstics policarbonats per a tot tipus d'usos, i el qual diversos estudis de les últimes dècades han relacionat amb nombrosos problemes de salut i disfuncions en diversos sistemes i òrgans. Atesos els efectes tòxics associats a l'exposició de tots aquestos EDCs, la seua vigilància i monitoratge ha anat també en augment [16].

En quant als compostos de producció no intencionada, també s'han afegit nous compostos al llistat de la Convenció d'Estocolm, com és el cas dels naftalens policlorats. Aquest compost, que també es sintetitza de forma industrial, és un derivat dels hidrocarburs policíclics aromàtics (*polycylic aromatic hidrocarbons, PAHs*), que encara que estan considerats com a semipersistents, també han estat catalogats com a contaminants orgànics des de fa temps, i un gran nombre d'ells es troben registrats al llistat de contaminants prioritaris de l'USEPA [7]. Els PAHs consisteixen en compostos formats per diversos anells aromàtics, i es generen a partir de la combustió incompleta en processos industrials o de transport. Encara que també es poden originar de forma natural, la major part de les emissions són antropogèniques. A més a més, la seua habitual presència en aire i aigües suposa un risc importat per a la població ja que els PAHs han estat relacionats amb efectes carcinògens i mutagènics, així com altres efectes perjudicials per a les persones i els ecosistemes [17–19].

Finalment, també requereixen una menció especial els compostos orgànics volàtils (*volatile organic compounds, VOCs*), un terme que comprén un ampli grup de més de 500 compostos de diversos tipus amb la característica comuna de la seua volatilitat, incloent alcans i alquens, hidrocarburs aromàtics, alcohols o

aldehids, entre altres. Per això, la seua presència en l'atmosfera és molt habitual, ja siga per emissions naturals o antropogèniques com la indústria o els mitjans de transport. A més a més, els efectes tòxics amb què s'associen molts d'ells han provocat també la seua regulació i els més importants es troben també inclosos en l'esmentat llistat de contaminants prioritaris [7], com per exemple els dissolvents coneguts com BTEX (benzè, toluè, etilbenzè i xilens) o diversos compostos fenòlics com el fenol o els alquilfenols [20,21].

Atesa la presència de tots els contaminants esmentats en el medi que ens envolta, i al marge de la Convenció d'Estocolm, la majoria de països del món han pres part també en aquesta vigilància i han establert una legislació cada vegada més estricta per al control i la regulació de totes aquestes substàncies, principalment pel que fa a les aigües. En el cas de la Unió Europea, diverses directives comunitàries són les que regulen la presència de tots aquestos contaminants en el medi ambient, per tal de limitar-hi així el contacte de la població. Així, la Directiva 2013/39/EU [22] assenyala els contaminants més importants a vigilar, i estableix concentracions límit permeses per a diversos d'ells i els seus metabòlits en el cas de les aigües continentals superficials. Igualment, altres directives prenen també aquest llistat com a referència, com és el cas de la Directiva 2006/118/EC [23] en el cas de les aigües subterrànies. Igualment, per la part de les aigües destinades al consum humà, la Directiva 98/83/EC [24] regula la presència de diversos contaminants orgànics, i estableix límits per a certs compostos com és el cas dels plaguicides (0.1 µg L^{-1} per a cada pesticida i 0.5 µg L^{-1} per al total), els PAHs (0.1 µg L^{-1} per a tots els PAHs especificats a la directiva, i 0.01 µg L^{-1} en el cas del benzo(a)pirè), o el benzé (1 µg L^{-1}). Igualment, governs d'altres països i altres organismes internacionals també han establert límits de concentracions per a molts d'aquestos compostos, com és l'exemple de l'Organització Mundial de la Salut (*World Health Organization, WHO*), o l'USEPA, principalment en el cas dels pesticides i altres compostos que han estat vigilats des de fa ja vàries dècades [25]. En aquest sentit, cal destacar també que la majoria d'aquesta legislació fa referència a compostos àmpliament coneguts com puguen ser els pesticides, hidrocarburs policíclics aromàtics, o els metalls pesants, però totes aquestes directives encara es troben endarrerides pel que respecta als contaminants emergents, com puguen ser els retardants de flama o els compostos poli- i perfluoroalquilats.

De manera similar, són diversos els estudis realitzats per tal de monitoritzar la presència dels contaminants orgànics en l'aire. En aquest sentit, cal destacar d'una banda el seu control a xicoteta escala, començant per l'avaluació de riscos laborals, a través de la qual es pretén conéixer l'exposició a un o diversos contaminants en un moment i lloc concret, com puga ser l'aplicació de pesticides o la fabricació i utilització de compostos químics a nivell industrial. En aquestos casos, diversos organismes estableixen també nivells de concentració tolerables en l'atmosfera, coneguts com límits d'exposició laboral (*Occupational Exposure Levels, OEL*) [26], per tal de garantir la seguretat de treballadors i usuaris.

Concretament en el cas de l'estat espanyol, l'Institut Nacional de Seguretat i Salut en el Treball emet anualment un llistat amb els compostos a vigilar, juntament amb els límits permesos per a garantir la seguretat [27]. No obstant, la majoria d'aquestos compostos, atesa la seua persistència i volatilitat, s'estenen molt més enllà del seu lloc d'emissió o aplicació, i esdevenen un seriós problema per a la salut pública a causa de l'exposició de la població general als seus efectes, fet que ha originat també l'aparició de diverses directives europees per intentar regular-los [28,29]. I, a més a més, d'altra banda, el seu transport de llarg abast incrementa encara més l'interés del control dels contaminants orgànics, i els converteix en una problemàtica global. Així, les tècniques de mostreig d'aire a gran escala, han originat nombrosos estudis a nivell mediambiental que han demostrat la seua presència, no sols en les zones més desenvolupades o industrialitzades, sinó també a quilòmetres de distància del lloc d'emissió [30–32].

Així doncs, una de les conseqüències més importants d'aquesta creixent presència de contaminants a nivell mediambiental, és l'absorció que es pot produir per par part dels humans, comportant múltiples problemàtiques de salut. Diversos estudis s'han centrat en les últimes dècades a establir els efectes adversos que poden tenir aquestes substàncies per als humans i, si bé és complicat determinar la relació directa de cada contaminant amb una afecció concreta, tots els POPs han presentat un alt potencial de tenir propietats altament nocives per a l'organisme ja siga com a disruptors endocrins, agents cancerígens o amb activitat tòxica sobre el sistema nerviós, immunològic, reproductor, o sobre algun òrgan vital [33–35]. Així, encara que aquesta absorció es pot donar a través de distintes vies com pot ser la via respiratòria a partir de la contaminació ambiental, o la via dèrmica, una de les principals rutes d'entrada és a través de la via digestiva, bé siga a partir de l'aigua de consum humà, tal i com s'ha comentat, o a través de la ingesta d'aliments.

Els aliments que consumim diàriament, tant d'origen animal com vegetal, es troben contínuament exposats a una gran varietat de contaminants orgànics, ja siga per exposició directa, com és el cas de l'aplicació de fitosanitaris, per absorció a través de la contaminació de l'aire o del sòl, o a causa dels tractaments previs a la seua comercialització [36]. Aquesta exposició pot comportar la presència de residus en el moment de la seua ingesta, ja siguen de la pròpia substància contaminant o d'algun metabòlit que també pot ser nociu per a la salut. Per aquest motiu, diversos organismes han determinat nivells d'ingesta tolerable, tant diaris com mensuals. És el cas de l'Organització Mundial de la Salut i l'Organització de Nacions Unides per a l'Alimentació i l'Agricultura (*Food and Agriculture Organization, FAO*), que en diversos estudis estableixen directrius i nivells tolerables per a diversos POPs, així com d'altres contaminants, a més de certs additius alimentaris [37–39]. La legislació europea (1881/2006/CE) també estableix valors límits per a molts d'aquestos contaminants ambientals com és el cas dels PAHs, PCBs o les dioxines, segons el tipus de producte i el seu origen [40]. A més a més, atés que el cas dels pesticides és especialment notori pel seu

contacte directe amb l'alimentació, la Unió Europea estableix també a través de diverses directives els nivells màxims de residu (*maximum residue level, MRL*) per a cadascun dels pesticides autoritzats, és a dir, les quantitats màximes que pot contenir el producte en el moment de la seua comercialització [41]. Igualment, els aliments d'origen animal també són especialment sensibles en quant a la presència de substàncies contaminants. Per una banda, la presència de contaminants orgànics en els animals pot vindre donada per la seua exposició a ells, principalment a partir de la contaminació dels pinsos o altres aliments [42,43] i, per altra banda, tal i com ja s'ha comentat, a causa de la presència de medicaments que s'utilitzen en el tractament del bestiar com puguen ser els antibiòtics o les hormones [44], i que poden estar presents també en el producte final comercialitzat, fet que requereix també el seu control i vigilància.

Per altra part, cal destacar que la contaminació dels aliments pot tenir altres orígens a part de la presència de contaminants orgànics ambientals o d'alguna altra font externa, com és el cas de les micotoxines. Les micotoxines són metabòlits secundaris produïts per fongs filamentosos que poden contaminar els aliments o els cultius i que són altament nocius per a persones i animals, fet que ha provocat que esdevinguen una preocupació important per a la seguretat alimentària. D'entre les més de 400 micotoxines que es coneixen actualment, les més comunes són les aflatoxines, ocratoxines, zearalenona, patulina, fumonisines, i tricotecens com el desoxinivalenol. Aquest problema es veu agreujat pel fet que la seua aparició és inevitable fins i tot quan s'apliquen les pràctiques agrícoles d'emmagatzematge o processament de manera correcta. De fet, segons la FAO, la contaminació per micotoxines afecta al 25% de totes les plantacions mundials, ja siga durant el seu cultiu o durant l'emmagatzematge. Això ha provocat també l'aparició, no sols de recomanacions i protocols de prevenció, sinó també de legislacions per tal de limitar les concentracions permeses de micotoxines en diversos tipus d'aliments per tal de garantir la seguretat de la població. A nivell europeu, la ja esmentada Regulació 1881/2006/CE [40] estableix també els límits màxims de les micotoxines més importants per a diversos tipus d'aliments, amb concentracions permeses d'entre 10 i 2000 µg kg^{-1} en el cas de micotoxines com la patulina, el desoxinivalenol, la zerealenona o les fumonisines, però amb límits molt més restrictius en el cas de les aflatoxines (0,025-15 µg kg^{-1}) o l'ocratoxina A (0,5-10 µg kg^{-1}) degut a la seua alta activitat tòxica a nivell hepàtic, nerviós, immunològic o genètic, presentant algunes d'elles també un potencial caràcter cancerigen. A més de l'aparició de les micotoxines en aliments d'origen vegetal, la contaminació dels pinsos pot provocar també l'absorció de les micotoxines per part dels animals que se n'alimenten i, en conseqüència, la contaminació dels productes alimentaris derivats d'ells, com és el cas de la llet [45–47]. A més a més, els efectes del canvi climàtic, com per exemple l'augment de temperatures, afavoreixen la proliferació dels fongs productors d'aquestes micotoxines. Aquest fet, juntament al creixement de les pràctiques d'agricultura intensiva per tal d'abastir a una creixent població, ha agreujat de manera notable en les últimes dècades la presència de micotoxines en aliments [48].

Finalment, la constatació de la presència dels contaminants orgànics en l'aire, aigua o aliments, ha comportat també una preocupació per saber quina n'és la presència al nostre organisme, fet que ha donat lloc a nombrosos estudis de biomonitoratge. L'objectiu d'aquestos estudis, a més d'avaluar els potencials riscos associats a l'exposició dels contaminants o substàncies nocives, és també identificar noves exposicions a productes químics, avaluar els canvis o les tendències d'aquestes exposicions, establir la distribució de la presència dels contaminants entre la població per poder identificar grups vulnerables, determinar com els canvis tecnològics afecten les exposicions, desenvolupar estudis epidemiològics o avaluar l'eficàcia de les regulacions i la legislació respecte d'aquestos compostos. Això ha provocat grans esforços dirigits a l'anàlisi de tot tipus de matrius biològiques, així com a la recerca dels biomarcadors adequats, centrant-se en l'estudi no sols d'aquestos compostos, sinó també dels seus metabòlits. Així doncs, un gran nombre de mètodes han anat sorgint a partir de l'anàlisi de diferents matrius, com són la sang (sèrum i plasma), orina, llet materna, saliva, cabells, ungles, entre altres [49,50].

Amb tot açò, la presència de contaminants i substàncies nocives en el medi en què vivim, tal i com ja s'ha dit, ha augmentat notablement en les últimes dècades amb la creixent industrialització, el necessari abastiment a una població mundial en constant augment, i els efectes del canvi climàtic, fet que ens ha abocat a un control i vigilància continu de totes aquestes substàncies per tal de garantir el compliment de la legislació i, en última instància, la nostra salut i la dels ecosistemes. I és en aquest punt on la química analítica actual ha pres un paper fonamental, desenvolupant i perfeccionant nombroses tècniques tant a nivell instrumental com de tractament de mostra, per tal d'encarar aquest gran repte.

2. Determinació de contaminants orgànics

En les últimes dècades la química analítica s'ha nodrit del creixent desenvolupament tecnològic per implementar nombroses tècniques instrumentals que, cada vegada més, obrin noves possibilitats per a la creació de mètodes d'anàlisi més selectius, sensibles, ràpids, exactes i precisos. En el cas de la determinació de contaminants orgànics les tècniques cromatogràfiques de separació han suposat una eina fonamental, ja que permeten la determinació simultània de diversos contaminants d'una manera eficient. En aquest sentit, les tècniques més àmpliament utilitzades per a la determinació de compostos orgànics, tant pel que fa a l'anàlisi mediambiental com d'aliments, han estat la cromatografia de gasos (*gas chromatography, GC*) i la cromatografia líquida d'alta resolució (*high resolution liquid cromatography, HPLC*). La combinació d'aquestes dues tècniques ofereix un gran ventall de possibilitats per a la determinació de compostos orgànics de propietats molt diverses en quant a volatilitat, polaritat, grandària molecular, etc. A més a més, en aquesta línia destaquen també les tècniques electroforètiques com l'electroforesi capil·lar de

zona (*capillary zone electrophoresis, CZE*) per a la separació d'espècies carregades, encara que aquestes tècniques són, en general, menys sensibles [35].

D'una banda, la GC és bastant utilitzada per a la determinació de molts dels compostos orgànics, principalment aquells amb una alta volatilitat. En el cas dels compostos orgànics poc polars, la separació se sol dur a terme amb columnes capil·lars de 5% fenil 95% dimetilpolisiloxà, estant la columna més àmpliament utilitzada, encara que columnes amb una polaritat més alta també s'empren per a anàlits més polars. A més a més, com a gas portador se sol utilitzar tant nitrogen com heli, encara que la proliferació dels detectors d'espectrometria de masses (*mass spectrometry, MS*), tal i com s'explica més endavant, ha fet que aquest últim siga, de lluny, el més utilitzat. Cal destacar també l'aparició als últims anys de la GC bidimensional (*GCxGC*) que ha esdevingut la tècnica cromatogràfica multidimensional més utilitzada per a mostres complexes. En aquesta tècnica, mitjançant la connexió de dos columnes amb un modulador, s'aconsegueix millorar la capacitat de separació de pics (i amb això la selectivitat), així com la sensibilitat respecte de la GC convencional [34].

En segon lloc, les tècniques d'HPLC han permés expandir la determinació de contaminants orgànics cap a molts tipus de substàncies, incloent compostos polars, iònics, o no volàtils, que no es poden separa mitjançant GC. Encara que altres tipus de columnes han estat també proposades, les fases estacionàries més àmpliament utilitzades en aquestos casos han estat sempre les columnes basades en C18. En aquest sentit, cal destacar l'evolució en els últims temps de l'HPLC cap a tècniques més sofisticades que ofereixen una resolució encara major, com és l'UHPLC (*ultra-high resolution liquid cromatography*), on mitjançant l'ús de columnes amb una menor grandària de partícula (<2 µm) s'aconsegueixen eficiències cromatogràfiques molt més altes, així com temps d'anàlisi més curts, i és per això que, cada vegada més, està esdevenint la tècnica més àmpliament utilitzada. Així, encara que els dissolvents utilitzats per a la separació són molt diversos (generalment fases mòbils hidroorgàniques), l'acoblament a tècniques de MS ha fet que aquest siga també un aspecte important a tenir en compte en quant a la detecció, ja que la composició de la fase mòbil pot afectar també a la qualitat de la posterior determinació al detector d'MS. Per últim, encara que molt menys utilitzada, la cromatografia de fluids supercrítics (*packed column supercrital fluid chromatography, pSFC*), també ha estat proposada per a la determinació de compostos orgànics, especialment aquells tèrmicament làbils [34,51].

Quant a la posterior determinació dels anàlits, des de l'aparició de les tècniques cromatogràfiques diversos detectors han estat desenvolupats per tal de quantificar els compostos orgànics. En primer lloc, pel que fa a la GC, partit del clàssic detector d'ionització en flama (*flame-ionization detector, FID*), altres detectors selectius han estat desenvolupats com puguen ser el detector selectiu de nitrogen-fòsfor (*nitrogen-phosphorus detector, NPD*), el detector de captura electrònica (*electron capture detector, ECD*) selectiu per a compostos halogenats, o el detector fotomètric de flama (*flame photometric detector, FPD*), selectiu per a

compostos de fòsfor i sofre. A més a més, en el cas de l'LC, destaquen els detectors òptics com són el d'ultravioleta-visible (UV-Vis), ja siga d'un sol díode o de fila de díodes (*diode array detector, DAD*) que permet la mesura a diverses longituds d'ona, així com el detector de fluorescència (*fluorescence detector, FLD*), que presenta una gran sensibilitat i selectivitat per als compostos amb activitat fluorescent. No obstant, tal i com ja s'ha comentat, totes aquestes tècniques de detecció s'han vist desplaçades en els últims anys amb l'acoblament de detectors d'espectrometria de masses a les tècniques cromatogràfiques [52,53].

L'acoblament dels detectors MS a les tècniques cromatogràfiques permet superar les deficiències dels detectors clàssics, incloent els més selectius, pel que fa a la inequívoca confirmació i identificació, així com l'obtenció d'informació estructural i isotòpica. A més a més, ofereixen una gran selectivitat que permet diferenciar fins i tot entre compostos que coelueixen, així com minimitzar el soroll de fons, fet que augmenta la sensibilitat. Així, encara que aquest acoblament resulta bastant sofisticat, la millora en les interfases entre el sistema cromatogràfic i l'analitzador de masses, així com la major disponibilitat d'equips i el seu abaratiment han suposat la universalització d'aquestes tècniques tant per a l'anàlisi dirigit com no dirigit o *screening* [34,51].

Atés que la interfase entre el sistema cromatogràfic i l'analitzador, així com el tipus de detector utilitzat són crucials per a una bona determinació dels anàlits, les investigacions dels últims anys han donat pas, en primer lloc, a diverses tècniques d'ionització dels anàlits, que es poden utilitzar en funció de les propietats químiques dels compostos estudiats. D'una banda, les tècniques d'ionització d'alt buit han estat majoritàriament utilitzades en equips de GC-MS, sent la ionització electrònica (*electron ionization, EI*) la més utilitzada, encara que també està bastant estesa la ionització química, principalment en la modalitat d'ionització negativa (*negative-ion chemical ionization, NICI*). D'altra banda, les tècniques d'ionització a pressió atmosfèrica (*atmosferic presure ionization, API*) han estat utilitzades de forma majoritària en el cas de LC-MS, encara que el seu ús en GC-MS ha anat en augment en els últims anys. Entre aquestes, a més de la fotoionització (*photoionization, APPI*) i la ionització química (*APCI*), destaca sobretot la ionització per *electrospray* (*ESI*), àmpliament utilitzada per a compostos més polars o amb una volatilitat menor. En segon lloc, són diversos també els tipus d'analitzadors de masses que s'han anat desenvolupant i acoblant a les tècniques cromatogràfiques, ja siguen espectròmetres de baixa resolució (*low resolution, LRMS*), especialment els quadrupols (*Q*), o d'alta resolució (*high resolution, HRMS*) com les trampes d'ions (*ion trap, IT*) o els analitzadors de temps de vol (*time-of-flight, ToF*). A més a més, en els últims anys, l'aparició d'analitzadors de masses en format tàndem (*MS/MS*) ha donat lloc a tècniques de detecció molt més ràpides, sensibles i selectives, amb el desenvolupament de nous detectors com el de triple quadrupol (*QqQ*) o el de quadrupol-temps de vol (*QToF*), que a poc a poc estan esdevenint els detectors més àmpliament utilitzats per a la determinació de compostos orgànics tant en LC com GC [34,35,51].

No obstant, i malgrat totes aquestes innovadores tècniques instrumentals, rarament la determinació de contaminants orgànics pot realitzar-se directament sense un tractament de mostra previ, especialment a nivell de traces. Aquest fet es deu principalment a les concentracions de tots aquestos compostos que sovint es troben al voltant dels límits de detecció (malgrat la gran sensibilitat de totes aquestes tècniques). També a l'alta presència d'interferents, fet que suposa una gran problemàtica sobretot quan s'analitzen mostres amb complexes matrius mediambientals o d'aliments, on la qualitat de l'anàlisi depén fonamentalment del tractament de mostra escollit [1,54]. De fet, algunes enquestes estimen en un 61% el temps que s'empra en el tractament de mostra en relació a la resta d'etapes d'una anàlisi cromatogràfica, i atribueixen un 30% de l'error que es comet en l'anàlisi també a la preparació de mostra (Figura 1) [55]. Açò posa de manifest la importància d'aquesta etapa, així com dels estudis enfocats a millorar-la en quant a temps i rendiment. Amb tot açò, el tractament de mostra esdevé crucial en l'anàlisi de contaminants orgànics amb l'objectiu de transformar la mostra a una forma més adequada per a la seua anàlisi, a través de tres vies principals [56]:

- La transformació de l'anàlit a una forma més adequada per a l'anàlisi instrumental.
- La simplificació de la matriu a través de la seua neteja o *clean-up*.
- La preconcentració de l'anàlit per tal de millorar els límits de detecció del mètode.

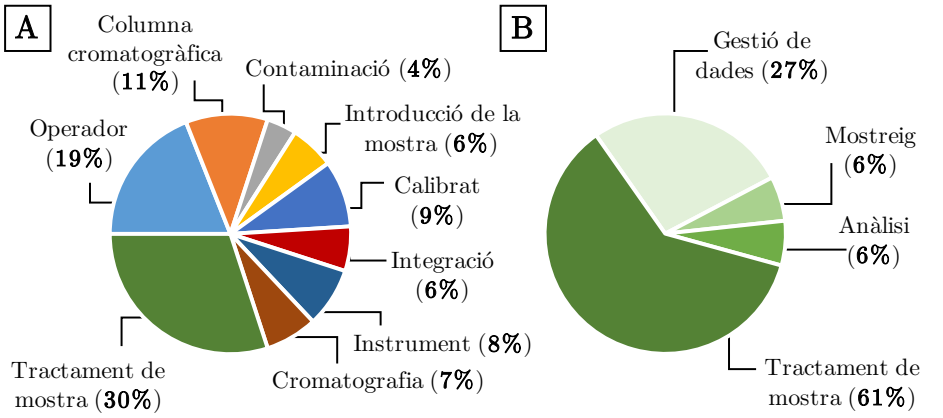

Figura 1. Importància de l'etapa de tractament de mostra en les anàlisis cromatogràfiques: percentatge d'error atribuït a cadascun dels elements de l'anàlisi cromatogràfica (A), i de temps emprat en cascuna de les etapes de l'anàlisi (B) [55].

Amb aquestos objectius, són molts els tractaments de mostra que s'han proposat en les darreres dècades, principalment partint de les dos tècniques d'extracció més comunes, com són l'extracció líquid-líquid (*liquid-liquid extraction, LLE*) i l'extracció en fase sòlida (*solid-phase extraction, SPE*). Encara que aquestes han anat evolucionant i donant lloc a noves metodologies, la majoria de protocols actuals es basen en els principis d'aquestes dues tècniques.

D'una banda, l'LLE és una tècnica molt popular des de fa temps a causa de la seua simplicitat i eficiència, i es basa en la diferència de solubilitat dels anàlits en diversos dissolvents per tal d'obtenir una extracció quantitativa dels compostos d'interés. Atés que l'LLE és una tècnica fàcil d'operar i no requereix de cap equipament ni tecnologia especial, ha estat utilitzada històricament per a un gran nombre de mètodes oficials. No obstant, també és una tècnica que requereix grans quantitats de dissolvents orgànics (generalment tòxics), així com llargs temps d'extracció, fet que n'ha provocat el desús en els últims temps [57,58]. Amb l'objectiu de pal·liar aquestos desavantatges, se n'han anat reportant diverses modificacions, generalment enfocades a la seua miniaturització per tal de fer-la més ràpida i sostenible. En aquest sentit, les més utilitzades per a l'extracció de contaminants orgànics, principalment en mostres aquoses, són les tècniques de microextracció en fase líquida (*líquid-phase microextraction, LPME*), que han aparegut en les últimes dècades, oferint una preconcentració i neteja de la matriu amb un baix cost, facilitat d'operació i alta eficàcia. Entre aquestes destaquen les LPMEs assistides per membranes, la microextracció en gota (*single-drop microextraction, SDME*) o la microextracció líquid-líquid dispersiva (*dispersive liquid-liquid microextraction, DLLME*) [57]. Aquesta última es basa en la dispersió d'una xicoteta quantitat de dissolvent extractant en la mostra mitjançant l'ús d'un agent dispersant, que se separa posteriorment per centrifugació [58]. Totes aquestes tècniques miniaturitzades han estat aplicades per a la determinació de tot tipus de contaminants orgànics com per exemple disruptors endocrins com els bisfenols [57], pesticides [58], o micotoxines [59].

D'altra banda, l'SPE va sorgir als anys 50, es va adaptar posteriorment als anys 70 per a quantitats menudes d'adsorbent, i actualment és una de les tècniques de tractament de mostra més àmpliament utilitzada per a tot tipus d'anàlisis, principalment perquè evita gran part dels inconvenients atribuïts a les extraccions LLE. Així, es tracta d'una tècnica simple on els anàlits són adsorbits de forma selectiva a una fase sòlida, per ser posteriorment eluïts amb una xicoteta quantitat d'eluent, afavorint així la preconcentració i neteja de la matriu d'una manera efectiva (Figura 2). A més a més, alguns altres dels seus principals avantatges són l'ús d'una quantitat menor de dissolvents, la rapidesa i simplicitat, i la possibilitat d'automatització i de combinar-la amb tècniques de detecció tant en línia (*on-line*) com seqüencialment (*off-line)*.

Cal destacar que, si bé l'empaquetament de la fase adsorbent se sol preparar en forma de columna o cartutx, també es pot trobar en altres formats com són els discs. També, un dels principals avantatges de les tècniques d'SPE és la disponibilitat d'una gran varietat de materials adsorbents que poden ser utilitzats com a fases sòlides, amb estructures i propietats químiques molt diverses, que poden donar lloc a un ampli rang de mecanismes d'extracció per a tot tipus d'anàlits, tal i com es vorà a continuació [1,56]. Igualment que amb les tècniques d'LLE, la tendència a la miniaturització i reducció de costos i temps d'anàlisi s'ha observat amb l'aparició de diverses tècniques fruit de la modificació de l'SPE. En

aquest sentit, destaca la microextracció en fase sòlida (*solid-phase microextraction, SPME*) desenvolupada per Arthur i Pawliszyn en 1990 [60], amb l'objectiu de minimitzar l'ús de dissolvents i reduir el temps de l'anàlisi, dos dels principals inconvenients de l'SPE clàssica. Des d'ençà, l'SPME ha anat guanyant popularitat per a la determinació d'una gran varietat de compostos en diverses matrius. Dins d'aquesta tècnica, són moltes les possibilitats d'operació en funció del tipus de mostra a analitzar, donant lloc a noves tècniques com la micro-SPE (μ-SPE) o l'extracció dinàmica en fase sòlida (*solid-phase dynamic extraction, SPDE*) [61]. Aquestes tècniques, a més, han donat lloc a nous formats per a l'empaquetament de la fase sòlida, com puguen ser les puntes de pipeta, xeringues, o les plaques de pous múltiples o *multi-well plates* [56].

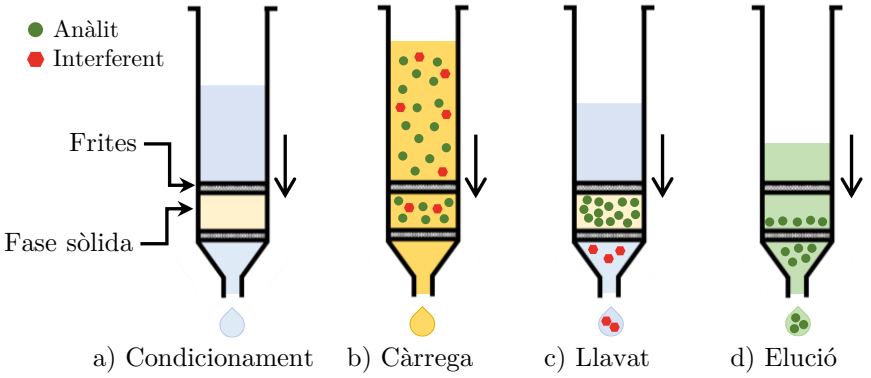

Figura 2. Esquema bàsic de les principals etapes de l'extracció en fase sòlida convencional: a) Condicionament de la fase sòlida; b) Càrrega de la mostra; c) Llavat de les interferències; d) Elució dels anàlits.

A més de l'SPME, també trobem altres alternatives a l'SPE tradicional, com puguen ser l'SPE dispersiva (*dispersive SPE, dSPE*), on la fase sòlida no es troba empaquetada en un cartutx, sinó que es dispersa a la mostra a analitzar per afavorir l'extracció. És un cas particular d'aquesta també l'anomenada SPE magnètica (*magnetic SPE, MSPE*), on es fa ús de nanopartícules magnètiques per tal d'afavorir la posterior separació de la fase dispersada amb l'ajuda d'un imant. També cal destacar l'extracció adsorbent amb vareta agitadora (*stir-bar sorptive extraction, SBSE*), on la fase sòlida es troba ancorada a una barra imantada que agita la dissolució per provocar l'adsorció selectiva dels anàlits [1,56,61]. No obstant, i a pesar de totes aquestes modificacions que fan els mètodes més ràpids i sostenibles, els mètodes miniaturitzats presenten també encara alguns inconvenients, com és l'encariment de les fibres utilitzades en el cas de l'SPME, la dificultat de reutilització dels materials i, sobretot, una capacitat de càrrega relativament baixa que dificulta el tractament de grans quantitats de mostra, fet que suposa un gran inconvenient per tal d'assolir límits de detecció baixos principalment pel que fa a l'anàlisi mediambiental a gran escala. Per aquestos motius, l'SPE clàssica és encara molt utilitzada per a molts tipus d'anàlisi com és el cas de l'anàlisi mediambiental, i per a l'anàlisi de matrius complexes [5,57,62].

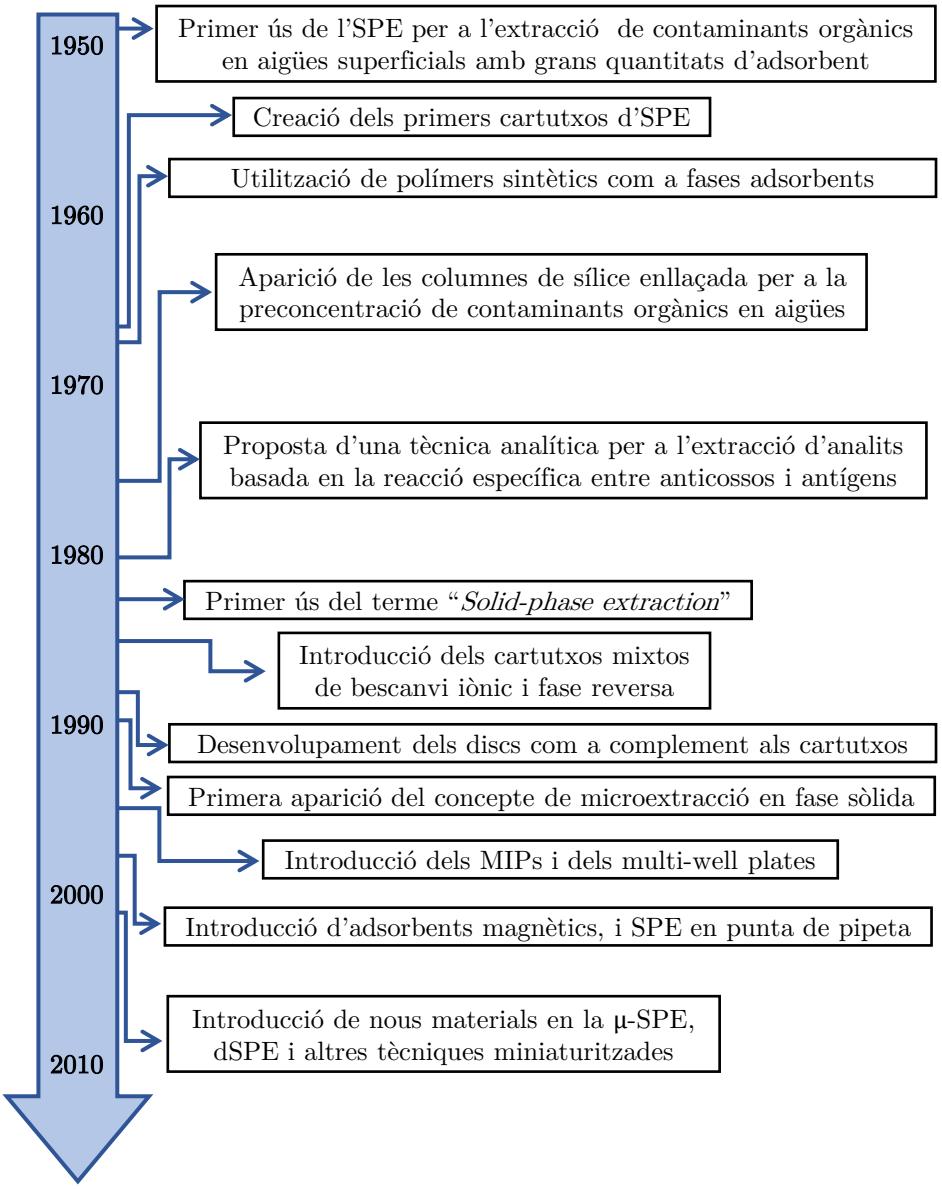

Figura 3. Fites històriques més importants en el desenvolupament de les tècniques d'SPE [56,61].

A més de les clàssiques tècniques d'extracció SPE i LLE i les seues posteriors modificacions, caldria destacar de forma especial el que es coneix com el procediment QuEChERS. Aquest procediment, que rep el seu nom de les sigles en anglés dels adjectius, ràpid, fàcil, barat, eficient, robust i segur (*quick, easy, cheap, efficient, rugged, safe*), va ser publicat inicialment per l'AOAC (*Association of Official Analytical Chemists*), i es basava en una primera extracció

amb acetonitril assistida per l'addició de sals com el $MgSO_4$ o el NaCl, seguida d'una dSPE en presència d'una amina secundària primària [63]. La metodologia QuEChERS, inicialment dissenyada per a la determinació de residus de pesticides en vegetals i fruites, ha estat aplicada per a l'extracció de tot tipus de contaminants amb diverses modificacions respecte del protocol inicial, com és la introducció de nous dissolvents o sals, o l'ús d'altres fases adsorbents per a l'etapa de *clean-up*. Aquesta tècnica és molt utilitzada també en procediments oficials, principalment per a l'anàlisi de mostres d'aliments amb matrius molt complexes, on sovint no es pot aplicar directament una SPE convencional o algun dels seus derivats, encara que també s'utilitza en anàlisi mediambiental o clínic [64].

Totes aquestes metodologies de tractament de mostra s'apliquen principalment a mostres sòlides com puguen ser els aliments o el sòl, i sobretot a mostres líquides, aquoses en la seua majoria, tant pel que fa a l'anàlisi d'aigües a nivell mediambiental, l'anàlisi d'aliments líquids com la llet, o l'anàlisi clínic de fluids biològics. No obstant, mereix una atenció especial el cas de les mostres gasoses, com puga ser la determinació de contaminants atmosfèrics, ja que es podria considerar que el tractament de mostra comença en la mateixa etapa de mostreig. En aquest cas, la tècnica més comunament utilitzada és la de fer passar l'aire a mostrejar a través d'una fase adsorbent per tal de retenir els anàlits objectiu, ja siga de forma passiva deixant l'adsorbent en contacte amb l'aire a mostrejar durant un període de temps llarg, o de forma activa mitjançant una bomba. En aquest cas, se solen utilitzar mostrejadors compostos de dues etapes: una primera amb un filtre per tal d'atrapar la fase particulada de l'aire, i una segona amb el material adsorbent per tal de mostrejar la fase gasosa (Figura 4). Donada la semivolatilitat de molts dels contaminants orgànics, a nivell mediambiental aquestos es poden trobar en ambdues fases, fet que fa necessària l'extracció dels compostos d'ambdues parts. Una vegada retinguts els anàlits, la seua extracció es pot dur a terme per diferents tècniques, principalment mitjançant la utilització de dissolvents orgànics en tècniques com el Soxhlet. No obstant, aquesta tècnica requereix el consum de grans quantitats de dissolvent i també de temps, per la qual cosa s'han desenvolupat altres tècniques d'extracció com l'extracció assistida per microones (*microwave-assisted extraction, MAE*), l'extracció amb fluids pressuritzats (*pressurized liquid extraction, PLE*) o l'extracció accelerada per dissolvents (*accelerated solvent*

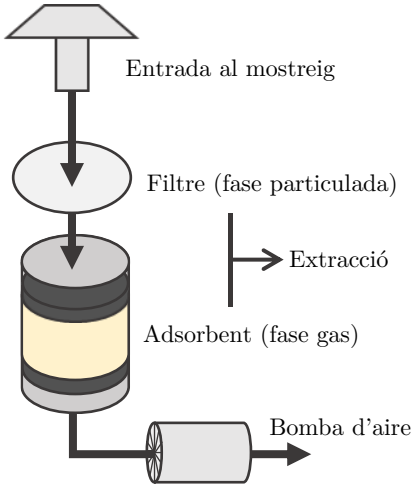

Figura 4. Esquema general del sistema de mostreig actiu utilitzat en anàlisi mediambiental [65].

extraction, ASE), així com metodologies per a la desorció tèrmica directa sense l'ús de dissolvents [34,65].

Amb tot açò, es pot extraure de la discussió el paper fonamental que les fases adsorbents juguen en els mètodes de tractament de mostra actuals. Tant el mostreig ambiental de contaminats orgànics com els mètodes de preparació de mostra basats en l'SPE per a la preconcentració o neteja de la matriu, requereixen de materials que asseguren una retenció quantitativa i selectiva dels anàlits, fet que, en les últimes dècades, ha propiciat un augment notori dels estudis enfocats al desenvolupament de nous materials per tal de donar resposta a aquesta necessitat.

3. Fases adsorbents utilitzades per a l'extracció de contaminants orgànics

Com ja s'ha comentat, des de l'aparició de les tècniques d'SPE, un gran nombre de fases sòlides han estat utilitzades per a la retenció de tot tipus de compostos. En el cas dels contaminants orgànics, diverses fases han estat àmpliament utilitzades en mètodes oficials i altres protocols, principalment les fases més clàssiques com la C18. No obstant, l'augment dels estudis enfocats al disseny de noves fases adsorbents ha donat lloc a un gran nombre de nous materials. Totes aquestes fases es poden classificar de distintes formes, ja siga segons el seu objectiu, segons la composició dels materials que les formen, o segons el tipus d'interaccions que estableixen amb els anàlits [56]. A continuació es detallen les fases més importants que s'han proposat per a la retenció de contaminants orgànics, agrupades segons la seua composició i mecanisme d'actuació.

3.1. Fases adsorbents clàssiques de sílice enllaçada

Les fase sòlides més utilitzades històricament han estat les fases de sílice enllaçada, modificada amb diversos grups funcionals orgànics que interaccionen amb els anàlits durant l'extracció. La sílice enllaçada es forma a partir de la reacció d'organosilans amb sílice activada, donant lloc a un adsorbent amb els grups funcionals units al substrat de sílice mitjançant enllaços silil èter. Enllaçats a aquesta base de sílice podem trobar una gran varietat de grups funcionals que atorguen a la fase unes propietats i una polaritat determinada, donant lloc als anomenats cartutxos de fase normal (polars) o de fase reversa (apolars). A la Taula 2 es mostren els grups funcionals més comunament utilitzats. Sense dubte, la fase més utilitzada per a la retenció de contaminants orgànics ha estat la fase amb ocatadecil com a grup funcional, anomenada C18. En aquest material els anàlits són retinguts per mecanismes principalment apolars, la qual cosa suposa molt bons rendiments d'extracció en el cas de la majoria de compostos orgànics, encara que els més apolars presenten dificultats en l'etapa de l'elució [66]. De fet,

nombrosos mètodes descrits al llarg de les últimes dècades han utilitzat aquest tipus de fase per a la determinació d'una gran varietat de contaminants orgànics [67–69], així com alguns mètodes oficials com per exemple en la determinació de pesticides [70].

Taula 2. Principals grups funcionals utilitzats en les fases adsorbents de sílice enllaçada [66].

Nomenclatura	Grup funcional	Estructura	Polaritat
C18	Octadecil (*Octadecyl*)	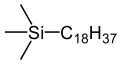	Apolar
C8	Octil (*Octyl*)	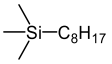	Apolar
C2	Etil (*Ethyl*)	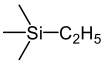	Apolar
CH	Ciclohexil (*Cyclohexyl*)	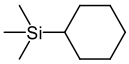	Apolar
PH	Fenil (*Phenyl*)	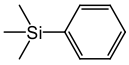	Apolar
CN	Cianopropil (*Cyanopropyl*)	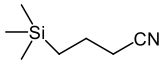	Polar
2OH	Diol	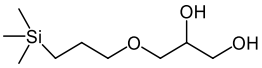	Polar
SI	Sílice (*Silica*)		Polar
NH2	Aminopropil (*Aminopropyl*)	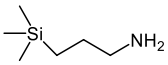	Polar
PSA	N-propil etilendiamina (*N-propylethylenediamine*)	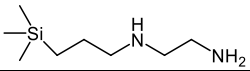	Polar

No obstant això, el major inconvenient d'aquestes fases és la seua baixa selectivitat, ja que retenen molts components de la matriu que posteriorment poden interferir en la determinació, principalment quan es tracta de mostres aquoses. Per aquest motiu, moltes de les alternatives que s'han anat proposant en les darreres dècades han anat en favor d'una retenció més selectiva dels anàlits que garantisca una major neteja.

Com s'ha dit, entre aquestes fases trobem també les de fase normal com és el cas de les fases de sílice, que també han anat evolucionant en els darrers temps cap a nous materials. És el cas dels cartutxos Florisil, compostos de silicat de magnesi, que també han estat aplicats en diverses ocasions per a la determinació de contaminants polars com és el cas dels PCBs [71].

3.2. Fases polimèriques

Dins dels cartutxos de fase reversa, en les darreres dècades han anat prenent protagonisme els materials polimèrics, principalment basats en el poliestiré-divinilbenzé (*poly(styrene-divinilbenzene), PS-DVB*), que poden presentar diverses estructures en funció dels monòmers utilitzats. Entre ells destaquen principalment els cartutxos Oasis HLB, formats per un copolímer macroporós que presenta un equilibri entre un monòmer lipòfil i un altre hidròfil, per la qual cosa es coneixen com fases d'equilibri hidròfil/lipòfil (*hydrophilic-lipophilic balanced, HLB*). Aquest equilibri li atorga propietats excel·lents per a l'adsorció de contaminants orgànics, ja que la part hidròfila contribueix a la humectació del material i afavoreix la transferència de massa, mentre que la part lipòfila ofereix una bona retenció dels anàlits orgànics. Així, aquestos materials es poden aplicar a la retenció d'un gran nombre de compostos dins d'un espectre de polaritats bastant ampli i en moltes matrius [72]. No obstant, aquesta característica comporta també una baixa selectivitat d'aquestes fases, fet que suposa el seu major inconvenient [62]. Així, aquestos cartutxos han estat aplicats per exemple a l'extracció de fàrmacs, productes de cura personal i hormones en sòls [73], a l'extracció de pesticides [74], o a la determinació de retardants de flama organofosforats en aigües mediambientals [5].

3.3. Adsorbents de bescanvi iònic

Altres fases adsorbents estesament utilitzades són les de bescanvi iònic, on una fase carregada reté selectivament els ions amb una determinada càrrega o polaritat. La base d'aquestos materials pot ser de sílice, encara que als últims anys han proliferat els cartutxos de tipus mixt amb una base polimèrica, i un grup funcional format per una cadena orgànica que acaba en alguna espècie carregada. Per altra banda, i depenent del grup funcional utilitzat, podem trobar fases de bescanvi aniònic carregades positivament, o de bescanvi catiònic. A més a més, depenent de l'espècie carregada poden ser fases de bescanvi fort o feble, donant lloc a cartutxos de bescanvi aniònic fort o feble (*strong or weak anionic exchange, SAX, WAX*) que contenen generalment amines quaternàries o secundàries respectivament, així com de bescanvi catiònic fort amb àcid sulfònic com a grup funcional (*strong cationic exchange, SCX)* o de bescanvi catiònic feble si conten àcids carboxílics (*weak cationic exchange, WCX*) [66,72]. Aquestes fases han estat menys utilitzades per a compostos orgànics atesa la seua apolaritat en termes generals, encara que sí que tenen un gran ús per a espècies molt polars o inclús carregades, principalment els d'interaccions iòniques dèbils. De fet, els cartutxos WAX han estat utilitzats en múltiples ocasions per a la retenció de PFASs en mostres aquoses, atés el seu caràcter majoritàriament iònic [5], o els WCX han sigut aplicats per exemple a la retenció d'antibiòtics com les fluoroquinolones en la seua forma protonada [75]. De manera similar, altres contaminants han sigut determinats amb aquestes fases com són els bisfenols o els corticosteroides en mostres alimentàries, o les toxines en mostres de sang [76].

Un cas particular de materials de bescanvi iònic serien també els hidròxids dobles en capes (*layered double hydroxides, LDHs*) que consten d'argiles aniòniques sintètiques formades per capes apilades d'hidròxids dobles de cations divalents i trivalents, amb anions hidratats dispersos entre elles. Aquesta estructura afavoreix l'intercanvi d'ions i la retenció d'espècies carregades tant orgàniques com inorgàniques. Si bé aquestos materials han estat utilitzats per a l'eliminació de contaminants, en els últims anys s'han començat a utilitzar també per al tractament de mostra, encara que de forma menys estesa, principalment degut als problemes en l'elució dels anàlits [1,56]. Entre alguns exemples, trobem estudis que han aplicat aquestos materials a l'adsorció i determinació d'àcids fenòlics en mostres de suc [77,78], o a la determinació de ftalats en aigües mediambientals [79].

3.4. Xarxes organometàl·liques

Les xarxes organometàl·liques (*metal-organic frameworks, MOFs*) han rebut una gran atenció en els últims anys en el camp de la química analítica pel seu ús per al tractament de mostra, i els estudis de la seua síntesi, caracterització i aplicacions han crescut de forma exponencial en els darrers anys [80,81]. Es tracta de polímers de coordinació porosos que es componen d'ions metàl·lics (*clusters*) units a connectors orgànics o *linkers*, i donen lloc a una xarxa de porositat molt alta i propietats úniques, com són la uniformitat de les cavitats, polaritat adaptable, bona estabilitat tèrmica i una alta àrea superficial d'entre 1000 i 10000 $m^2\ g^{-1}$. Totes aquestes propietats poden ser adaptables mitjançant l'ús de nous metalls o connectors, fet que ha propiciat la seua aplicació per a l'extracció d'una gran quantitat d'anàlits, principalment en la seua aplicació a tècniques miniaturitzades com l'SPME (utilitzats en la fabricació de les fibres d'extracció) o la dSPE, encara que en mètodes d'SPE convencional també s'utilitzen [81]. A la Figura 5 es poden veure, a tall d'exemple, les estructures simulades de diversos MOFs utilitzats per a la retenció de contaminants de diversa naturalesa [82].

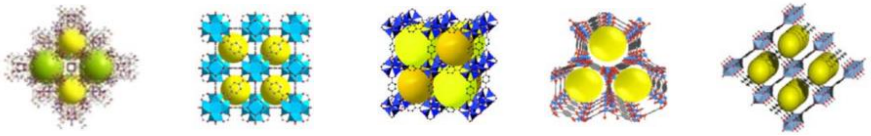

Figura 5. Simulació de l'estructura de diversos MOFs utilitzats per al tractament de mostra en la determinació de contaminants. Les esferes representen les cavitats disponibles per a la retenció dels anàlits. Figures prèviament publicades [82].

Així, a la bibliografia podem trobar un gran nombre de mètodes basats en la utilització de MOFs per a l'extracció de contaminants orgànics, sobretot pel que fa a l'anàlisi mediambiental o d'aliments com per exemple l'extracció d'OCPs [83]

o PCBs [84] en aigües mediambientals, la determinació de PAHs [85] o antibiòtics [86] en aigües i aliments, o la determinació d'EDCs com els bisfenols en mostres de suc i llet [87]. No obstant, també trobem aplicacions en el camp de l'anàlisi clínica com és el cas de la determinació de pesticides organofosforats en mostres de cabell o orina [88].

3.5. Materials basats en carboni

Els materials basats en carboni han estat utilitzats des de fa molts anys per a la retenció de contaminants ambientals, principalment per a la seua eliminació per adsorció, com per exemple alguns contaminants orgànics com productes farmacèutics [35], encara que també en diverses aplicacions en el tractament de mostra. Les propietats d'aquestos materials com són la gran capacitat d'adsorció, la seua gran estabilitat tèrmica, química i mecànica, i el seu baix cost han propiciat la seua aplicació com a fases adsorbents. En aquest sentit, el carbó actiu ha estat àmpliament emprat tant per a la retenció i determinació de contaminants orgànics com d'ions de metalls pesants [1]. Dins d'aquest grup de fases adsorbents destaca el grafit, un material natural i cristal·lí que també ha estat àmpliament aplicat a la cromatografia i SPE atesa la seua alta àrea superficial i capacitat d'adsorció. Aquest material ha donat lloc també a múltiples fases com són les de carboni grafititzat, comercialment denominades ENVI-Carb, àmpliament utilitzades per a l'anàlisi mediambiental i d'aliments [72], com per exemple en el *clean-up* per a la determinació de pesticides [89], compostos fenòlics [90], o PFASs en combinació amb els cartutxos WAX [91].

A més a més, totes les seues atractives propietats es van veure amplificades amb el descobriment del grafé (*G*), que és essencialment un capa única de grafit que dona lloc a una estructura planar d'un àtom de grossor, que pot formar interaccions molt fortes amb els anàlits gràcies als seus electrons π deslocalitzats. Aquest material ha estat també àmpliament modificat per tal de millorar les seues propietats com a fase adsorbent, principalment a partir del seu derivat l'òxid de grafé (*graphene oxide, GO*). Tant a partir de la funcionalització de la superfície del grafé com del GO, s'han desenvolupat tot tipus de materials, com per exemple a partir de l'addicció de nanopartícules magnètiques com òxids de ferro [1,56]. Tots aquestos materials han permés elaborar mètodes per a la determinació de contaminants orgànics com per exemple estròg ens [92], PAHs [93] i pesticides clorats [94] en aigües mediambientals, o micotoxines [95] i pesticides organofosforats [96] en mostres d'aliments.

Entre aquestos materials destaca també l'aparició en les últimes dècades dels nanotubs de carboni (*carbon nanotubes, CNTs*). Des del seu descobriment al 1991, els CNTs han estat emprats per a una gran varietat d'aplicacions, entre elles com a fases per a l'adsorció, purificació i preconcentració de compostos apolars en SPE. Aquestos poden ser utilitzats en el seu format d'una sola capa (*single-wall CNTs, SWCNTs*) o en format multicapa (*multi-wall CNTs, MWCNTs*). No obstant, aquestos materials presenten dos grans inconvenients, principalment pel que fa a

la seua aplicació en tècniques de dSPE com són la dificultat de dispersió i de recol·lecció després de l'extracció. Així, diverses funcionalitzacions han estat proposades per tal de pal·liar aquestos inconvenients, així com per tal d'ampliar el seu camp d'aplicació cap a compostos més polars [1,56]. A través d'aquestes modificacions, els CNTs han estat aplicats també a la determinació d'un gran nombre de contaminants orgànics com per exemple bisfenols en mostres de suc [97], PAHs en olis comestibles [98], o productes farmacèutics en mostres d'aigua [99]. A la Figura 6 es pot veure una representació esquemàtica de les estructures principals de tots aquestos nous materials basats en carboni.

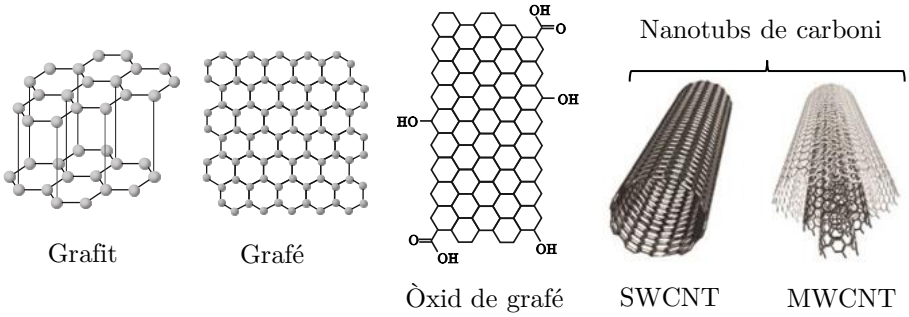

Figura 6. Esquema de les estructures dels principals nous materials amb base de carboni utilitzats per a l'extracció de contaminants orgànics [100].

3.6. Materials de reconeixement molecular

Els materials de reconeixement molecular han estat també de gran interès pel que fa a les seues aplicacions en adsorció, ja que es tracta de materials amb una alta selectivitat. Encara que aquestos materials poden ser de naturalesa molt diversa, tots ells presenten una resposta específica o molt selectiva cap a un anàlit o família d'anàlits determinada, fet que suposa un gran avantatge per al seu ús com a fases sòlides en SPE.

Per una banda, la utilització d'anticossos ha oferit grans resultats per a la retenció selectiva de certs compostos orgànics, donant lloc al que s'anomenen immunosorbents. Els immunosorbents es formen a partir de la immobilització d'anticossos, glicoproteïnes produïdes per un cos o una cèl·lula com a resposta a un antigen, sobre un suport sòlid com puga ser sílice, alúmina, o algun polímer. Així, aquestes fases fan ús de la interacció anticòs-antigen per oferir una interacció específica cap a una molècula determinada, permetent el tractament eficaç de grans quantitats de mostra, i assolint límits de detecció molt bons. No obstant, una de les limitacions més gran d'aquestos materials és la fabricació d'aquestos anticossos i el seu cost, ja que es requereix de cultius cel·lulars per a la seua obtenció. L'especificitat d'aquestos materials ha propiciat inclús la seua classificació com una tècnica d'SPE específica anomenada SPE d'immunoafinitat (*immunoaffinity SPE, IASPE*) [56,61]. Aquest tipus de cartutx és molt emprat principalment per a la determinació de micotoxines, ja que presenta una gran

selectivitat, encara que també s'utilitzen per determinar altres compostos com puguen ser hormones com l'estradiol [46,61].

En aquest sentit, podem trobar també els materials basats en aptàmers, bastant prometedors atés el seu baix cost, facilitat de preparació i estabilitat, a més de la selectivitat característica d'aquestos materials. Els aptàmers són cadenes d'oligonucleòtids, és a dir, fragments d'ADN o ARN, que presenten una estructura tridimensional específica amb plegaments que per la seua grandària i els grups funcionals disponibles presenten una gran selectivitat, similar a la dels anticossos, front una molècula determinada, que pot ser algun compost orgànic de grandària menuda. A la Figura 7 es pot veure un exemple d'un material que fa ús d'un aptàmer per a l'extracció i determinació d'aflatoxina B_2 en mostres d'aliments [101]. Aquesta gran selectivitat ha propiciat també la seua aplicació a la determinació de contaminants orgànics principalment en tècniques d'SPE miniaturitzades en l'anàlisi d'aliments [56,102], com puga ser la determinació de PCBs en peix [103] o aflatoxina M_1 en llet [104].

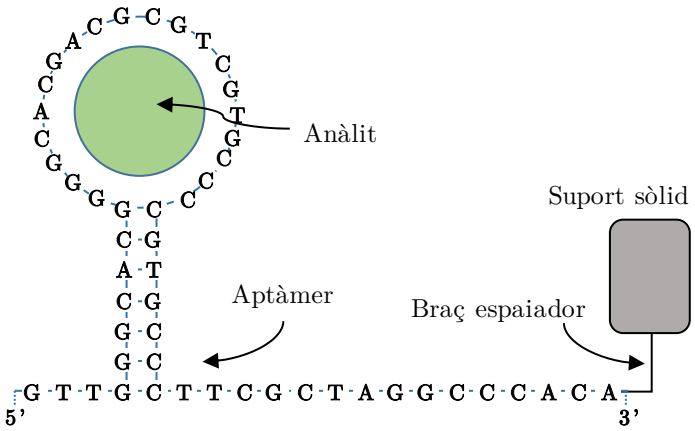

Figura 7. Esquema d'un material amb un aptàmer ancorat per a la retenció d'aflatoxina B_2 [101].

Per altra banda, els polímers de reconeixement molecular (*molecularly imprinted polymers, MIPs*) han rebut una gran atenció en les tècniques de detecció de residus, ja que són considerades com una de les fases més selectives que es poden utilitzar per a SPE. Aquestos polímers es preparen mitjançant la copolimerització d'un o més monòmers funcionals amb capacitat per interaccionar amb els anàlits, amb un agent entrecreuant, i en presència d'una molècula plantilla o *template*, molt similar a l'anàlit objectiu. Una vegada finalitzada la polimerització, la molècula plantilla s'extrau, donant lloc a cavitats que són llocs de reconeixement específic d'un anàlit diana, assegurant una gran selectivitat i especificitat [1,56]. Aquesta tècnica ha permés preparar MIPs amb cavitats selectives a un rang molt ampli de contaminants orgànics, donant lloc a mètodes

tant per a l'anàlisi d'aigües mediambientals, com per exemple en la determinació de bisfenol A [105], hormones [106] o compostos fenòlics [107], com per a la determinació de pesticides [108] o antibiòtics [109] en aliments.

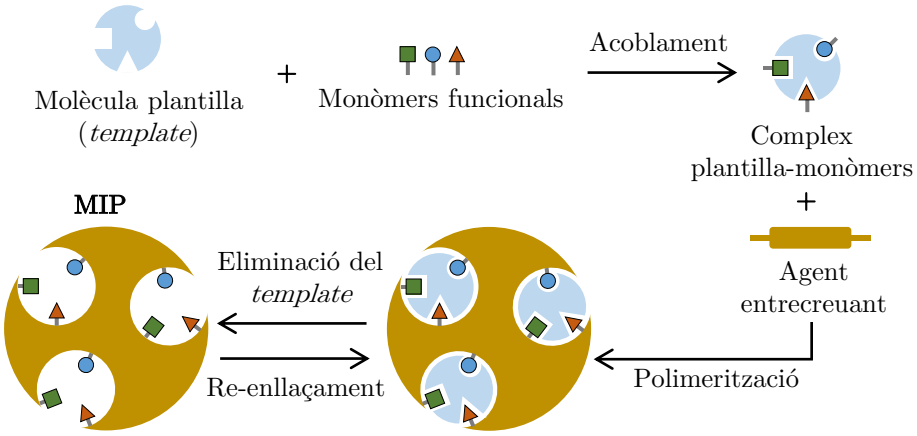

Figura 8. Esquema de la preparació i estructura d'un MIP [45].

3.7. Materials d'accés restringit

Els materials d'accés restringit (*restricted access materials, RAM*) presenten grans avantatges per a l'anàlisi de mostres amb matrius complexes en presència de macromolècules. Mitjançant l'ús de barreres hidròfiles i els mecanismes d'exclusió per grandària, permeten el pas cap als porus del material sols als compostos orgànics de grandària menuda, excloent altres macromolècules com les proteïnes. Aquestos materials han estat utilitzats principalment per a l'anàlisi de mostres d'aliments, on la presència de molècules molt grans com les proteïnes suposa un repte important en l'etapa de neteja de la matriu [56], com per exemple en aplicacions per a la determinació d'antibiòtics en llet [110], o per a la determinació de pesticides organofosforats en mostres de mel, en combinació amb un MIP [108].

3.8. Materials amb ciclodextrines

Les ciclodextrines (*cyclodextrins, CD*) són una família d'oligosacàrids cíclics obtinguts a partir de la unió de monòmers de glucosa. Gràcies a la seua forma de con truncat, són capaces de formar complexos d'inclusió amb molècules orgàniques menudes, depenent de la seua grandària i polaritat. Així, depenent del nombre de monòmers i, en conseqüència, de la seua grandària, es pot diferenciar entre la α-, β-, i γ-ciclodextrina, que junt a les seues formes modificades formen un conjunt de centres actius que poden ser utilitzats per a la retenció d'un gran nombre de compostos orgànics. De fet, en els últims anys han rebut una gran atenció per al tractament d'aigües residuals gràcies a les seues propietats fisicoquímiques, estabilitat química i excel·lent selectivitat per a determinats

contaminants. Això ha donat lloc també a la seua aplicació com a fases sòlides per a la preconcentració de contaminants, ancorant aquestes CDs a diversos suports, ja siguen amb base de sílice o polimèrica, per ser utilitzades com a centres actius per a l'adsorció en el tractament de mostra i determinació de contaminants orgànics en matrius mediambientals o d'aliments, o per a la determinació de fàrmacs en matrius biològiques. A més a més, els materials modificats amb CDs han estat utilitzats també per al desenvolupament de mostrejadors per a diversos contaminants orgànics volàtils [111].

3.9. Materials basats en sílice mesoporosa

Recentment, els materials mesoporosos han anat guanyant interés pel que fa al tractament de mostra gràcies a les seues favorables propietats com són l'alta àrea superficial, volums de porus molt grans, grandària i distribució dels porus modificable, i la possibilitat de modificar la seua superfície. A més a més, en concret els materials de sílice mesoporosa presenten una gran estabilitat tèrmica, química i mecànica [112]. Gràcies a totes aquestes propietats, aquestos materials han estat àmpliament utilitzats com a estructures selectives de grandària, permetent l'adsorció de molècules orgàniques tant menudes com grans, i han supost tres grans avantatges respecte dels materials microporosos: l'ordre de la seua xarxa de porus amb grandàries molt controlades, l'augment considerable en l'àrea superficial i el volum de porus, i una major estabilitat. En aquest sentit, l'interés d'aquestos materials es va veure incrementat amb l'aparició dels sòlids M41S de la Mobil Oil Corporation [113], que feien ús de surfactants durant la seua síntesi per tal d'obtenir una xarxa de mesoporus ordenada. De tots aquestos materials, l'MCM-41 ha sigut el més utilitzat per a diverses aplicacions com el tractament de mostra. A més a més, les àmplies possibilitats de funcionalització d'aquestos materials ha suposat la seua aplicació per a la retenció d'un gran nombre de contaminants, en diversos àmbits, no només de la MCM-41, sinó també de molts altres sòlids similars com el SBA-15 o l'UVM-7 [114–116]. Més endavant, al Capítol 1, es discutirà més àmpliament al voltant de les característiques i aplicacions analítiques més importants que s'han desenvolupat amb aquestos sòlids, ja que són els materials que vertebren aquesta tesi.

4. Fases adsorbents utilitzades per al mostreig de contaminants orgànics en aire

Encara que no s'emmarcaria estrictament dins de l'etapa del tractament de mostra, el mostreig de contaminants orgànics en aire també requereix del desenvolupament de materials que asseguren una retenció quantitativa dels compostos objectiu. En aquest sentit, i seguit el sistema de mostreig que s'ha explicat anteriorment, els filtres utilitzats per a recollir la fase particulada de l'aire són principalment els de fibra de vidre i els de fibra de quars, sent aquesta etapa més senzilla atés que es tracta d'una simple filtració de la matèria particulada

[18,65]. No obstant, la retenció dels contaminants en la fase gasosa comporta impediments més grans atesa la dificultat de trobar materials que permeten el mostreig de grans quantitats d'aire evitant la pèrdua dels anàlits.

En aquest sentit, un dels materials més utilitzats són les resines polimèriques de tipus XAD. Aquestos adsorbents universals consten de copolímers reticulats de poliestiré amb una alta superfície que poden interaccionar amb els anàlits mitjançant forces de Van der Waals i interaccions π-π amb els anells aromàtics. Entre aquestes, destaquen la resina XAD-2 molt utilitzada per al mostreig de pesticides, igual que la resina XAD-4, encara que en menor mesura [65,117]. Aquestes resines s'han utilitzat per al mostreig, no només a nivell mediambiental, sinó també per a l'avaluació de riscos laborals, sent el XAD-2 la fase recomanada en alguns mètodes oficials com els del NIOSH (*National Institute for Occupational Safety and Health*) [118]. De manera similar, altres resines estan recomanades també per al mostreig d'altres compostos com és el cas del XAD-7 per al mostreig de fenols [119].

Unes altres fases adsorbents àmpliament emprades són les Tenax, en especial el Tenax TA, una resina polimèrica porosa basada en l'òxid de 2,6-difenilfenol, especialment dissenyada per atrapar contaminants volàtils i semivolàtils en mostres d'aire. Aquestos materials han estat aplicats a la retenció de molts contaminants com els PAHs, i també han estat contemplats en diversos mètodes oficials com l'USEPA TO-17 [120] o l'IP-1B [121] per al mostreig i determinació de compostos orgànics volàtils [18], encara que tenen una major aplicació per a mostrejos de baix volum com en el cas de l'avaluació de riscos laborals [65].

A més a més, en el cas del mostreig mediambiental, alguns d'aquestos mètodes recomanen també la utilització de l'espuma de poliuretà (*polyurethane foam, PUF*), ja siga sola o en combinació amb altres materials com el XAD-2 o el Tenax TA. De fet, el PUF ha estat aplicat tant en mostrejadors actius com passius, no sols per a la determinació de pesticides, sinó també per al mostreig de tot tipus de POPs, com per exemple compostos clorats com els PCBs, ésters organofosforats, o altres compostos semivolàtils [65,122,123], i està recomanat també en alguns mètodes oficials de mostreig com l'USEPA TO-10A [124] .

Igualment, altres materials també s'han utilitzat per al mostreig de contaminants orgànics en aire, com són els tubs de polidimetilsiloxà (*polidimethylsiloxane, PDMS*), o els tubs reblerts de carboni actiu en distintes formes, com puguen ser el Carbopack C o el Tenax G [18].

OBJECTIVES AND WORKING PLAN

The main **objective** of this PhD Thesis is to evaluate the potential of UVM-7 materials as sorbents for the retention and extraction of organic pollutants and hazardous compounds, in order to develop analytical methods for their determination. As stated in the Introduction, the growing presence of contaminants in our daily life makes it necessary to find new materials that allow their reliable preconcentration and determination. Thus, the aim of this work is to address this important challenge of analytical chemistry.

UVM-7 materials were developed by a group of the Institute of Materials Science of the University of Valencia (ICMUV), starting from the emergence of mesoporous silicas thanks to the use of surfactants as templates to control their porous structure. Thus, the use of these materials for a wide variety of applications, mainly to catalysis, has been widely studied, although their analytical applications as sorbents have not been yet assessed. The aim of this work is to take profit from the excellent features of the hierarchical porous structure of these materials to develop sorbents for the efficient determination of organic hazardous compounds.

Hence, the objectives of the thesis can be divided as follows:

Objective 1. To synthesize blank UVM-7 materials with suitable porosity for the retention of aflatoxins from food samples. The bimodal porosity of the solid is expected to propitiate the retention of analytes thanks to size-exclusion mechanisms due to the mesopore and macropore size and distribution.

1.1. To determine the best strategy for the surfactant removal

1.2. To develop analytical methods for the determination of aflatoxins in aqueous food samples such as tea or milk with UVM-7 material.

1.3. To understand the role of the UVM-7 bimodal porous structure in the retention of aflatoxins through size-exclusion mechanisms and the interaction of the analytes with the silica.

Objective 2. To modify the UVM-7 structure with the addition of metals (M), namely Ti and Fe, through different strategies such as co-hydrolysis and impregnation, to enhance its selectivity towards organophosphorus compounds, and develop analytical methods for their determination. The interaction between Ti and Fe and phosphate groups are expected to lead to more selective retention.

2.1. To develop samplers containing the most appropriate M-UVM-7 materials for organophosphorus pesticides air sampling for occupational risk assessment.

2.2. To develop an SPE method for the extraction of organophosphorus pesticides from environmental water samples, by using the synthesized M-UVM-7 materials.

2.3. To develop SPE cartridges to enhance the extraction efficiencies of the organophosphorus flame retardants determination, in the case of the analysis of water samples.

Objective 3. To impregnate the UVM-7 structure with Au nanoparticles in order to obtain Au/UVM-7 materials that may be suitable for the selective retention of organochlorine compounds.

3.1. To develop an SPE method for organochlorine pesticides determination in environmental water samples.

3.2. To prove the interaction between chlorinated analytes and the Au nanoparticles of the material.

Objective 4. To apply the Fe-containing silica materials to the extraction of fluorine-containing organic compounds such as perfluoroalkyl substances, with the aim of developing an analytical method for their determination. Since these compounds present a huge variety in their chain length, the possibility of modifying the pore size of the material through the modification of the surfactant is also considered.

Objective 5. To develop a new material with the attachment of β-CD centers to the silica structure, to retain endocrine-disrupting chemicals. The ability of cyclodextrins to form host-guest complexes with aromatic compounds can lead to selective retention of endocrine-disrupting chemicals such as parabens or bisphenols.

5.1. To modify the UVM-7 synthesis procedure to achieve the β-CD incorporation.

5.2. To apply the developed β-CD-UVM-7 material to the design of an analytical method for the extraction and determination of parabens and bisphenol A in urine samples.

In order to achieve all these objectives, a general **working plan** has been designed, consisting of two differentiated parts: synthesis and characterization of silica materials, and application of these materials to the determination of organic hazardous compounds.

Synthesis and characterization of silica materials

Firstly, UVM-7 silica materials will be synthesized, either pure or modified with metallic heteroelements or organic functionalization. The versatility of sol-gel processes and the atrane route employed on UVM-7 synthesis allow the introduction of a wide variety of modifications in the solid structure. At this point, several modifications or aspects will be studied:

- Different strategies will be studied for surfactant removal, namely acidic extraction and calcination.
- The incorporation of Fe and Ti by co-hydrolysis with a modification of the same one-pot procedure will be studied.
- The incorporation of Ti by impregnation in a later step will be also considered in order to assess the best strategy.
- The modification of the pore size using different surfactants, simultaneously with the incorporation of metallic heteroelements will be also explored for the first time.
- The incorporation of Au nanoparticles to the UVM-7 structure will be also studied through an impregnation strategy, as well as the influence of the Ti in the attachment.
- The incorporation of CD will be also explored. For this purpose, the CD will be firstly functionalized with silane groups in order to obtain a UVM-7 material with the CD centers bonded to the silica structure.
- Metal-containing and CD-containing xerogels will be also synthesized for comparison. In the first case, the metal incorporation will be carried out by impregnation. Likewise, other porous silica materials with different structures will be synthetized also for comparative purposes.

Once all these solids will be synthesized their structure will be properly characterized to assess the influence of the different modifications introduced during the synthesis processes, understand their final structure and properties, and evaluate their potential abilities for organic pollutants retention. This characterization will be carried out by several techniques such as electron microscopy, energy-dispersive X-ray spectroscopy, X-ray diffraction, porosimetry and N_2 adsorption-desorption, nuclear magnetic resonance, Raman and UV-Vis spectroscopy, elemental analysis, or thermogravimetric analysis.

Application of the materials to the determination of organic compounds

Once the solids will be synthesized and characterized, they will be evaluated as sorbents for the retention of the target compounds, and the best material will be selected in each case to develop the analytical method. Thus, their application to extraction methods is considered for matrices such as water, food, and biological samples, as well as their use in the selective sampling step in air analysis. For this purpose, different cases should be taken into account:

- For air sampling methods, the optimization will be carried out through the contamination of the designed samplers, followed by air pumping through the material to simulate the sampling process, with the later extraction of the analytes from the material. Then, the analytical figures of merit will be assessed in the same way with optimized parameters.

- In the case of water samples, for the optimization steps, synthetic samples will be prepared. For the first steps, spiked ultrapure water will be used, whilst spiked real matrices will be considered for the next steps as well as for the analytical figures of merit evaluation.
- In the case of food and biological samples, previous steps will be also introduced when needed, such as a previous extraction or an enzyme deconjugation. These steps will be based on previous publications and reoptimized if necessary. Then, for SPE optimization, spiked ultrapure water will be used in the first steps, although real matrices will be used for the analytical figures of merit evaluation.

Apart from these considerations, the same general protocol will be applied in all studies for method optimization and evaluation:

1. Comparison among the developed materials in order to assess the best option for the method development. This comparison has also the aim of understanding the interaction between the material and the analytes, thus explaining the possible differences. After that, the best material will be selected in each case.
2. Optimization of the main analytical parameters of the protocol such as sorbent type and amount, solvent nature and volume for the desorption or elution, or sampling and loading conditions. After the optimization of the method, the main features will be described, such as the loading capacity, breakthrough volume, or reusability.
3. Description of the main analytical figures of merit of the developed method regarding sensitivity, linearity, repeatability, extraction efficiency, recoveries, and matrix effects.
4. Comparison of the main analytical parameters of the method with other similar methods previously reported in the literature, to assess the advantages and drawbacks of the protocol.
5. Application of the developed method to the analysis of real samples in comparison to a reference method, to ascertain its feasibility. In the cases where no target compounds are detected in none of the analyzed samples, the analysis of synthetic samples prepared by spiking real matrices will be considered.

With the exposed working plan all proposed objectives will be properly approached.

METHODS, RESULTS, AND DISCUSSION

SECTION A

Chapter 1

Synthesis of porous materials for analytical purposes

1. Introduction

From an analytical standpoint, an ideal solid-phase support for chemical applications includes several key properties such as large surface area, interconnected pores, an open framework, the ability to be doped with organic or inorganic reagents during synthesis or post-synthesis, mechanical and chemical stability, and feasibility of construction in terms of cost and time. In this sense, silica-based materials, and among them sol-gel-derived materials, meet many of these requirements, and therefore, they have been widely applied for a long time in the analytical chemistry field [112].

The interest in the sol-gel processing of inorganic ceramic and glass materials began as early as the mid-1800 and has experienced huge steps since then. Mainly in the XX century, a large number of novel ceramic oxide compositions were reported, as well as the commercial development of colloidal silica powder thanks to the work of Iler et al. [125]. Besides, Stöber et al. [126] extended Iler's findings using ammonia as a catalyst to control both the morphology and size of the powders, giving rise to the so-called Stöber spherical silica powder [127]. Since all these findings, the versatility of the usual low-temperature sol-gel processing has allowed its use for a wide variety of applications [112].

Sol-gel processing of silica is an intrinsically simple process that usually involves the hydrolysis of a silicon alkoxide precursor, and the catalytic polycondensation to produce a macromolecular network of siloxane bonds (Figure 9). Although less common aqueous silicates can also be used as precursors, tetramethyl orthosilicate (TMOS) and tetraethyl orthosilicate (TEOS) are the most widely used, jointly with a solvent to dissolve the precursor, a catalyst, and water [112].

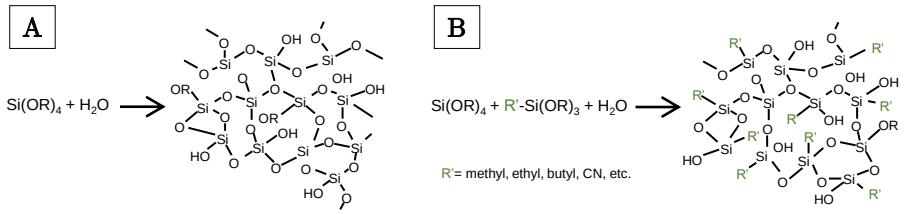

Figure 9. A simplified view of sol-gel processing of silica (A) and organosilica (B) [112].

Hence, although gel formation from alkoxides has been performed for more than 150 years, only in recent decades we have seen a revolution in the area of sol-gel-derived materials, concerning both our understanding of their properties and their applications to analytical chemistry. This increased prominence can be attributed, in part, to three significant factors: the ability to generate an almost infinite number of organic-inorganic hybrids, the fact that sol-gel-derived materials can be used to encapsulate biomolecules in a functional state, and the discovery of the supramolecular template approach, which can generate ordered mesostructures, as further discussed later. Besides, the sol-gel process also provides flexibility in controlling the shape and porosity of materials, their hydrophilic/hydrophobic balance, and most importantly, their chemical reactivity via a wide range of appropriate functionalization. Because of that, and among many other applications, porous sol-gel materials such as xerogels and aerogels have been used in several fields of analytical chemistry, and more concisely for the retention of organic compounds either as solid-phase, for separations sciences, sensors development, or electrode design [112].

In this sense, the porosity of these materials as analytical sorbents becomes crucial for most analytical applications particularly those that require analyte molecules to be separated and detected. An increase in the specific surface area of materials often enhances reactivity and improves recognition properties, which helps to ensure high sensitivities. Furthermore, wide-open structures are likely to impart more rapid mass transport. Because of that, in recent years, significant efforts have been made with the emergence of ordered mesoporous silicates prepared by the surfactant template route to further increase the porosity of these materials, from the specific surface areas of the silica gels ($S > 200$ m^2 g^{-1}), to surface areas above 1000 m^2 g^{-1} and pore sizes in the range of 1.5-10 nm [112].

This research on ordered mesoporous silica materials suffered a turning point by the discovery of the M41S silicas, firstly synthesized by the Mobil Research and Development Corporation, whose success was based on the use of long-chain quaternary ammonium surfactants as "structural directing agents" [113]. Since this publication, a large amount of related work was published in a very short time, as can be seen in Figure 10 [115]. Among them, MCM-41 is, by far, the most known material. This solid presents regular arrays of uniform channels, the dimensions of which can be tailored through the choice of the surfactant. This pore architecture has involved its application to analytical chemistry as sorbent and, more concisely, for sample treatment procedures. Thus, MCM-41 derivatives have been applied, for instance, to the trapping of VOCs from air samples for their determination [128], and also as SPE or µ-SPE sorbents for the extraction and determination of PFASs in environmental, food, and bioanalysis [129–131], for the extraction of pesticides from fruits [132], or functionalized with cyanopropyl groups for the determination of parabens and UV-filters in water [133]. Following the MCM-41, other mesoporous solids were also developed, most of them with a wide variety of analytical applications regarding analyte retention, and other SPE or miniaturized-SPE applications have been described. Some of them were based on SBA-15 solids, that have been used in food analysis for the determination of veterinary drugs such as steroids in meat or milk, for the extraction of EDCs or hormones from drinking waters, apart from other applications such as the design of sensors or HPLC stationary phases [114,134,135]. Finally, other mesoporous silica sorbents have been also employed in these fields, such as HMS or MCM-48 [114,136,137].

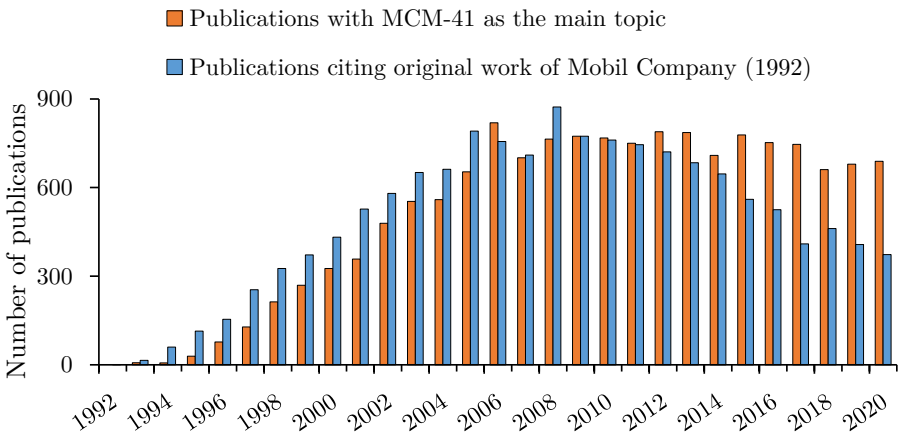

Figure 10. Evolution of the impact of MCM-41-related solids on the published content. Elaborated by the author from *Web of Science* data.

However, it has been argued that the periodic and unimodal mesoporous structure pore system of the M41S-related silicas, with narrow pore size distributions, could not offer specific advantages for certain applications such as

the retention of organic compounds, since the bulk materials might suffer from hindered accessibility to the active sites because of partial or total pore-blocking phenomena [116]. This drawback is also enhanced by the difficulties of introducing metal doping agents to their structure regarding the prediction of the amount of dopant incorporation, the reproduction of the mesophase of the pure silica system, and the stability of the resulting mesoporous material [115].

At this point, it seems important to state that, in practice, two different types of pathways can lead to the formation of mesostructured materials (Figure 11). On the one hand, in the route of the liquid-crystal templating mechanism (LCT) used in the synthesis of solids such as MCM-41, the inorganic phase grows and occupies the intermicellar space of a previously formed ordered organic mesophase ("supramolecular template") [113,138]. On the other hand, the other approach relies more on conventional colloid chemistry, where cooperative self-assembling procedures involve the formation of composite (inorganic-organic) micelles that organize to form particle nuclei that flocculate after a more or less lengthy growing stage. In opposition to the LCT approach, where very high surfactant amounts are used, in this case, surfactant concentrations around the critical micellar concentration (cmc) are considered. Thus, the principal synthetic advances in this field have resulted from developments of the chemistry that underlies the cooperative self-assembling processes at low surfactant concentrations [115]. However, in these cases, the starting organic precursor and their chemical features become essential tools for the search of new synthesis designs, as well as other parameters such as pH or temperature.

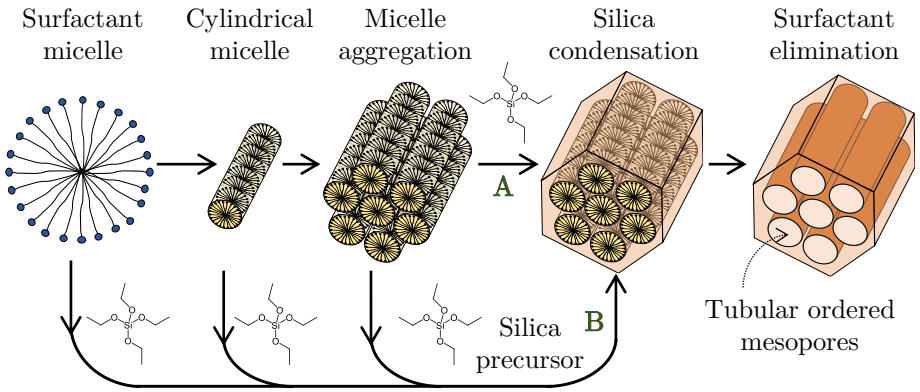

Figure 11. Schematic representation of the two possible synthesis pathways of surfactant-assisted mesoporous ordered silicas such as MCM-41: liquid-crystal phase initiated (A) and silicate anion initiated (B) [138].

In this sense, Cabrera et al. [115] described a generalized synthesis process to achieve ordered mesoporous silicas in combination with several heteroelements, thanks to the modification of the atrane route. In this process, triethanolamine (TEA) was proposed as an ideal ligand to harmonize the reactivity of the

corresponding precursors, forming atrane complexes simultaneously unstable and inert in an aqueous solution. Thus, the formation of atrane complexes that remain unchanged for long periods, leads to mesoporous metal-containing solids with high homogeneity, thus maintaining the silica mesostructure. Among all these solids, UVM-7 material (University of Valencia Material -7) [139] stands out due to its particular architecture consisting of a continuous silica framework constructed from soldered small mesoporous nanoparticles that generate a non-ordered system of large pores (between large-meso and macro), giving rise to a bimodal pore structure. This architecture has permitted its application to the retention of organic compounds in several fields, mainly in catalysis [140–142], or as nanocontainers [143,144]. Moreover, the synthesis procedure allows the introduction of metallic heteroelements through co-hydrolysis and co-condensation processes, leading to an M-UVM-7 structure [145,146]. In addition, other post-synthesis functionalizations have been reported, such as metallic impregnation [141,147], or the attachment of organic ligands such as amino or isocyanate groups, C18, or EDTA [148]. Otherwise, El Haskouri et al. [116] described the control of the pore size of these mesoporous solids through the modification of the surfactant, leading to similar solids with larger or smaller mesopores, being this an important feature for their application as solid phases. Also, other modifications have been introduced in the mentioned atrane route to obtain a wide variety of materials for different applications, such as UVM-11 material, synthesized in the absence of surfactant [149]. However, it should be noticed that the combination between the pore size modification and the introduction of metal heteroelements at the same time has not been yet studied.

Thanks to all these features, UVM-7 materials have been also applied as solid phases for the extraction and determination of several compounds. On the one hand, Shirkhanloo et al. reported numerous studies by using amino-functionalized UVM-7 material for the extraction and determination of several metal ions in both environmental and human urine samples, such as Pb (II), Ni (II), Cd (V), and the speciation between Cr (III) and (V), and As (III) and (V) [150–154]. On the other hand, regarding organic compounds determination, several sensors have been also developed with the functionalization of UVM-7 materials in the field of food analysis, for the quality control of turkey, pork sausages or chicken meat [155–157], or the detection of long-chain carboxylates [158], anionic compounds, or amines in water [159,160]. Moreover, the use of UVM-7 materials for the extraction and determination of phospholipids in human milk samples has been reported [161], as well as its employing for the designing of organo-silica hybrid monolithic columns for alkylbenzenes separation [162]. Also, Pérez-Cabero et al. [163] studied the adsorption properties of a carbon material synthesized by using this mesoporous silica as a template (C/UVM-7) for the retention of several pesticides in water solution, although no analytical method was developed. Thus, the UVM-7 application to the retention and preconcentration of organic hazardous compounds for analytical purposes has not been yet studied.

In other matters, as stated in the Introduction, cyclodextrins (CDs) are a family of cyclic oligosaccharides obtained from the binding of glucose monomers that have been also widely used for the retention of organic compounds in analytical applications. The natural occurrence of CDs can be classified into α-, β-, and γ-cyclodextrin, which are composed of 6, 7, and 8 glucose units respectively, thus increasing the diameter with the number of them (Figure 12). Due to their truncated-cone shape jointly with the orientation of their hydroxyl groups and their inside hydrophobic zone, they can form stable host-guest complexes with small organic compounds depending on the diameter of each type of CD. These features have positioned CDs as promising nanoscale carriers. Further, CDs can be modified, for instance by amination, esterification, or etherification of their hydroxyl groups in the external hydrophilic zone, which is an important tool to suit analytical applications [111,164].

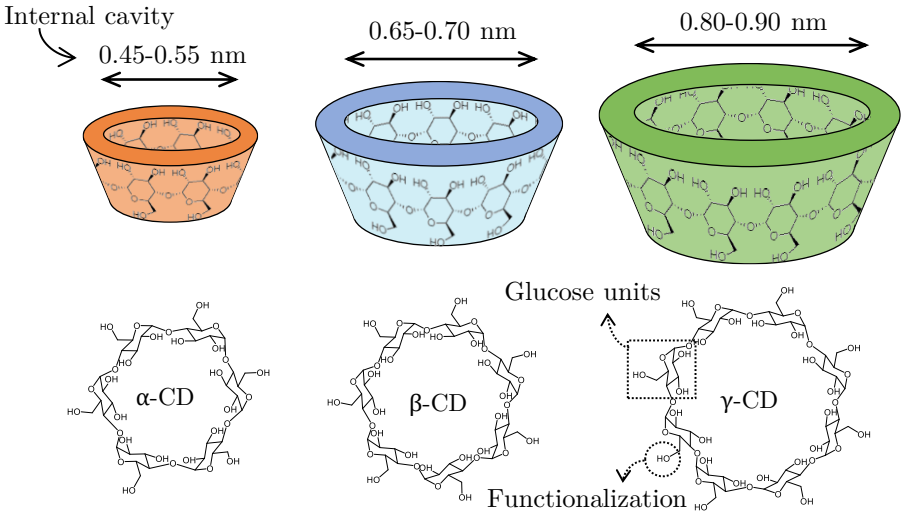

Figure 12. Schematic representation of the native α-, β-, and γ-cyclodextrin: molecular structure, shape, and internal cavity diameter [111].

Thus, several structures have been proposed for CD immobilization to use them as active centers for analyte retention, including polymeric supports, metal-organic frameworks (MOFs), or other complex nanocomposites, However, silica materials are one of the most used supports [111]. In this sense, a wide variety of CD-containing silica materials have been synthesized, both classical silica gel materials and through sol-gel chemistry strategies. These materials have been applied as solid phases for the preconcentration and clean-up of a wide variety of organic pollutants such as pesticides, pharmaceuticals, PAHs, phenolic compounds, or PCBs, in all kinds of environmental, food, and biological matrices [17,111,164–166]. However, substantially fewer studies have combined ordered and mesoporous silica with CDs as active centers for the retention of organic compounds for analytical purposes [111,164].

2. Synthesis of silica materials

2.1. Materials and reagents

For all synthesis of silica materials, both mesoporous materials and xerogels, all reagents were used in reagent grade: tetraethyl orthosilicate (TEOS), triethanolamine (TEA), tetrabutyl orthotitanate (TBOT), iron chloride (II) tetrahydrate ($FeCl_2 \cdot 4H_2O$), and titanium (IV) oxyacetylacetonate ($TiO(acac)_2$) were purchased from Fluka (Buchs, Switzerland), ethanol from VWR ProLabo Chemicals (Radnor, PA, USA), cetyl trimethylammonium bromide (C_{16}TAB) dodecyl trimethylammonium bromide (C_{12}TAB) and decyl trimethylammonium bromide (C_{10}TAB) from Sigma-Aldrich (St Louis, MO, USA), and $HAuCl_4$ hydrate from Strem Chemicals (Newburyport, MA, USA). Also, ultrapure water was obtained from an Adrona purification system (Riga, Latvia).

In the case of CD-containing silica materials, β- and γ-CD were purchased from Cyclolab (Budapest, Hungary). Dry pyridine from Panreac AppliChem (Darmstadt, Germany) and 3-isocyanatopropyltriethoxysilane from Sigma-Aldrich were also employed. Also, NaOH was purchased from Scharlab (Barcelona, Spain), and HCl from VWR Chemicals. A Büchi rotary evaporator (Flawil, Switzerland) and an Azbil Telstar LyoAlfa 10/15 lyophilizer (Shonan, Japan) were also used during the cyclodextrin functionalization.

2.2. Synthesis of mesoporous silica materials type UVM-7

The synthesis of UVM-7 materials was based on the procedure previously described, by a one-pot surfactant-assisted procedure, which is a modification of the so-called atrane route [115,139]. All pure UVM-7 silicas were prepared by the same general method and using the following molar ratios of reagents: 2 Si: 7 TEA: 0.5 C_{16}TAB: 180 H_2O. In a typical synthesis of UVM-7 pure silica, 25 mL of TEA were added to 11.2 mL of TEOS, and the mixture was warmed at 140 °C. Then, the mixture was allowed to cool at room temperature and 4.56 g of C_{16}TAB were added to the mixture at 120 °C. Subsequently, at 85 °C, 80 mL of water were slowly added under vigorous stirring. This mixture was aged at room temperature overnight and the resulting solid was collected by filtration, washed with water and ethanol, and dried with vacuum. To prepare the final mesoporous material, the surfactant was removed either by calcination at 550 °C for 5 h, leading to calcined UVM-7, or by acid extraction, giving rise to extracted UVM-7. In this case, 100 mL of ethanol and 8.5 mL of HCl 37% were added for each gram of the synthesized material and mixed under vigorous stirring at 60 °C for 12 h. The general synthesis procedure for UVM-7 materials is schematized in Figure 13, as well as its modification for the addition of metallic heteroelements and cyclodextrins by co-hydrolysis, as explained below.

Heteroelement (M) incorporation in UVM-7 was achieved by simply adding variable amounts of the respective metallic precursor to the first silatrane-containing solution, and following the procedure described above [145]. In that case, and depending on the desired Si/M molar ratio, the proportion of the reagents was modified as follows: 2-x Si: x M: 7 TEA: 0.5 C_{16}TAB: 180 H_2O. In the case of Ti-containing solids, amounts of 0.17, 0.33, 0.65, 1.55, and 2.84 mL of tetrabutyl orthotitanate were added in order to prepare materials with a Si/Ti nominal molar ratio of 100, 50, 25, 10, and 5 respectively, named as Ti-UVM-7 materials. Likewise, in the case of solids with iron, $FeCl_2 \cdot 4H_2O$ were added to the initial mixture to obtain UVM-7 materials with a Si/Fe nominal molar ratio of 100, 50, 25, and 10 (0.095, 0.19, 0.38, and 0.95 g respectively), leading to Fe-UVM-7 solids. For all these M-UVM-7 materials, surfactant removal was carried out by calcination.

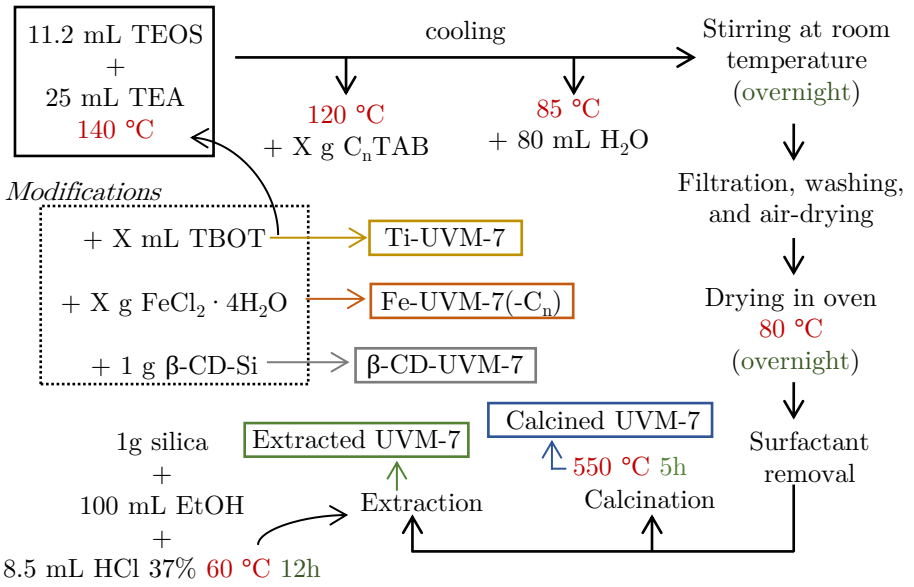

Figure 13. Schematic representation of the synthesis procedure of UVM-7 materials, either blank or modified by co-hydrolysis.

In this last case, the modification of the mesopore size was also explored simultaneously with the iron incorporation (with a Si/Fe molar ratio of 50 in all cases). For this purpose, and according to previous publications, surfactants with shorter tail lengths were used, namely C_{12}TAB and C_{10}TAB [116]. It should be noted that, in order to maintain the nanometric size of the primary UVM-7 particles, and according to the discussion previously exposed in the introduction of this Chapter, it is mandatory to increase in a significant way the amount of surfactant as its tail length decreases according to their respective cmc values. In this way, the synthesis strategy guarantees in all cases (surfactants) the presence of similar and adequate concentrations of micelles in the solution. Thus, regardless of the surfactant used, a very rapid nucleation process of UVM-7 type

nanoparticles takes place followed by limited growth. Hence, the desired materials were obtained following the previously described synthesis for C_{16}TAB (Figure 13) and preserving the previously molar ratio of the reagents except for the surfactant value: 1.96 Si: 0.04 Fe: 7 TEA: m C_nTAB: 180 H_2O (m= 4.2 and 16.7 for C_{12}TAB and C_{10}TAB, respectively). In those cases, when de differentiation among the surfactants used in the synthesis is needed, it was stated in the solid nomenclature (Fe50-UVM-7-C_{16}, Fe50-UVM-7-C_{12}, and Fe50-UVM-7-C_{10}).

For comparison, titanium incorporation was also carried out by impregnation in a later step, following the procedure previously described [141]. For this purpose, the ratio Ti/(Ti+SiO_2) was considered as 3.7 wt%. For the modification, 200 mL of deionized water were slowly added to a solution of 200 mL of ethanol containing 0.8 g of $TiO(acac)_2$. Then, 2.4 g of UVM-7 silica were added, and the mixture was aged under stirring for 2 h. After filtration, the resulting powder was washed with water and ethanol, dried at 80 °C overnight, and calcined at 300 °C for 5 h. In this case, the resulting solid was named as TiO_2-UVM-7 (see Figure 14).

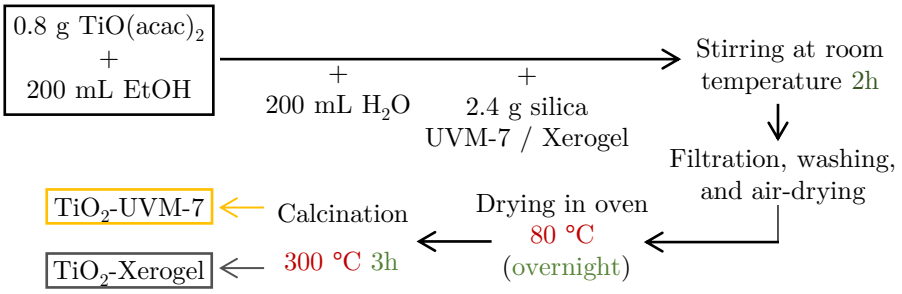

Figure 14. Schematic representation of the experimental procedure for titanium impregnation of silica materials.

On the other hand, and because of the impossibility of adding Au nanoparticles by co-hydrolysis during UVM-7 synthesis as already explained for the titanium or iron incorporation, the impregnation in a later step was also considered. In this sense, based on previous works [147], the inefficiency of Au deposition on silica surfaces was solved by adding titanium to the structure. Thus, Au-containing sorbents were synthesized starting from the already described Ti-UVM-7 solids. In these solids, small nano or subnanodomains of TiO_2 can be formed, thus becoming fixing centers for the Au impregnation and favoring its attachment. The Au impregnation procedure was based on previous works [167], as shown in Figure 15. Briefly, 0.38 g of $HAuCl_4$ hydrate were solved in 220 mL of ultrapure water, and the solution was heated at 70 °C in a water bath, wrapped in aluminum foil to prevent light degradation. The initial acidic pH (around 2) was slowly neutralized until pH 7 by drop-wise addition of NaOH 0.1 M. When pH was constant for 30 min, 2.5 g of desired blank or Ti-containing UVM-7 material were

dispersed in the solution. pH variations observed in the acidic region (pH 5-6) were adjusted with NaOH 0.1 M until pH was constant for 15 min. Then, the suspension was stirred for 1 h at the same temperature. After that, it was cooled, filtered, and washed with ultrapure water. The resulting powder was dried in the oven at 80 °C overnight and stored at 4 °C protected from light. Thus, several Au-containing materials were synthesized either with blank UVM-7 or Ti-containing silica materials with Si/Ti molar ratios of 50 and 5, leading to Au/Ti-UVM-7 materials.

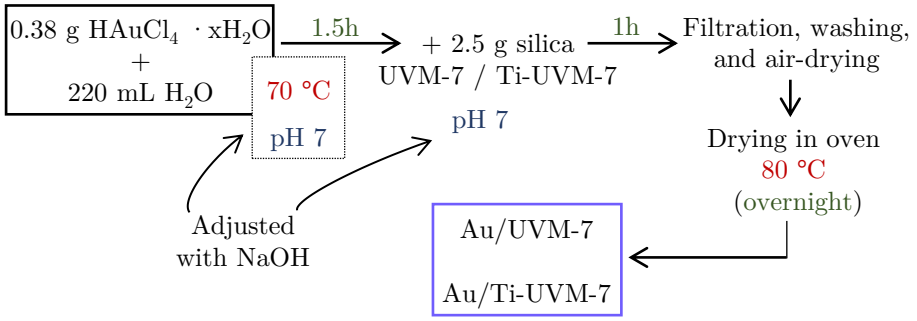

Figure 15. Schematic representation of the experimental procedure for gold impregnation of silica materials.

Finally, UVM-7 materials containing cyclodextrins as active sites were also synthesized for the first time. For this, β-CD was previously functionalized according to the procedure described by Mahmud and Wilson [168] (Figure 16). For this purpose, 9.3 mL of 3-isocyantopropyltriethoxysilane were added to a stirred solution of 10.7 g of lyophilized β-CD in 132 mL of dry pyridine. The solution was stirred at 70 °C for 48 h under an N_2 atmosphere. Once the reaction was finished, the solvent was rotary evaporated and the reagent (CD-Si) isolated.

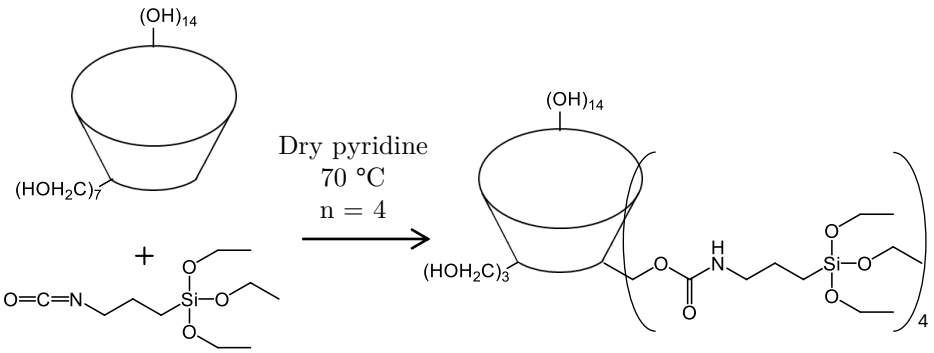

Figure 16. Schematic representation of the functionalization reaction of β-CD [168].

Once the cyclodextrin was modified with silane groups, hierarchical porous silica with UVM-7 structure was synthesized through a modification of the previously described one-pot procedure (Figure 13). In this case, he molar ratio of the reagents was modified as 2-x Si: x CD: 7 TEA: 0.5 C_{16}TAB: 180 H_2O (x = 0.02, that corresponds to a TEOS:β-CD = 99:1 ratio). The synthesis procedure was modified as follows: 0.96 g of functionalized β-CD (β-CD-Si) was solved in 10.6 mL of TEA at 140 °C. On the other hand, TEOS (10 mL) was mixed with the rest of the TEA (10.6 mL) at 140 °C until homogeneous solution. Then, both solutions were mixed at 140 °C and let cool at room temperature. Next, the procedure was continued as same as in the pure UVM-7 synthesis, by adding 4.15 g of C_{16}TAB at 120 °C. The silane hydrolysis and silica framework formation were achieved by adding 73.7 mL of ultrapure water at 85 °C. The final mixture was vigorously stirred at room temperature overnight, and the resulting powder was filtered, washed with water and ethanol to remove any free surfactant, and dried in the oven at 80 °C. Then, the surfactant removal was achieved through the same acidic extraction previously described.

2.3. Synthesis of other silica materials for comparative purposes

The synthesis of xerogel materials was carried out according to a modification of previous works [166]. Thus, 40 mL of deionized water were mixed with 32 mL of TEOS at pH 1.7, adjusted with diluted hydrochloric acid. After 2 h of stirring at room temperature, the hydrolysis and condensation of the silicon alkoxide are produced. Then, the mixture was allowed to dry for 24 h to evaporate the ethanol generated in the hydrolysis and favor the condensation. The formed xerogel was dried at 40 °C for another 24 h, triturated, and sieved below 600 µm.

This xerogel material was also modified by the incorporation of titanium by impregnation at the same Ti/(Ti+SiO_2) ratio as before (3.7 wt%). Thus, the same procedure described above was followed, but using 2.4 g of the xerogel instead of UVM-7 silica and resulting in the TiO_2-Xerogel material.

Besides, xerogel materials containing cyclodextrins were also synthesized, with the attachment of the functionalized CDs, also through a co-hydrolysis process. In this case, the stoichiometry of the materials followed the general formula: $(CD)_xSiO_{1.5}(OH)_{0.5} \cdot 0.7H_2O$, where the x value depends, among other parameters, on the CD type. After CD functionalization as described above, 40 mL of a 0.015 M solution of the modified sugar was added to the desired amount of TEOS. The hydrolysis and co-condensation processes were achieved in the same condition as described for pure xerogels, thus obtaining β-CD-Xerogel and γ-CD-Xerogel materials. Finally, materials were washed with ultrapure water before their use in order to remove the formed NaCl during pH adjustment.

Finally, other silica materials were synthesized for comparison. Firstly, UVM-11 material was synthesized following the procedure previously described [149]. In this case, the same procedure as for the UVM-7 synthesis was used, except for the absence of any surfactant, in order to achieve a similar solid to the UVM-7

with the absence of the mesopores. Hence, in this case, the molar relation of the reagents was modified as 1 Si: 2 TEA: 30 H_2O. Briefly, 33.1 mL of TEOS were added to liquid 39.3 mL of TEA and heated at 150 °C for 5 min. The resulting solution was cooled down to 80 °C and 80 mL of water were added while stirring. After a few hours, the obtained transparent gel was hydrothermally treated at 175 °C for 24 h to modulate both the particle and pore sizes.

On the other hand, Stöber spherical particles were also synthesized, either massive or mesoporous, by following the well-known procedure previously described [126], and using ammonia as a catalyst during the tetraalkyl silicate hydrolysis and condensation.

3. Instrumental characterization of the synthesized materials

The structure of the synthesized materials was characterized by several instrumental techniques, in order to assess their suitability for the desired analytical purposes.

Firstly, all materials were characterized by electron microscopy techniques, mainly transmission electron microscopy (TEM), by using a Jeol (Tokyo, Japan) model JEM-1010 microscope operating at 200 kV. In these cases, a MegaView III camera was used for obtaining images provided with the AnalySIS image data acquisition system. On the other hand, high-resolution transmission electron micrographs (HRTEM) were also acquired in some cases with a Jeol-2100F microscope operating at 200 kV. Also, for the Au incorporation evaluation in Au-UVM-7 and Au/Ti-UVM-7 materials, scanning transmission electron microscopy—high-angle annular dark-field (STEM-HAADF) images were obtained with the same equipment.

Moreover, the metal content of metal-containing synthesized solids was assessed by energy-dispersive X-ray spectroscopy (EDX), using either a Philips XL30 ESEM (Amsterdam, Netherlands) or a Hitachi S-4800 (Chiyoda, Japan) scanning electron microscope.

The silica porous architecture of the materials was also evaluated by X-ray diffraction (XRD) with either a Seifert 3000TT θ-θ diffractometer (Massillon, OH, USA) or a Bruker D8 Advance diffractometer (Billerica, Massachusetts, USA) operating at 40 kV and 40 mA. In both cases, a CuKα monochromatic source was used for obtaining de X-ray diffractograms. Patterns at the low-angle range were collected in steps of 0.02° (2θ) over the angular range 1–10° (2θ), with an acquisition time of 10 s per step. Additionally, patterns were recorded over a wider angular range, 10-80° (2θ) to determine the presence of segregated crystalline phases.

Moreover, the porosity was also evaluated with the recording of the N_2 adsorption-desorption isotherms at 77 K with a Micrometrics ASAP2010

automated sorption analyzer (Norcross, GA, USA). Samples were degassed at 90 °C in a vacuum overnight. Specific surface areas were calculated from the adsorption data in the low-pressure range using the Brunauer-Emmett-Teller (BET) model. Pore size was determined following the Barrett-Joyner-Halenda (BJH) method.

For the evaluation of Ti and Fe centers in M-UVM-7 materials, their Raman spectra were also obtained. For this, a Horiba Jobin Yvon iHR320 spectrometer (Kyoto, Japan) with Peltier-cooled CCD and a 532 nm and 785 nm doubled YAG laser excitation source was used, as well as a Horiba-MTB Xplora equipment, using a 785 nm laser excitation source. Room-temperature diffuse reflectance spectra were also recorded using a Shimadzu UV-Vis 2501PC spectrophotometer (Kyoto, Japan).

For nuclear magnetic resonance (NMR) studies, ^{29}Si and ^{13}C spectra were measured with a Bruker Avance III 400 MHz and a Varian Unity 300 MHz instruments, both operating in magic angle spinning (MAS) mode.

Besides, the organic content in the functionalized samples (CD-UVM-7 material) was determined by elemental CNH analysis, with an elemental analyzer CHNS1100 of CE Instruments Ltd. (Hindley Green, United Kingdom). This determination was confirmed through thermal gravimetric analysis (TGA) by using a Setaram Setsys 16/18 thermobalance (Setaram Instrumentation, Caluire-et-Cuire, France) working under an air atmosphere flowing at 25 mL min^{-1} (heating rate of 5 °C min^{-1}). In order to appreciate the homogeneous CD distribution, we used a confocal microscopy Olympus FV1000 (Tokyo, Japan). For this study, difluoro{2-[1-(3,5-dimethyl-2H-pyrrol-2-ylidene-N)ethyl]3,5-dimethyl-1H-pyrrolato-N}boron (Bodipy-Me) was purchased from Sigma-Aldrich, and dimethylformamide (DMF) from Alfa Aesar (Haverhill, MA, USA).

4. Conclusions

The synthesis of several UVM-7-type silicas has been presented here, including their functionalization with the addition of metals through different procedures, as well as organic centers such as cyclodextrins. Thanks to the so-called “atrane route”, the presented one-pot procedure is expected to lead to a hierarchical porosity in the final material, as will be characterized through the described techniques.

Besides, the synthesis of other comparative solids has been also presented, embracing materials with different porosity that will allow understanding the retention mechanisms in the UVM-7 materials. Also, in order to assess the role of each functionalization strategy, the incorporation of metals and organic ligands has been also considered for these comparative silicas.

SECTION B

Chapter 2

Characterization of UVM-7 materials and other comparative porous silicas

1. Introduction

In this chapter, the silica structure of synthesized pure UVM-7 materials is presented. As stated, these materials can be considered as a nanometric version of the well-known MCM-41 silicas [113], with an architecture consisting of a continuous network constructed from aggregated mesoporous nanoparticles. As explained in the synthesis part (Chapter 1), the use of the surfactant C_{16}TAB as a template in the modification of the atrane route is expected to lead to bimodal porous silica with a high surface area [115]. Moreover, the effect of the two surfactant elimination strategies explored during the synthesis in the final solid features is also studied in this Chapter.

For comparative purposes, the structure of other synthesized silica solids (Chapter 1) is also studied in this part, according also to their expected features as sorbents. On the one hand, the effect of the non-surfactant-assisted synthesis process in the UVM-11 material is assessed [149]. On the other hand, Stöber spherical particles, both massive or mesoporous are also presented, in order to confirm their typical structure [126].

2. Characterization of porous silica materials

Firstly, TEM micrographs were obtained for UVM-7 materials, showing the continuous silica network constructed from aggregated small mesoporous nanoparticles (Figure 17).

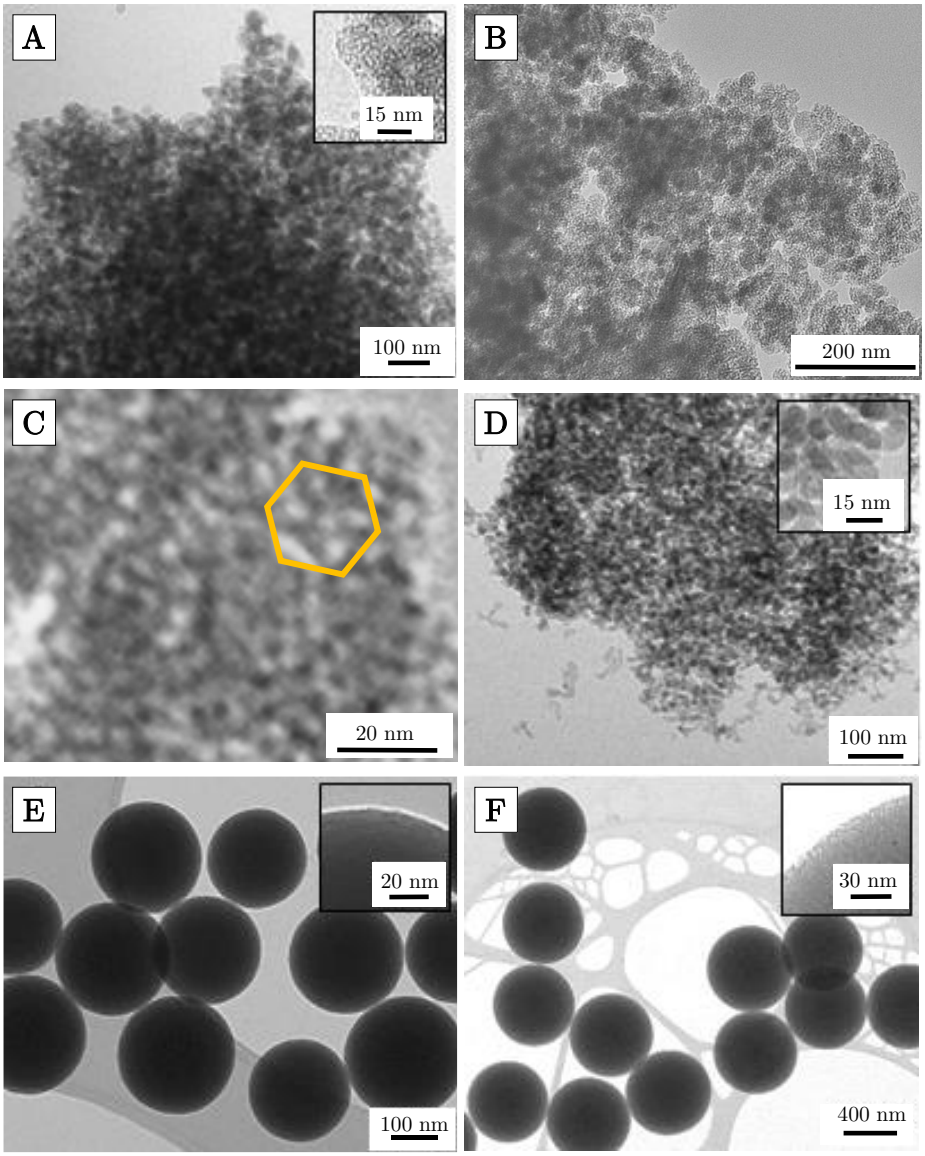

Figure 17. Representative TEM images in different zones or regions of the UVM-7 material (A, B, C), in different magnification, and other silica materials used for the comparison and study of the aflatoxin retention: UVM-11 (D), massive Stöber spherical particles (E), and mesoporous Stöber spherical particles (F). Images obtained with Jeol JEM-1010 microscope.

These observations confirm its framework combining large interparticle non-ordered macropores and intraparticle mesopores showing a hexagonal disordered array, as shown in Figure 17C.

In order to understand the influence of the porosity on the aflatoxin retention, three other silica materials (with different porous systems and morphologies) such as UVM-11 material and Stöber spherical particles were tested as SPE sorbents, as later described. These materials were also characterized by TEM. As can be seen in Figure 17, UVM-11 material presents a continuous silica network constructed from aggregated small solid nanoparticles. This results in an architecture similar to UVM-7 materials, with the presence of non-ordered large pores and the absence of the mesopores, as can be confirmed in the inset of Figure 17D. Likewise, the spherical structure of Stöber particles was observed, either in the massive silica spheres (Figure 17E) or with the presence of mesopores, depicted in the inset of Figure 17F.

Besides, the surface area and pore size distribution of the prepared mesoporous materials were also determined from the nitrogen adsorption-desorption isotherms (Figure 18). In the case of UVM-7 silicas, two adsorption steps were evidenced in both calcined and extracted material. The first, at intermediate partial pressures ($0.1 < P/P_0 < 0.4$), is due to capillary condensation of N_2 inside the intrananoparticle mesopores. The second step, at high relative pressure ($P/P_0 > 0.8$), corresponds to the filling of the large interparticle pores. This confirms their bimodal network and its great accessibility.

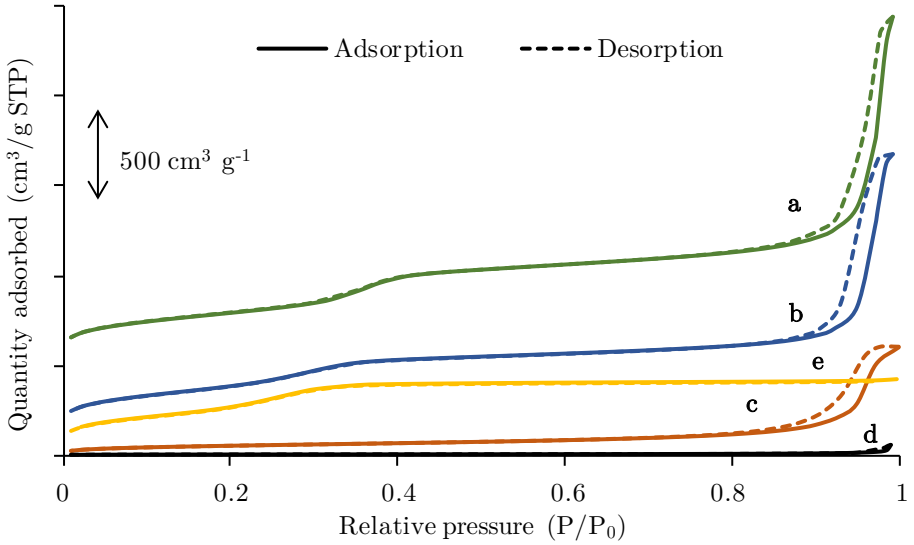

Figure 18. N_2 adsorption-desorption isotherms of the synthesized silica materials: extracted UVM-7 (a), calcined UVM-7 (b), UVM-11 (c), massive Stöber spherical particles (d), and mesoporous Stöber spherical particles (e).

Regarding their textural parameters, although the cell contraction previously highlighted on the calcined material also affects in a subtle way the nitrogen adsorption-desorption isotherms, both silicas, chemically extracted and calcined, show very similar porosity. As can be seen in Table 3, the existence of mesopores (2.67-2.87 nm) and large macropores (44.8-45.5 nm) confirm their bimodal porosity and high surface areas.

The other synthesized silica materials were also compared in terms of their adsorption-desorption isotherms and porosity data (Figure 18 and Table 3). As can be seen, the presence of macropores was confirmed in UVM-11 solid, as well as the availability of mesopores in mesoporous Stöber spheres. It should be noted that the presence of mesopores on these particles causes a significant increase in the surface area available for retention (from 19 to 976 $m^2\ g^{-1}$). In the same way, the absence of mesopores in UVM-11 material entails a significant surface area decrease in comparison with UVM-7, which is expected to affect the retention of analytes.

At the sight of these results, it should be highlighted the presence of the bimodal porosity of the UVM-7 materials, in comparison with the unimodal porosity observed in the UVM-11 and mesoporous Stöber particles (being its single pore size in the macro and meso range respectively) and also with the absence of any porosity in the case of massive Stöber particles.

Table 3. Selected physical parameters of UVM-7, UVM-11, and Stöber (mesoporous and massive) solids.

Material	Particle size[a] (nm)	Surface area[b] ($m^2\ g^{-1}$)	Mesopores		Macropores	
			Pore size[c] (nm)	Pore volume[c] ($cm^3\ g^{-1}$)	Pore size[c] (nm)	Pore volume[c] ($cm^3\ g^{-1}$)
Extd. UVM-7	36	1058	2.87	0.99	45.5	1.91
Calcd. UVM-7		1033	2.67	0.83	44.8	1.71
UVM-11	19	216	-	-	28.5	0.94
Massive Stöber particles	199	19	-	-	-	-
Mesoporous Stöber particles	580	976	2.45	0.73	-	-

[a]Determined by TEM

[b]Surface area estimated according to the BET model

[c]Pore sizes and volumes calculated using the BJH method from the adsorption branch of the isotherms. Intra-particle pores ($P/P_0 < 0.7$). Inter-particle pores ($P/P_0 > 0.7$)

Moreover, XRD patterns of synthesized materials were taken. As expected, none of the materials provided X-ray diffractograms with signals in the high angle domain, due to the amorphous nature of the silica-rich pore walls of all the solids. However, in the case of calcined and extracted UVM-7 (Figure 19), a broad signal at low angles (2° (2θ)), and a shoulder at ca. 3-4° (2θ) were observed, that can be associated with the (100) and the overlapped (110) and (200) reflections of an MCM-41-like hexagonal cell, respectively. These patterns are characteristic of hexagonal disordered mesoporous UVM-7 materials, and they only inform us about the existence of the intraparticle mesoporous system. Thus, similar diffractograms were obtained for both materials, except for a slight shift of this peak towards higher 2θ values, due to cell contraction associated with the increase in the condensation degree of the silica walls by calcination. As also observed in this figure, the presence of mesopores on the mesoporous Stöber particles was also confirmed with a similar broad peak, whereas the absence of any order in the porosity of massive spheres and UVM-11 materials lead to planar X-ray diffractograms.

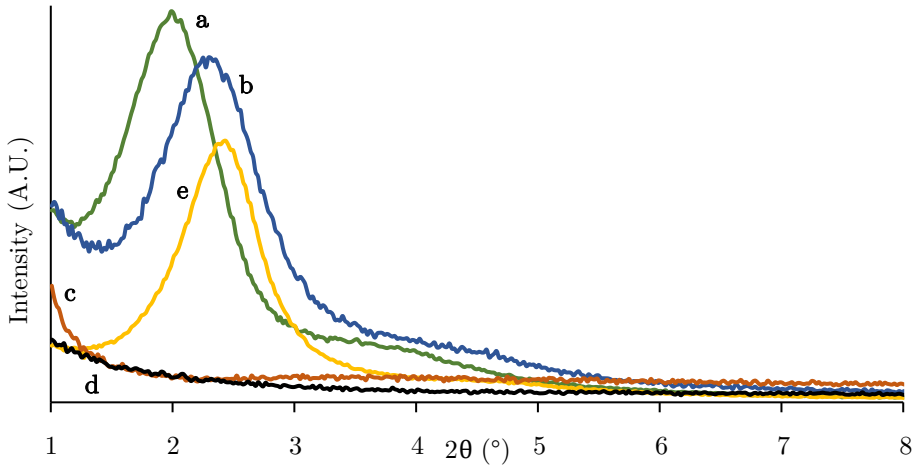

Figure 19. X-ray diffractograms of synthesized silica materials, obtained from CuKα radiation: extracted UVM-7 (a), calcined UVM-7 (b), UVM-11 (c), massive Stöber spherical particles (d), and mesoporous Stöber spherical particles (e). Obtained with Seifert 3000TT θ-θ diffractometer.

Finally, ^{29}Si NMR MAS spectra were obtained for both UVM-7 materials. As shown in Figure 20, an important decrease in Q^3 centers ($Si(OSi)_3(OH)$), and Q^2 centers ($Si(OSi)_2(OH)_2$) to a lesser extent, compared to Q^4 centers ($Si(OSi)_4$), were observed in calcined material, due to the formation of siloxane linkages during the calcination process at high temperature, thus entailing a greater presence of silanol groups in the material surface. This effect leads to a significant variation in the $Q^4/(Q^2+Q^3)$ ratio, being it of 1.4 and 2.8 for the chemically extracted and calcined samples, respectively.

Then, although the surfactant elimination method used does not affect the mesostructured architecture (only assumes a slight contraction of the cell observed in the position of the diffraction peak), it has an important effect on the surface nature due to changes in the condensation degree. Hence, the surfactant elimination process determines the density of silanol groups and, in consequence, its greater or lesser hydrophilic character and its ability to interact through hydrogen bonds with guest species.

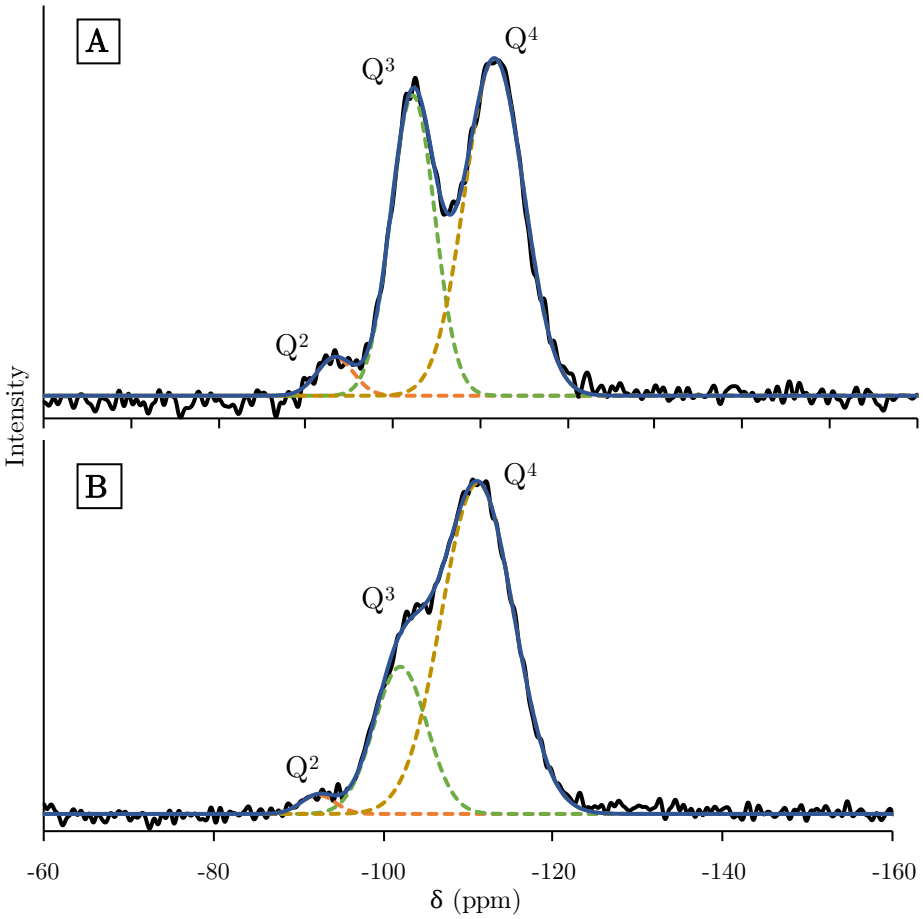

Figure 20. ^{29}Si NMR MAS spectra of extracted (A) and calcined (B) UVM-7, and its deconvolution in Q^2, Q^3 and Q^4 peaks. Obtained with Varian Unity 300 MHz spectrometer.

3. Conclusions

The typical UVM-7 structure was confirmed for synthesized materials. Both extracted and calcined materials have proved to present a hierarchical porosity with a continuous silica network constructed from aggregated small mesoporous nanoparticles, leading to a high surface area and mesoporous sizes in the range of 2-3 nm, which are expected to present good features for small organic compounds retention. The only difference between both materials is confirmed to be the density of silanol groups, significantly higher in extracted material, which can play a key role in the interaction with analytes.

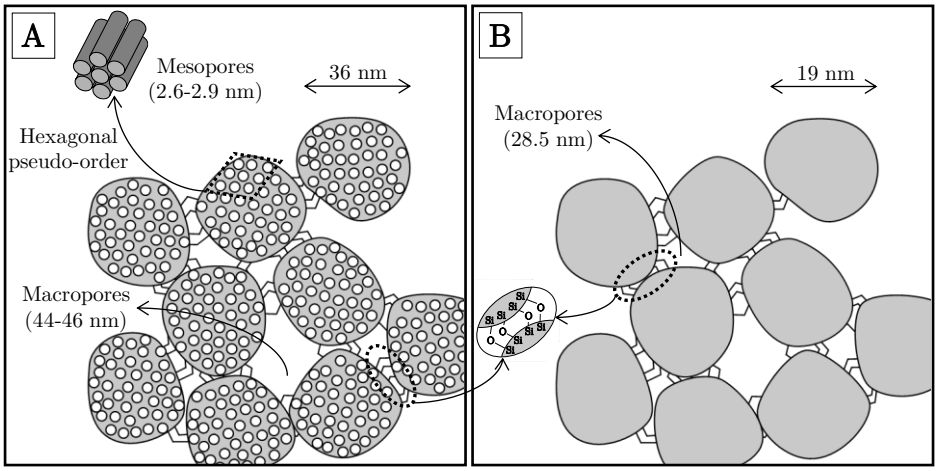

Figure 21. Schematic representation of the characterized structure for UVM-7 (A) and UVM-11 (B) materials.

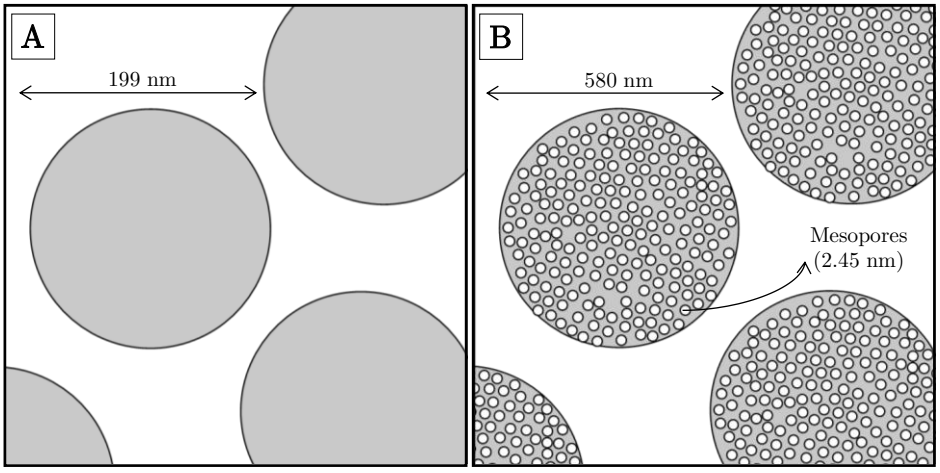

Figure 22. Schematic representation of the Stöber spherical particles: massive (A) and mesoporous (B).

As can be seen in Figure 21 and Figure 22 the differences among UVM-7 materials and other silica materials have been assessed, thus obtaining a material with the same macroporous architecture as UVM-7, although with the absence of the mesopores (UVM-11), silica spheres with the only presence of those mesopores, and silica particles with the absence of any porosity. With these materials, the pore role in the analyte retention can be evaluated, as discussed in the next Chapter.

Chapter 3

Application of UVM-7 mesoporous silica to aflatoxins extraction from food samples

1. Introduction

Mycotoxins are metabolites produced by fungi contaminating various food and feed crops, being a risk for both human and animal health. Hence, mycotoxin contamination is an ongoing global concern, as it is considered an unavoidable and unpredictable problem, even when good agricultural, storage, and processing practices are implemented. In fact, according to the FAO, 25% of the world's crops are contaminated with mycotoxins during growth or storage. Currently, more than 400 different types of mycotoxins have been identified, as stated previously, but among them, aflatoxins (AFs) are the most toxic, commonly present naturally, and significant regarding economic burden to agriculture. These toxins are produced by *Aspergillus flavus* and *Aspergillus parasiticus* and, until now, eighteen different types of AFs have been identified wherein aflatoxin B_1 (AFB_1), B_2 (AFB_2), G_1 (AFG_1), and G_2 (AFG_2) are the most toxic and commonly found. Indeed, they have been classified as Group 1 carcinogens by the International Agency for Research on Cancer (IARC), being AFB_1 the most significant form considering incidence and toxicity [45–47,169].

Even though these compounds can be found in several kinds of food, their presence is especially frequent in vegetable products such as nuts, cereals, corn, rice, peanuts, oilseeds, and certain spices, as well as products processed and derived from them. Thus, the European Commission regulation [40] sets specific limits for these kinds of products, being them in the range 4-15 μg kg^{-1} for total AFs and 2-12 μg kg^{-1} for AFB_1 [170]. Nevertheless, some studies have found aflatoxins in several other food products not specified in this regulation, such as beer [171–174], jelly, tea [175–177], and other medicinal herbs [178–181]. In these cases, in Spain [182] the limits are set at 10 μg kg^{-1} for total AFs and 5 μg kg^{-1} for AFB_1 for food products in general [170]. In this sense, minor aflatoxin concentrations have been found in nutraceutical products such as tea or medicinal herbs, although their control is advisable due to their current high consumption [176].

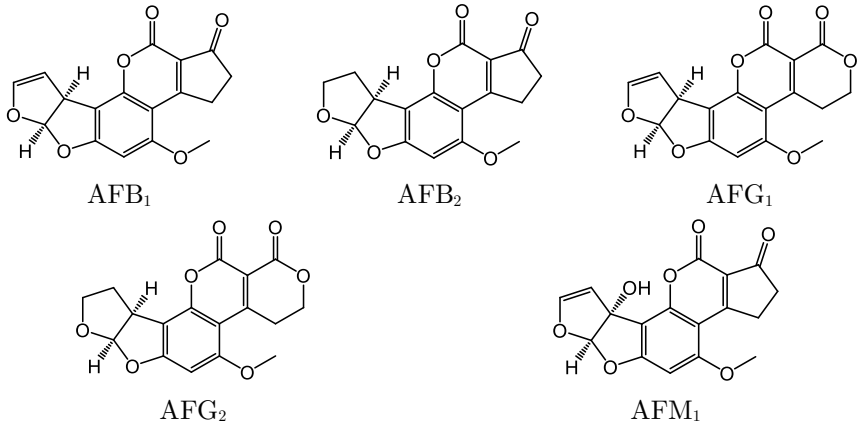

Figure 23. Molecular structure of the main aflatoxins present in food products.

Likewise, special attention has also received aflatoxin M_1 (AFM_1). This toxin is the major oxidized metabolite of AFB_1 and has become a global concern regarding human health since it has been also classified as Group 1 carcinogenic substance by the IARC [46,183]. Due to the aflatoxin contamination of feed, its presence in milk and dairy products has become an important avenue for human exposure to aflatoxins [184,185]. Moreover, several studies have proved the resistance of AFM_1 to heat processes used for milk conservation, such as pasteurization or boiling [186]. In this case, the same European legislation previously mentioned establishes the limit value of 0.05 μg kg^{-1} for AFM_1 in milk and its derivatives, although lower limits are considered in the case of milk powder for children (0.025 μg kg^{-1}) [40].

In order to achieve these regulatory limits and ensure the correct control and vigilance of food products, there is a special interest in developing sensitive and reliable methods for aflatoxin determination. On the one hand, several techniques have been developed for aflatoxin fast and simple screening, mainly based on the use of antibodies in immunoassays. The most commonly used is the enzyme-linked

immunosorbent assay (ELISA), a simple technique that enables simultaneous testing of multiple samples with a precise detection, using low sample volume. In the same way, lateral flow immunoassay (LFIA) is a membrane-based immunoassay that works as a competitive method, using a labeled antibody as a signal reagent. Also, several types of biosensors have been used for aflatoxin rapid detection [45]. However, most aflatoxin determinations are carried out by chromatographic techniques, both in food and feed samples. Although thin-layer chromatography (TLC) has been used for several years as a rapid screening method, the most common technique used is, by far, liquid chromatography. Apart from the universal UV-Vis detector, the fluorescence detector has been widely used for aflatoxins quantification due to their native fluorescence with a high quantum yield. However, because of the increasing availability of sensitive and specific MS detectors over the past two decades, many works have been reported by using this instrumentation. Thus, LC-MS and LC-MS/MS techniques have proved to be a good standard tool to deal with the analytical challenges of food and feed safety analysis, and provide one of the most reliable and sensitive results for simultaneous determination of several aflatoxins, as well as other multi-mycotoxin analyses [45,46,169,187]. It should be noted that, to a lesser extent, gas chromatography techniques have been also used for this purpose although because of the low volatility of the analytes and their high polarities a derivatization step is required [45].

In addition, due to the low established limits, the use of sample treatment for the pre-concentration and clean-up is mandatory. In this sense, extraction procedures based on QuEChERS have been widely applied, as well as other techniques based on LLE such as DLLME or PLE, although even in these cases a later purification step is advised due to the complexity of food matrices [45,169,188]. For this purpose, immunoaffinity columns (IAC) coating pre-treatment is the most common and reliable method due to their selective isolation and is the conventional method for the clean-up of many food matrices in AFs determination. In these cartridges, the retention of AFs is achieved thanks to the presence of monoclonal antibodies, whilst water-soluble impurities are removed during the washing step. Due to the specificity of the antibody-antigen interaction and the minimum level of interfering matrix components, IACs are a very sensitive and selective method for purification and determination of aflatoxins [45,169,189], and their use is recommended by several official organizations such as the AOAC [190]. However, IAC methods require very expensive and disposable cartridges, which are generally designed for only one type of toxin, reducing the method multiresiduality [169]. Because of that, several alternatives have been proposed for aflatoxin purification and clean-up, being the most common those based on SPE.

Although other purification methods have been also used with satisfactory results, such as SPME [191,192], dSPE [59,193], or the already mentioned DLLME [187], solid-phase extraction is a rapid, efficient, and reproducible technique that

is widely used for this purpose. In this case, there is a wide range of commercially available columns with different sorbents that have been applied for aflatoxin extraction, such as C18 [184,185,194] or Oasis HLB [181,195], but the majority of the commercial cartridges present several drawbacks for mycotoxins screening [45,46]. Because of that, other sorbents have been developed based on novel technologies such as MIPs [196,197], aptamers [104], carbon nanotubes [198], graphene oxides [95], or MOFs [199,200], highlighting the growing interest in developing new SPE sorbents for this purpose.

In this sense, the molecular diameters of the target analytes seem to be appropriate for pore sizes of mesoporous materials that are comprised in the range of 2-3 nm. Also, the stability of silica materials, their large surface area, and their ability to interact through hydrogen bonds give them great utility in this field. As discussed in Chapter 1, among mesoporous silicas, MCM-41 materials are the best-known mesoporous silica materials, even though their large particle size may cause diffusion problems, and reduce the accessible surface area for the analyte retention. On the other hand, in UVM-7 materials, which can be considered as a nanometric version of the MCM-41 silicas, the particle size decreases from the micro to the nanodomain, and it necessarily implies a similar decrease in the intraparticle mesopore length. This fact combined with the preservation of the mesopore diameter and silica wall thickness confers to the UVM-7 silicas improved accessibility for the analytes to the whole internal surface area [116]. Hence, UVM-7 calcined and extracted materials show great potential for the retention of aflatoxins from aqueous food matrices.

2. Materials, reagents, and instrumentation

Aflatoxin standards were purchased from LGC Standards (Teddington, Middlesex, UK), as a multicomponent solution in acetonitrile of concentration 2 mg L^{-1} for B_1 and G_1, and 0.5 mg L^{-1} for B_2 and G_2. In the case of aflatoxin M_1, the solid standard was purchased from Sigma-Aldrich (St. Louis, MO, USA), and dissolved in methanol HPLC grade. Working standard solutions were prepared by dilution of these mixtures and stored in darkness at -18 °C.

For extraction and analysis procedures, methanol (MeOH), ethanol, and acetonitrile (ACN) from HPLC grade quality were purchased from Panreac AppliChem (Darmstadt, Germany), as well as hexane from Scharlab (Barcelona, Spain). Ultrapure water from Adrona (Riga, Latvia) purification system was also employed. Acetic acid (HAcO) from Sigma-Aldrich and sodium chloride (NaCl) from Scharlab were also used for the milk extraction.

In addition, for the validation of the method, commercial IAC (Supel™ Tox AflaZea cartridges) were purchased from Supelco (Bellefonte, PA, USA), following the corresponding reference method for each determination [190,201].

For SPE procedures, a Vac Elut 20 connected to a vacuum pump system was employed. Tea samples were previously filtered with polyamide 0.45 µm Sartorius Stedim Biotech filters (Goettingen, Germany). Also, a miVac sample concentrator from SP Scientific (Warminster, PA, USA) was used for solvent evaporation. For the AFM_1 extraction from milk samples, a Hettich EBA 20 laboratory centrifuge (Tuttlingen, Germany) was also employed.

During the optimization stage, and for sample analysis in the case of AFM_1, aflatoxins were determined using an LC-2000 Plus liquid chromatograph equipped with an FP-2020 Plus Intelligent Fluorescent Detector, a PU-2089 Plus Quaternary Gradient Pump with integrated degasser, and an I/FLC/NetII/ADC interface from Jasco (Madrid, Spain). The separation was carried out using a Kromasil C18 column from Análisis Vínicos (Ciudad Real, Spain) at 35 °C under an isocratic flow of 1 mL min^{-1}, and water:ACN:MeOH as a mobile phase. In the case of the determination of aflatoxins, the ratio of the eluents was 65:25:10 respectively, whilst this proportion was slightly modified for AFM_1 determination (70:20:10). The fluorimetric detection was carried out at λ_{ex} = 365 nm and λ_{em} = 435 nm.

On the other hand, for sample analysis and identification checking, samples were injected into the UHPLC-MS/MS system. For this purpose, an Acquity UPLC Waters liquid chromatograph was used (Milford, MA, USA), equipped with a triple quadrupole mass spectrometry (MS/MS) detector programmed in ESI+. In this case, a C18 BEH Waters column was used (2.1 x 50 mm, 1.7 µm particle size), and the separation was carried out at 30 °C using a mixture of MeOH and water (containing ammonium formate 0.15 mM and formic acid 0.1%) under gradient conditions (described in Table 4). The specific transition ion pairs monitored for each aflatoxin are given in Table 5.

Table 4. UHPLC-MS/MS mobile phase composition used in the determination of aflatoxins.

t (min)	Water (%)	Methanol (%)
0	95	5
2	75	25
13	0	100
15	0	100
15.1	95	5
18	95	5

In order to study the aflatoxin retention in UVM-7 material, new porosity data were collected with a Micrometrics ASAP2010 automated sorption analyzer recording nitrogen adsorption-desorption isotherms at 77 K. Pore size and volume, and surface area were calculated from the adsorption data in low-pressure range using BET model. Fourier-transform infrared (FTIR) spectrometer Bruker Tensor

27 (Massachusetts, USA) was also employed. Confocal images were acquired with a Leica TCS-SP2 confocal microscope (Leica Microsystems, Heidelberg, Germany) equipped with an ultraviolet light source of continuous wavelength argon excitation laser beam (λ_{ex} = 365 nm, λ_{em} = 435 nm). The gain was adjusted by using aflatoxin-free UVM-7 pure silica as blank, and later this same gain value was used to record the remaining images. Under these identical conditions, the aflatoxin-containing silica leads to emission signal saturation, indicating conclusively its presence and dispersion.

Table 5. UHPLC-MS/MS detection parameters for the target aflatoxins.

Compound	Quantifier transition ion pair, Q (m/z)	Qualifier transition ion pairs, q (m/z)	Cone voltage (V)
AFB_1	313 > 285	313 > 241	45
AFB_2	315 > 287	315 > 259	45
AFG_1	329 > 243	329 > 283 329 > 311	40
AFG_2	331 > 257	331 > 217 331 > 285	45
AFM_1	329 > 273	329 > 229	45

3. Extraction and determination of aflatoxins in tea samples by using UVM-7 silica

In this part, the potential of pure UVM-7 mesoporous silica for the extraction of aflatoxins from nutraceutical products has been studied. For this purpose, extracted and calcined UVM-7 materials were considered, being their main difference in the density of silanol groups available for the interaction with analytes. Thus, an SPE method has been developed for the preconcentration of aflatoxin B_1, B_2, G_1, and G_2 from tea samples, with their later determination by HPLC-FLD and UHPLC-MS/MS. For this purpose, relevant features of the method have been established, and the method has been applied to the analysis of real samples, in comparison with a reference method.

3.1. SPE protocol and experimental procedure

SPE cartridges were prepared by packing the desired amount of UVM-7 material (either calcined or extracted) between two polyethylene frits of 20 µm into 6 mL empty polypropylene cartridges. After optimization, the recommended SPE procedure consisted in using 100 mg of extracted UVM-7 material, which was previously conditioned with 5 mL of MeOH and 5 mL of ultrapure water.

Then, spiked ultrapure water containing aflatoxins (AFB_1, AFB_2, AFG_1, and AFG_2) was passed through the cartridge. After that, the cartridge was dried with air for 10 min and analytes were eluted with 3 mL of MeOH. After their concentration by evaporation (60 °C) and recomposition with 250 µL of MeOH, the extracts were analyzed by HPLC-FLD or UHPLC-MS/MS.

The optimization study was carried out based on the recovery obtained from spiked water with AFs, by varying one parameter at a time and keeping the other parameters constant. For the application of the method to real samples, green and black tea samples from different origins were purchased, both from commercial bags (containing 1.5 g of tea) and herbalists. In order to find out the aflatoxin contamination of the consumable liquid portion of the tea, sample treatment was carried out by immersing tea bags in 250 mL of water at 80 °C for 20 min. In the case of herbalist tea (purchased in bulk), the same amount as in the bags was treated. This liquid portion was homogenized, filtered, and 25 mL of the filtrate were analyzed according to the protocol described above. Likewise, the matrix effect was studied by analyzing a triplicate of spiked tea samples (600 ng L^{-1} for AFB_1 and AFG_1; 150 ng L^{-1} for AFB_2 and AFG_2) following the same protocol.

In addition, results were compared with those obtained with the AOAC reference method [190] using IAC cartridges for aflatoxin extraction.

3.2. Results and discussion

3.2.1. Optimization of SPE conditions

The comparison between calcined and extracted was firstly carried out, as well as the study of sorbent amount. For this purpose, SPE cartridges were prepared with 25, 50, and 100 mg of each material, and 10 mL of spiked ultrapure water (150 ng L^{-1}) were loaded into each cartridge. After elution with 3 mL of MeOH, the best recoveries were obtained for 100 mg of extracted UVM-7, being these recoveries greater than 90%, as observed in Figure 24. Thus, these cartridges were selected for method development. Additionally, these results are consistent with those obtained in the NMR characterization of pure UVM-7 materials. As discussed in Chapter 2, extracted UVM-7 shows fewer Q^4 centers, which means that more silanol groups are available to interact with analytes. It should be noted that the optimization was carried out with AFB_2 and AFG_2, while all analytes were studied in the analytical figures of merit and the analysis of real samples.

Then, loading conditions such as ionic strength and pH were studied. Firstly, the effect of the pH was studied. For this purpose, several spiked solutions were used with different pH values (between 4.5 and 7.1). Results indicated that the recovery of the analytes was not affected by the loading pH, since aflatoxins acid-base activity is expected to be negligible, and the working pH range is not below silica isoelectric point (2-3) [125]. Secondly, the influence of ionic strength was also studied, in order to reduce the solubility of the analytes in the aqueous phase,

while increasing their retention into the sorbent. Different contents of NaCl (up to 2 M) in the spiked sample were studied and the results indicated that recoveries were not affected by ionic strength variation. Consequently, the use of sodium chloride was discarded.

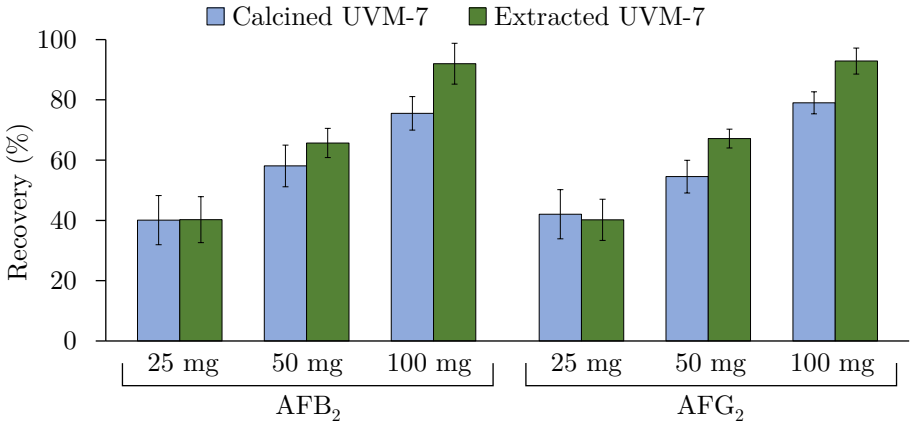

Figure 24. Influence of the type and amount of mesoporous silica sorbent on the recovery of AFB_2 and AFG_2 from spiked ultrapure water samples. Conditions: 10 mL of water spiked with 150 ng L^{-1}; elution with 3 mL of methanol.

Even though recoveries obtained with methanol as elution solvent were satisfactory (> 95.9%), other solvents were tested as eluents in order to increase these recoveries. Thus, acetonitrile and ethanol were investigated. For this purpose, 3 mL of each solvent were used as eluent. Low recoveries were obtained with ethanol, whilst the use of more polar solvents such as MeOH and acetonitrile gave higher recoveries. In fact, the best extraction efficiencies were obtained using methanol for both analytes, being also this solvent less toxic than acetonitrile. These observations can be explained not only based on the higher polarity of these solvents but also because of the interaction between methanol and silica (in comparison to ethanol), with implies more efficient desorption [202]. Subsequently, eluent solvent volume was studied. In this way, volumes from 1 to 4 mL of MeOH were investigated, in order to assure the minimum solvent volume required to elute retained aflatoxins. The greatest extraction efficiencies (103-104%) were obtained when 3 mL of MeOH were used.

In addition, the possibility of increasing the sensitivity of the procedure by evaporating the solvent at 60 °C using a rotatory evaporator, was assessed. Then, the residue was redissolved either in 250 µL, 500 µL, 1 mL, or 2 mL of MeOH. Results showed that after evaporation of the solvent and its redissolution, no significant differences in the recoveries were observed with none of these volumes (variations < 5%), which indicates that it is possible to carry out this preconcentration step.

In order to obtain reliable analytical results and high preconcentration factors, it is relevant to achieve satisfactory recoveries for all analytes in large sample volumes. For the study of the breakthrough volume, volumes between 10 and 100 mL of aflatoxin-spiked sample were passed through the SPE cartridge following the procedure previously described and keeping the absolute amount of analytes constant (1.5 ng). Experimental results showed satisfactory recoveries with 50 mL (95.7-98.0%) as well as with 100 mL (97.1-101.2%). For this reason, depending on sample concentration, this material allows treating up to at least 100 mL of sample in order to achieve the maximum limits established in the legislation.

Finally, the loading capacity of the sorbent was also studied by passing through the cartridge 50 mL of spiked deionized water (concentrations from 0.05 µg L^{-1} to 2 µg L^{-1}). No significant differences were observed in the analyte recoveries. This confirms that this material can be used for SPE clean-up within these concentrations.

3.2.2. Analytical figures of merit

The optimized SPE protocol was evaluated in terms of linearity, selectivity, and precision. Calibration standards were prepared and injected twice, both in HPLC-FLD and UHPLC-MS equipment in order to determine the sensitivity of the method by using both techniques. The sensitivity of the method in terms of limit of detection (LOD) and quantification (LOQ), was calculated with a confidence level of 95%, and following the latest IUPAC recommendations [203]. In both cases, limits were expressed in terms of absolute amount, as well as in tea sample, considering the recommended procedure. Linearity range was estimated following these recommendations, considering the LOQ as the lower limit of linearity [32]. As can be seen in Table 6, LODs were lower than 0.7 µg kg^{-1} using both systems, and LOQs were below 2.1 µg kg^{-1}. Thus, this method is sufficiently sensitive for quantifying the maximum aflatoxin concentration established in the legislation [40,182]. Likewise, our values were better or comparable than those reported in the scientific literature, by other extraction methods for aflatoxin determination in similar matrices (Table 7).

The precision of the SPE procedure was evaluated by measuring the repeatability (intra- and inter-day) of extractions of spiked water samples, in terms of relative standard deviation (RSD). The intra-day precision was estimated by analyzing a triplicate within a day, whereas the inter-day precision was determined with three series of three independent extractions analyzed on three different days (Table 8). The SPE procedure showed good precision, with RSDs below 5.1%. As can be seen in Table 8, good extraction efficiencies were achieved (between 96% and 99%) for all studied aflatoxins. Also, these obtained recoveries are better than those presented by other methods reported in the literature, as well as the resulting RSD values that also improve the precision of reported methods (Table 7).

Table 6. Analytical figures of merit of the method combined with HPLC-FLD and UHPLC-MS/MS systems.

Analyte	HPLC-FLD					UHPLC-MS/MS				
	Linearity (µg L^{-1})	Absolute amount (ng)		Tea sample (µg kg^{-1})		Linearity (µg L^{-1})	Absolute amount (ng)		Tea sample (µg kg^{-1})	
		LOD	LOQ	LOD	LOQ		LOD	LOQ	LOD	LOQ
AFB_1	-	-	-	-	-	0.8-19.3	0.068	0.207	0.45	1.4
AFB_2	0.26-4.8	0.021	0.064	0.14	0.43	0.8-4.8	0.067	0.204	0.45	1.4
AFG_1	-	-	-	-	-	1.0-19.3	0.079	0.240	0.52	1.6
AFG_2	0.26-4.8	0.021	0.065	0.14	0.43	1.3-4.8	0.105	0.321	0.70	2.1

Table 7. Comparison of the method with other reported methods.

Sample	Clean-up procedure	Recovery (%)	LOD (µg kg^{-1})	LOQ (µg kg^{-1})	RSD (%)	Analytical technique	Ref.
Tea	UVM-7 SPE	88-102	0.14-0.7	0.43-2.1	1.4-5.1	UHPLC-MS	This work
Black tea	IAC	75-110	0.2-1	-	-	HPLC-FLD	[175]
Green tea	QuEChERS-C18	76-115	2-10	5-20	9-25	UHPLC-HRMS	[176]
Medicinal herbs	IAC	64.7-112	0.03	0.1	2.3-8.3	LC-MS/MS	[178]
Medicinal herbs	QuEChERS	68.1-95.6	-	1.2-3.8	0.9-12.7	HPLC-MS/MS	[180]
Medicinal herbs	Oasis HLB	77.6-110	10[a]	25[a]	5.0-13.1	LC-MS/MS	[181]

[a]These values are given in terms of total amount of aflatoxin (ng)

Table 8. Repeatability, extraction efficiency, and matrix influence ($\bar{x} \pm s$) of the SPE protocol.

Analyte	Repeatability RSD (%)		Extraction efficiency (%)	
	Intra-day	Inter-day	Water	Tea matrix
AFB_1	4.5	5.1	96 ± 3	88.3 ± 1.8
AFB_2	1.7	2.0	98.2 ± 1.2	102 ± 8
AFG_1	3.8	4.2	96 ± 2	97 ± 3
AFG_2	1.4	2.3	96.2 ± 1.4	92 ± 9

Then, the reusability of extracted UVM-7 cartridges was also evaluated. The results indicate that no significant decrease in the recoveries was observed when the cartridges were reused up to six times. Is important to note that this is a significant advantage over commercial disposable IAC cartridges.

3.2.3. Sample analysis and matrix influence

The recommended SPE procedure using UVM-7 cartridges was applied for the analysis of different tea samples and the evaluation of the matrix effect. As can be seen in Table 8, extraction efficiencies in the tea matrix were slightly affected, being these recoveries above 88% for all aflatoxins. Thus, results indicate that these cartridges can be properly used for the extraction of aflatoxins in tea matrices, although standard addition calibration may be used in order to eliminate the matrix effect. In addition, according to AOAC guidelines [190], recoveries should be over 80% for AFB_1, AFB_2, and AFG_1, and over 60% for AFG_2, in the studied concentration range. Thus, the extraction efficiencies are appropriate.

In order to validate the viability of the method using UVM-7 material, the SPE protocol was used for the determination of aflatoxins in eight tea samples. These samples were from commercial bags, both green (M1, M2, M3) and black (M4, M5, M6), and also from herbalists (M7 green and M8 black). The standard addition calibration method was applied in order to eliminate the influence of the matrix. As can be seen in Table 9, no target compounds were found, except for AFG_2 in samples M1, M4, and M6, being both green and black tea samples. However, although these values were over the quantification limit, none of them were above the Spanish legislation [182] for total aflatoxin concentration (10 µg kg^{-1}), except sample M3. Is important to notice that this sample was stored for several years in bad conditions (in contact with atmospheric air and at 25-35 °C) and its consumption is not recommended.

In addition, these positive samples (M1, M4, and M6) were also analyzed following the AOAC reference method by using IAC cartridges [190]. As shown in Table 3, it can be concluded that results are comparable among them by using

the paired t-test for comparing individual differences [204] for a 95% of confidence level. Thus, both protocols gave comparable results, being our cartridges (100 mg of sorbent costs less than 1 euro) significantly less expensive than commercial ones (more than 10 euros each cartridge). Hence, the method provided good results by using an inexpensive and reusable material being an alternative to commercial expensive IAC cartridges. In addition, the material permits the multiresidual analysis, thus improving its scope. As a disadvantage, although the purification of the samples is achieved with our material, the selectivity of the extraction can lead to the extraction of other undesired species from the matrix. Nevertheless, the use of a selective instrumental technique, such as UHPLC-MS/MS allows to properly quantify the analytes.

Table 9. Results for aflatoxin determination in tea samples, and comparison with the reference method ($\bar{x} \pm s$, $n = 3$).

Sample	Method	Concentration (μg kg^{-1})			
		AFB_1	**AFB_2**	**AFG_1**	**AFG_2**
M1	UVM-7	< LOD	< LOD	< LOD	5.0 ± 1.2
	IAC	< LOD	< LOD	< LOD	4.4 ± 0.4
M2	UVM-7	< LOD	< LOD	< LOD	< LOD
	IAC	-	-	-	-
M3	UVM-7	< LOD	< LOD	(1.0)[a]	13.1 ± 1.7
	IAC	< LOD	< LOD	< LOD	13.5 ± 1.0
M4	UVM-7	< LOD	< LOD	< LOD	(1.7)[a]
	IAC	-	-	-	-
M5	UVM-7	< LOD	< LOD	(0.6)[a]	5.8 ± 0.7
	IAC	< LOD	< LOD	< LOD	6.4 ± 0.7
M6	UVM-7	< LOD	< LOD	< LOD	(1.9)[a]
	IAC	-	-	-	-
M7	UVM-7	< LOD	< LOD	(0.5)[a]	7.8 ± 0.4
	IAC	< LOD	< LOD	< LOD	9.4 ± 0.4
M8	UVM-7	< LOD	< LOD	< LOD	(1.4)[a]
	IAC	-	-	-	-

[a]Values below LOQ

4. Bimodal porous silica as sorbent for the determination of aflatoxin M_1 in milk and dairy products

In this point, pure UVM-7 silica has been applied to the extraction and determination of aflatoxin M_1 in milk samples and dairy products, through the design of an SPE method. As previously explained, the effect of the density of silanol groups was also assessed by comparing extracted and calcined UVM-7. After the optimization of the main analytical parameters, and thanks to the use of this material, the determination of AFM_1 by HPLC-FLD has been properly carried out in real samples, in comparison with a reference method.

4.1. Sample clean-up protocol and experimental procedure

The AFM_1 extraction from milk and dairy products samples was carried out through a modification of the procedure proposed by Campone et al. [185], and using UVM-7 material for the sample clean-up. The complete extraction and clean-up procedure is summarized in Figure 25. Briefly, 2 g of NaCl were dissolved in 10 g of milk or yogurt sample. Then 7.6 mL of ACN and 100 µL of acetic acid were added, and the mixture was manually shaken for 30 s. After centrifugation at 6000 rpm for 10 min, the upper phase, containing AFM_1, was transferred into a glass tube, evaporated under vacuum at 60 °C, and redissolved with 10 mL of ultrapure water for the SPE clean-up step. In the case of powder milk samples, 3 g of each sample were dissolved in 30 mL of deionized water. Then, an aliquot of 10 g of the resulting milk was treated in the same way as described above.

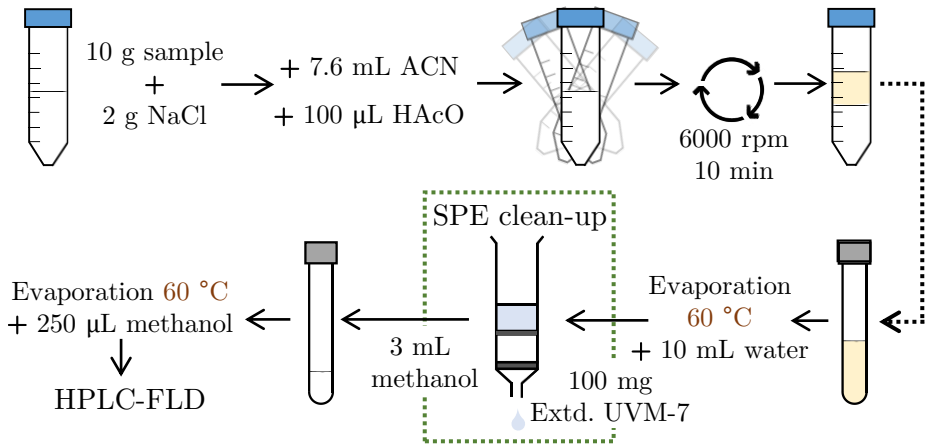

Figure 25. Schematic summary of the recommended protocol for the extraction and clean-up of aflatoxin M_1 from milk samples using extracted UVM-7 material.

Hence, several parameters such as the amount of solid phase, type and amount of elution solvent, and loading conditions were optimized, by varying one parameter at a time and keeping the other parameters constant. After

optimization, the recommended SPE procedure consisted in using cartridges with 100 mg of extracted UVM-7 material, previously conditioned with 5 mL of methanol and 5 mL of ultrapure water. Then, the aqueous solution from sample extraction was passed through the cartridge and washed with 5 mL of ultrapure water followed by 3 mL of hexane. The material was dried with air for 10 min and AFM_1 was eluted with 3 mL of methanol. Then, the organic extract was evaporated and recomposed with 250 µL of methanol. Next, the concentrated extracts were analyzed by HPLC-FLD.

For the application of the method to real samples, whole and skimmed commercial milk samples were analyzed, as well as a fresh milk sample from a farm. Likewise, commercial yogurt and powder milk samples were considered. Moreover, in all cases, the matrix effect was studied by analyzing a triplicate of a sample spiked with 0.5 µg kg^{-1} of AFM_1 following the described procedure.

For the assessment of the main analytical parameters of the method, 7 calibration points were prepared with concentrations of 0, 0.5, 1, 3, 5, 12, and 25 µg L^{-1} in the injection solution. Through the injection of calibration standards in the HPLC-FLD system, the linearity of the method was evaluated, as well as the sensitivity and the limits of detection (LOD) and quantification (LOQ). All values were calculated according to the latest IUPAC recommendations, with a confidence level of 95% for the limits and considering the LOQ as the lower limit of the linear range [203].

The feasibility of the described method was validated by comparing the obtained results with another validated method. Thus, some samples were also analyzed through the reference extraction method following the application note described by Sigma-Aldrich [201]. The results obtained through both protocols were compared with the t-student statistic test, considering a 95% confidence interval.

4.2. Results and discussion

4.2.1. Optimization of sample treatment parameters

SPE parameters using mesoporous silica materials were studied. For this purpose, spiked water solutions were used. Firstly, the type and the amount of solid sorbent were evaluated. Hence, SPE cartridges were prepared to contain several amounts (25, 50, and 100 mg) of either calcined or extracted UVM-7, and 10 mL of spiked ultrapure water were loaded into each cartridge (0.5 µg L^{-1} of AFM_1 in the aqueous sample). The analyte was then eluted with 3 mL of methanol. As also observed in the previous study, a recovery of 99.2% was obtained using 100 mg of extracted UVM-7, being this extraction more efficient than those using calcined UVM-7 (80.8%). Thus, these cartridges were selected for further studies. It should be noticed that these observations are consistent with results obtained for the retention of other AFs, as well as with the results obtained in the NMR characterization (see Chapter 2). Thus, as stated, the higher

presence of Q^3 centers ($Si(OSi)_3(OH)$) in extracted UVM-7 in comparison to the Q^4 centers ($Si(OSi)_4$), implies the higher availability of silanol groups for the interaction with the analyte. This high density of silanol groups, along with the pore structure of the material, implies good retention of the analyte. As can be seen also in the porosimetry analysis, the mesopore size is suitable for the AF molecular structure, as proved also in the previous point of the present Chapter.

Once the cartridge was selected, the elution step was also studied. Several solvents, namely ethanol and ACN, were also tested in comparison with methanol. In this case, spiked ultrapure water was treated as described above and 3 mL of each solvent were used for the desorption of the analyte. The results showed worse recoveries using these alternative solvents, mainly with ethanol (38 ± 7%). Although ACN recovery was slightly better (50 ± 6%), the best results were achieved by using methanol as eluent solvent (100 ± 7%), in agreement with what was previously observed for other AFs. Likewise, the solvent volume was studied, in order to use the minimum but enough amount of methanol in the optimized procedure. Thus, similar extractions were carried out by using volumes of 1, 2, 3, and 4 mL of methanol for the elution. As can be seen in Figure 26, results showed that, although AFM_1 was quantitatively eluted by using 2 mL, the elution was complete when 3 mL of methanol was used, selecting this volume as the recommended to desorb any remaining traces of analyte from the solid phase.

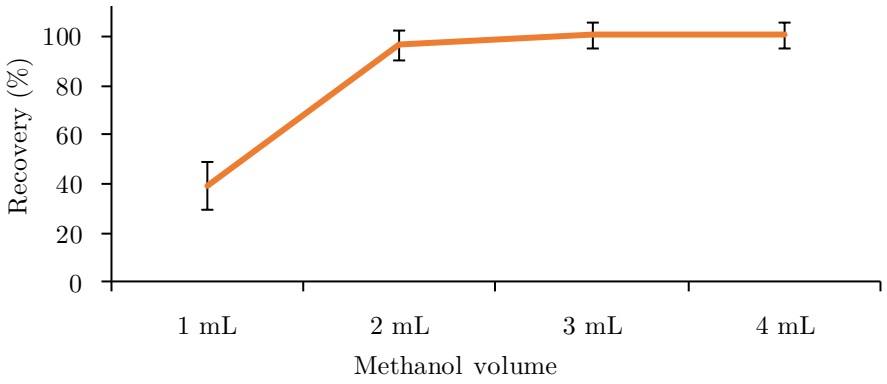

Figure 26. Influence of the methanol volume used in the elution on the AFM_1 recovery. Conditions: 100 mg of extracted UVM-7; 10 mL of water spiked with 0.5 µg L^{-1} of AFM_1.

Also, the possibility of concentrating the extract by evaporation was studied. The evaporation was carried out under vacuum at 60 °C, followed by redissolution with volumes of 250-2000 µL of methanol, and no significant variations were observed in the recoveries (variations < 5%) since AFM_1 is expected to be stable at this temperature. Thus, this concentration step is recommended, using 250 µL of methanol for the redissolution, thus increasing considerably the pre-concentration factor of the method.

In addition, loading conditions were also optimized. The effect of the loading pH was assessed by changing the pH of the sample in the loading step (4.5-7.1), as well as the influence of the ionic strength through the modification of the NaCl content (0-2 M). In both cases, the results showed that AFM_1 recovery was affected neither by pH nor ionic strength variations. As previously commented, these observations are expected, taking into account the stability of the silica material above silica isoelectric point (2-3) [125], as well as the negligible acid-base activity of the analyte in this pH range. Hence, the modification of the sample pH or ionic strength was discarded, in order to reduce the time and resources employed in the method during the sample treatment step.

Other analytical parameters such as loading capacity and breakthrough volume were also evaluated. For this purpose, several spiked water samples were treated following the optimized SPE procedure and varying either sample volume or AFM_1 concentration each time. Results showed that the variations observed with AFM_1 concentrations in the range of 0.05-6 µg L^{-1} can be due to the dispersion of the results and not to the concentration influence. Likewise, no loss of the analyte was observed by loading sample volumes up to 50 mL (recovery 100 ± 4%), whilst using 100 mL a lower recovery and a higher dispersion were obtained (76 ± 20%). These results indicate that sample analysis in this concentration range can be carried out by using these mesoporous silica cartridges, and aqueous extracts up to 50 mL can be treated by using this material, being this volume more than enough for the treatment of milk and dairy products samples with a good method sensitivity.

Due to the inability to carry out the SPE clean-up directly with the complex milk matrix, a previous treatment is needed. Once the SPE parameters were established, several modifications were introduced in the liquid-liquid extraction procedure described by Campone et al. [185]. In order to increase the sensitivity of the method, in this case, the possibility of working with 10 g of milk was studied, as well as the possibility of treating the whole extract volume through the SPE clean-up, as described above. In all cases, obtained recoveries from spiked milk samples were above 92%, as referred to in the procedure selected for sample treatment. Likewise, several washing options were tested, and after using 5 mL of ultrapure water followed by 3 mL of hexane, quantitative AFM_1 recoveries were obtained (>95%), as well as the proper clean-up of the matrix interferences.

4.2.2. Evaluation of the linearity and sensitivity of the method

As described, the linearity of the method in the working range was evaluated, with a linear range in the injection solution between 0.6 and 25 µg L^{-1} (correlation coefficient r^2 of 0.996). Likewise, both LOD and LOQ were calculated in both final extract (0.2 and 0.6 µg L^{-1} respectively), and milk samples considering the described procedure (0.005 and 0.015 µg kg^{-1} respectively). Results showed that good sensitivity was achieved by using the fluorescence detector, being the LOQ low enough to achieve the quantification of the AFM_1 below the regulatory limits

established by the European Commission Regulation [40], both for milk products and powder milk for children. Thus, owing to the proper clean-up of the sample using cheap and simple UVM-7 silica cartridges, satisfactory and enough sensitivity was achieved by using traditional equipment such as HPLC-FLD.

4.2.3. Repeatability, matrix influence, and real sample analysis

The precision of the method was evaluated by measuring the repeatability from extractions of spiked samples (0.5 µg kg^{-1}) and expressed in terms of relative standard deviation. Likewise, the extraction efficiency of the described method was measured with the recovery from the analysis of these spiked samples, using cartridges with 100 mg of extracted UVM-7. As shown in Table 10, in both cases the evaluation was carried out in ultrapure water, as well as in several sample matrices such as whole and skimmed milk or yogurt, in order to assess the matrix influence. As can be seen, good recoveries were achieved for all sample matrices, being them higher than 94% for all milk matrices, and slightly lower for the more complex yogurt matrix (85 ± 7%). In this last case, a result correction with matrix recovery is advisable. In the same way, good repeatability was achieved for all matrices, being the RSD values under 9% in all cases. Hence, the described extraction and clean-up procedure allows the quantitative and efficient extraction, concentration, and determination of AFM_1 in several kinds of milk and dairy products matrices.

Table 10. Recoveries obtained for AFM_1 in spiked samples from several matrices (n = 9 for ultrapure water and n = 3 for real food matrices).

Matrix	Spiking level (µg kg^{-1})	Recovery (%)	Recovery RSD (%)
Ultrapure water	0.5	101 ± 4	4
Whole milk	0.5	94 ± 4	4
Skimmed milk	0.5	100 ± 9	9
Yogurt	0.5	85 ± 7	9

Moreover, the feasibility of the described method was assessed by applying it to the determination of AFM_1 in real samples. For this purpose, whole (M1, M2) and skimmed milk (M3, M4) samples were analyzed, as well as a fresh milk sample (M5) collected directly from a farm. Likewise, commercial yogurt (M6, M7) and powder milk samples (M8, M9) were considered. In all cases, cartridges with 100 mg of extracted UVM-7 were used for the clean-up step. As can be seen in Table 11, since no target compound was detected in any analyzed sample (apart from concentrations below LOQ in sample M6), some of these samples were spiked with 0.5 µg kg^{-1} and analyzed through the described method. In all cases, obtained concentrations were comparable to theoretical values, being all relative errors below 16%. In addition, sample M3 was also analyzed through the reference method, and a concentration of 0.52 ± 0.09 µg kg^{-1} was obtained. Thus, as can be seen, the obtained results are statistically comparable, using a 95% confidence level interval.

Table 11. Concentration of AFM_1 obtained in the analysis of real milk and dairy product samples, following the described method, and the measured concentrations in spiked samples.

Sample	Matrix	Concentration (µg kg^{-1})	Spiked sample (0.5 µg kg^{-1})	
			Obtained concentration (µg kg^{-1})	Relative error (%)
M1	Whole milk	< LOD	0.50 ± 0.02	0.02
M2	Whole milk	< LOD	0.42 ± 0.04	-16.1
M3	Skimmed milk	< LOD	0.45 ± 0.11	-9.7
M4	Skimmed milk	< LOD	-	-
M5	Fresh milk	< LOD	-	-
M6	Yogurt	< LOQ (0.008)	0.50 ± 0.04	0.2
M7	Yogurt	< LOD	-	-
M8	Powder milk	< LOD	-	-
M9	Powder milk	< LOD	-	-

Finally, the reusability of the developed cartridges containing extracted UVM-7 material (100 mg) was also tested. For this purpose, after each extraction, SPE cartridges were washed with 2 mL of MeOH. Then, after the proper conditioning as described above, a fresh spiked water sample was loaded into the sorbent. Results did not show important variations on the recoveries after 5 reuses of the same cartridge (above 96%). The advantage of these cartridges is they can be reused at least up to 6 times without analyte loss as compared to other commercial cartridges such as the disposable IAC.

To evaluate the developed method, some similar protocols described in the literature for the determination of AFM_1 in milk and dairy products have been summarized in Table 12, in order to compare the described method with them. As can be seen, the recoveries found are comparable or better than those reported in other similar works, being the influence of the matrix lower than those of similar procedures presented in the table. Also, the repeatability of the described method is satisfactory with RSD values in the same range as those reported. Hence, satisfactory extraction results were achieved with the developed method regarding other reported procedures, by using a cheap solid phase for the sample clean-up and allowing the extraction of AFM_1 with low solvent and time consumption. Also, the obtained LOD and LOQ values were comparable or even better than those reported by other methods. In any case, the limits presented here are low enough for the determination of AFM_1 according to the European Union legislation, using conventional equipment without the need for post-column derivatization.

Table 12. Comparison of the described method with other methods reported in the literature for the determination of AFM_1 in milk and dairy products.

Sample clean-up	Sorbent	Analytical technique	Recovery (%)	RSD (%)	LOD (ng kg^{-1})	LOQ (ng kg^{-1})	Reference
SPE	UVM-7	HPLC-FLD	85-100	4-9	5	15	This work
SPE	rGO/Au[a]	UHPLC-MS/MS	71.7-87.3	2.3-14.3	10[b]	20[b]	[95]
Online SPE	C18	UHPLC-MS/MS	86-95	2-8	0.5-0.7	1.5-2.4	[185]
SPE	C18	HPLC-FLD	89.3-94.0	3.8-5.8	100	250	[184]
dSPE	Oleic acid- Fe_3O_4	Fluorimetry	91.3-99.5	2.1-4.3	13[b]	-[c]	[59]
Online SPE	C_4/NH_2 macroporous silica-gel	UHPLC-MS/MS	105-136	2-9	0.3	-[c]	[205]
dSPE	PSA[d]	HPLC-FLD[e]	80-92	5.5-10	1.2	10	[193]
SPE	C18	HPLC-FLD[e]	89-90	2.5-4	1	-[c]	[194]

[a]Reduced graphene oxide with gold nanoparticles

[b]Expressed in ng L^{-1}

[c]Not reported

[d]Primary secondary amine

[e]Post-column derivatization

5. Study of aflatoxin retention in the UVM-7 porous structure

Once the suitability of the UVM-7 material for aflatoxin retention was proved, it seems important to understand the interaction between the structure of the mesoporous solid and analytes. For this purpose, several studies were carried out to study the potential of UVM-7 material to retain AFs.

Firstly, and assuming the beneficial effect of a rich-silanol density at the silica surface, we intend to understand the influence of the porosity on aflatoxin retention. This aspect is key to interpreting the high efficiency as SPE sorbent achieved for the UVM-7 silica with aflatoxins. With this aim, three other silica materials (with different porous systems and morphologies) such as UVM-11 material [149] and Stöber spherical particles [126] were tested as SPE sorbents. As described in the characterization in Chapter 2, UVM-11 material presents a continuous silica network constructed from aggregated small solid nanoparticles. This results in an architecture similar to UVM-7 materials, with the presence of non-ordered large pores and the absence of the mesopores (Figure 21). Likewise, the spherical structure of Stöber particles was confirmed, either in the massive silica spheres or with the presence of mesopores (Figure 22).

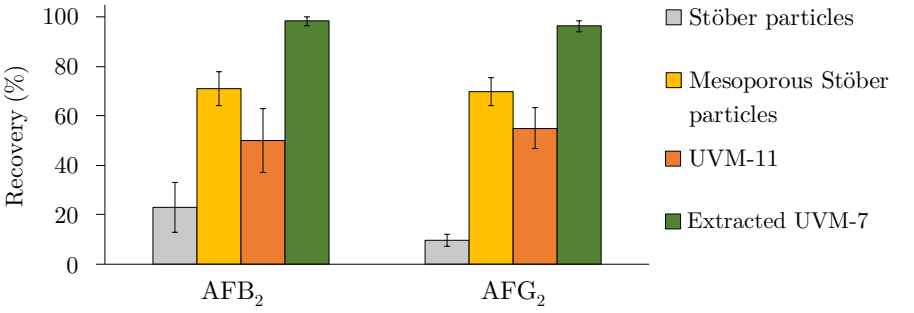

Figure 27. Comparison of the recoveries for aflatoxins B_2 and G_2 by using silica materials with different architectures.

Thus, 10 mL of spiked ultrapure water (150 ng L^{-1} of each AF) were loaded into cartridges containing these materials, and analytes were extracted and determined. As can be seen in Figure 27, poor recoveries were obtained using massive Stöber particles due to the absence of any porous cavities, whereas the best retention was achieved with the bimodal porous architecture of UVM-7 material. Regarding other porous materials, macropores from UVM-11 materials improved the retention of the analytes. However, the presence of mesopores is necessary to overcome the 50% of aflatoxin recovery, being results obtained with mesoporous spherical particles significantly better. In short, the aflatoxin retention increases as follows: massive Stöber < UVM-11 < mesoporous Stöber < UVM-7. Thus, it can be concluded that the presence of intraparticle mesopores plays a key role in the retention of aflatoxins, due to their appropriate size and shape, whilst the presence of macropores in the UVM-7 give it an optimal

architecture for the retention of these compounds. These interparticle textural macropores can play a dual role, as efficient and large routes to favor the diffusion of the analytes and also as an additional pore able to interact with the aflatoxins through hydrogen bonds, thus achieving excellent recoveries.

On the other hand, the aflatoxin retention in UVM-7 material was studied through the characterization of this silica containing retained aflatoxins. Although from a qualitative point of view the general trend of the isotherm can be ascribed to a typical UVM-7 material, there are appreciable differences in the porosity due to the aflatoxin retention in both mesopores and macropores of the material. This effect is observed even at low aflatoxin concentration, much smaller than the maximum loading capacity associated with the volume of mesopore. In any case, the fact that BET surface area, and pore sizes and volumes decrease confirms the ability of the silica surface to interact with the analytes (Table 13).

Table 13. Porosimetry data for extracted UVM-7 material and the material containing aflatoxins (extracted UVM-7 data already presented in Chapter 2).

Material	Surface area[a] (m^2 g^{-1})	Mesopores		Macropores	
		Pore size[b] (nm)	Pore volume[b] (cm^3 g^{-1})	Pore size[b] (nm)	Pore volume[b] (cm^3 g^{-1})
UVM-7[c]	1058	2.87	0.99	45.5	1.91
UVM-7[c] + AFs	648	2.37	0.34	17.7	0.23

[a]Surface area estimated according to the BET model
[b]Mesopore sizes and volumes calculated using the BJH method from the adsorption branch of the isotherms (intra-particle pores $P/P_0 < 0.7$; inter-particle pores $P/P_0 > 0.7$)
[c]Extracted UVM-7

As shown in Figure 28, the presence of aflatoxin in the charged material was also proved by the FTIR spectra. This spiked material was also analyzed by confocal microscopy (Figure 29). After excitation at 365 nm, the presence of aflatoxin is clearly observed due to the fluorescence blue signal. This signal is absent in the case of the pure UVM-7 silica (used as blank) and confirms not only the retention of the aflatoxins but also its homogeneous distribution through the silica particles at a micrometric scale.

Finally, and taking into account the beneficial role played by the mesopores, it is expected that aflatoxins diffuse relatively well through these pores. In this case, a good size and shape adequacy must be required. The geometry of the aflatoxins was studied and the approximated molecular size of the different stable conformations was estimated. For this purpose, a conformational search considering a microcanonical ensemble and using stochastic dynamics via Verlet velocity algorithm and Amber force field [206] was performed with the Gabedit program [207]. Then, in order to have an idea of the volume of the molecules, the longest distance and the perpendicular ones were calculated. As can be seen in Table 14, molecular diameters in the range of 0.9-1.2 nm were obtained for all

conformers of these compounds. These observations are consistent with results obtained for both reported methods for aflatoxin determination, as this size is appropriate for the molecule adsorption in UVM-7 mesopores with diameters around 2.7 nm (Figure 30).

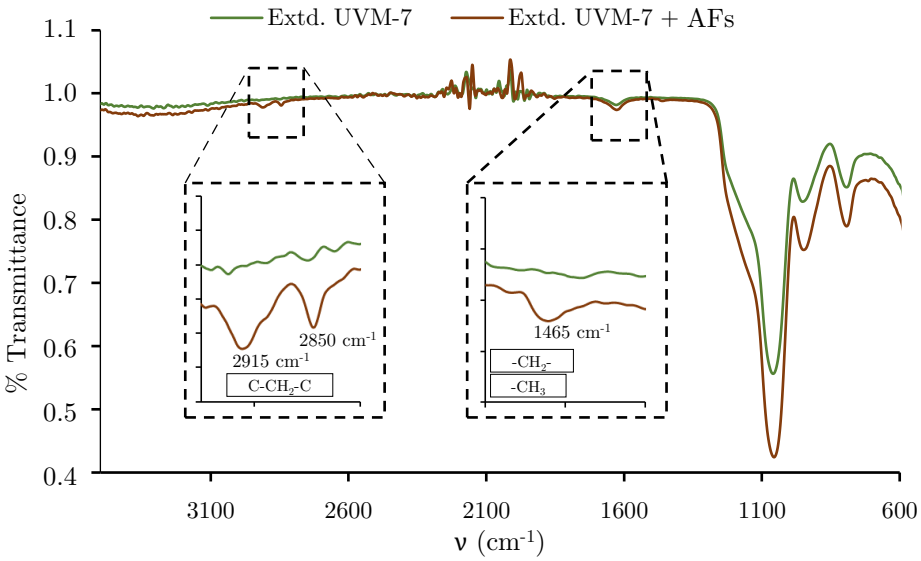

Figure 28. FTIR spectra of the extracted UVM-7 material and the material containing aflatoxins.

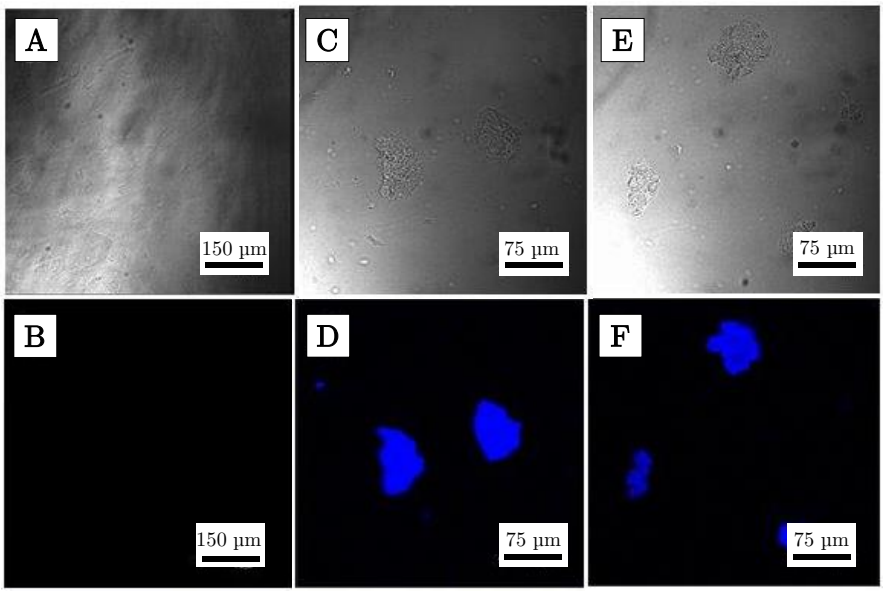

Figure 29. Confocal micrographs (up) and their fluorescence after excitation at 365 nm (down) of the extracted UVM-7 material (A, B) and UVM-7 containing aflatoxins (C, D, E, F).

Table 14. Molecular size of the conformers of aflatoxins B_1, B_2, G_1, and G_2, where Z means the longest distance and X, Y are the perpendicular ones (Å).

Conformer	AFB_1		
	Z	X	Y
1	9.94253129	6.44274773	5.6850608
2	9.94343143	7.4132654	4.73008645
3	9.9668795	6.01503343	5.89378495
4	10.075958	5.44190083	5.44190083
5	10.0948166	6.14080674	5.7256686
6	10.0953813	5.51825543	7.51093779
	AFB_2		
	Z	X	Y
1	9.42360575	7.6044009	5.8058127
2	9.42373186	7.67200618	4.73848415
3	10.0860891	7.22725029	5.10362319
4	9.31993671	7.50055278	5.47255971
5	9.43155694	7.59731684	5.82248262
	AFG_1		
	Z	X	Y
1	10.0412105	6.23208547	6.89809298
2	10.0002732	6.42667569	7.00595474
3	10.0670259	5.42606945	7.13102756
4	10.0736682	6.66138884	5.69391919
	AFG_2		
	Z	X	Y
1	11.5815011	7.9901092	3.34850149
2	10.076505	6.78160542	5.52033835
3	10.0274921	7.34438278	5.69170499

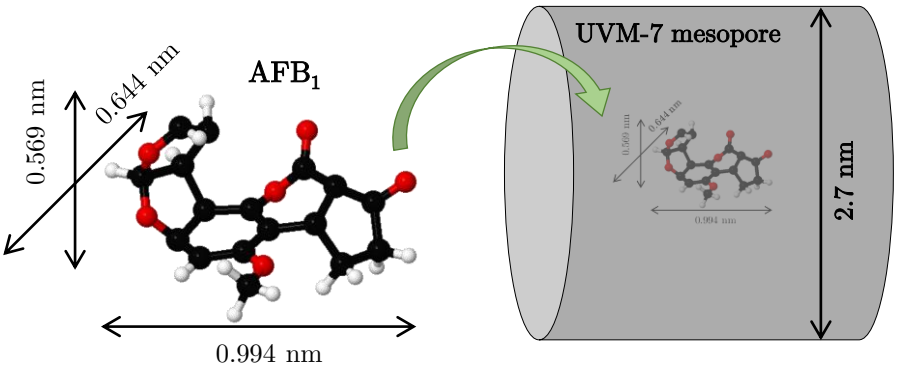

Figure 30. Schematic representation of the geometry of one AFB_1 conformer (1), in relation to a scale representation of the mesopore size of UVM-7 materials.

6. Conclusions

In the present chapter, the potential of UVM-7 materials for the retention of aflatoxins has been properly assessed. As described, the preference of extracted UVM-7 against calcined UVM-7 was clearly observed and explained according to materials characterization already presented in Chapter 2, as well as the interaction of the analytes with silanol groups.

Thus, this ability of mesoporous silica materials was applied through the development of two methods for the determination of aflatoxins in food samples. On the one hand, the developed method for the extraction of aflatoxins B_1, B_2, G_1, and G_2 from tea samples, has shown great analytical parameters, with excellent extraction efficiencies and repeatability. Likewise, the protocol for the determination of aflatoxin M_1 in milk and dairy products has also provided good results. Indeed, extraction efficiencies above 85% have been obtained in both cases for all studied matrices, and above 90% for most of them, as well as RSD values under 10% in all cases. Both designed methods have shown good sensitivity, being the reported LOQs satisfactory for aflatoxin determination in food samples, according to legal limits established by the previously mentioned European Regulation [40]. Moreover, all these analytical features are better or, in some cases, similar to those reported by other reported methods for aflatoxins extraction.

It should be noted that the feasibility of both methods has been assessed with their comparison with reference methods using IAC cartridges, which are the most commonly used solid-phase. Thus, UVM-7 materials allow the extraction and determination of aflatoxins in food samples with good results by using an inexpensive and reusable material being an alternative to commercial expensive IAC cartridges and other sorbents proposed for this purpose.

In addition, these good results were also explained through the study of the aflatoxin retention on UVM-7 material, and the key role of the bimodal porosity of the material has been proved. In this sense, the presence of the intra-particle mesopores has been stated as the most important feature according to aflatoxins size and shape, taking into account also the importance of the textural macropores in the analyte diffusion and retention. All these features allow the homogeneous retention of the aflatoxins for their extraction.

As a disadvantage, although the purification of the samples is achieved with our material in both cases, the selectivity of the extraction can lead to the extraction of other undesired species from the matrix, since silica materials are able to retain organic analytes with a certain polar character from an aqueous solution. Nevertheless, the UVM-7 morphology, and the possibility of controlling pore sizes through the surfactant-assisted synthesis, give it a proper structure for the retention of these compounds. Since the retention inside the pore cavities is significantly greater, size-exclusion mechanisms can favor the adsorption of

aflatoxins against other compounds. Thus, although some other species may be also retained, the combination of this sorbent with separation techniques such as liquid chromatography with selective detectors (FLD or MS/MS) allows the preconcentration and determination of aflatoxins in complex food matrices.

SECTION C

Chapter 4

Characterization of metal-containing silica materials

1. Introduction

In this chapter, the effects of the metal introduction in the M-UVM-7 materials are assessed. The porous silica structure of synthetized materials containing metallic heteroelements has been characterized, as well as the features of metal incorporation in terms of amount, homogeneity, distribution, coordination, and chemical environment. As stated in Chapter 1, different strategies have been explored for metal incorporation. On the one hand, the one-pot procedure of the UVM-7 synthesis allows, in some cases, to introduce the correspondent metal by co-hydrolysis [145,146], thus obtaining Ti-UVM-7 and Fe-UVM-7 materials with the incorporation of titanium and iron respectively. On the other hand, the metal impregnation in a later step has been also studied, in the case of TiO_2-UVM-7 and Au/UVM-7 materials [141,147], for the incorporation of titanium and gold. The properties of the incorporated metals, as well as their effect on the architecture of the final solid, are here explored. It should be noted that, in all metal-containing UVM-7 materials, the surfactant removal was carried out by calcination.

In the same way, as previously stated, the possibility of modifying the mesopore size through the choice of the surfactant gives to the material even more versatility. Indeed, Haskouri et al. [116] described the structure of UVM-7 materials synthetized with different surfactants, although the combination between the pore size modification and the introduction of metal heteroelements at the same time has not been yet studied, and is here presented for the first time.

Besides, the structure of xerogel materials, synthetized in the absence of surfactant, has been also characterized in this chapter in comparison to UVM-7 solids, as well as the incorporation of metals by impregnation in the case of TiO_2-Xerogel material. The properties of the materials with different porous systems were compared in order to test them for analyte retention and understand the role of both the metal incorporation and the porous structure in the final properties of the material for the adsorption of organic compounds.

Finally, xerogels containing cyclodextrins have been previously studied as sorbents for the retention of organic pollutants in environmental matrices [17,166]. Several characterization data, as well as some comments, are also presented in this Chapter (along with Ti-containing materials) for comparative purposes since they have also been applied in further studies (Chapter 5), although these materials are not the specific target of this characterization part.

2. Characterization of silica materials modified with Ti

All synthetized silica materials containing titanium were characterized, paying special attention to Ti25-UVM-7 and Ti50-UVM-7 solids, since they have been used for the development of analytical methods, as later described. Firstly, TEM and HRTEM micrographs were obtained for all Ti-containing UVM-7 materials. In the case of the incorporation of Ti by co-hydrolysis, the heteroelement did not modify the typical architecture of the UVM-7 pure silicas. Representative images of Ti-UVM-7 materials are given in Figure 31 showing the organization based on the aggregation of primary mesoporous nanoparticles, where an additional hierarchic continuous pore system of non-ordered large pores is evidenced, being these images similar to those observed for UVM-7 pure silica (Chapter 2). Specifically, for Ti25-UVM-7 and Ti50-UVM-7 materials, the presence of the pseudo ordered mesopore system was proved with the magnified images (Figure 31A and B), also observing the absence of titanium oxide ordered domains.

Otherwise, in the case of the addition of Ti by impregnation, although the preservation of silica structure is also observed in TEM images (Figure 32A), the introduction of the metal did not lead to a well-distributed organization, thus observing crystalline domains of TiO_2 (Figure 32B). These observations are also supported by the STEM mapping results, which showed a good heteroelement dispersion and a homogeneous distribution of Ti throughout the silica network in the case of Ti-UVM-7 material (Figure 33A), in opposition to the relatively

inhomogeneous dispersion observed for TiO_2-UVM-7 solid (Figure 33B), which could imply important differences in the availability of the titanium as an active site for the retention.

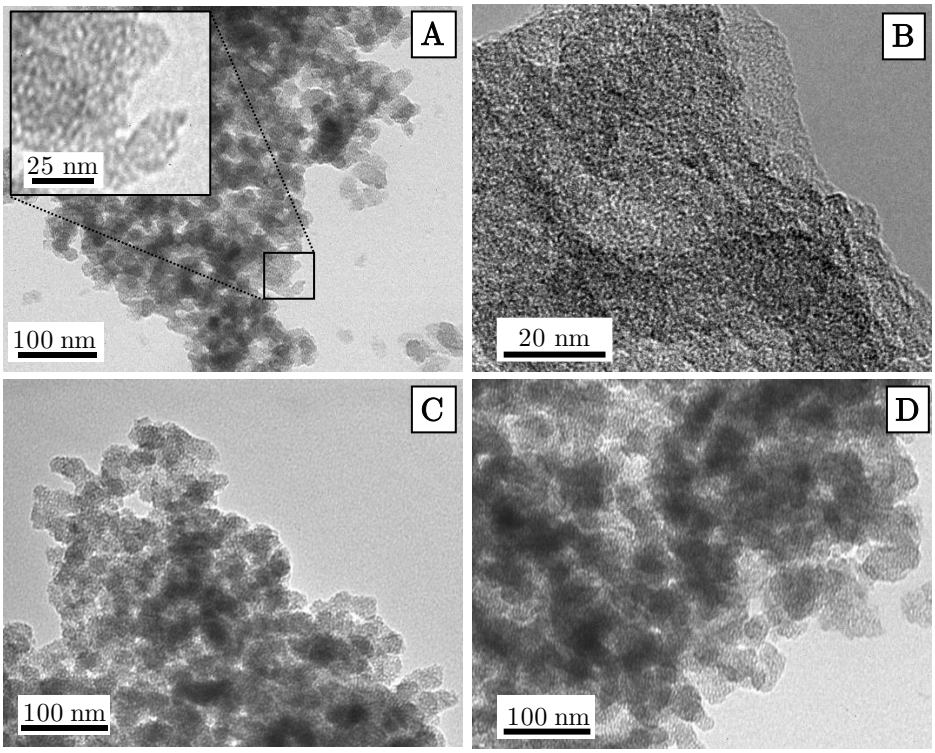

Figure 31. Representative TEM micrographs of Ti50-UVM-7 (A), Ti25-UVM-7 (B), Ti100-UVM-7 (C), and Ti5-UVM-7 (D), with different magnifications, showing that the typical architecture of the UVM-7 material is preserved. Obtained with Jeol JEM-1010 microscope.

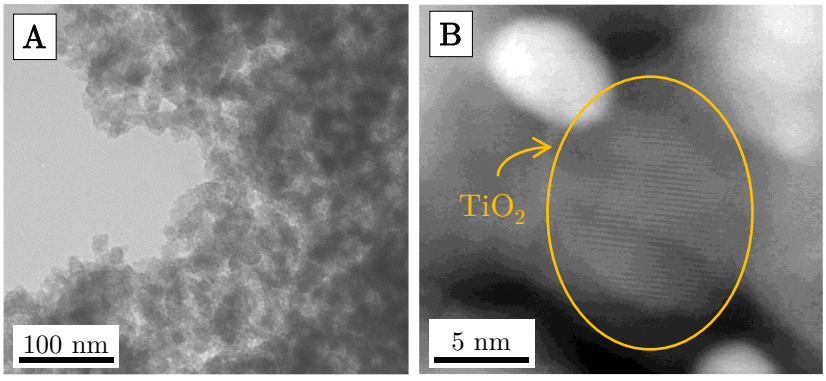

Figure 32. Representative micrographs of TiO_2-UVM-7 material: TEM image (A) and HRTEM image displaying the presence of crystalline TiO_2 nanodomains (of ca. 10-15 nm) (B). Obtained using Jeol JEM-2100F and JEM-1010 microscopes respectively.

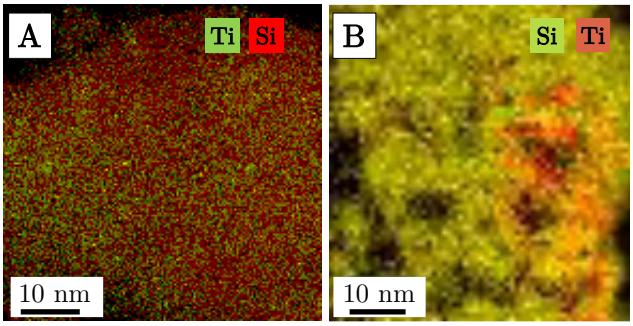

Figure 33. Mapping images of Ti25-UVM-7 (A) and TiO_2-UVM-7 (B) materials showing the differences in the distribution of Si and Ti. Obtained with Philips XL30 ESEM microscope.

On the other hand, in TEM images obtained for xerogels, the differences in both the particle size and the porous architecture were evidenced, showing a microporous structure typical of xerogel silicas, as well as the formation of titanium oxide domains in its addition by impregnation (Figure 34). Similar architecture to the xerogel material was obtained also for β-CD and γ-CD-Xerogel, as characterized in previous works [17,166], thus showing the existence of micrometric particles without well-defined forms containing a homogeneous distribution of small micropores.

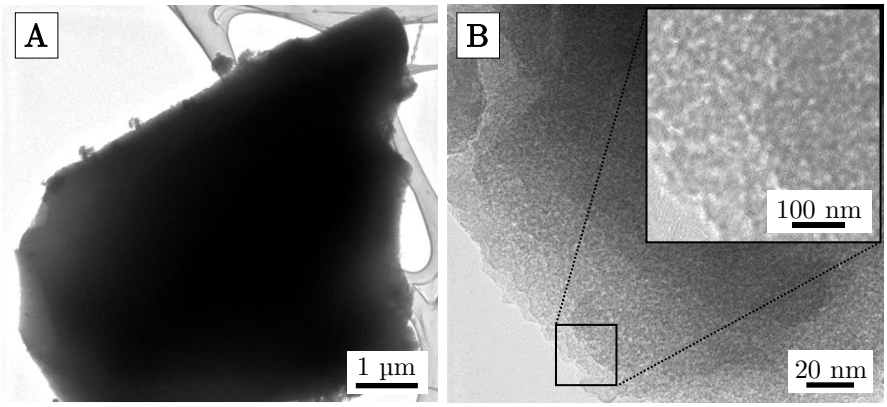

Figure 34. Representative TEM images of the TiO_2-Xerogel material, showing the relatively large size of the particles (A), and the disordered microporous distribution (B). Obtained with Jeol JEM-1010 microscope.

Likewise, the real Si/M ratio was also measured by EDX (Table 15), thus obtaining in all cases metal concentrations higher than theoretical ones, due to the lower solubility of the titanium in comparison to silica, which can lead to an enrichment in the metallic heteroelement. This effect is even more notable when the titanium amount introduced is lower, because of the lower concentration of the metal (thus entailing a lower enrichment). Anyway, real ratios of 22 and 38 (Si/Ti) were obtained for Ti25- and Ti50-UVM-7 materials respectively.

Table 15. Comparison between theoretical and real Si/Ti ratio of synthesized Ti-UVM-7 materials.

Material	Theoretical Si/Ti molar ratio	Measured Si/Ti molar ratio
Ti50-UVM-7	50	38.1
Ti25-UVM-7	25	18.1
Ti10-UVM-7	10	8.2
Ti5-UVM-7	5	4.0

As expected, none of the materials (with UVM-7 or xerogel architecture) have X-ray diffractograms with signals in the high-angle domain. Firstly, this is due to the amorphous nature of the silica-rich pore walls in both silica structures [208] and, on the other hand, because the ordered oxidic domains of TiO_2, present in some of them, are too small to diffract. However, there are clear differences at low angles in their respective diffractograms. As can be seen in Figure 35, the solids with UVM-7-type organization have an intense and broad signal at around 2° (2θ), thus confirming the presence of a hexagonal pseudo-order in the mesopore network (according also to TEM images) typical from these materials, as also observed in the pure materials in Chapter 2. This observation is not affected by the introduction of the material either by co-hydrolysis or impregnation. Otherwise, the absence of any template agent used in the preparation of the xerogels leads to disordered materials [149], both at nano and mesoscale, resulting in the absence of XRD peaks along the complete diffractogram (Figure 36), as also observed for xerogel materials with the incorporation of cyclodextrins [17,166].

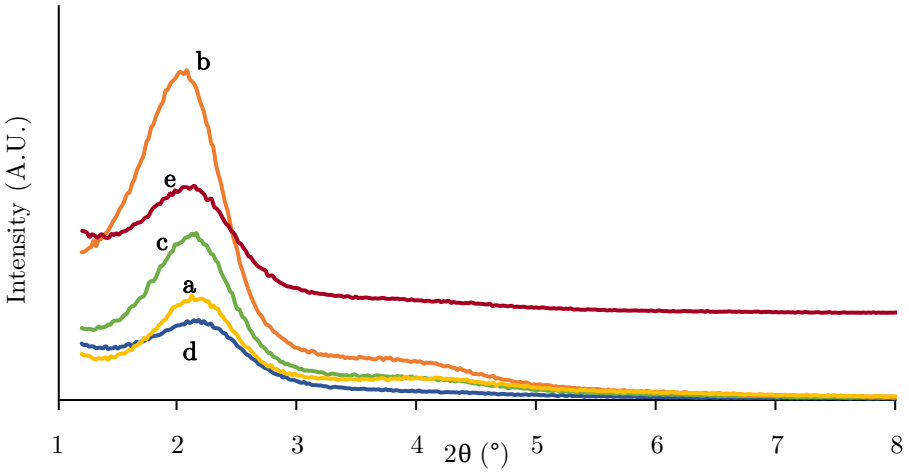

Figure 35. XRD diffractograms of the synthetized Ti-containing UVM-7 materials, obtained from Cu Kα radiation: Ti50-UVM-7 (a), Ti25-UVM-7 (b), Ti10-UVM-7 (c), Ti5-UVM-7 (d), and TiO_2-UVM-7 (e). Obtained with Seifert 3000TT θ-θ diffractometer.

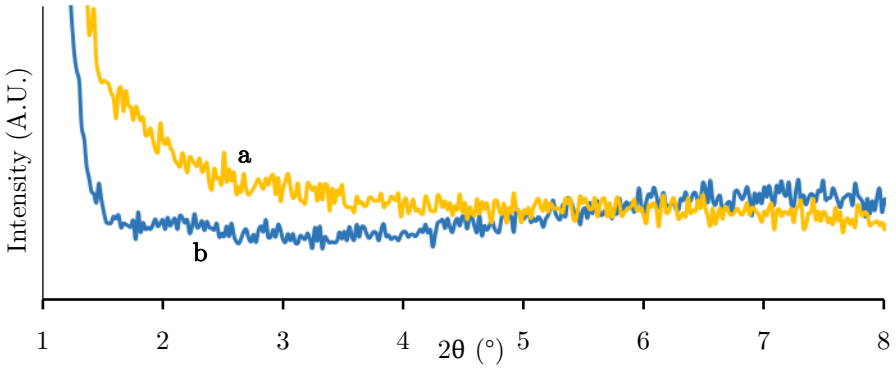

Figure 36. XRD diffractograms of the synthetized xerogel materials, obtained from Cu Kα radiation: Xerogel (a) and TiO_2-Xerogel. Obtained with Seifert 3000TT θ-θ diffractometer.

Then, the surface area and pore-size distribution of the prepared UVM-7 materials were determined from the nitrogen adsorption-desorption isotherms. In all UVM-7 silica-based materials, two adsorption steps were evidenced independently of the metal introduction, thus confirming their bimodal framework and its high accessibility. However, significant differences were observed in some cases for the textural parameters (Table 16). As can be observed, high surface areas were obtained for almost all materials synthetized by co-hydrolysis (between 980 and 1010 m^2 g^{-1}) with mesopores in the range of 2.3-2.7 nm and large macropores in the range 32.8-46.0 nm. However, it should be noted that it is an exception Ti5-UVM-7 material, where a lower surface area and pore volumes and sizes were obtained. It indicates that the titanium introduction does not modify the silica porous structure, except when the introduced amount is high, in which case the morphology is clearly altered. On the other hand, in the case of the titanium addition by impregnation, is important to notice that the modification entails a notable decrease in both surface area and pore size, because of the formation of TiO_2 clusters and the worse distribution of the heteroelement. This effect is even more notable in the case of xerogels since the possible blocking of the small micropores (by TiO_2 nanocrystals) implies a huge decrease in the surface area and pore size. This observation is also confirmed in their isotherms, where the only step observed (because of the unimodal micropores) is clearly affected by the titanium introduction.

It should be also noted that the porosity of xerogels is also deeply affected by the incorporation of bonded cyclodextrins into the structure, as reported in previous works [17,166]. As shown in the table, the introduction of β-CD entails an important reduction in the surface area and a decrease in the pore volume, whilst the addition of γ-CD causes an almost complete loss of both the surface area and the pore volume, because of the pore blocking caused by the cyclodextrin presence, being this effect more notable in the case of γ-CD due to its bigger size.

Table 16. Textural parameters of the Ti-containing silica materials synthetized by different procedures, and the CD-Xerogel materials (calcined UVM-7 data were already presented in Chapter 2).

Material	Surface area (m^2 g^{-1})	Mesopores / Micropores		Macropores	
		Pore size (nm)	Pore volume (cm^3 g^{-1})	Pore size (nm)	Pore volume (cm^3 g^{-1})
UVM-7	1033	2.67	0.83	44.8	1.71
Ti100-UVM-7	1010	2.57	0.56	32.80	1.21
Ti50-UVM-7	995	2.74	0.66	43.60	1.57
Ti25-UVM-7	987	2.72	0.64	42.70	1.53
Ti10-UVM-7	980	2.68	0.40	46.00	0.83
Ti5-UVM-7	743	2.27	0.30	43.90	0.50
TiO_2-UVM-7	880	2.74	0.72	42.0	0.94
Xerogel	952	0.7	0.51	-	-
TiO_2-Xerogel	14	<0.7	0.002	-	-
β-CD-Xerogel	347	0.63	0.17	-	-
γ-CD-Xerogel	< 10	< 0.7	-	-	-

*Surface area estimated according to the BET model. Pore sizes and volumes calculated using the BJH method from the adsorption branch of the isotherms
*Porosity data of CD-Xerogels were already reported in previous works [17,166]

In addition to the support architecture at a mesoscopic scale, the size, shape, and nature of active centers play a key role in the interaction with analytes. Hence, UV-Vis and Raman spectra were obtained for both blank and modified UVM-7 materials, as well as for anatase and rutile TiO_2 as reference. In the case of UV-Vis spectra of Ti-UVM-7 materials (Figure 37), in all solids the presence of both tetrahedral and octahedral titanium centers was confirmed. However, the proportion of octahedral centers was increased when higher amounts of titanium were introduced in the material, being these centers less favored for the interaction with other species such as the phosphate group of the analytes. This behavior is expected, since the introduction of more titanium atoms in the framework could lead to the formation of more Ti-O-Ti bonds, thus conforming octahedral titanium centers and even small domains of TiO_2 [209].

In fact, in the case of Ti5-UVM-7 material where high amounts of titanium were introduced, the presence of anatase domains is clearly confirmed in the Raman spectra, with a defined peak around 615 cm^{-1} (Figure 38). Hence, although the presence of titanium in UVM-7 materials does not imply a modification of their porous morphology, the ratio between octahedral and tetrahedral centers is clearly increased in high Ti-containing materials.

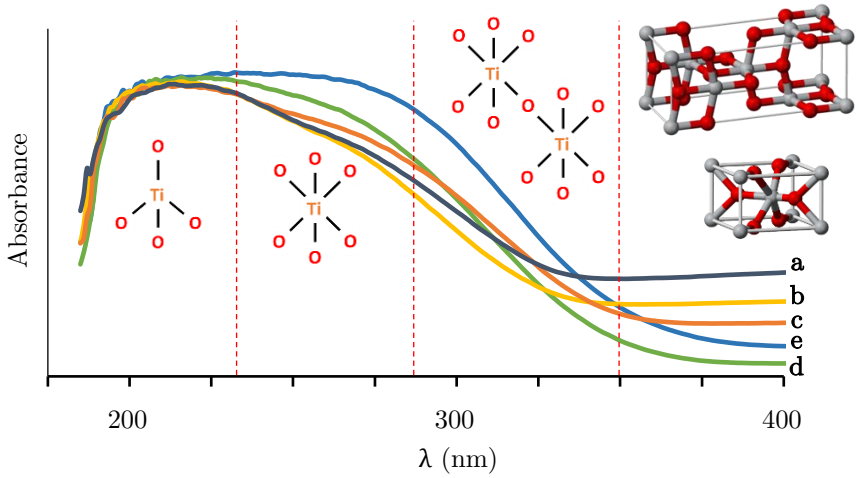

Figure 37. UV-Vis spectra of Ti-UVM-7 materials synthetized by co-hydrolysis, showing the increase of octahedral centers when high amounts of Ti are introduced: Ti00-UVM-7 (a), Ti50-UVM-7 (b), Ti25-UVM-7 (c), Ti10-UVM-7 (d), and Ti5-UVM-7 (e).

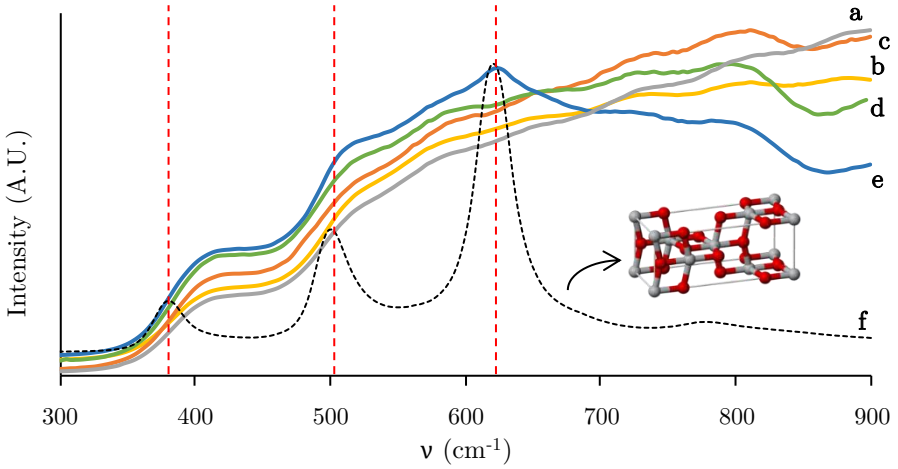

Figure 38. Raman spectra of Ti-UVM-7 materials synthetized by co-hydrolysis and TiO_2 anatase reference: UVM-7 (a), Ti50-UVM-7 (b), Ti25-UVM-7 (c), Ti10-UVM-7 (d), Ti5-UVM-7 (e), and anatase (f). Spectra obtained with a Horiba Jobin Yvon iHR320 spectrometer.

Besides, these characteristic anatase peaks are also observed in the Raman spectra of both Ti-containing materials synthetized by impregnation (TiO_2-UVM-7 and TiO_2-Xerogel), as can be seen in Figure 39. These observations regarding the nature of Ti centers are important for the Ti availability to interact with the analytes, being an important advantage of materials such as Ti25-UVM-7 or Ti50-UVM-7 where the titanium has been incorporated into the silica network by means of isomorphic substitution, leading to a predominance of the tetrahedral environments.

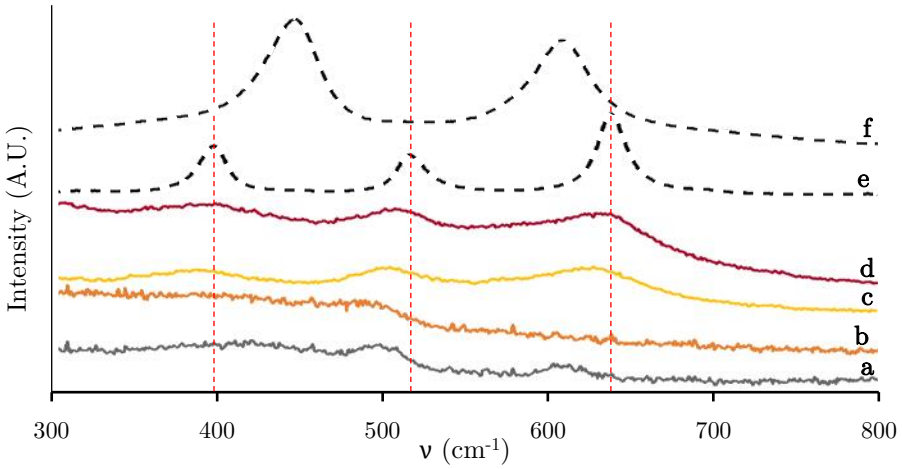

Figure 39. Raman spectra of Ti-containing materials synthetized by impregnation, and TiO_2 and Ti25-UVM-7 as reference: UVM-7 (a), Ti25-UVM-7 (b), TiO_2-Xerogel (c), TiO_2-UVM-7 (d), anatase (e), and rutile (f). Spectra obtained with a Horiba Jobin Yvon iHR320 spectrometer.

3. Characterization of Fe-UVM-7 materials

Iron-containing UVM-7 materials were also characterized, taking into account that the simultaneous incorporation of the heteroelement by co-hydrolysis and the modification of the mesopore size through the use of different surfactants, were considered in this case. Thus, as previously described in Chapter 1, materials with different contents of Fe were synthesized using the C_{16}TAB surfactant. Then, other materials were also prepared with shorter surfactants (C_{12}TAB and C_{10}TAB), keeping the same iron content (Si/Fe nominal molar ratio of 50).

Thus, TEM images were also obtained for all these materials, thus observing that regardless of the Fe content or the surfactant used, the nanoparticulated bimodal porous structure typical of UVM-7 silicas is preserved. All materials present a continuous nanometric organization built from aggregates of small mesoporous nanoparticles that generate a hierarchic non-ordered system of inter-particle large pores. In Figure 40A, B, and C, the micrographs of some of these materials are shown as an example.

The Fe incorporation has been evaluated by EDX, to assess the stoichiometry and chemical homogeneity of the adsorbents. EDX data (see Table 17) showed that all reported samples are chemically homogeneous at the scale spot area (ca. 1 μm). The real Fe content in the final solid is higher than the present in the stock solution. In the case of the solids synthesized with the C_{16}TAB surfactant, an approximately stable increase, in the 30-40% range, is observed. It is also noted that, for an identical nominal molar ratio Si/Fe = 50, when the size of the

surfactant decreases, the enrichment in Fe is somewhat higher: 52 and 62% for the solids prepared with C_{12}TAB and C_{10}TAB, respectively. This fact indicates the preferential incorporation of Fe into the final silica network due to the iron oxide insolubility when compared to that of silica.

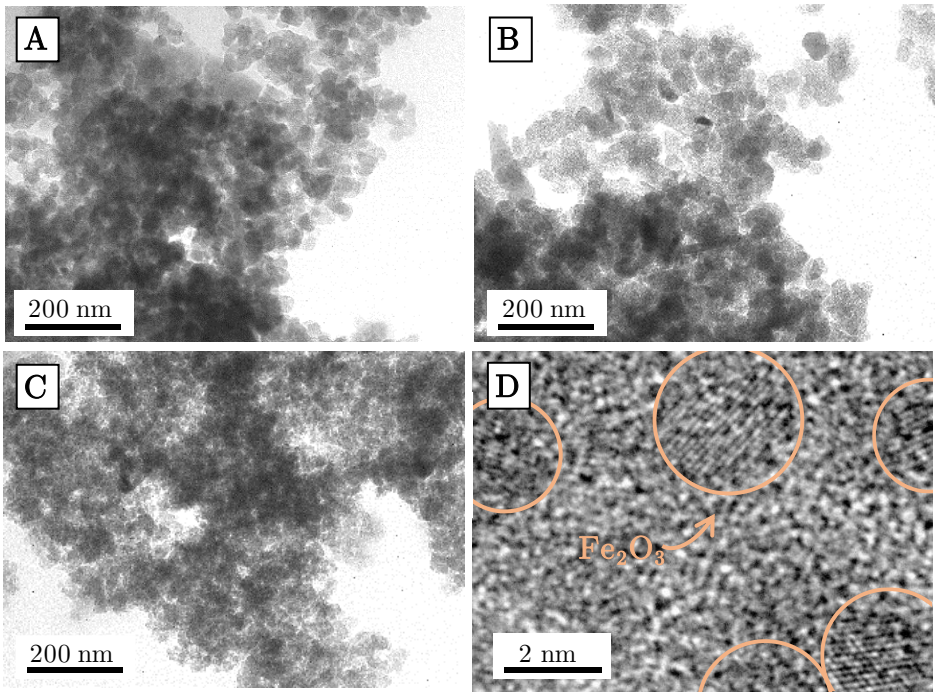

Figure 40. Selected TEM images of some of the synthesized Fe-containing materials: Fe50-UVM-7-C_{16} (A), Fe10-UVM-7-C_{16} (B), Fe50-UVM-7-C_{10} (C), and HRTEM image of the Fe25-UVM-7-C_{16} material. Obtained with a Jeol JEM-1010 microscope.

Table 17. Comparison between theoretical and measured Si/Fe molar ratio of the synthesized materials and d_{100} spacing obtained from XRD diffractograms.

Material	Theoretical Si/Fe molar ratio	Measured Si/Fe molar ratio	d_{100} (nm)
Fe100-UVM-7-C_{16}	100	63	4.12
Fe50-UVM-7-C_{16}	50	29	4.25
Fe25-UVM-7-C_{16}	25	14	4.15
Fe10-UVM-7-C_{16}	10	6	4.18
Fe50-UVM-7-C_{12}	50	24	3.02
Fe50-UVM-7-C_{10}	50	18	2.71

All Fe-containing solids display similar low-angle XRD patterns as other described UVM-7 silicas, with one strong peak, associated with the (100) reflection as discussed, and one broad signal of relatively low intensity (Figure 41), as also explained previously. Regardless of the iron content, the position of the XRD signals is practically unchanged (see d_{100} spacing values in Table 17) for solids synthesized with the same surfactant (C_{16}TAB). Nevertheless, as expected, a gradual shift towards higher 2θ values (lower d_{100} spacing) occurs as the tail length of the surfactants decreases.

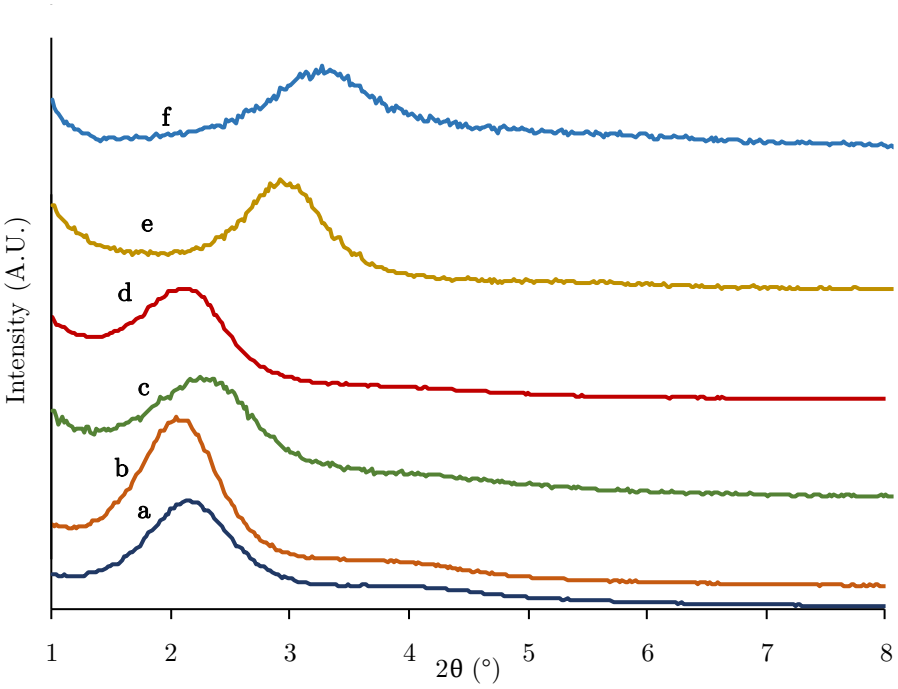

Figure 41. XRD patterns of the synthesized materials measured at low angles: Fe100-UVM-7-C_{16} (a), Fe50-UVM-7-C_{16} (b), Fe25-UVM-7-C_{16} (c), Fe10-UVM-7-C_{16} (d), Fe50-UVM-7-C_{12} (e), and Fe50-UVM-7-C_{10} (f). Obtained with a Bruker D8 Advance diffractometer.

Moreover, taking into account the high-angle XRD patterns of the materials (Figure 42), in the case of the Fe10-UVM-7-C_{16} sample, where the highest content of Fe was introduced, the low-intensity peaks associated with Fe_2O_3 nanodomains are clearly observed, which indicates the presence of iron oxide domains to a greater extent and, subsequently, a worse dispersion of the metal. This observation is also supported by the Raman spectrum of this solid (Figure 43) which clearly shows the presence of hematite-like nanodomains in this solid.

It should be noticed that, although this fact is not observed in the other materials with lower Fe contents, the presence of small nanodomains of iron oxide (Fe_2O_3) is not completely discarded. Indeed, as an example, the Raman spectrum

of the Fe25-UVM-7-C_{16} sample was measured irradiating the material at relatively high energy, and the presence of these hematite-like nanodomains was proved (Figure 44).

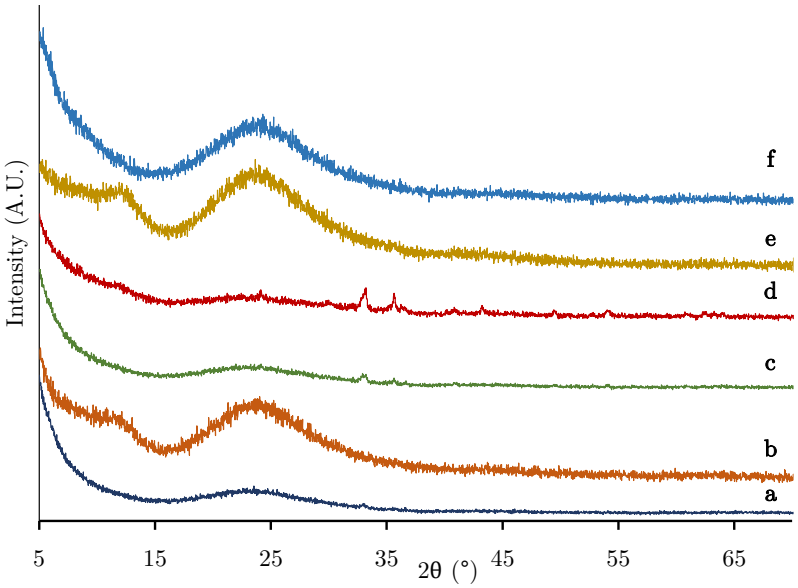

Figure 42. XRD patterns of the synthesized materials measured at high angles, showing the presence of Fe_2O_3 nanodomains in some cases: Fe100-UVM-7-C_{16} (a), Fe50-UVM-7-C_{16} (b), Fe25-UVM-7-C_{16} (c), Fe10-UVM-7-C_{16} (d), Fe50-UVM-7-C_{12} (e), and Fe50-UVM-7-C_{10} (f). Obtained with a Bruker D8 Advance diffractometer.

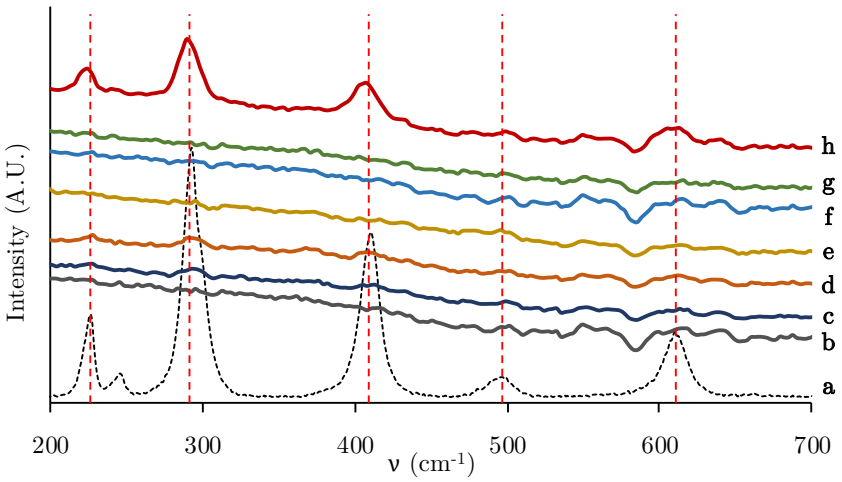

Figure 43. Raman spectra obtained for all Fe-containing UVM-7 materials: Fe_2O_3 hematite reference (a), UVM-7 (b), Fe100-UVM-7-C_{16} (c), Fe50-UVM-7-C_{16} (d), Fe50-UVM-7-C_{12} (e), Fe50-UVM-7-C_{10} (f), Fe25-UVM-7-C_{16} (g), and Fe10-UVM-7-C_{16} (h). Spectra obtained with a Horiba-MTB Xplora spectrometer (785 nm laser excitation source).

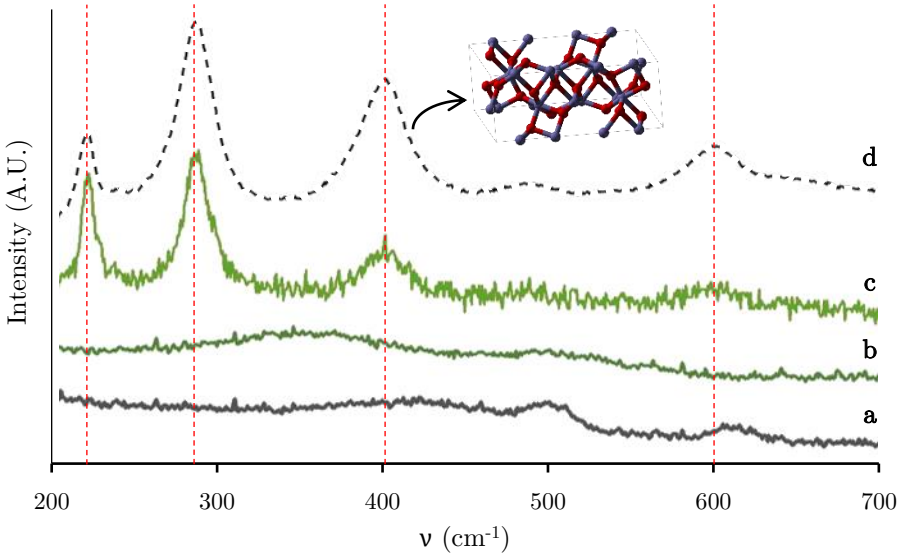

Figure 44. Raman spectra obtained for pure UVM-7 (a) and Fe25-UVM-7-C_{16} irradiated at low energy (b, 15 mW during 10 s) and at relatively high energy (c, 100 s at 30 mW followed by 100 mW during 10 s), with a Fe_2O_3 hematite reference (d). Spectra obtained with a Horiba Jobin Yvon iHR320 spectrometer.

Likewise, although TEM images did not show any heterogeneity on the Fe incorporation, the measurement of the micrographs at high resolution (HRTEM) allowed the observation of the presence of small iron oxide nanodomains, as shown in Figure 40D. However, except for the Fe10-UVM-7-C_{16} sample, the presence of these nanodomains is expected to be negligible in comparison to the amount of iron introduced, thus entailing an almost homogeneous dispersion of the heteroelement in almost all the samples. It could be stated that this fact, in comparison to the complete homogeneity observed for the titanium incorporation, can be explained due to the less favored exchange between Si (IV) and Fe (III) or Fe (II), in comparison to Ti (IV).

The bimodal porous system was further characterized by N_2 adsorption-desorption isotherms (Figure 45). In all cases, the solids show typical curves of UVM-7 silicas, with the two well-defined steps already explained in Chapter 2. All solids show very high BET surface area values, greater than 1000 $m^2\ g^{-1}$, except for solids with higher iron content, in which the area is slightly lower (Table 18). The interparticle pore shows a moderate heterogeneity in sizes and volumes already observed in other UVM-7 type materials. Thus, the mean size is 37.5 ± 9 nm and the volumes are always greater than 1.20 $cm^3\ g^{-1}$, except for the two Fe-richest solids, for which the interparticle BJH volume gradually decreases as the Si/Fe ratio decreases. In any case, taking into account the size of organic pollutants the interparticle pore system does not represent any barrier to their easy diffusion.

More significant differences were seen in intraparticle porosity. The size of the mesopore, as well as the BJH pore volume, is affected both by the incorporation of Fe as well as by the size of the tail of the surfactant used. In the case of materials synthesized from C_{16}TAB, the mesopore size decreases from ca. 2.8 to 2.5 nm by increasing the amount of Fe incorporated. However, the greatest size reduction is observed when modifying the length of the surfactant tail: 2.26 and 2.01 nm when starting from C_{12}TAB and C_{10}TAB, respectively. Hence, we have combined here for the first time, with satisfactory results, the modification with heteroelements and the use of short-chain alkyl trimethylammonium-type surfactants.

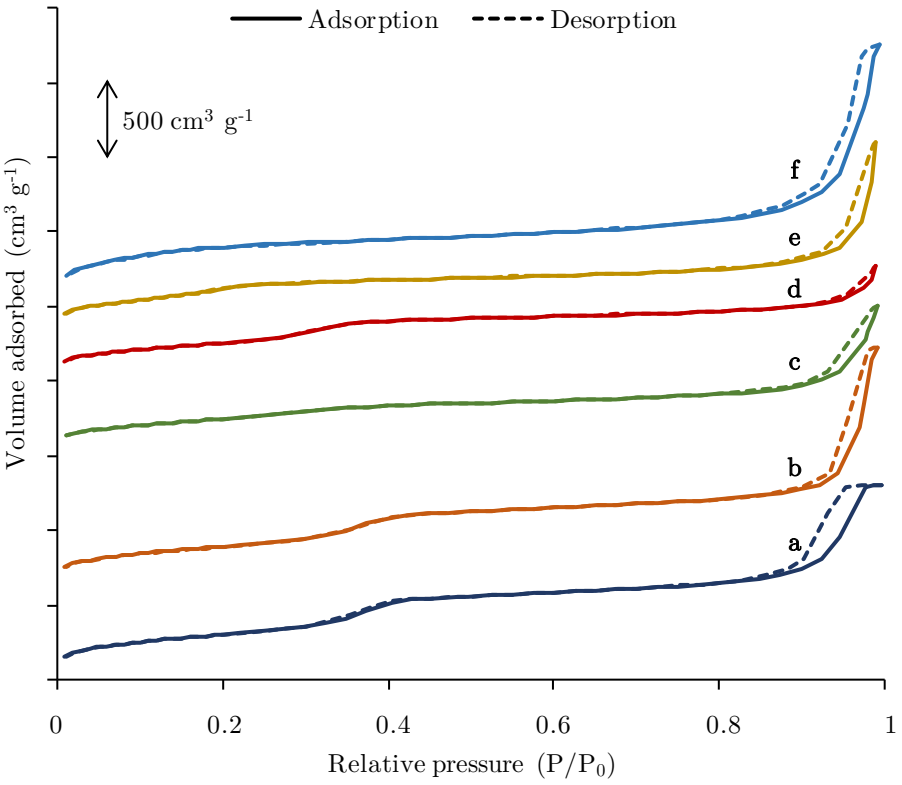

Figure 45. N_2 adsorption desorption isotherms of the synthesized materials: Fe100-UVM-7-C_{16} (a), Fe50-UVM-7-C_{16} (b), Fe25-UVM-7-C_{16} (c), Fe10-UVM-7-C_{16} (d), Fe50-UVM-7-C_{12} (e), and Fe50-UVM-7-C_{10} (f).

Table 18. Textural parameters of the synthesized Fe-containing materials.

Material	Surface area (m^2 g^{-1})	Mesopores		Macropores	
		Pore size (nm)	Pore volume (cm^3 g^{-1})	Pore size (nm)	Pore volume (cm^3 g^{-1})
Fe100-UVM-7-C_{16}	1109	2.81	0.82	27.4	1.20
Fe50-UVM-7-C_{16}	1067	2.83	0.77	44.4	1.75
Fe25-UVM-7-C_{16}	907	2.58	0.45	36.4	1.05
Fe10-UVM-7-C_{16}	931	2.55	0.57	34.9	0.55
Fe50-UVM-7-C_{12}	1171	2.26	3.02	43.3	1.47
Fe50-UVM-7-C_{10}	1046	2.01	2.71	34.7	1.28

*Surface area estimated according to the BET model. Pore sizes and volumes calculated using the BJH method from the adsorption branch of the isotherms

4. Characterization of UVM-7 materials impregnated with Au

The characterization of the appropriate structure of synthesized Au-containing materials was proved, thus assessing the effect of the Au impregnation on UVM-7 and Ti-UVM-7 materials. Firstly, TEM images were obtained for all synthesized materials. As can be seen in Figure 46A, the UVM-7 morphology was proved for all materials (Au/Ti50-UVM-7 is shown in the figure as a representative example), thus observing the characteristic architecture formed by small aggregated mesoporous nanoparticles. Moreover, the Au nanodomains were observed in the case of modified materials, as shown in Figure 46B (HRTEM), as well as in the STEM-HAADF image (Figure 46C). These techniques showed the presence of these Au nanoparticles in the 5-9 nm size range.

In addition, in the case of Au/Ti50-UVM-7 material, the homogeneity of the Ti (already observed in the characterization of Ti-containing materials) and Au incorporation was also evaluated with EDX images, as observed in Figure 47. Worse distribution was observed for non-Ti-containing materials impregnated with Au, as it is shown in Figure 46D, with the formation of larger Au domains, thus proving the anchoring-effect of the Ti-rich domains in the Au impregnation. This favors a good homogeneous dispersion of the gold nanoparticles along the whole silica surface. Moreover, this Ti effect was also corroborated with an estimation of the Au content by EDX. As shown in Table 19, an increase in the Au content was observed when higher amounts of Ti were introduced in the silica structure, being these observations consistent with previous publications [147]. Hence, thanks to the variation in the Ti content of the materials, the synthesis of UVM-7 materials with different Au content has been achieved.

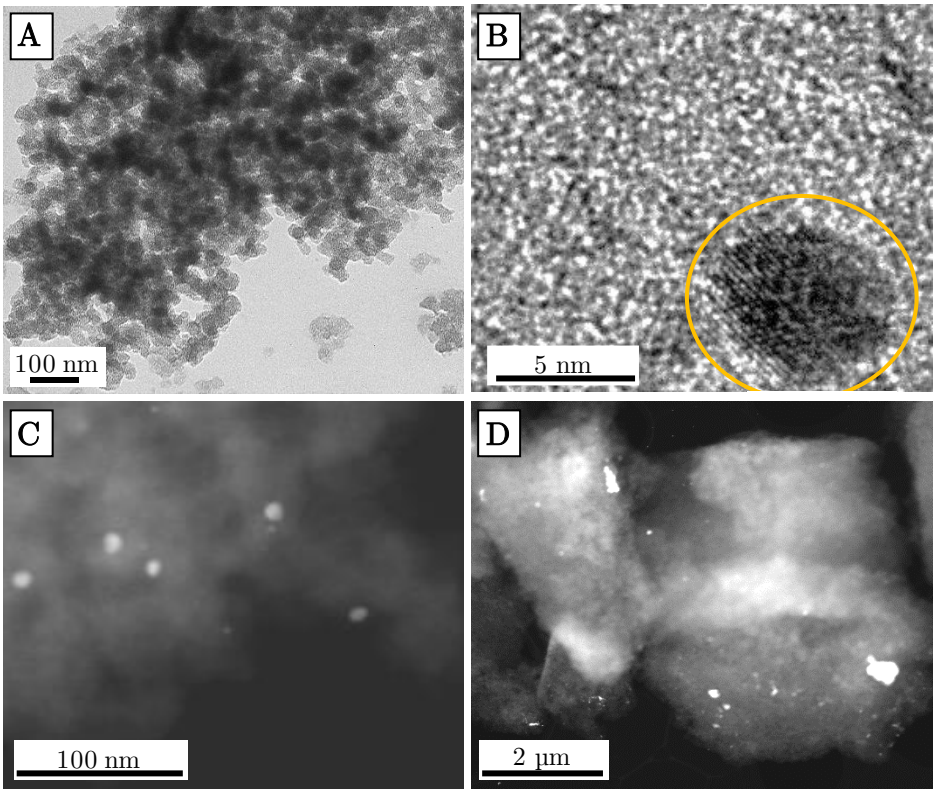

Figure 46. Representative micrographs of Au-containing materials: TEM images of Au/Ti50-UVM-7 material (A, B) and STEM-HAADF images of Au/Ti50-UVM-7 (C) and Au/UVM-7 (D) materials. Obtained with Jeol JEM-1010 and Jeol-2100F microscopes, respectively.

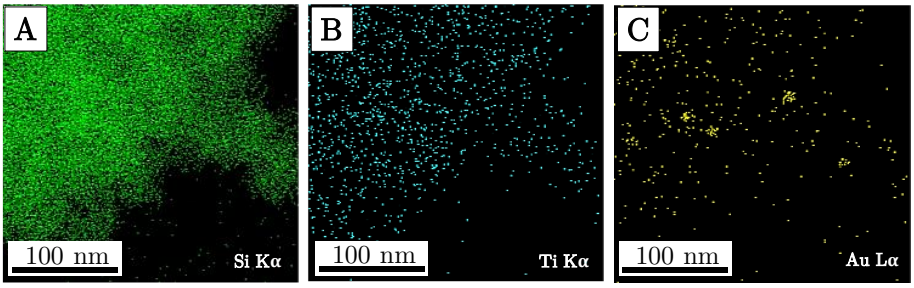

Figure 47. Mapping images of Au/Ti50-UVM-7 material showing the distribution of Si (A), Ti (B), and Au (C). Obtained with Hitachi S-4800 microscope.

Au-containing materials were also characterized by X-ray diffraction, thus confirming the UVM-7 architecture previously presented, as well as by nitrogen adsorption-desorption. In all diffractograms, the characteristic peak appears at ca. 2.2° (2θ) together with a broad signal (a shoulder) of very low intensity (at ca. 4° (2θ)) in the low angle regime. These features indicate the existence of a

certain organization in the intraparticle mesopore system characteristic of highly disordered hexagonal silicas. The intensity and resolution of this peak decrease significantly as the content of Ti (and Au) increases (Au/Ti5-UVM-7). Besides, no X-ray diffraction signals are observed in the high angle zone due both to the amorphous nature of the silica walls, as expected for UVM-7 materials, and also to the small size of the gold nanoparticles.

Moreover, as can be seen in the isotherms of Figure 48 and the textural parameters of Table 19, the presence of mesopores and macropores typical of the UVM-7 architecture was confirmed in all samples. The gold incorporation does not affect the isotherms from a qualitative point of view, except for a slight decrease in the first step because of the slight reduction of the mesopore size. However, depending on the Ti and Au content, certain parameters are modified. The richest Ti and Au sample (Au/Ti5-UVM-7) presents a mesopore size and an intraparticle mesopore volume significantly lower than the rest of the materials. Since this could hinder the accessibility of the analytes to the active centers, Au/Ti50-UVM-7 sample is expected to be the optimal one for the analytical study.

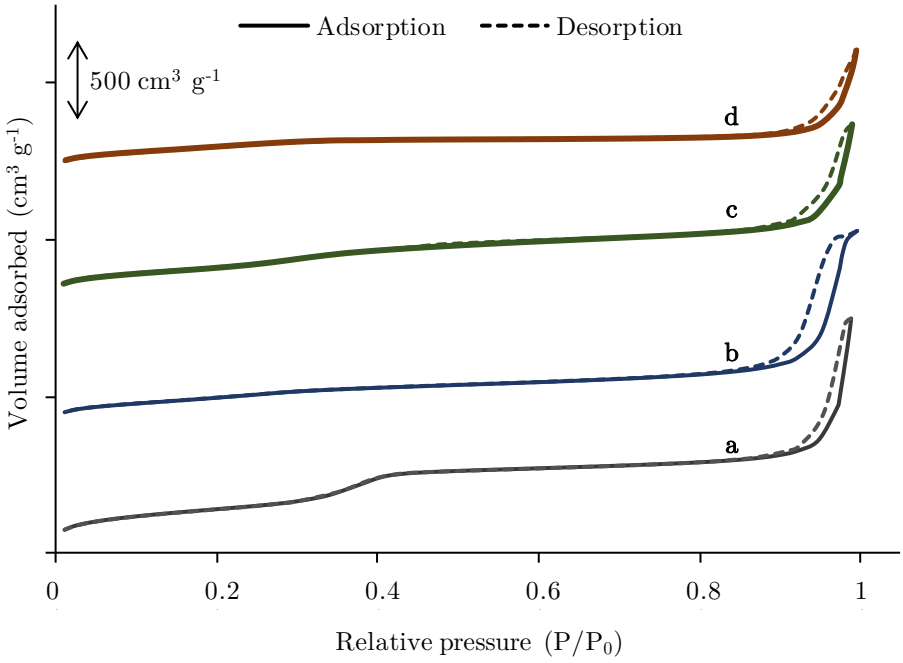

Figure 48. N_2 adsorption-desorption isotherms of the synthesized Au-containing materials: UVM-7 (a), Au/UVM-7 (b), Au/Ti50-UVM-7 (c), and Au/Ti5-UVM-7 (calcined UVM-7 data were already presented in Chapter 2).

Table 19. Textural parameters of the Au-containing silica materials synthetized (calcined UVM-7 data were already presented in Chapter 2).

Material	Surface area (m^2 g^{-1})	Mesopores		Macropores		Si/Au
		Pore size (nm)	Pore volume (cm^3 g^{-1})	Pore size (nm)	Pore volume (cm^3 g^{-1})	
UVM-7	1033	2.67	0.83	44.8	1.71	-
Au/UVM-7	718	2.71	0.53	36.76	1.61	1151
Au/Ti50-UVM-7	811	2.78	0.67	35.09	1.25	699
Au/Ti5-UVM-7	722	2.29	0.34	51.76	0.92	161

*Surface area estimated according to the BET model. Pore sizes and volumes calculated using the BJH method from the adsorption branch of the isotherms

5. Conclusions

The synthesized materials have been properly characterized and the main features of the metal incorporation have been assessed. On the one hand, the homogeneous incorporation of the titanium to UVM-7 structure through co-hydrolysis has been proved, as well as the preservation of the bimodal porous structure of the UVM-7 (Figure 49A). Thus, materials with a real Si/Ti molar ratio from 4 to 38 have been successfully obtained, and the formation of TiO_2 nanodomains has been only observed when high amounts of metal were incorporated. Besides, the predominance of tetrahedral environments of the Ti centers has been proved for the materials with moderate contents of heteroelement (Ti25-UVM-7 and Ti50-UVM-7), which is expected to imply more favorable interactions with the analytes. On the other hand, the incorporation of the titanium by impregnation in a later step has not provided a homogeneous dispersion due to the formation of larger domains of TiO_2 (Figure 49B). It implies the partial pore blocking in the UVM-7 materials, and the complete blocking of the microporosity of the xerogels. Thus, these materials are expected to be less favored for the proper retention of the analytes. In this sense, the structure of the xerogels has been also characterized, thus showing the disordered microporous network. The functionalization of these materials has been also studied, through the addition of both Ti and cyclodextrins, and the pore blocking of the micropores has been observed in both cases, which is expected to be an important drawback for their use as sorbents (Figure 50).

Although the addition of Fe by co-hydrolysis has also led to homogenous metal incorporation, the formation of small nanodomains of Fe_2O_3 is not discarded in this case, due to the less favored substitution of the Fe (II) and Fe (III) with Si (IV), in comparison to Ti (IV). However, except for the material with a high amount of Fe, this fact is expected to be negligible considering the total amount

of metal incorporated, and the UVM-7 bimodal structure is preserved in all cases (Figure 49C). In this way, the incorporation of the iron with the simultaneous modification of the mesopore size has been successfully carried out for the first time. The use of short-chain surfactants has proved to provide materials with the desired content of Fe and the same bimodal structure as the UVM-7, with a reduction on the mesopore size (from 2.8 to 2.26 and 2.01 for Fe50-UVM-7-C_{12} and Fe50-UVM-7-C_{10}, respectively).

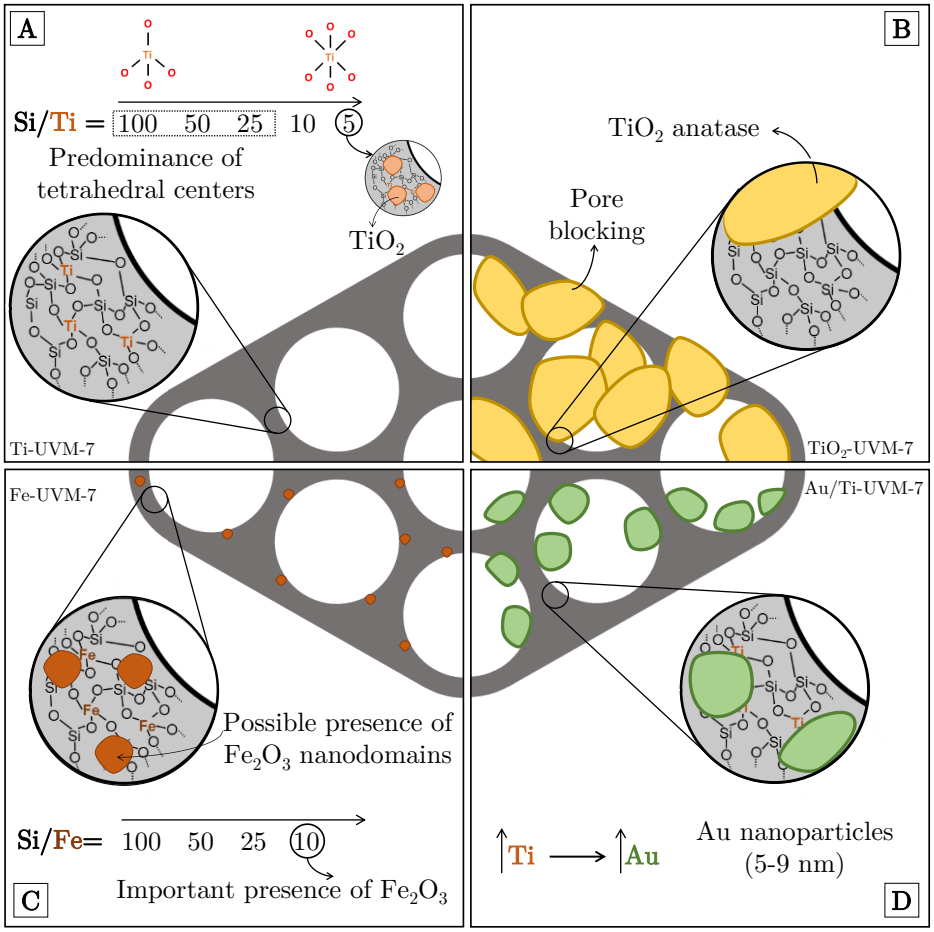

Figure 49. Schematic representation of the characterized structure for Ti-UVM-7 materials (A), TiO_2-UVM-7 solid (B), Fe-UVM-7 materials (C), and Au/Ti-UVM-7 materials (D).

Finally, the incorporation of Au nanoparticles through an impregnation procedure has also led to materials that preserve the UVM-7 structure (except for partial blocking of the mesopores), with the presence of Au nanoparticles of 5-9 nm of diameter (Figure 49D). The Ti key role on the Au incorporation (regarding both amount and homogeneity) has been proved, and materials with

different Au contents have been successfully synthesized through the modulation o the Si/Ti ratio of the precursor material.

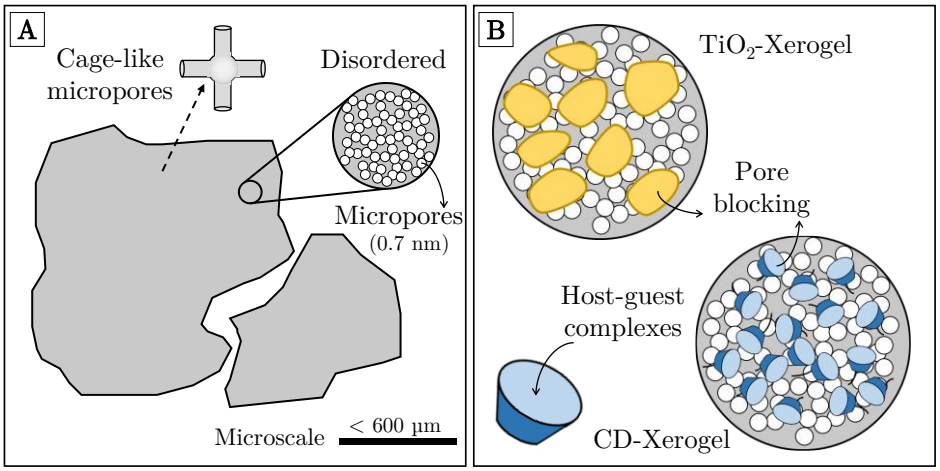

Figure 50. Schematic representation of the characterized structure for xerogel materials (A), and their modifications with Ti and cyclodextrins (B).

Chapter 5

Evaluation of metal-containing UVM-7 materials for pesticide determination in environmental analysis

1. Introduction

Nowadays, pesticides are widely used not only in agriculture but also in many areas of life. The range of applications of pesticides is continually expanding, and their consumption is ever growing since the increase in the population on the Earth entails a greater food demand. Besides, due to their resistance to environmental degradation, they have become one of the most concerning organic micropollutants [8]. Among them, organochlorine pesticides (OCPs) are characterized by containing chlorine groups in their structure and comprise mainly dichlorodiphenylethanes, chlorinated cyclodienes, chlorinated benzenes, and chlorinated cyclohexanes (Figure 51) [210]. Even though these pesticides have been used for more than a half-century for pest and insect control, their toxicity and persistence have forced their banning or restriction, since they have clearly demonstrated to cause several adverse effects in human health, such as endocrine-disrupting effects, cancer, or neurodegenerative disorders [8,211].

Indeed, as mentioned, many of them were banned in the Stockholm Convention, and their agricultural or domestic usage is not allowed in many European countries [4], such as DDT, aldrin, endrin, or chlordane. Nevertheless,

some specific OCPs, especially DDT and hexachlorocyclohexanes (HCHs), are still allowed in several countries around the world, and in 2005 about 1% of all applied pesticides were still OCPs. This fact, jointly with their considerable longevity (up to 30 years) and their long-range transportation by air and water, makes their environmental control and vigilance recommendable [8,212].

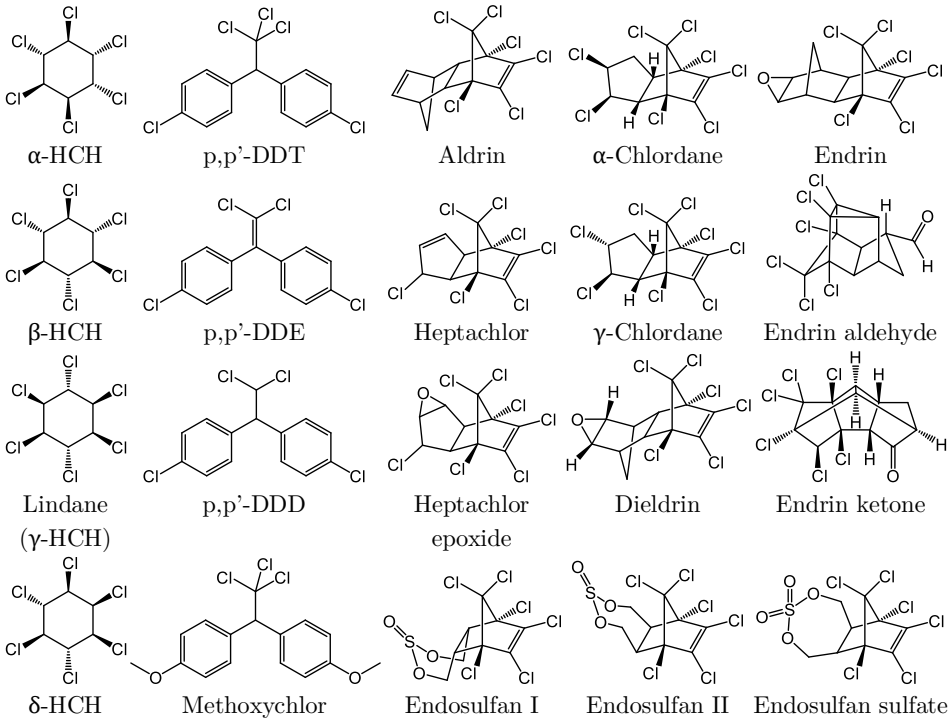

Figure 51. Molecular structures of the studied OCPs.

Moreover, the restriction of OCPs has caused their replacement by other compounds such as organophosphorus (OPPs) or organonitrogen pesticides (ONPs). They have become very popular because they are cheap and readily available, have a wide range of efficacy, are able to combat a large number of pest species, and have a shorter environmental half-life than their organochlorine predecessors. Among them, one of the principal classes of compounds used as insecticides is OPPs. This term embraces all P-containing pesticides, usually in the form of esters (Figure 52). It is estimated that OPPs are worth nearly 40% of the global market and they are expected to maintain dominance for some time into the future. Because of that, the presence of OPPs in water, air, or soil, has become an important risk to public health, due to their highly toxic effects on humans and other organisms [8,213,214].

Owing to the importance of this problem, pesticide use is regulated in Europe by the European Commission [215], although each country may have its own regulation for a specific pesticide. However, their emission to the environment is

still constant because of their increasing use, mostly during their spray application, since the percent of pesticide released to the ambient air can reach 20-30%. In addition, depending on their physicochemical properties and other environmental factors, they can be present both in particulate matter and air phase, mainly in the case of OPPs that are semi-volatile compounds [216]. Thus, their presence in air entails an important exposure risk by inhalation for the population, and mainly for sprayer operators, who are directly and constantly exposed both environmentally and occupationally [214,217]. For this reason, Spanish legislation set occupational exposure limits (OELs) for some of these compounds in the range 0.01-10 mg m^{-3}, although there are many pesticides not covered by these values [27,218]. In these cases, other OELs can be found, established by other organisms or pesticide companies, being in line with European legislation, as in the case of methyl-chlorpyrifos [219].

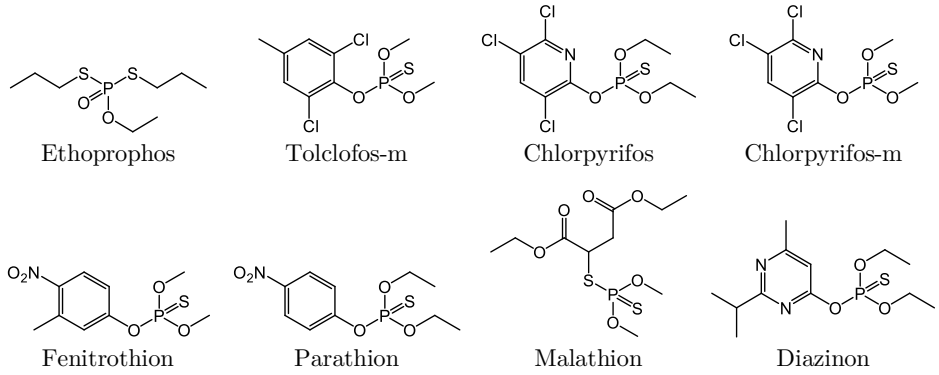

Figure 52. Molecular structures of the studied OPPs.

Likewise, the pesticide emission to the air, as well as their adsorption in soils, can cause water contamination, and because of that, the presence of residues of these compounds in water must be controlled and monitored. Indeed, the European legislation is very strict regarding allowed limits, fixing a general limit of 0.1 and 0.5 µg L^{-1} for individual and total pesticide concentration respectively in case of human consumption and groundwater, being these limits lower (0.03 µg L^{-1}) in the case of some OCPs such as aldrin, dieldrin, heptachlor, and heptachlor epoxide [23,24]. Also, in the case of surface water, several phosphorus, nitrogenous, and chlorinated pesticides are registered, and limits below 0.05 µg L^{-1} are considered in all cases for these listed compounds [22]. Likewise, similar regulations are considered in other countries, with higher permitted concentrations in certain cases [25]. Thus, regarding their occurrence in water samples, OCPs are not used to be found in European countries because of their strong regulation, with concentrations in the range of 50 ng L^{-1}, being these concentrations much higher in sediment samples due to the lipophilic nature of these compounds. However, larger concentrations were found in other regions such as Asian or African countries, with concentrations even above 500 µg L^{-1}. Besides, in the case of OPPs, their occurrence is significantly higher in developed countries

due to their extended use, with concentrations ranging from a few ng L^{-1} to more than 500 ng L^{-1}, also in European countries such as Spain [8,210,220].

Since these compounds have been used for a long time, there are many developed methods for their analytical determination, mainly based on liquid (LC) or gas chromatography (GC). Although OPPs can be determined either by LC or GC due to their semi-volatile nature, in the case of OCPs the GC is the most used technique taking into account their volatility and stability [8,210]. These chromatographic techniques have been widely used combined with selective detectors, such as the nitrogen-phosphorus detector (NPD) or the flame photometric detector (FPD) in the case of organophosphorus compounds, or the electron capture detector (ECD) in the case of chlorine-containing pesticides, being these detectors proposed in several reported and official methods [8,213,221–226]. However, the emergence of more sophisticated instrumentation has entailed the migration to the use of mass spectrometry detectors (MS), widely used now in most of the methods [8,65,216,227–231].

Moreover, despite the good sensitivity achieved with this instrumentation, generally, pesticides are at low concentration both in air and water matrices, which makes necessary the utilization of proper sampling and sample treatment strategies in order to preconcentrate them. Regarding air sampling, these techniques are based on the use of materials as trapping sorbents for analyte retention both in environmental and occupational analysis. As described, these sampling strategies could be either passive (diffusive) or active by pumping air through the material, thus retaining these pollutants. In these cases, several sorbent polymeric phases have been used for trapping OPPs from the air, such as PUF or XAD-4. However, the most used material is the cross-linked polystyrene resin XAD-2, being this sorbent used in most of the sampling methodologies recommended by official organizations such as NIOSH [65,117,118]. Also, and regarding the later desorption of the retained analytes, several solvent-consuming techniques have been used, being the most common the Soxhlet extraction [213], pressurized liquid extraction [65], or microwave-assisted extraction [230].

A similar case is the water analysis, where the determination of both OPPs and OCPs in water sources with complex matrices requires the development of pretreatment and clean-up steps in order to enhance sensitivity. In this sense, liquid-liquid extraction methods have been commonly used for pesticide extraction with solvents such as dichloromethane, hexane, or toluene, including modifications of this technique such as liquid-liquid microextraction (LLME or DLLME). However, the use of large amounts of harmful solvents has caused its substitution by other techniques based on solid-phase extraction (SPE), due to its many advantages such as low solvent consumption and high enrichment factors [8,232]. Other similar sample pretreatment methods have been also proposed, such as solid-phase microextraction (SPME) [223,233], micro solid-phase extraction (μ-SPE) [228,229,234], or stir bar sorptive extraction (SBSE) [8,227], although the high sample volumes used in water analysis makes necessary the use of larger

amounts of sorbent with the classical SPE. In that way, the conventional C18 or polymeric cartridges used in most published and official methods for this purpose [67,69,70,224,235–237] present some disadvantages, such as limited selectivity and poor reusability. Because of that, other materials have been proposed as an alternative, such as ionic liquids, carbon nanotubes, or molecularly imprinted polymers [8,227,235,238]. In this sense, there is considerable interest in developing new selective and efficient materials for extracting and isolating pesticides from complex environmental matrices, as well as for their retention from air samples [239].

For this purpose, the versatility of sol-gel chemistry offers great possibilities, since it enables us to generate a wide range of silica materials with controlled structure, morphology, and porosity [112], which have allowed their application for the retention of pesticides [240,241]. Likewise, these materials can be easily modified, for instance with the introduction of cyclodextrins, in order to retain environmental pollutants either in air or water samples [17,20,166].

On the other hand, mesoporous silica materials and, among them, UVM-7 solids, offer interesting features for their utilization as sorbents for the adsorption of both small and large molecules, as discussed in Chapter 4. Moreover, as also stated, the introduction of metallic heteroelements either by co-hydrolysis or by impregnation extends, even more, their scope as selective sorbents. In this sense, regarding OPPs retention and extraction, the addition of titanium and iron to the silica network, widely used in several adsorption processes due to their chemical affinity for phosphate groups, should increase the adsorption properties of the material [242,243]. In this way, as commented, Ti-UVM-7 materials have been already used for the retention of phospholipids in food matrices [161], although their application as SPE sorbents for the determination of organic pollutants such as pesticides in environmental samples has not been yet proposed.

Besides, the introduction of Au nanoparticles in the sorbent structure can be also useful for the retention of OCPs due to the presence of chlorine groups in their structure. Thus, some works have used Au-containing sorbents for the retention of OCPs by SPME [223] or as electrochemical sensors [244,245]. However, the use of Au/UVM-7 materials to develop an SPE method has not been yet studied, as well as its application to OCPs extraction.

2. Materials, reagents, and instrumentation

All organophosphorus pesticides were purchased as individual standards, being ethoprophos, diazinon, methyl chlorpyrifos (chlorpyrifos-m), methyl tolclofos (tolclofos-m), malathion, and parathion from Sigma-Aldrich (St. Louis, MO, USA) and fenitrothion and chlorpyrifos from LGC Standards (Teddington, Middlesex, UK). A standard stock multicomponent solution of OPPs was prepared in acetonitrile. On the other hand, in the case of organochlorine

pesticides, a standard OCP mix was purchased from Supelco (Bellefonte, PA, USA) containing 2000 mg L^{-1} of the 20 target pesticides in toluene:hexane (50:50, v/v): α-HCH, β-HCH, γ-HCH (lindane), δ-HCH, heptachlor, aldrin, heptachlor epoxide, α-chlordane, γ-chlordane, endosulfan I, p,p'-DDE, dieldrin, endrin, endosulfan II, p,p'-DDD, endrin aldehyde, endosulfan sulfate, p,p'-DDT, endrin ketone, and methoxychlor. Diluted solutions of OCPs were prepared with ethanol for all studies. All pesticide solutions were stored refrigerated in darkness.

During all optimization, sampling, and sample analysis steps, all solvents were used in HPLC grade, namely ethanol (EtOH), ethyl acetate (EtOAc), acetonitrile (ACN), acetone, n-hexane, dichloromethane (DCM), methanol (MeOH), tetrahydrofuran, purchased from Scharlau (Barcelona, Spain), VWR Chemicals (Radnor, PA, USA), Panreac AppliChem (Darmstadt, Germany), and Lab-Scan Analytical Sciences (Gliwice, Poland). Ultrapure water from an Adrona (Riga, Latvia) purification system was also employed. Besides, NaOH and HCl were purchased from Merck (Darmstadt, Germany) and diluted with ultrapure water before their use.

In addition, for the air sampling study, XAD-2 samplers were used as a reference method, obtained from SKC Inc. (Eighty Four, PA, USA), and containing 100/50 mg (front and backup section respectively). Likewise, in the case of water analysis for both OPP and OCP studies, commercial C18 cartridges containing 200 mg of sorbent were used as a reference method for pesticide enrichment, being them from Varian Bond Elut and Scharlau respectively.

For the air sampling step, APEX and TUFF Standards pumps were used from Casella (Kempston, England). An ultrasonic bath Elmasonic S40 (Singen, Germany), as well as a Vibromatic-Selecta wrist shaker and a rotator stirrer from JP Selecta (Barcelona, Spain), were also used for the analyte desorption. Besides, for SPE protocols, a vacuum pump system was used connected to a Vac Elut 20 chamber. Polyamide filters from Sartorius Stedim Biotech (Goettingen, Germany) with 0.45 µm pores were used for the filtration of the extract in air analysis, as well as for water samples filtration. Also, a miVac sample concentrator from SP Scientific (Warminster, PA, USA) was used for solvent evaporation.

OPPs were determined using an Agilent 7890A GC system from Agilent Technologies Inc. (Santa Clara, CA, USA) equipped with an ALS-7693A autosampler and an NPD system. For their separation, an analytical column Agilent HP-5 (30 m x 0.32 mm x 0.25 µm film thickness) was employed, using nitrogen as carrier gas at 1 mL min^{-1} flow rate. Sample injection (0.5 µL) was carried out in splitless mode using the following temperature gradient: 60 °C for 1 min, followed by a ramp at 5 °C min^{-1} up to 170 °C (hold 3 min), and ramp at 2 °C min^{-1} to 195 °C (hold 1.5 min). Under these conditions, a good resolution was achieved for all pesticides except for chlorpyrifos and parathion pair in the case of the water samples study (see Figure 53).

On the other hand, for air sample analysis in the occupation risk assessment study, a Focus GC gas chromatograph from Thermo Fisher Scientific (Waltham, MA, USA) with a DSQ II mass spectrometry detector was used. The separation of the analytes was carried out under the same conditions indicated above, working on selective ion monitoring mode. Likewise, in the case of the determination of OPPs in water samples, some analytical figures of merit were evaluated using an Agilent 7890B gas chromatograph coupled to an Agilent 5977A single quadrupole MS detector. For this purpose, the same separation conditions indicated above were used and selective ion monitoring mode was also employed. The specific ions monitored for each pesticide in each equipment are given in Table 20.

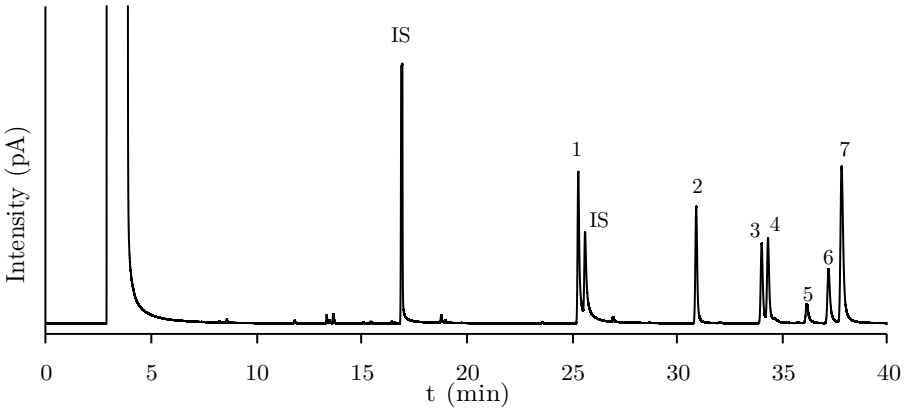

Figure 53. Example chromatogram of the GC-NPD system showing the separation of the analytes in the described conditions: ethoprophos (1), diazinon (2), tolclofos-m (3), chlorpyrifos-m (4), fenitrothion (5), and malathion (6). Chlorpyrifos and parathion (7) were not differentiated with this equipment.

Table 20. Monitored ions of each target OPP in both GC-MS equipment.

Compound	Monitored ions (m/z)	
	Focus DSQ II detector	Agilent 5977A detector
Ethoprophos	97, 158, 200	97, 139, 158
Diazinon	137, 152, 179, 199, 304	137, 152, 179
Chlorpyrifos-m	125, 286, 287	125, 286, 288
Tolclofos-m	250, 265, 267	250, 265, 267
Fenitrothion	109, 125, 260, 277	109, 125, 158, 277
Malathion	93, 125, 126, 158, 173	93, 125, 173
Chlorpyrifos	97, 197, 198, 314	197, 314, 349
Parathion	-[a]	97, 109, 291

[a]Not measured in that study

Also, to evaluate the non-retained OPPs remaining in water samples, a LaChrom chromatograph was used from Hitachi (Chiyoda, Tokyo, Japan), which was equipped with a LaChrom L-7100 pump, a Hitachi oven, a VWR L-7614 degasser, an Agilent Interface 35900E processer, and a LaChrom L-7614 UV-Vis detector at 225 nm. The separation was carried out using a C18 ZORBAX Eclipse Plus column from Agilent (4.6 x 100 mm, 3.5 µm particle size) at 30 °C and at a constant flow of 1 mL min^{-1}, with MeOH:water as mobile phase under the following elution gradient conditions: from 0-7 min from 50:50 (v/v) MeOH-H_2O increasing progressively up to pure MeOH (to 60:40 (v/v) for 7-12 min; 80:20 (v/v) for 12-15 min, and 100% MeOH for 2 more min). The injection volume was 20 µL. In this case, all analytes were separated properly under described conditions.

In the case of OCPs instrumental determination, a Thermo Scientific Trace GC Ultra gas chromatograph coupled to an electron capture detector (ECD) with a ^{63}Ni source was used. The separation of the analytes (Figure 54) was achieved with the same Agilent HP-5 column as above, but using the following modification of a temperature program previously described [221]: 100 °C for 5 min, followed by an increase to 250 °C at a rate of 5 °C min^{-1}, next at 20 °C min^{-1} to 270 °C. The injection volume was 0.3 µL in splitless mode (splitless time of 1 min), nitrogen at constant pressure (110 kPA) was used as the carrier gas, and the detector was set at 300 °C (250 °C for base temperature).

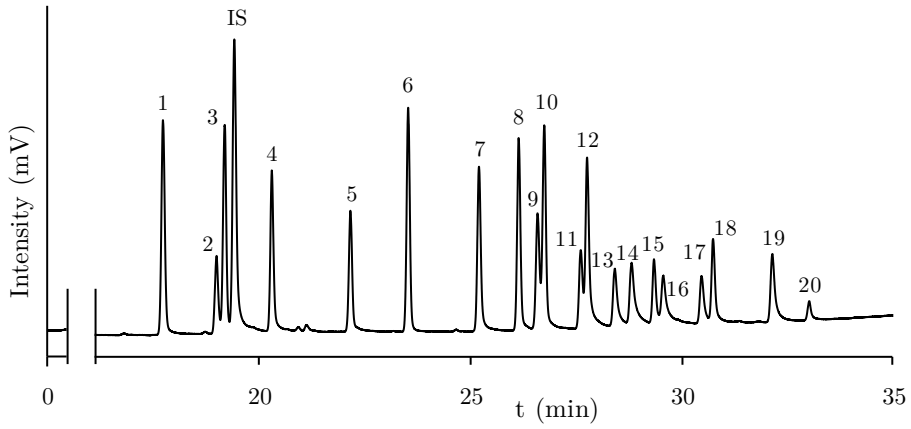

Figure 54. Example chromatogram of the GC-ECD system showing the separation of the analytes in the described conditions: α-HCH (1), lindane (2), β-HCH (3), δ-HCH (4), heptachlor (5), aldrin (6), heptachlor epoxide (7), γ-chlordane (8), endosulfan I (9), α-chlordane (10), dieldrin (11), p,p'-DDE (12), endrin (13), endosulfan II (14), p,p'-DDD (15), endrin aldehyde (16), endosulfan sulfate (17), p,p'-DDT (18), endrin ketone (19), and methoxychlor (20).

Likewise, samples were also injected in an Agilent 7890B gas chromatograph coupled to an Agilent 5977A single quadrupole MS detector. In this case, 2 µL of

extract were injected in split mode (split ratio 30:1), and the separation was carried out with helium as carrier gas and using the same temperature program previously mentioned. The MS detector temperature was established at 230 °C for source temperature and 150 °C for quadrupole temperature, with a fixed electron energy of 70 eV. The detector was programmed in selective ion monitoring mode, and the specific parameters and ions monitored for each pesticide are given in Table 21. This instrumentation was employed only for real sample analysis to confirm the presence or absence of target OCPs.

Table 21. Specific ions monitored for each pesticide in GC-MS analysis.

Compound	Monitored ions (m/z)	Dwell time (ms)
α-HCH	51, 109, 111, 181, 217, 219	50
β-HCH	51, 109, 111, 181, 217, 219	50
Lindane	51, 109, 111, 181, 217, 219	50
δ-HCH	51, 109, 111, 181, 217, 219	50
Heptachlor	100, 135, 237, 272, 337, 372	55
Aldrin	66, 91, 263, 293, 364, 366	55
Heptachlor epoxide	81, 151, 153, 237, 263, 386, 390	55
γ-Chlordane	237, 263, 272, 301, 375, 377, 410	60
Endosulfan I	195, 197, 265, 339, 406	60
α-Chlordane	237, 263, 272, 301, 375, 377, 410	60
Dieldrin	79, 263, 277, 279, 345, 380, 382	60
p,p'-DDE	105, 176, 210, 246, 248, 281, 316, 318, 320	60
Endrin	243, 245, 263, 281, 317, 345	60
Endosulfan II	159, 195, 241, 339, 406	65
p,p'-DDD	164, 195, 235	65
Endrin aldehyde	250, 279, 343, 345, 347	65
Endosulfan sulfate	229, 272, 387, 420, 422, 424	65
p,p'-DDT	165, 235, 237, 318, 354	65
Endrin ketone	67, 245, 281, 317, 345, 380	65
Methoxychlor	174, 227, 346	65

Finally, UV-Vis spectra in the plasmon coupling study were registered with a Shimadzu UV-2600 spectrophotometer (Nakagyo-ku, Kyoto, Japan), using an integrating sphere assembly.

3. Comparison of metal-containing silica-based materials for organophosphorus pesticides air sampling and occupational risk assessment

The aim of this work is to study the potential use of sol-gel and mesoporous silica materials (based on UVM-7 structure), doped with the addition of Ti and Fe, for the retention of organophosphorus pesticides during occupational air sampling, followed by their analysis by GC-NPD and GC-MS. Ti25-UVM-7 material, which provided the best results, was selected for the method development, and its relevant features were established. Additionally, the developed samplers were applied for the sampling of OPPs during real pesticide application and compared with commercial XAD-2 samplers.

3.1. Sampling methodology and experimental procedure

For the preparation of samplers, the desired amount of each silica material was packed into an empty tube between two frits. Then, during the optimization process, the material was spiked with 10 µL of a multicomponent solution of OPPs, and the air was pumped through the solid at 500 mL min^{-1}, in order to simulate the sampling process. Then, the sorbent was placed in a glass tube for the desorption of the analytes with an organic solvent, and their determination by GC-NPD.

After the optimization, samplers containing Ti25-UVM-7 material (40 mg in the front section and 20 mg in the backup section) were prepared. Air samples were collected in several orange plantations of Benifaió and Sollana (Valencia, Spain), both during and after the application of a commercial pesticide containing methyl-chlorpyrifos as the active agent. At the same time, the sampling was also carried out with samplers containing XAD-2 (100/50 mg) according to the NIOSH recommended procedure [118]. In both cases, the sampling flow was monitored and kept in the range 200-600 mL min^{-1}, and three replicates were collected. The pesticide application was carried out by spraying it, and the samplers were installed next to the operator. After the sampling, the tubes were stored refrigerated and desorbed with 2 mL of acetonitrile under vigorous shaking. After solvent evaporation and redissolution in 250 µL of acetonitrile, the final solutions were analyzed by GC-MS.

3.2. Results and discussion

In this study, different types of silica materials were studied, namely UVM-7 mesoporous solids, and xerogel materials, both pure and doped with metals. As described in the characterization of Chapter 4, they show significant differences in the pore system organization and particle size. In the case of UVM-7 materials, a hierarchical bimodal pore system with intraparticle hexagonally pseudo-ordered mesopores and large interparticle macropores is considered, whereas xerogels present a unimodal and completely disordered microporosity. Otherwise, an

important difference in the addition of the metallic heteroelement to the silica network should be noted, since both types of silica have been doped with Ti and Fe, either by co-hydrolysis (through the one-pot atrane method) or by impregnation of the material surface. Thus, depending on the silica framework and the metallic modification, their morphology, as well as their retention properties, are expected to be different.

3.2.1. Optimization of sampling parameters

The nature of the sorbent was firstly studied by preparing several samplers containing 50 mg of each silica material, either pure or modified. After spiking the material (4-16 µg of each pesticide), 10 L of air were pumped through the sampler and the later desorption was carried out with 2 mL of acetonitrile with a wrist shaker. As can be seen in Figure 55, best recoveries were achieved with UVM-7 type silicas, since their architecture is more suitable for target analytes due to its larger mesopores, in comparison with xerogel micropores. Moreover, the addition of Ti and Fe by co-hydrolysis entailed an improvement in the results, since the heteroelement is well-distributed in the silica network, as commented in Chapter 4. However, whilst the addition of Ti by impregnation improved the results for xerogels, the blocking of the pore structure makes the recoveries lower in UVM-7 materials. Finally, the worst recoveries were obtained for the diazinon, mainly for Fe25-UVM-7 material, probably because of the slight modification of the pore structure in the addition of the Fe, as observed in the material characterization. Thus, Ti25-UVM-7 material, which offered the best recoveries (92-115%), was selected as the best sorbent for further studies.

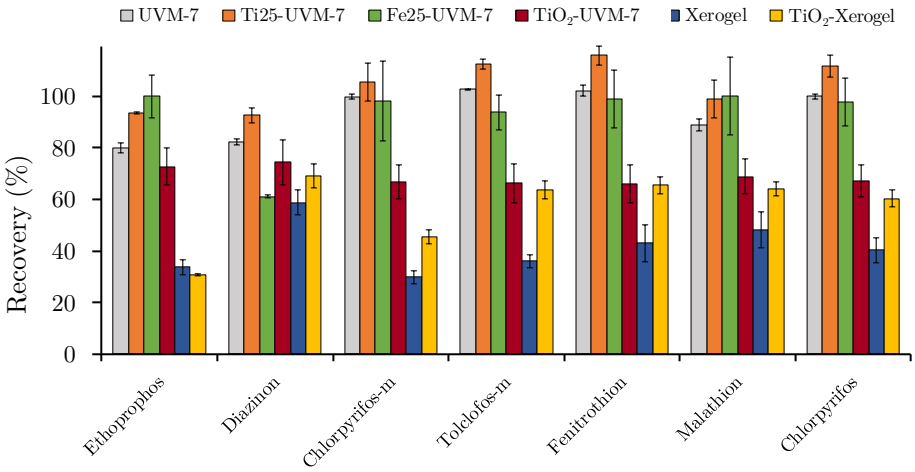

Figure 55. Effect of the sorbent nature on the recovery of OPPs. Conditions: 50 mg of sorbent; 10 L of air sampled; desorption by wrist shaking with 2 mL of acetonitrile (20 min); samplers spiked with 4 µg of diazinon, 8 µg of ethoprophos, tolclofos-m, fenitrothion, and malathion, and 16 µg of chlorpyrifos-m and chlorpyrifos.

Then, the desorption procedure was optimized. Firstly, other alternatives for the stirring were studied such as ultrasonication or rotator stirring, although significantly better results were obtained with wrist shaking. Likewise, several experiments were carried out as described above, by varying the shaking time between 5-20 min and the results showed that the complete desorption of the analytes was achieved after 15 min of stirring (Figure 56).

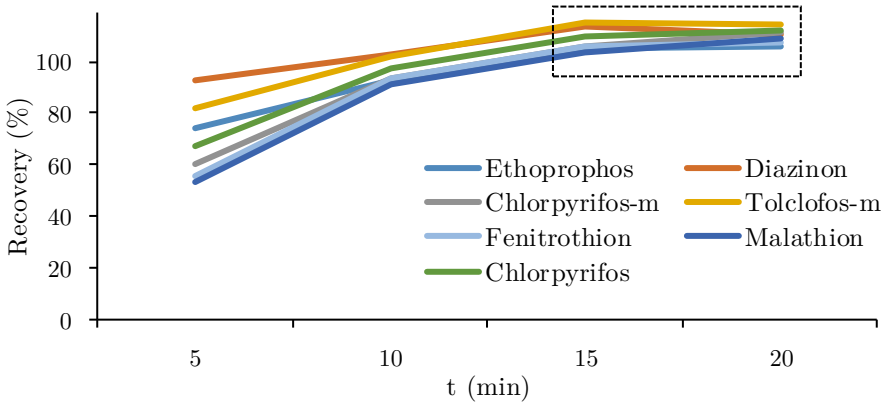

Figure 56. Effect of the stirring time on the recovery of OPPs with Ti25-UVM-7 material. Conditions: 50 mg of sorbent; 10 L of air sampled; desorption by wrist shaking with 2 mL of acetonitrile; samplers spiked with 4 µg of diazinon, 8 µg of ethoprophos, tolclofos-m, fenitrothion, and malathion, and 16 µg of chlorpyrifos-m and chlorpyrifos.

For the evaluation of the solvent nature, even though satisfactory recoveries were achieved with acetonitrile, other organic solvents were considered, such as ethanol, ethyl acetate, and acetone. These solvents were tested by following the described sampling procedure. However, best recoveries were obtained with acetonitrile (97-113%). Moreover, similar experiments were carried out by using 1, 2, and 3 mL of acetonitrile to assure the minimum but enough volume of solvent for the desorption of the analytes, and no variations were observed in the recoveries (Table 22). Finally, the possibility of concentrating the final solution by evaporation was assessed, in order to increase the sensitivity of the proposed procedure. The evaporation was carried out at room temperature and under vacuum, with the later redissolution with 250 µL of acetonitrile. After that, no significant differences in the results were observed (variations $< 5\%$) which indicates that it is possible to carry out this preconcentration step.

The amount of sorbent was also studied, by preparing samplers with 10, 20, 30, 40, and 50 mg of Ti25-UVM-7 (Figure 57). Results showed that whilst using up to 30 mg recoveries were under 90%, satisfactory recoveries were achieved with 40 mg (92-119%). With this amount of solid phase, the breakthrough volume was evaluated, in order to sample the largest volume of air possible, thus achieving better sensitivity in the sampling step. For this purpose, the samplers were tested by passing air volumes between 0 and 210 L after sorbent contamination. In all

cases, quantitative recoveries were obtained for 210 L (88-111%), except for diazinon (66%). However, acceptable results were obtained after sampling 55 L of air for this pesticide (recovery 75%). Hence, 40 mg of the designed sorbent allow sampling at least 210 L of air without analyte loss for all target compounds, except in the case of diazinon determination, when the sample volume should be lower than 55 L.

Table 22. Effect of the desorption solvent volume on the recovery of OPPs. Conditions: 50 mg of sorbent Ti25-UVM-7; 10 L of air sampled; desorption by wrist shaking with acetonitrile (15 min); samplers spiked with 4 µg of diazinon, 8 µg of ethoprophos, tolclofos-m, fenitrothion and malathion, and 16 µg of chlorpyrifos-m and chlorpyrifos.

Compound	1 mL	2 mL	3 mL
Ethoprophos	102 ± 6	100 ± 2	100 ± 5
Diazinon	106 ± 2	99 ± 1	99 ± 3
Chlorpyrifos-m	112 ±1 0	102 ± 5	103 ± 16
Tolclofos-m	108 ± 3	99 ± 3	102 ± 9
Fenitrothion	118 ± 5	100 ± 4	105 ± 19
Malathion	111 ± 17	103 ± 6	103 ± 25
Chlorpyrifos	111 ± 4	101 ± 4	102 ± 14

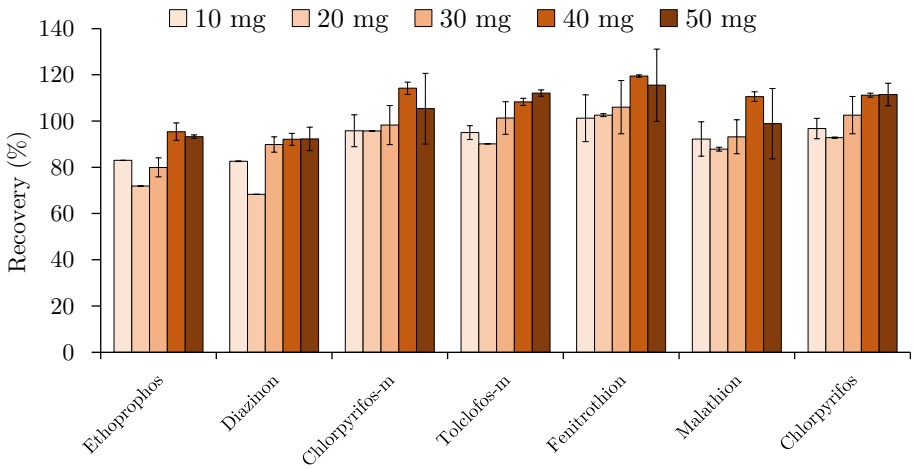

Figure 57. Effect of the sorbent amount (Ti25-UVM-7) on the recovery of OPPs. Conditions: 10 L of air sampled; desorption by wrist shaking with 2 mL of acetonitrile (15 min); samplers spiked with 4 µg of diazinon, 8 µg of ethoprophos, tolclofos-m, fenitrothion, and malathion, and 16 µg of chlorpyrifos-m and chlorpyrifos.

In the same way, the loading capacity was also evaluated. In this case, the sorbent was spiked with different amounts of OPPs (0.5-20 µg) and after the sampling simulation, the desorption was carried out under the optimum conditions. In this case, no significant differences were observed in any case, and the designed samplers can be applied for working in this range of concentrations.

3.2.2. Analytical figures of merit

The linearity, selectivity, and precision of the optimized sampling method were evaluated. Calibration standards were prepared and injected twice both in GC-NPD and GC-MS systems. The limit of detection and quantification were estimated with a confidence level of 95% and according to the latest IUPAC recommendations, as well as the linearity, considering the LOQ as the lower limit of the linear range [203]. LODs and LOQs were expressed in terms of the total amount as well as considering the sampling of the maximum permitted volume of air. As shown in Table 23 and Table 24, acceptable linearity and sensitivity were achieved by using NPD detection system (LOQs between 0.10-1.0 µg m^{-3}), although the best sensitivity was obtained using GC-MS, with LOQs in the range 0.06-0.5 µg m^{-3} for the air sampling, being these limits below those established by Spanish legislation for these pesticides in an occupational environment (0.01-10 mg m^{-3}) [27].

Table 23. Analytical figures of merit of the proposed sampling protocol combined with GC-NPD.

Compound	Linearity[a] (mg L^{-1})	Absolute amount (µg)		Air sample (µg m^{-3})	
		LOD	LOQ	LOD	LOQ
Ethoprophos	0.09-10	0.007	0.02	0.04	0.10
Diazinon	0.05-5	0.004	0.013	0.07	0.2
Chlorpyrifos-m	0.3-2	0.03	0.08	0.12	0.4
Tolclofos-m	0.12-10	0.010	0.03	0.05	0.14
Fenitrothion	0.6-10	0.05	0.16	0.3	0.8
Malathion	0.8-15	0.07	0.2	0.3	1.0
Chlorpyrifos	0.2-20	0.019	0.06	0.09	0.3

[a]Referred to the injection solution

Table 24. Analytical figures of merit of the proposed sampling protocol combined with GC-MS.

Compound	Linearity[a] (mg L^{-1})	Absolute amount (µg)		Air sample (µg m^{-3})	
		LOD	LOQ	LOD	LOQ
Ethoprophos	0.07-2	0.006	0.017	0.03	0.08
Diazinon	0.10-2	0.008	0.02	0.14	0.4
Chlorpyrifos-m	0.05-2	0.004	0.013	0.02	0.06
Tolclofos-m	0.11-2	0.009	0.03	0.04	0.13
Fenitrothion	0.07-2	0.006	0.017	0.03	0.08
Malathion	0.4-2	0.03	0.10	0.15	0.5
Chlorpyrifos	0.07-2	0.006	0.018	0.03	0.08

[a]Referred to the injection solution

The RSD of the developed sampling method was also calculated for each analyte, by preparing several samplers with 40 mg of Ti25-UVM-7 and testing them, following the optimized procedure, and sampling 10 L of air. Thus, three replicates within a day were done in order to estimate the intra-day precision, whilst three series of three independent experiments were carried out for establishing the inter-day precision. As can be seen in Table 25, RSD values below 13% were obtained for intra- and inter-day precision. These results are acceptable, taking into account the main sources of error in this sampling step, such as the variations in air concentrations during the time, and the sample handling during the desorption process. In the same way, an average recovery was also calculated for all analytes, thus obtaining good results for all target compounds, taking into account the recommended parameters [246], and recoveries above 90% for all pesticides except for diazinon (82%).

Table 25. Analytical figures of merit of the proposed sampling protocol in terms of repeatability and analyte recovery.

Compound	Repeatability RSD (%)		Recovery (%)
	Intra-day	Inter-day	
Ethoprophos	7	12	93 ± 8
Diazinon	4	11	82 ± 6
Chlorpyrifos-m	11	7	107 ± 7
Tolclofos-m	7	4	104 ± 5
Fenitrothion	12	9	108 ± 9
Malathion	13	12	98 ± 9
Chlorpyrifos	8	6	104 ± 7

Finally, the storage time of the material was also tested. In this case, after the sampling step, the samplers were properly covered and stored at 4 °C. After 24 h, no significant analyte loss was observed (recoveries 79-100%), although, after 5 days, similar recoveries were obtained only for chlorpyrifos-m, tolclofos-m, fenitrothion, and chlorpyrifos (79-96%), whilst recoveries under 67% were obtained for the other pesticides. Likewise, the reusability of the material was proved. After washing and drying the used material, new samplers were prepared and no significant differences were observed in recoveries, being this an important feature of the designed sorbent, taking into account the chemical stability and long lifetime in the working conditions.

3.2.3. Sampling and analysis of real samples

The designed cartridges containing Ti25-UVM-7 material were applied for the sampling of two different air samples, during the spray application of a pesticide containing methyl-chlorpyrifos in two orange plantations (P1 and P2).

Table 26. Concentration of chlorpyrifos-m in collected air samples, using both Ti25-UVM-7 and XAD-2 samplers, and the obtained exposure rate.

Plantation	Sampling	Ti25-UVM-7		XAD-2	
		Concentration (mg m^{-3})	Exposure rate	Concentration (mg m^{-3})	Exposure rate
P1	During application	0.07 ± 0.03	0.61	0.07 ± 0.02	0.61
P2	During application	0.072 ± 0.015	0.63	0.055 ± 0.002	0.48
P2	After application	0.015 ± 0.002	0.13	0.013 ± 0.002	0.11

Table 27. Comparison of the presented method with other methods reported in the literature.

Sorbent	Sampling	Instrumental technique	Extraction solvent	Recovery (%)	LOD (ng m^{-3})	RSD (%)	Ref.
Ti25-UVM-7	Active	GC-MS	1 mL acetonitrile	82-107	20-150	3.8-13	This work
XAD-2	Active	GC-NPD GC-NCI/MS	2 mL carbon disulphide	95-102	-[a]	4.5-9.0	[213]
SPMD[b]	Passive	HPLC-UV	60 mL acetone:hexane	81-105	1-2	2.1-6.9	[247]
Chromosorb 102	Active	GC-FPD	4 mL acetone	81-92	6-10	2-13	[225]
XAD-2	Active	GC-FPD	2.5 mL acetone:toluene (10:90)	88-104[c]	20-300	0.06-0.07[b]	[226]

[a]LOD of the complete sampling method no specified in the work

[b]Semipermeable membrane device

[c]Related to desorption efficiency, not to the complete sampling method

In the case of P2, another sample was also collected 10 minutes after the pesticide application, in order to check the quality of the air in the plantation after working. Moreover, samplers containing XAD-2 sorbent were employed for the validation of the method. In all cases, the sampling process was carried out successfully, since negligible concentrations of pesticides were found in the backup section. As shown in Table 26, the values obtained with both materials are statistically comparable by the t-student test, being in the same confidence interval (95% confidence level). It should be noted that high deviation was obtained for real air measurement, since pesticide concentrations in the air usually show great variations during its application, depending on time or position, being these factors important sources of error for these sampling protocols. Also, as expected, no concentrations above LOD were detected for the other target pesticides.

Regarding the obtained results, concentrations between 0.055 and 0.072 mg m^{-3} were obtained during the pesticide application. This entails exposure rates in the range 0.48-0.61, assuming a diary application time of 7 h and an OEL of 0.1 mg m^{-3} [219]. Hence, according to Spanish legislation [218], the air quality during the application is not extremely unsafe but its control and vigilance are advised (exposure rate in the range 0.1-1), which makes necessary the utilization of personal protective equipment. In the same way, 10 min after application, concentrations in the range 0.013-0.015 mg m^{-3} were obtained, as well as exposure rates above 0.1, which indicates that is not completely safe to work on these plantations after pesticide application.

3.2.4. Comparison with other samplers

As observed in Table 27, achieved recoveries in this work are in the same range of other similar studies in the literature, being also confirmed the acceptable repeatability of the method with RSDs comparable to other works. In addition, even though the LODs of the method are slightly higher than those presented in the literature, this sensitivity is enough for the risk assessment of the target pesticides.

It should be noted that in some reported methods, a long sampling time is needed to achieve those LODs (mainly in passive samplers, up to 7 days), in comparison to short sampling periods reported in this work. Nevertheless, the sensitivity can be increased by designing samplers with a higher amount of sorbent which would permit the sampling of higher volumes of air. In any case, a mild and more environmentally friendly desorption process has been presented in this work, since 1 mL of acetonitrile was used, compared to the other unfriendly desorption methods (microwave or Soxhlet extraction) with large volumes of more toxic solvents reported by other works. Thus, in the presented work, both sampling and desorption processes are cheaper, faster, and more environmentally friendly than other reported works, with similar or better analytical parameters. These features, along with the stability and ease of synthesis of the silica

materials, lead to a useful tool for its implementation in occupational risk assessment. Also, the reusability of the material has been proved, being an important advantage in comparison with other commercial samplers.

Thus, presented Ti25-UVM-7 samplers represent a cheap, effective, reusable, and less solvent-consuming alternative for the occupational risk assessment and systematic sampling and determination of organophosphorus pesticides.

4. Study of Ti-UVM-7 materials as sorbents for organophosphorus pesticides determination in environmental water samples

The aim of this work is to study the potential use of mesoporous silica materials based on UVM-7 structure doped with Ti and Fe as SPE sorbents for the extraction of OPPs from water samples followed by their analysis by GC-NPD. In addition, a comparison with silica materials modified with immobilized CDs was initially done. Ti25-UVM-7 solid provided the best extraction performance and therefore it was selected. Its relevant features (such as breakthrough volume, reusability, etc.) were established and the optimal SPE procedure was then applied to the preconcentration of OPPs in environmental water samples. Additionally, these results were compared with those obtained with a commercial C18 sorbent.

4.1. Experimental SPE protocol and analysis of water samples

For the preparation of the SPE cartridges, 50 mg of the UVM-7 materials (either pure or doped with Ti or Fe) were packed between two polyethylene frits into 3 mL empty propylene cartridges. For silica-based materials modified with β- or γ-CDs, 100 mg of each solid phase were placed into the same empty propylene cartridges.

Thus, several SPE parameters such as the amount of sorbent, type and volume of eluting solvent, pH, and ionic strength of the sample were studied. This optimization procedure was performed with deionized water spiked with OPPs as a test mixture. In particular, OPP concentrations used during SPE optimization were: 50 μg L^{-1} for diazinon; 125 μg L^{-1} for ethoprophos, tolclofos-m, fenitrothion, and parathion; and 250 μg L^{-1} for chlorpyrifos, malathion, and chlorpyrifos-m.

After optimization, the optimum SPE conditions were achieved with cartridges containing 75 mg of Ti25-UVM-7 material, which were previously conditioned with 5 mL of MeOH and 5 mL of ultrapure water. Next, a known volume of either ultrapure water or a real sample, spiked with OPPs, was passed through the cartridges. Then, the cartridge was dried with air for 5 min and analytes were eluted with 1 mL of hexane and 1 mL of ethyl acetate followed by GC-NPD analysis.

Water samples from different sources such as well water (Borriana, Castelló, Spain) and irrigation ditch (Algemesí, València, Spain) were collected. Also, wastewater samples were taken from the effluent and influent of a wastewater treatment plant (WWTP) of the region of Valencia. The precleaned bottles were covered with aluminum foil and stored in the dark at 4 °C until analysis. Prior to analysis, samples were filtered to remove any particulate matter.

These real water samples were analyzed according to the protocol described above. To evaluate the influence of matrix on pesticide recovery, these samples were spiked with the OPPs at several levels of concentrations (12.5-50 µg L^{-1}) in triplicate. Additionally, these samples were analyzed using a commercial C18 cartridge since it is often used as a reference sorbent in environmental analysis for sample enrichment of OPPs [67,69]. In this case, the elution was carried out by using 2 mL of ethyl acetate and 2 mL of dichloromethane followed by injection into the GC system.

4.2. Results and discussion

In this work, we explore the ability of two silica-based porous materials as SPE supports for the pesticide preconcentration in complex water samples. The two solids differ both in the organization of the pore system as well as the interaction with the analytes. In the case of xerogels containing CDs, a unimodal microporous system is present, whereas the UVM-7, as previously mentioned, can be considered as a bimodal pore system combining meso and large pores. Regarding the sorbent-analyte interaction, as previously commented in the case of the Ti/Fe-UVM-7 solids, the local affinity of the phosphorus moiety of the pesticides for Ti or Fe sites must be the responsible factor that would provide an enhanced interaction. On the other hand, in the case of the CD-based derivatives, the interaction must be controlled by the host-guest inclusion mechanism typical of these supports.

4.2.1. Optimization of SPE parameters

The study of sorbent nature was firstly evaluated by testing either pure UVM-7 silica or doped with Ti or Fe. For this purpose, SPE cartridges containing 50 mg of each material (UVM-7, Ti25-UVM-7, and Fe25-UVM-7) were selected. Thus, 25 mL of ultrapure water containing target OPPs in concentrations of 125-500 μL^{-1} were loaded into each cartridge. After elution with 4 mL of ethyl acetate, the results of this study showed that Ti25-UVM-7 gave the best recoveries for OPPs (reaching values up to 69.1%), and it was selected for the following studies.

Then, this material was compared with xerogel materials with immobilized CDs. Thus, cartridges containing 50 mg of Ti25-UVM-7 or 100 mg (minimum amount of material to be properly packed) of CD-based materials were prepared and 25 mL of deionized water spiked with OPPs was introduced in each cartridge. Then, analytes were eluted with ethyl acetate. As can be seen in Figure 58, the results showed that these latter materials using either β- or γ-CDs provided large

retention values (93.8-100%) for OPPs containing aromatic rings, mainly those that have chlorinated functional groups (chlorpyrifos-m, tolclofos-m, and chlorpyrifos). This fact could be explained due to the ability of CDs to form host-guest complexes with OPPs containing these functional groups. Indeed, low retentions, and therefore low recoveries (below 20%), were obtained for analytes without aromatic groups (e.g. ethoprophos and malathion) using β-CD-based xerogel material. A slight improvement in the recovery values (up to 25%) was obtained for these analytes when γ-CD material was tried, probably due to the bigger size of this CD.

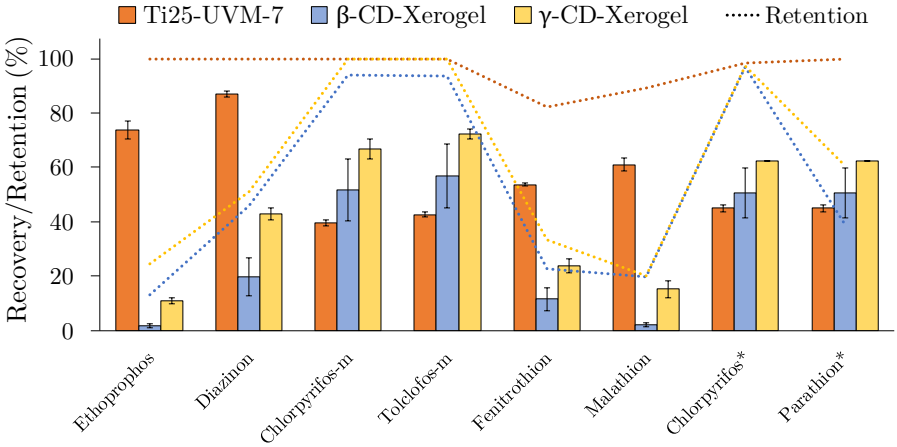

*Chlorpyirifos and parathion retentions are presented separately, although the recovery values are the same, obtained from the joint determination.

Figure 58. Effect of the sorbent nature on the recovery and the retention of OPPs. Conditions: 50 mg of Ti25-UVM-7 and 100 mg of xerogel sorbents; sample volume, 25 mL; eluent, 4 mL of ethyl acetate; deionized water spiked with 500 μg L^{-1} of diazinon, 1000 μg L^{-1} of ethoprophos, tolclofos-m, fenitrothion, and parathion, and 2000 μg L^{-1} of chlorpyrifos, malathion, and chlorpyrifos-m. Retention was obtained from the measurement of non-retained analytes in water.

In contrast, using Ti25-UVM-7 material, retentions over 80% were obtained for all analytes and, in some cases, close to 100%. Although these values were obtained using an un-optimized elution procedure, these results clearly demonstrated that UVM-7-based materials are more appropriate than xerogel materials modified with CDs. The enhanced ability of Ti-UVM-7 solid to interact with a large variety of P-containing pesticides when compared to the CD-containing silica xerogels is based on two aspects: the higher accessibility derived of the open architecture of UVM-7 solids, and a support-analyte interaction more generic and independent of the pesticide size.

Then, several SPE parameters were evaluated. The amount of sorbent (25-100 mg) was first studied using Ti25-UMV-7 as a filler of the SPE cartridge. As can be seen in Figure 59, the best recoveries were found at 75 mg, being this amount chosen for further studies.

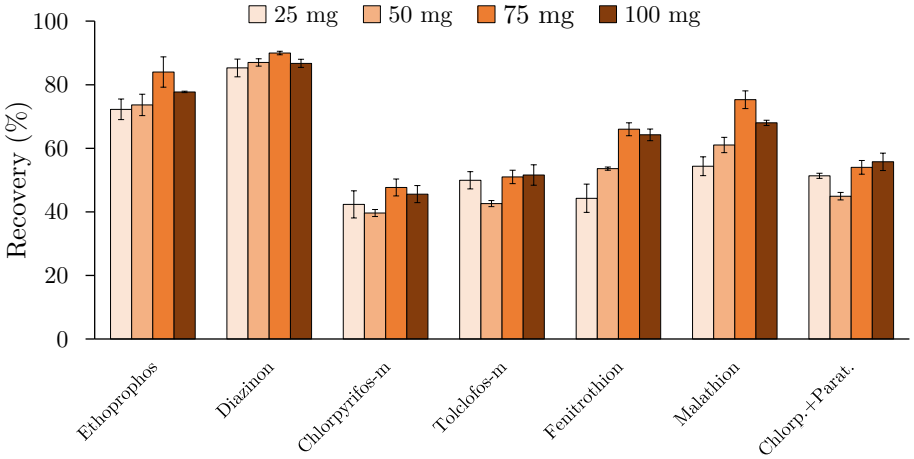

Figure 59. Effect of the amount of solid phase (Ti25-UVM-7) on the recovery of OPPs. Conditions: sample volume, 25 mL; eluent, 4 mL of ethyl acetate; deionized water spiked with 50 μg L^{-1} of diazinon, 125 μg L^{-1} of ethoprophos, tolclofos-m, fenitrothion and parathion, and 250 μg L^{-1} of chlorpyrifos, malathion, and chlorpyrifos-m.

In order to increase the recoveries, the influence of eluent type was then considered. In this sense, several eluting solvents of different polarities namely ethyl acetate, acetonitrile, methanol, dichloromethane, hexane, and tetrahydrofuran were investigated. For this purpose, an elution volume of 4 mL was selected. As shown in Figure 60, the best results were achieved using ethyl acetate and hexane, depending on the analyte. Thus, both solvents were selected to carry out the study of eluent solvent volume. In this way, volumes from 1 to 4 mL of hexane or ethyl acetate were investigated to assure the minimum but enough volume required to elute the retained OPPs to achieve the highest sensitivity. The highest recoveries (83.4-108.3%) were obtained when 1 mL of hexane followed by 1 mL of ethyl acetate were used.

Then, the influence of pH on the recoveries by changing the pH value of the sample solution between 4.0 and 7.0 was studied. For this study, the loading step was adequately adjusted to the pH conditions to achieve the highest extraction efficiency. Results indicated that sample pH did not affect the retention of the analytes, as their acid-base properties are practically negligible, and the working pH range is above silica isoelectric point (2-3) [125], as previously commented. Thus, neutral pH was chosen for the next studies. Likewise, the effect of ionic strength was also studied in order to reduce the solubility of analytes in the aqueous phase while enhancing their partitioning into the sorbent. Different contents of sodium chloride (up to 2 M) in the sample were studied. Results indicated that when salt concentration increased, the recoveries for all the OPPs decreased, probably due to the competitive interaction of Na^+ ions with silanol moieties. Consequently, the use of NaCl was discarded.

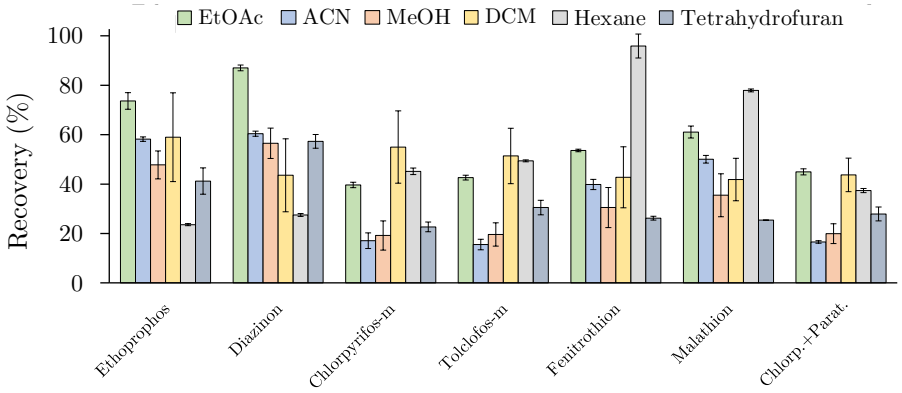

Figure 60. Effect of the type of eluting solvent on the recovery of OPPs. Conditions: sample volume, 25 mL; sorbent amount, 75 mg; eluent volume, 4 mL; deionized water spiked with 50 µg L^{-1} of diazinon, 125 µg L^{-1} of ethoprophos, tolclofos-m, fenitrothion, and parathion, and 250 µg L^{-1} of chlorpyrifos, malathion, and chlorpyrifos-m.

In order to obtain reliable analytical results and high preconcentration factors, it is relevant to achieve satisfactory recoveries for all analytes in the largest sample volume possible. To establish the breakthrough volume, variable volumes (between 25 and 100 mL) of the OPPs solution were passed through the SPE material. Experimental results showed recoveries comprised between 86.9-113.3% for OPPs up to 50 mL, whereas a considerable decrease in the recoveries of OPPs was observed at volumes of 100 mL. Consequently, 50 mL was adopted as the volume for the analysis of real water samples.

The loading capacity of SPE sorbent was also evaluated by loading different amounts of OPPs (50 mL of spiked 4-250 µg L^{-1} deionized water). Results indicated that no significant differences in the recoveries were found for the different concentrations tested, which suggested that the studied material could be properly used for SPE extraction within these concentrations.

4.2.2. Analytical figures of merit

The optimized SPE protocol was validated concerning linearity, sensitivity, and precision. Calibration curves were prepared and injected twice. The limit of detection (LOD), as well as the limit of quantification (LOQ), were estimated according to the latest IUPAC recommendations, with a confidence level of 95% [203]. Linearity range was estimated following these recommendations, considering the LOQ as the lower limit of linearity. In the same way, calibration solutions were injected into a GC-MS system to evaluate these parameters for chlorpyrifos and parathion separately, as well as to establish the linear range and sensitivity of the method (Table 28). As can be seen, LODs were lower than 1.3 µg L^{-1} for several OPPs, such as ethoprophos, diazinon, chlorpyrifos-m, and tolclofos-m using NPD detector, whereas using GC-MS instrumentations LODs below 1.4 µg L^{-1} were achieved for all analytes.

Table 28. Analytical figures of merit of the proposed SPE protocol combined with GC-NPD method, and GC-MS systems.

Compound	GC-NPD			GC-MS		
	Linearity[a] (mg L^{-1})	LOD (µg L^{-1})	LOQ (µg L^{-1})	Linearity[a] (mg L^{-1})	LOD (µg L^{-1})	LOQ (µg L^{-1})
Ethoprophos	0.10-2.5	1.3	4.1	0.03-2.5	0.4	1.2
Diazinon	0.03-1.25	0.4	1.7	0.012-1.25	0.2	0.5
Chlorpyrifos-m	0.09-5	1.2	3.7	0.06-5	0.7	2.2
Tolclofos-m	0.09-2.5	1.2	3.8	0.02-2.5	0.2	0.7
Fenitrothion	0.2-2.5	3.1	9.3	0.04-2.5	0.5	1.7
Malathion	0.2-5	2.8	8.6	0.06-5	0.8	2.3
Chlorpyrifos	-	-	-	0.11-5	1.4	4.4
Parathion				0.03-5	0.4	1.2

[a]Referred to the final injection solution

The precision of the SPE combined with the GC-NPD method was evaluated by studying the intra- and inter-day repeatabilities of extractions of 50 mL of spiked water samples. The intra-day precision was determined by analyzing three replicates within a given day, whereas the inter-day precision was estimated by analyzing three series of three independent experiments carried out on three different days (Table 29). The method showed good precision with relative standard deviation (RSD) values below 12%. Also, good extraction efficiencies were achieved (between 81-104%), and enrichment factors (EF) in the range of 20.4 to 26.1 were obtained for all analytes, calculated by considering 50 mL of sample volume and 2 mL of final extract, through the following general expression:

$$EF = R \frac{V_S}{V_E} \quad (1)$$

where R is the recovery rate for each analyte, V_S is the analyzed sample volume, and V_E is the volume of the final extract.

Table 29. Repeatability and extraction efficiency of the developed SPE-GC-NPD method.

Compound	Repeatability RSD (%)		Extraction efficiency (%)	EF
	Intra-day	Inter-day		
Ethoprophos	3.8	4.8	95 ± 2	23.7 ± 0.5
Diazinon	2.6	3.2	104.5 ± 1.5	26.1 ± 0.4
Chlorpyrifos-m	6.4	9.8	81 ± 4	20.4 ± 0.9
Tolclofos-m	3.2	6.0	84 ± 2	21.0 ± 0.6
Fenitrothion	7.8	12.0	90 ± 5	22.4 ± 1.2
Malathion	5.9	9.0	98 ± 4	24.5 ± 1.0
Chlorpyrifos	2.9	6.6	83 ± 2	10.3 ± 0.3
Parathion				

4.2.3. Sample analysis and matrix influence

The proposed SPE protocol using Ti25-UVM-7 material was applied for the analysis of different environmental water samples and the study of the matrix influence. Table 30 shows the recovery values obtained in several matrices. As can be seen in Table 29 and Table 30, for Ti25-UVM-7 material, recovery rates in these water samples were significantly affected by the matrix. In any case, the results showed that WWTP water underwent the highest matrix effect, whereas the well water showed the lowest one, although the influence was, in general, similar for all matrices. Anyway, the results obtained demonstrate that the use of standard addition calibration would be advisable for future applications, due to the matrix type influence.

Table 30. Matrix influence on the OPP recovery (%) using the proposed method.

Compound	$C_{additioned}$ (µg L^{-1})	WWTP water	Well water	Irrigation water
Ethoprophos	25.5	87 ± 9	93 ± 4	83 ± 9
Diazinon	12.8	77 ± 15	78 ± 2	82 ± 7
Chlorpyrifos-m	51.2	59 ± 10	61 ± 2	57 ± 7
Tolclofos-m	25.7	59 ± 11	57 ± 2	55 ± 11
Fenitrothion	25.3	48 ± 5	69 ± 4	52 ± 7
Malathion	50.7	49 ± 8	68.8 ± 1.5	49 ± 9

To validate the feasibility of the proposed SPE protocol using Ti25-UVM-7 material, a commercial C18 SPE sorbent was also used for comparison. Thus, both SPE protocols were applied to the determination of these OPPs in seven water samples collected from the following origins: WWTP influent (M1) and effluent (M2) channels, Borriana irrigation ditch (M3), several Borriana water wells (M4, M5, M6) and Algemesí irrigation network (M7). As shown in Table 31, most of OPP concentrations were below LODs and all of them below LOQs using both Ti25-UVM-7 and C18 materials. Tolclofos-m and diazinon were present in samples M1, M2, and M5, whereas in the rest of the samples these target OPPs or others were not found. Additionally, it seems relevant that OPP concentrations found in M1 and M2 samples (influent and effluent WWTP water) were quite similar since these plants are not designed to remove micropollutants [248]. Since no target OPPs were detected, some water samples (M1 and M3) were spiked (M1S and M3S) and analyzed through both SPE protocols. The results obtained (Table 32) showed that both methodologies are completely comparable (comparison of variances by Fisher-Snedecor's test and comparison of means by Student's test, 95% of confidence level).

Then, the reusability of Ti25-UVM-7 material in a real matrix (irrigation water) was also evaluated. The results indicated that the cartridges were reused up to three times without a significant decrease in the recoveries for OPPs (differences on the recoveries below 5% for all OPPs). In addition, this re-used solid phase can be re-calcined (5 h) and used again for new extraction cartridges reaching large recovery values and differences under 8% from first use.

Table 31. Results obtained (µg L^{-1}) for OPPs determination in water samples (M1, M2, and M5), using Ti25-UVM-7 material and C18 commercial cartridges.

Compound	M1		M2		M5	
	Ti25-UVM-7	C18	Ti25-UVM-7	C18	Ti25-UVM-7	C18
Ethoprophos	< LOD	< LOD	< LOD	< LOD	< LOD	< LOD
Diazinon	< LOQ (0.4)	< LOQ (0.8)	< LOQ (0.5)	< LOQ (0.8)	< LOD	< LOQ (0.6)
Chlorpyrifos-m	< LOD	< LOD	< LOD	< LOD	< LOD	< LOD
Tolclofos-m	< LOD	< LOQ (1.9)	< LOQ (1.9)	< LOD	< LOD	< LOQ (1.8)
Fenitrothion	< LOD	< LOD	< LOD	< LOD	< LOD	< LOD
Malathion	< LOD	< LOD	< LOD	< LOD	< LOD	< LOD

Table 32. Results obtained (µg L^{-1}) for OPPs determination in spiked water samples (M1S and M3S), using Ti25-UVM-7 material and C18 commercial cartridges, and their relative error (%).

Compound	$C_{additioned}$	M1S				M3S			
		C18		Ti25-UVM-7		C18		Ti25-UVM-7	
		Concentration	Error	Concentration	Error	Concentration	Error	Concentration	Error
Ethoprophos	25.5	25.7 ± 1.9	1.0	25.6 ± 0.6	-0.4	25.4 ± 0.6	-0.4	27.5 ± 1.7	8.2
Diazinon	12.8	12.7 ± 0.5	-1.2	13.8 ± 0.6	1.8	13.1 ± 0.3	1.8	13.9 ± 0.4	8.1
Chlorpyrifos-m	51.2	50 ± 4	-1.5	54 ± 4	2.2	52 ± 3	2.2	59 ± 4	14.8
Tolclofos-m	25.7	25.2 ± 1.7	-1.9	29 ± 3	2.5	26.4 ± 1.3	2.5	27.6 ± 1.5	7.4
Fenitrothion	25.3	24.9 ± 1.2	-1.7	23.3 ± 0.8	2.3	26 ± 3	2.3	29.5 ± 1.4	16.5
Malathion	50.7	50 ± 7	-0.8	51 ± 3	1.4	51 ± 2	1.4	50.9 ± 1.4	0.4

At the sight of previous results, our material showed similar results for the analysis of real samples compared to commercial C18 cartridges, although a great advantage over this sorbent was its reusability, which undoubtedly makes more economically attractive its application to extract these OPPs in complex sample matrices.

The developed material was also compared with previous extraction methods reported by Korrani et al. [241] that use sol-gel silica mesoporous materials as SPE sorbent. In particular, the mean recovery values assayed for diazinon in this work were in the same order of magnitude as those previously found in water samples. However, this analytical parameter or others (e.g. reusability) were evaluated using spiked deionized water or samples with relatively simple matrices (tap water, drinking water, and mineral water) in contrast to those considered here. Concerning the LODs, our values were better than those reported using SPE with cyano cartridges, although slightly higher than that found by Korrani et al. (0.4 vs 0.1 µg L^{-1} for diazinon). In any case, the SPE protocol developed here constitutes a good alternative for the effective extraction of OPPs since it can be performed in a short time (ca. 6 samples per hour) and with low cost, with acceptable analytical parameters.

5. Application of UVM-7 materials doped with Au nanoparticles as sorbents for organochlorine pesticides determination in water samples

The aim of this work is to develop a method for the extraction and determination of OCPs in water samples by using UVM-7 silica materials doped with Au. For this study, the 20 target pesticides were selected according to the USEPA method for organochlorine pesticides determination [221], to include the most significant OCPs in the method development. The extraction is carried out through an SPE method and later determination of the analytes is achieved with GC-ECD and GC-MS equipment. Once the main features of the SPE procedure are established, the method is applied to the determination of OCPs in real water samples. The results obtained were also compared with a reference USEPA method [70].

5.1. Experimental part: SPE procedure and sample analysis

SPE cartridges were prepared by packing the desired amount of mesoporous silica into an empty polypropylene cartridge, between two polyethylene frits. After optimization, the recommended procedure was developed by using sandwich cartridges containing 150 mg of Au/Ti50-UVM-7 and 150 mg of blank UVM-7, separated with a frit. After conditioning with 6 mL of MeOH and 6 mL of ultrapure water, 100 mL of sample were adjusted to pH 6-7 and loaded into the cartridge. Then, the cartridge was dried under vacuum for 30 min, and the elution

was carried out with 6 mL of a mixture of dichloromethane/ethyl acetate (50:50). Subsequently, the extract was evaporated under N_2 stream in a 30 °C water bath, reconstituted with 250 µL of acetone, and injected in GC-ECD under described conditions.

Water samples were collected from several points of the irrigation system in the region of Valencia (Spain), both from water wells (M1, M2, and M3) and irrigation ditches (M4 and M5). Cleaned bottles were used for the sampling, and stored at 4 °C in the darkness. Before analysis, all samples were filtered in order to remove any particulate matter. Since no target compounds were detected in any sample, some of them were spiked (0.3 µg L^{-1}) and 100 mL were analyzed through the described procedure. Additionally, the same volume of these spiked samples was also analyzed by a reference method (USEPA method 3535A) [70] by using C18 cartridges for comparison. In this case, cartridges containing 200 mg of sorbent were used, previously conditioned with 15 mL of MeOH and 15 mL of ultrapure water. The later elution was carried out with 2.5 mL of acetone and 7.5 mL of dichloromethane. After evaporation, under the same conditions described above, the redissolution was done with 500 µL of acetone, prior to GC-ECD analysis. All extracts of real samples were also analyzed through GC-MS in the described conditions in order to confirm the identification or the absence of the target compounds.

The sensitivity of the method was evaluated in terms of limits of detection (LOD) and quantification (LOQ), estimated as 3 and 10 times the signal-to-noise ratio respectively. The linearity was also described, considering the LOQ as the lower limit of the linear range. The repeatability of the SPE protocol was evaluated through the analysis of replicates of 100 mL of the spiked real matrix (0.3 µg L^{-1}) following the recommended procedure. The intra-day precision was estimated by analyzing three replicates within a day, while inter-day precision was assessed with three series of three independent extractions. Besides, in order to evaluate the extraction efficiency of the method and the matrix effect, triplicates of analysis of spiked real samples at three different spiking levels (0.1, 0.3, and 1 µg L^{-1}) from irrigation ditch and water well were analyzed through the described method.

5.2. Results and discussion

5.2.1. Optimization of the SPE protocol

The influence of the Au content in the sorbent was firstly studied. For this purpose, cartridges containing 100 mg of synthesized materials were prepared. After conditioning, 10 mL of spiked ultrapure water (15 µg L^{-1}) were loaded into the cartridge. The later elution was carried out with 3 mL of dichloromethane. As can be seen in Figure 61, an improvement in the OCPs retention was observed in most of the analytes when Au nanoparticles were introduced in the sorbent structure due to their interaction with them. However, it should be noted that

this increase is slighter in the case of the material where the Ti has not been used for the Au impregnation. This observation is expected since the Au deposition in this material is proved to be poor and less homogeneous (see Chapter 4), and this amount is clearly not enough to interact with analytes. Thus, the best results were obtained with Au/Ti50-UVM-material, where a compromise between enough Au for analyte retention and the preservation of the UVM-7 porous structure is achieved, as previously commented. However, some special cases should be mentioned, such as δ-HCH and endrin aldehyde, where the recoveries are clearly reduced with the introduction of Au. Hence, in order to achieve the complete retention of the analytes, but including the contribution and selectivity of the Au, a sandwich cartridge was proposed, containing 50 mg of Au/Ti50-UVM-7 and 50 mg of pure UVM-7. As included in Figure 61, the best recoveries were achieved for this mixture, with recoveries above 60% in all cases, and these cartridges were selected for further studies.

The elution solvent was also studied. Several solvents, namely dichloromethane, ethyl acetate, hexane, and acetone were tested for the elution step for both selected materials. As shown in Figure 61, even though the worst recoveries were clearly obtained when 3 mL of hexane were used (32-84%), better recoveries in the range of 50-104% were obtained using 3 mL of the other solvents. Because of that, several mixtures of these three solvents were also tested (50:50). After the treatment of 10 mL of synthetic sample (15 µg L^{-1}) with a cartridge containing 50 mg of Au/Ti50-UVM-7 and 50 mg of UVM-7, the elution was carried out with 3 mL of each mixture. As can be seen, better results were obtained using a mixture of DCM/EtOAc (50:50), thus selecting this mixture as eluent.

In addition, the influence of the pH and ionic strength of the sample in the analyte retention was also studied. In this case, several extractions were carried out in the same conditions, but varying the pH of the sample in the range 3-8, or adjusting the ionic strength with concentrations of NaCl up to 2 M. Results showed that no influence of the NaCl was observed; however, an improvement in the OCPs retention was obtained when neutral pH was used (6-7), thus selecting these conditions for the next steps.

To assess the breakthrough volume, greater amounts of sorbent were used in order to allow the treatment of higher volumes. Thus, as described in the recommended procedure, cartridges containing 150 mg of Au/Ti50-UVM-7 and 150 mg of pure UVM-7 were prepared. After conditioning, several volumes of real matrices from the irrigation system, spiked with the same amount of each OCP (200 ng) were loaded into the cartridge, and the later elution was done with 3 mL of DCM/EtOAc 50:50. Results showed that significant recoveries were achieved for the analysis of 50 and 100 mL, thus allowing the method to treat up to 100 mL of real samples.

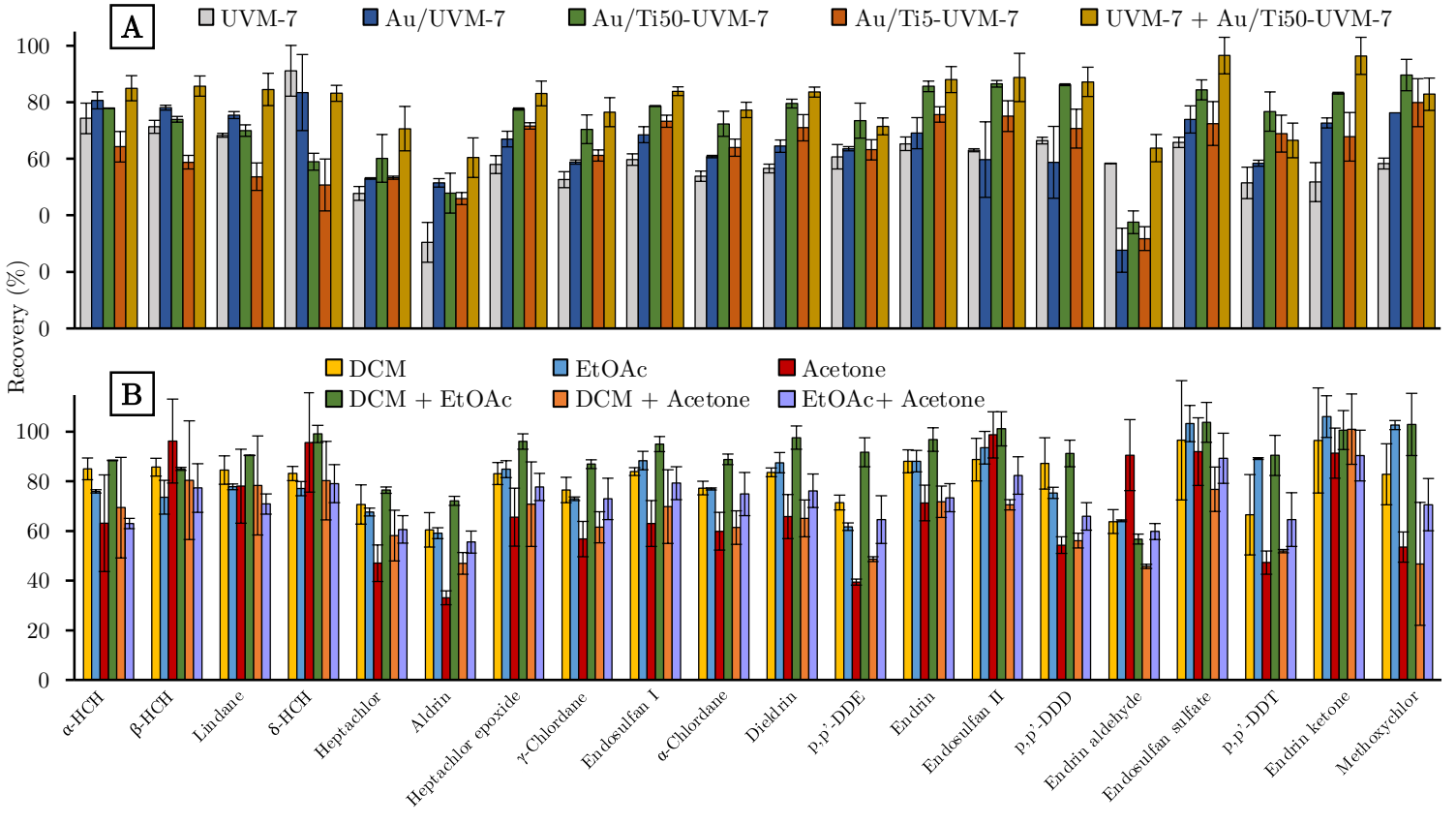

Figure 61. Effect of the Au content (A, 100 mg of sorbent) and the elution solvent nature (B, 50 mg of Au/Ti50-UVM-7 + 50 mg of UVM-7) on the OCPs recovery. SPE conditions: sample 10 mL of spiked ultrapure water (15 µg L^{-1}), elution 3 mL of each solvent or mixture.

Finally, the elution profile was evaluated, by analyzing 100 mL of a spiked real matrix (2 µg L^{-1}) and using volumes from 1 to 9 mL of the selected eluent, and it was proved that all retained analytes were eluted with 6 mL. Moreover, the possibility of concentrating the extract by evaporation was studied. Thus, extracts containing OCPs were evaporated under N_2 stream in a 30 °C water bath. After redissolution with 250 µL of acetone, and taking into account the internal standard correction, no loss of the analytes was observed. Thus, the elution with 6 mL of DCM/EtOAc and the later concentration with N_2 evaporation was considered for the final protocol.

The reusability of the designed cartridges was also proved. For this purpose, several extractions were carried out under described conditions, by using the same cartridge. It should be noted that the cartridge was washed with 5 mL of DCM/EtOAc, and conditioned again as described before the next extraction. The results showed that no significant differences were observed in analyte recoveries when cartridges were reused up to 4 times, being this an important advantage of this material.

5.2.2. Analytical figures of merit and sample analysis

Linearity and sensitivity were evaluated. As shown in Table 33, good LODs were achieved with the described method, being them below 2.5 ng L^{-1} in all cases except for lindane, DDT, and methoxychlor, where worse sensitivity was observed. In comparison with other reported methods from the literature, summarized in Table 34, the sensitivity achieved in this work is comparable or even better than the reported by using other alternative sorbents, even than those using more sophisticated equipment such as GC-MS. Also, in all cases except for methoxychlor, the obtained LOQs are below 0.02 µg L^{-1}, thus allowing the determination of OCPs in water samples concerning the European legislation [22,24].

Besides, the repeatability for a triplicate of analysis of real samples within a day was proved to be satisfactory (RSDs in the range 4-20%), being the deviation slightly higher when inter-day repeatability is considered (8-22%), as can be seen in Table 33. As observed in the comparison with other sorbents, even though the repeatability is in some cases better, our values are greater than some reported works, and the RSDs obtained are in general great for OCP determination in real matrices.

Moreover, the extraction efficiency of the proposed method was evaluated in two different matrices, and at three different spiking levels. As can be seen in Table 35, absolute recoveries above 60% were obtained in all cases for irrigation ditch and well water matrices, and above 70% for most of them, being heptachlor, aldrin, and DDE, the analytes with the worst recoveries. Besides, for most of the analytes, these recoveries are in the range 80-110%, being these recoveries in general comparable with those reported in other works (Table 34), and in some cases better taking into account that in some studies relative recoveries were

reported. Thus, these absolute recoveries were achieved with good enrichment factors (EFs, see equation (1)), also reported in Table 35, in the range 275-430. Besides, these values are higher than most of the methods summarized in the table, except for methods where greater amounts of sorbent were used. However, from these results, it can be observed that these recoveries are, in some cases, different depending on the studied matrix, with variations even of 20%. This fact proves the presence of a notable matrix effect, and consequently, the use of an addition standard calibration is advised, and it was considered for real sample analysis. It should be also noted that a low solvent-consumption method is reported in comparison with other procedures, except in the case of miniaturization techniques (implying a significant decrease of the enrichment factors). Hence, satisfactory results were obtained with the reported method, by using a cheap and reusable material for OCPs extraction and using simpler instrumentation such as GC-ECD.

Table 33. Analytical figures of merit of the proposed SPE-GC-ECD method for OCPs enrichment and determination.

Compound	Repeatability RSD (%)		Sensitivity (ng L^{-1})		Linearity (µg L^{-1})[b]
	Intra-day	Inter-day	LOD[a]	LOQ[a]	
α-HCH	11	12	0.4	1.1	0.5-100
β-HCH	4	9	4	13	5-100
Lindane	15	10	0.6	1.9	0.7-100
δ-HCH	18	18	1.7	5	2.1-100
Heptachlor	14	22	0.4	1.2	0.5-100
Aldrin	19	21	0.4	1.3	0.5-100
Heptachlor epoxide	12	11	0.4	1.3	0.5-100
γ-Chlordane	16	14	0.6	1.9	0.8-100
Endosulfan I	15	15	0.3	1.0	0.4-100
α-Chlordane	15	16	0.3	0.9	0.4-100
Dieldrin	8	11	0.6	1.9	0.8-100
p,p'-DDE	16	17	1.2	4	1.5-100
Endrin	14	17	0.9	3	1.1-100
Endosulfan II	11	17	0.7	2.2	0.9-100
p,p'-DDD	20	20	2.4	7	3-100
Endrin aldehyde	11	22	1.4	4	1.7-100
Endosulfan sulfate	11	11	1.5	4	1.8-100
p,p'-DDT	11	14	6	18	7-100
Endrin ketone	9	8	1.1	3	1.3-100
Methoxychlor	12	17	20	61	24-100

[a]Referred to the water sample

[b]Referred to the injection extract

Table 34. Comparison of the analytical features of the developed method with other SPE-based methods using alternative sorbents for OCP enrichment.

Analytical technique	Sorbent	LOD (ng L^{-1})	LOQ (ng L^{-1})	Recovery (%)	RSD (%)	EF (EF_{max})	Solvents	Ref.
SPE GC-ECD	Au/Ti-UVM-7 (300 mg)	0.3-20	1-61	62-118	4-22	275-430 (400)	6 mL MeOH, 3 mL DCM, 3 mL EtOAc	This work
SPE GC-ECD	C18 (1g)	0.8-7.4	-[a]	75-212	6-26	375-1060[b] (500)	4 mL acetone, 4 mL hexane, 1.5 mL MeOH, 5 mL DCM	[222]
SPME GC-ECD	PA-AuNPs[c,d]	130-240	440-810	85-97.1[e]	6.7-1.5	-[a]	-[f]	[223]
SPE GC-ECD	Sep-Pack Plus C18 (500 mg)	-	-	70.5-92.4	1.0-17.2	352.5-462[b] (500)	15 mL hexane,5 mL MeOH	[224]
SB-µ-SPE GC-MS	ILs[g] (1 mg)	250-1410	-[a]	32-83.8[b]	3.9-12.5	16.1-41.9 (50)	0.1 mL hexane, 0.1 mL toluene	[227]
SPE GC-MS	PEP[c,h]	440-1880	890-6260	70-118	0.5-17.8	70-118[b] (100)	5 mL MeOH, 22 mL hexane	[237]
D-µ-SPE GC-MS	C18/Forisil/Chromasorb (100 mg)	0.51-22.4	1.71-74.5	99.3-50.4	1.9-19.6	100-199 (200)	0.5 mL EtOAc, 1 mL IPA	[229]
µ-SPE GC-MS	MOF MIL-101 (4 mg)	2.5-16	17-74	87.6-98.6[e]	4.2-11	87.6-98.6[b] (100)	100 µL EtOAc	[228]
D-µ-SPE GC-ECD	1D-PANI[i] (3 mg)	7.4-46.8	24.4-154.4	73.6-107[e]	0.6-11.9	73.6-107[b] (100)	65 µL hexane	[234]

Table 34 (*continued*)

Analytical technique	Sorbent	LOD (ng L^{-1})	LOQ ng L^{-1})	Recovery (%)	RSD (%)	EF (EF_{max})	Solvents	Ref.
SPE GC-MS	SilprImN-DMIP[j] (150 mg)	7-126	-[a]	83.8-112.7	0.9-9.7	167.6-225.4[b] (200)	3 mL MeOH, 0.5 mL hexane, 12 mL DCM	[238]
SPE GC-MS	Graphene (50 mg)	1.50-9.38	5-31.3	83.9-107.3	2.9-7.4	83.9-107.3[b] (100)	20 mL MeOH, 12 mL EtOAc	[249]
SPE GC-MS	Cigarette filters (120 mg)	200	-[a]	76.4-103.7	3.2-13.6	76.4-103.7[b] (100)	8 mL MeOH, 2 mL EtOAc, 4 mL hexane, 1 mL acetone	[250]
MSPE GC-MS	MNPs[k] (50 mg)	-[a]	6-48	45-108	1-4	22.5-54[b] (50)	6 mL MeOH	[251]

[a]Not reported

[b]Not reported. Calculated from the reported experimental procedure and other reported data

[c]Sorbent amount not reported

[d]Polyacrylate commercial fiber with Au nanoparticles

[e]Reported as relative recovery

[f]Thermal desorption

[g]Ionic liquids (4-methylbenzenaminium tetrachloroferrate (III) and 1-naphthylammonium tetrachloroferrate (III))

[h]Polarity Enhanced Polymer

[i]One dimensional polyaniline

[j]Ionic liquid (SilprImN) with dummy molecularly imprinted polymer (DMIP)

[k]Magnetic nanoparticles coated with oleic acid

Table 35. Extraction efficiency for studied matrices at different spiking levels (expressed as recovery ± s) and average EF obtained with the proposed SPE-GC-ECD method for OCPs enrichment and determination.

Compound	Well water matrix				Irrigation ditch matrix			
	Recovery (%), spiking level			EF	Recovery (%), spiking level			EF
	0.1 µg L^{-1}	0.3 µg L^{-1}	1 µg L^{-1}		0.1 µg L^{-1}	0.3 µg L^{-1}	1 µg L^{-1}	
α-HCH	87 ± 16	95 ± 11	101.7 ± 1.3	377 ± 30	68 ± 8	71 ± 16	88.8 ± 0.8	300 ± 50
β-HCH	81 ± 10	95 ± 9	88 ± 3	343 ± 18	68 ± 17	87 ± 3	78 ± 3	288 ± 20
Lindane	86 ± 12	89 ± 13	94 ± 2	367 ± 19	74 ± 8	71 ± 9	82 ± 2	320 ± 30
δ-HCH	86 ± 9	83 ± 15	86 ± 3	340 ± 8	81 ± 7	70 ± 3	66 ± 5	290 ± 30
Heptachlor	75 ± 4	67 ± 15	73 ± 4	286 ± 18	70 ± 30	78 ± 3	75 ± 2	300 ± 20
Aldrin	72.3 ± 1.0	62 ± 13	72 ± 3	280 ± 20	63.0 ± 0.7	65 ± 20	70.1 ± 0.4	265 ± 15
Heptachlor epoxide	86 ± 9	98 ± 11	97 ± 6	380 ± 30	82 ± 12	91 ± 18	97 ± 2	360 ± 30
γ-Chlordane	68 ± 3	75 ± 11	81 ± 8	300 ± 20	75 ± 16	70 ± 15	74 ± 3	292 ± 11
Endosulfan I	99 ± 14	98 ± 14	100 ± 7	395 ± 3	100 ± 20	91 ± 20	95 ± 3	381 ± 19
A-Chlordane	79 ± 20	79 ± 13	83 ± 6	322 ± 8	89 ± 11	90 ± 20	80 ± 5	342 ± 18
Dieldrin	96 ± 23	104 ± 12	97 ± 9	396 ± 19	84 ± 13	87 ± 18	85 ± 4	343 ± 6
p,p' -DDE	68 ± 25	68 ± 12	71 ± 5	275 ± 8	63 ± 12	76 ± 30	68 ± 8	280 ± 30
Endrin	85 ± 9	90 ± 15	89 ± 11	352 ± 12	102 ± 10	100 ± 12	101 ± 11	403 ± 4
Endosulfan II	97 ± 11	96 ± 17	94 ± 6	383 ± 6	71 ± 14	65 ± 4	71 ± 18	276 ± 14
p,p' -DDD	82 ± 7	83 ± 16	89 ± 7	340 ± 15	107 ± 5	108 ± 2	95 ± 7	410 ± 30
Endrin aldehyde	86 ± 5	94 ± 21	76 ± 6	340 ± 40	81 ± 14	86 ± 10	83 ± 9	333 ± 9
Endosulfan sulfate	100 ± 30	104 ± 12	97 ± 7	401 ± 14	96 ± 17	90 ± 14	92 ± 8	370 ± 11
p,p' -DDT	102 ± 21	118 ± 16	100 ± 14	430 ± 40	97 ± 11	97 ± 18	93 ± 8	382 ± 8
Endrin ketone	103 ± 12	107 ± 9	100 ± 20	417 ± 10	98 ± 4	102 ± 20	95 ± 8	393 ± 15
Methoxychlor	114 ± 24	102 ± 18	90 ± 20	413 ± 40	81 ± 15	80 ± 12	94 ± 20	340 ± 30

Regarding sample analysis, no target OCPs were detected in any of the five analyzed samples. This fact can be expected since, although OCPs are still in use around the world, most of them are currently banned by European legislation. Because of the absence of positive samples, and in order to ascertain the feasibility of the method for the analysis of real samples, two synthetic samples were prepared from both studied matrices (M1S and M5S). Both samples were spiked at the same level (0.3 μg L^{-1}), and 100 mL of them were analyzed through the recommended procedure, as well as the reference method with C18 cartridges, as described above. Quantified results are presented in Table 36. As observed, obtained concentrations are close to the theoretical value. Moreover, a t-student test was carried out comparing each concentration with the same concentration obtained through the reference method. Thus, results obtained for the test indicated that all results are statistically comparable considering a 95% confidence level. Hence, the reported method presents analytical parameters comparable or better than those reported in the literature, with low solvent consumption, and can be properly applied to the determination of OCPs in water samples, being a reliable alternative for this purpose.

Table 36. Concentrations obtained (μg L^{-1}) for the analysis of spiked real water samples (spiking level 0.3 μg L^{-1}, n = 3).

Compound	M1S		M5S	
	Au/Ti-UVM-7	C18	Au/Ti-UVM-7	C18
α-HCH	0.30 ± 0.02	0.30 ± 0.02	0.30 ± 0.07	0.31 ± 0.02
β-HCH	0.32 ± 0.05	0.31 ± 0.02	0.28 ± 0.04	0.32 ± 0.12
Lindane	0.272 ± 0.011	0.295 ± 0.008	0.28 ± 0.05	0.294 ± 0.010
δ-HCH	0.30 ± 0.04	0.31 ± 0.03	0.264 ± 0.012	0.3 ± 0.2
Heptachlor	0.22 ± 0.04	0.29 ± 0.02	0.278 ± 0.012	0.283 ± 0.009
Aldrin	0.30 ± 0.08	0.299 ± 0.015	0.29 ± 0.10	0.30 ± 0.02
Heptachlor epoxide	0.31 ± 0.04	0.31 ± 0.02	0.28 ± 0.06	0.32 ± 0.03
γ-Chlordane	0.28 ± 0.07	0.31 ± 0.03	0.27 ± 0.07	0.31 ± 0.04
Endosulfan I	0.29 ± 0.05	0.29 ± 0.02	0.27 ± 0.07	0.30 ± 0.04
α-Chlordane	0.30 ± 0.04	0.31 ± 0.04	0.28 ± 0.08	0.31 ± 0.04
Dieldrin	0.294 ± 0.006	0.31 ± 0.04	0.27 ± 0.06	0.31 ± 0.03
p,p'-DDE	0.30 ± 0.07	0.30 ± 0.04	0.26 ± 0.12	0.30 ± 0.03
Endrin	0.33 ± 0.02	0.31 ± 0.05	0.27 ± 0.04	0.31 ± 0.04
Endosulfan II	0.33 ± 0.03	0.31 ± 0.04	0.24 ± 0.02	0.31 ± 0.03
p,p'-DDD	0.29 ± 0.03	0.305 ± 0.012	0.300 ± 0.005	0.32 ± 0.04
Endrin aldehyde	0.34 ± 0.04	0.31 ± 0.05	0.26 ± 0.04	0.30 ± 0.04
Endosulfan sulfate	0.29 ± 0.09	0.28 ± 0.03	0.28 ± 0.07	0.29 ± 0.05
p,p'-DDT	0.297 ± 0.015	0.30 ± 0.04	0.25 ± 0.06	0.30 ± 0.04
Endrin ketone	0.30 ± 0.03	0.28 ± 0.05	0.26 ± 0.06	0.27 ± 0.05
Methoxychlor	0.30 ± 0.02	0.31 ± 0.06	0.26 ± 0.06	0.30 ± 0.04

5.2.3. Study of the interaction of analytes with gold nanoparticles

Finally, the interaction between Au nanoparticles and analytes was studied. For this purpose, a cartridge containing 100 mg of Au/Ti50-UVM-7 was loaded with 10 mL of spiked water at a high concentration (150 µg L^{-1}). After air-drying the material, the UV-Visible spectrum of both blank and charged silica was measured. As seen in Figure 62, in the absence of analyte, a typical plasmon band centered at a wavelength value of 540 nm is observed along with a shoulder of less intensity at ca. 700 nm. The most intense band may be associated with the presence of isolated Au nanoparticles smaller than 10 nm, while the shoulder band can be due to a certain degree of aggregation between the Au particles, forming larger clusters [252,253]. This observation is also in good accordance with the electron microscopy study (Chapter 4). This phenomenon is called plasmon coupling and it translates into a significant shift in the overall extinction peak at higher wavelengths when the spacing between particles is reduced [252,253]. As observed, the addition of analyte causes a disaggregation or separation among the individual Au nanoparticles. Consequently, it greatly decreases the intensity of the shoulder and increases the signal centered at 540 nm. Although the phenomenon is reversible, it is proof of the preferential interaction of the analyte on the surface of the Au nanoparticles, favouring their separation and avoiding plasmon coupling.

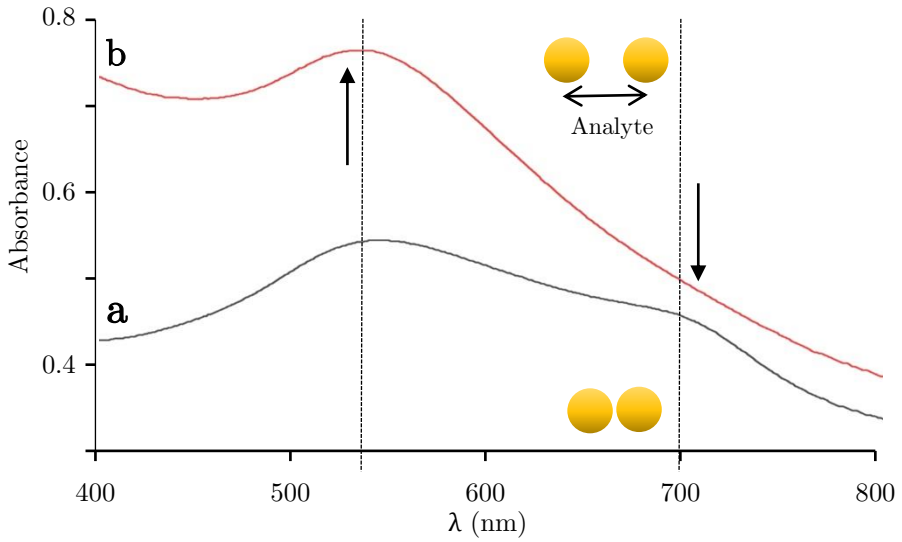

Figure 62. UV-Vis spectra of blank (a) and OCP charged (b) Au/Ti50-UVM-7 material, showing the increase in the plasmon band of Au nanoparticles due to their separation because of the interaction with analytes.

6. Conclusions

In this chapter, the ability of UVM-7 materials doped with metallic heteroelements for the retention of pesticides has been proved. The presence of Ti centers in Ti-UVM-7 materials has been demonstrated to play a key role in the retention of organophosphorus pesticides, due to its interaction with phosphate groups, in comparison with blank UVM-7. Also, Ti incorporation by co-hydrolysis has proved to be more effective than the presence of Fe for the extraction of OPPs from both air and water matrices because of the proper distribution of the metal throughout the silica network, as described in Chapter 4. Besides, the characteristic architecture of this material has proved also to be better for the target analytes than xerogels, either doped with metals by impregnation or containing cyclodextrins. Likewise, the modification of these materials with Au nanoparticles by impregnation has been also demonstrated to provide good sorbents for OCPs retention and extraction, and the preferential interaction between these active centers and chlorine groups of the target analytes has been also proved through the plasmon coupling study.

Thus, with the Ti25-UVM-7 material, two analytical methods have been successfully developed. On the one hand, samplers designed with this material have proved to be an alternative for OPPs sampling from air in occupational risk assessment, with good recoveries for all studied analytes (above 82%) and acceptable repeatability taking into account the main sources of error such as the variations in the air concentrations, which strongly depend on parameters such as the time and sampling position. Besides, good sensitivity has been also reported, being this method a mild and more environmentally friendly alternative. In addition, the method has been successfully applied for the determination of methyl-chlorpyrifos in a real risk assessment study, in comparison with XAD-2 samplers. In this study the presence of unsafe pesticide concentrations in the workplace has been demonstrated, both during the pesticide application and before the application, thus proving the need for personal protective equipment. Therefore, all these features of the Ti25-UVM-7 samplers, stand them out as a useful tool for its implementation in occupational risk assessment.

Likewise, a method for OPPs extraction from water samples has been developed with Ti25-UVM-7 material, with recoveries above 81% for spiked water samples. However, in this case, an important matrix effect was demonstrated in complex environmental matrices being recommended a standard addition calibration. Besides, the protocol developed also provided satisfactory sensitivity using common equipment accessible in most analytical laboratories, as well as LODs in the range 0.2-1.4 µg L^{-1} using a GC-MS system. In summary, the present SPE method is simple, cost-effective, and showed good reusability of material.

Finally, a similar method has been developed for OCPs determination in water samples, by using the Au/Ti50-UVM-7 material. In this case, good extraction efficiencies were obtained for most of the 20 target analytes, with recoveries in

the range of 80-110% for most of them in several environmental matrices. Moreover, other good analytical features were achieved such as good sensitivity for the determination of OCPs according to European regulations [22,24]. Thus, analytical parameters comparable or better than other alternative sorbents have been reported, being this method a simple, cheap, and environmentally-friendly alternative, using accessible and straightforward instrumentation.

In both cases, the feasibility of methods designed for pesticides extraction from water samples was assessed in comparison with C18 commercial cartridges, and comparable results were obtained for the analysis of spiked real samples. Also, results from the analysis of real samples provided negative results in all cases for OCPs determination due to the strong regulations in European countries for these compounds, although low concentrations were detected for OPPs since their use is more widespread in developed countries. However, concentrations below LOQs were obtained in all cases. Hence, synthesized materials showed satisfactory results for these analytes and better reusability than the commercial support, being a good alternative for pesticide extraction and determination in environmental water samples.

Chapter 6

Extraction of emerging pollutants from environmental water samples with M-UVM-7 materials

1. Introduction

As commented, currently, there is a rising concern about the presence of new organic synthetic compounds in the environment, which are called emerging pollutants. Although in many cases these compounds have been present in the environment since a long time ago, they have not been identified until the development of more sensitive analytical methods. Because of that, some of them are not regulated and their effects are not completely studied [5]. However, most of them are starting to be regulated by several organizations such as the Stockholm Convention on Persistent Organic Pollutants, which is doing great efforts to identify these potentially hazardous compounds to vigilante them [4].

Among these emerging pollutants, flame retardants (FRs) have received great attention since two decades ago. These compounds are chemical additives widely used to prevent combustion or delay fire propagation. For many years, halogenated flame retardants were highly used, mainly brominated FRs such as polybrominated diphenyl ethers (PBDEs), currently listed in the Stockholm Convention. However, their persistence, bioaccumulation, and toxicity, led to their restriction and ban.

For this reason, phosphorus flame retardants (PFRs) were considered as a suitable alternative to these compounds (Figure 63) [4,5,254,255]. Despite this, these additives are not chemically bonded to the product, which means that they can be easily released to the environment by volatilization, abrasion, and dissolution [256,257]. In addition, although their effects have not been studied to the same extent as brominated flame retardants, several studies have shown their potential carcinogenic effects as well as high environmental persistence, especially in the case of chlorinated PFRs, being an ongoing global concern regarding public health [5,255,258,259].

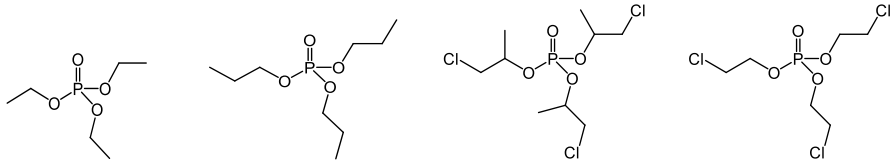

Triethyl phosphate (TEP) | Tripropyl phosphate (TPP) | Tris(2-chloroisopropyl) phosphate (TCIPP) | Tris(2-chloroethyl) phosphate (TCEP)

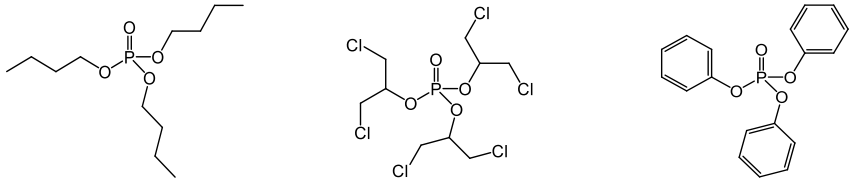

Tri-n-butyl phosphate (TnBP) | Tris(1,3-dichloro-2-propyl) phosphate (TDCIPP) | Triphenyl phosphate (TPhP)

Figure 63. Molecular structure of studied phosphorus flame retardants.

In the same way, perfluoroalkyl and polyfluoroalkyl substances (PFASs) are a group of anthropogenic chemicals that have been widely used since 1950 for a wide range of industrial applications such as polymer production or as surfactants [12]. Due to their persistence, ubiquity, and long-range transport potential, they have been detected in the environment, wildlife, and humans [260,261]. Despite their non-volatility and low water solubility, the most frequently detected PFASs are the perfluoroalkyl carboxylates (PFCAs) and perfluoroalkyl sulfonates (PFSAs) [260,262], with an increasing concern about their presence because of their bioaccumulation and adverse effects on humans [263,264].

Perfluorooctanoic acid (PFOA) | Perfluorooctane sulfonic acid (PFOS)

Figure 64. Molecular structure of PFOA and PFOS, as a representative example of the structure of studied PFCAs and PFSAs respectively.

Even though the regulation of these compounds is still ongoing, strong restrictions are being applied to them, mainly to perfluorooctanoic acid (PFOA) and perfluorooctane sulfonic acid (PFOS) (Figure 64), which are included in Annex A and B of the list of the Stockholm Convention, respectively, for their elimination or regulation [4,264–266]. Indeed, the evaluation of these and other emerging pollutants is currently ongoing, not only by the United Nations in the Stockholm Convention, but also by other organizations such as the European Chemicals Agency, which has added several of these PFASs and PFRs to the Candidate List of Substances of Very High Concern [9,267,268], or the United States Environmental Protection Agency (USEPA) [255].

Because of that, their monitoring and environmental vigilance have been increased in the last decades, and many studies have been carried out to assess the presence of these pollutants in environmental matrices. In the case of flame retardants, PFRs are expected to be present in higher concentrations than brominated compounds due to their water solubility. Indeed, several studies have reported their presence in environmental water samples, with concentrations ranging from few ng L^{-1} to several µg L^{-1} in the case of European countries [254,257]. Likewise, several studies have reported the presence of significant concentrations of PFASs around the world. Although in European countries lower concentrations of PFASs were detected [267,269,270], higher concentrations have been found in Asian countries such as China, where concentrations up to several µg L^{-1} were reported [271–273].

Specifically, Lorenzo et al. [264] reported the presence of high concentrations of these emerging pollutants in Mediterranean wetland in Valencia (Spain), with mean concentrations of the order of 50-500 ng L^{-1} in the case of PFRs (mainly TCIPP, TDCIPP, and TPhP), and maximum concentrations of PFASs in the range of 20-60 ng L^{-1}, being these concentrations up to 100 ng L^{-1} in the case of wastewater. Indeed, wastewater treatment plants (WWTP) were identified as the major source of polluted water since both PFASs and PFRs are not expected to be completely removed in these plants [271,274]. Thus, high contents have been found in some studies regarding WWTP both effluent and influent channels, with concentrations even of the order of µg L^{-1} of some PFRs [255,275], as well as significant concentrations of several PFASs in both influent and effluent channels from plants at a global level [271]. Moreover, the long-range transport of these compounds has also been studied, being a global concern [30,257,276–278]. Hence, there is an important interest in developing new methodologies for the determination and environmental control of these pollutants.

These results have led to the development of a wide variety of methods for PFR and PFASs preconcentration, enrichment, and determination in environmental samples. In the case of PFRs, due to the wide range of physical and chemical properties, these compounds are detected by using either gas (GC) or liquid chromatography (LC) [5,254]. However, in the case of PFASs, although some groups such as the fluorotelomers can be determined by GC [260,279], in

some cases with previous derivatization [280], the most commonly employed technique for the quantification of these analytes is the LC. In these cases, although high-resolution liquid chromatography (HPLC) has been widely used for the separation, the appearance of more sophisticated techniques has caused the migration to ultra-high-resolution liquid chromatography (UHPLC) [5,281]. Besides, mass spectrometry detectors (MS or MS/MS) are the most frequently used due to their selectivity and their advantages for identification, although selective detectors such as nitrogen-phosphorus detector [282] and flame photometric detector [255] have been also used for organophosphorus compounds.

However, and despite the great sensitivity of these techniques, the low concentrations generally present in some samples make the preconcentration step mandatory for environmental analysis. For this purpose, in the case of water samples, the most used technique is the solid-phase extraction (SPE), although some studies using liquid-liquid extraction (LLE) have been reported, using several organic solvents such as dichloromethane, toluene, methyl *tert*-butyl ether, or acetonitrile [283–287]. However, the high organic solvent consumption, the long extraction time, as well as the foam formation, and the difficulties for automatization, represent great disadvantages for the adoption of these protocols [254,255,288]. Likewise, other miniaturized techniques have been also proposed for PFASs enrichment from water samples, such as solid-phase microextraction (SPME) with fibers, or dispersive liquid-liquid microextraction (DLLME), although a significantly lower volume of water can be treated in these cases, thus entailing poor enrichment factors concerning environmental analysis [5]. Thus, SPE is preferred for water extraction, since its time of analysis is shorter and its solvent consumption is lower, thus providing better enrichment factors [289].

For SPE methods development, several sorbents have been proposed for the enrichment of these emerging pollutants. On the one hand, several sorbents have been used for PFASs retention and extraction [5,287], including the classical C18 cartridges, but the most commonly used are the weak anionic exchange (WAX) cartridges, such as the Oasis WAX [262,290,291] or Strata-X AW [292–295], or the hydrophilic/lipophilic balanced Oasis HLB cartridges [296]. Although comparable recoveries have been reported for both of them, WAX cartridges are proved to be more efficient for short-chain PFASs, mainly in the case of ionic PFCAs and PFSAs, being the most frequently used ones [287]. On the other hand, in the case of PFRs, the most commonly used materials are also the C18 cartridges such as ENVI-18, amberlite resins such as XAD-2, and also the above-mentioned Oasis HLB cartridges. With these materials, although quantitative recoveries were achieved for some analytes in many studies, the extraction yields are still insufficiently good in some cases with recoveries in the range of 40-45% for certain compounds (mainly for triethyl phosphate) [254,264,288]. Hence, there is an important interest in developing new materials and methods for PFASs and PFRs quantitative retention and extraction from aqueous matrices, to address all these extraction problems and ensure a feasible quantification.

In this sense, and as discussed in previous Chapters 2 and 4, UVM-7 materials present great features for the retention of both small and large molecules, being a promising sorbent for organic pollutants retention. Besides, the possibility of controlling the pore size through the modification of the surfactant used during the one-pot synthesis allows adapting the silica architecture to target analytes, thus expanding the scope of these materials [116]. Also, their modification through the introduction of heteroelements by co-hydrolysis can lead to selective sorbents thanks to the use of metallic centers as active sites for the retention, as previously presented [145,146]. In this sense, as stated in Chapter 5, the addition of titanium and iron to the silica network seems to be a good option for organophosphorus compounds retention due to the interaction of Ti and Fe with phosphate groups [161,242,243], as previously applied in organophosphorus pesticides determination (Chapter 5). Likewise, the presence of iron has proved to improve the effectiveness of the sorption of PFASs in some studies focused on pollution removal, thus being the addition of this metal a possible strategy to enhance the selectivity of SPE sorbents for the extraction of these compounds [297,298].

2. Materials, reagents, and instrumentation

PFR standards such as triethyl phosphate (TEP), tripropyl phosphate (TPP), tri-n-butyl phosphate (TnBP), tris(2-chloroethyl) phosphate (TCEP), tris(2-chloroisopropyl) phosphate (TCIPP), tris(1,3-dichloro-2-propyl) phosphate (TDCIPP) and triphenyl phosphate (TPhP) were purchased from Sigma-Aldrich (St. Louis, MO, USA). A standard stock multicomponent solution of 750 mg L^{-1} was prepared in acetonitrile for all studies. All PFR solutions were stored in darkness at 4 °C.

In the case of PFASs, A multicomponent solution in methanol was purchased from Wellington Laboratories (Southgate, Canada) containing 2000 µg L^{-1} of perfluoro-n-butanoic acid (PFBA), perfluoro-n-pentanoic acid (PFPA), perfluoro-n-hexanoic acid (PFHxA), perfluoro-n-heptanoic acid (PFHpA), perfluoro-n-octanoic acid (PFOA), perfluoro-n-nonanoic acid (PFNA), perfluoro-n-decanoic acid (PFDA), perfluoro-n-undecanoic acid (PFUnDA), perfluoro-n-dodecanoic acid (PFDoDA), perfluoro-n-tridecanoic acid (PFTrDA), perfluoro-n-tetradecanoic acid (PFTeDA), perfluoro-1-butanesulfonic acid (PFBS), perfluoro-1-hexanesulfonic acid (PFHxS), perfluoro-1-octanesulfonic acid (PFOS), and perfluoro-1-decanesulfonic acid (PFDS). A concentrated solution of perfluoro-n-[$^{13}C_8$]octanoic acid ($^{13}C_8$-PFOA) of 50 mg L^{-1} in methanol was also purchased from Wellington Laboratories and used as an internal standard. These stock solutions were stored refrigerated in the darkness, and diluted with methanol for their use.

All solvents used in extraction and analysis procedures were of HPLC grade quality: ethanol, n-hexane, ethyl acetate (EtOAc), methanol (MeOH), acetonitrile (ACN), and dichloromethane (DCM), purchased from Panreac AppliChem

(Darmstadt, Germany), Scharlau (Barcelona, Spain), Lab-Scan Analytical Sciences (Gliwice, Poland), and VWR Chemicals (Radnor, PA, USA). Ultrapure water from an Adrona (Riga, Latvia) purification system was also employed. In addition, acetic acid from Sigma-Aldrich, NaOH from Scharlau, and NH_4F from Merck (Darmstadt, Germany) were also employed.

For sample analysis, commercial C18 cartridges (Varian Bond Elut, 200 mg) were used as reference sorbents for extraction of PFR, and Oasis WAX cartridges containing 150 mg of sorbent were used from Waters (Milford, MA, USA) in the case of PFASs.

During SPE procedures, a Vac Elut 20 was used, connected to a vacuum pump system. Water samples were filtered prior to analysis with polyamide 0.45 µm from Sartorius Stedim Biotech filters (Goettingen, Germany). For solvent evaporation, a miVac sample concentrator from SP Scientific (Warminster, PA, USA) was employed.

Regarding instrumental determination of PFRs, a Focus GC gas chromatograph from Thermo Fisher Scientific (Waltham, MA, USA) with a DSQ II mass spectrometry detector was employed. For the separation, an analytical column Agilent HP-5 (30 m x 0.32 mm x 0.25 µm film thickness) was used from Agilent Technologies Inc. (Santa Clara, CA, USA), with helium as carrier gas (1 mL min^{-1}). A sample volume of 0.5 µL was injected in splitless mode (splitless time of 1.5 min) using the following temperature gradient: 40 °C for 4 min, followed by a ramp at 5 °C min^{-1} up to 170 °C (hold for 5 min), ramp at 10 °C min^{-1} to 230 °C (hold for 5 min), ramp at 5 °C min^{-1} to 250 °C, and ramp at 10 °C min^{-1} to 300 °C [284]. Selective ion monitoring mode was selected for mass detection, and the specific ions monitored for each compound are shown in Table 37. Likewise, the proper separation of the target compounds under these conditions is given in Figure 65.

Table 37. Monitored ions for each target analyte using GC-MS equipment.

Compound	Monitored ions
TEP	99, 109, 127, 155
TPP	99, 123, 141, 153
TnBP	99, 155, 211
TCEP	99, 143, 205, 249
TCIPP	99, 125, 157
TDCIPP	99, 155, 191, 209
TPhP	170, 214, 233, 325

*The dwell time for each monitored ion was 100 ms

Moreover, in some optimization steps where higher concentrations were used, a Thermo Scientific Trace GC Ultra gas chromatograph coupled to a flame ionization detector was employed. In this case, nitrogen was used as carrier gas

(2.7 mL min^{-1}) and 0.3 µL were injected in split mode (split ratio 5). The separation was achieved with the same oven temperature program described above.

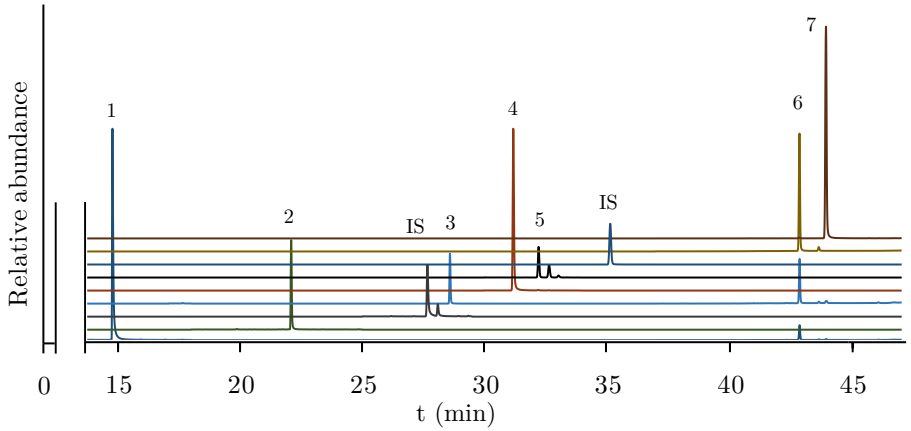

Figure 65. Extracted ion chromatogram from specific ions used for each compound, showing the proper separation of target PFR: TEP (1), TPP (2), TnBP (3), TCEP (4), TCIPP, (5), TDCIPP (6), TPhP (7).

On the other hand, the instrumental determination of PFASs was carried out with an ExionLC AD liquid chromatograph coupled to a triple quadrupole QTRAP 6500+ mass spectrometry detector from Sciex (Framingham, MA, USA). The separation of the analytes was achieved with a Kinetex C18 column (100 Å x 2.1 mm x 1.7 µm) from Phenomenex (Torrance, CA, USA), and using a mobile phase composed of water and methanol, containing 2,5 mM of NH_4F in both cases. The proportion of both solvents and the programmed gradient is shown in Table 38 (flow 0.3 mL min^{-1}). Instrumental parameters of the MS/MS detector, including selected transitions for each analyte, are displayed in Table 39.

Table 38. Mobile phase gradient used in UHPLC-MS/MS system for PFASs separation. Components: water (2.5 mM of NH_4F) and methanol (2.5 mM of NH_4F).

Time (min)	Methanol (%)
0	5
0.5	30
12	96
20	95
29	30

Table 39. Instrumental parameters of the MS/MS detector in the determination of target PFASs.

Compound	Quantifier transition				Qualifier transition			
	Q (m/z)	DP (V)	CE (V)	CXP (V)	q (m/z)	DP (V)	CE (V)	CXP (V)
PFBA	213 > 169	-80	-5	-10				
PFPeA	263 > 219	-80	-5	-10				
PFBS	299 > 99	-140	-38	-10	299 > 80	-140	-26	-10
PFHxA	313 > 269	-70	-5	-10	313 > 119	-70	-5	-10
PFHpA	363 > 319	-25	-5	-37	363 > 169	-25	-5	-37
PFHxS	399 > 99	-30	-78	-15	399 > 80	-30	-86	-9
PFOA	413 > 369	-32	-14	-31	413 > 169	-32	-14	-31
$^{13}C_8$-PFOA	417 > 372	-25	-14	-23	417 > 169	-25	-14	-23
PFNA	463 > 419	-30	-16	-17	463 > 219	-30	-16	-17
PFOS	499 > 99	-135	-108	-7	499 > 80	-135	-106	-9
PFDA	513 > 469	-60	-17	-49	513 > 269	-60	-17	-49
PFUnDA	563 > 519	-22	-14	-45	563 > 269	-22	-14	-45
PFDS	599 > 99	-80	-80	-10	599 > 80	-80	-80	-10
PFDoDA	613 > 569	-90	-5	-10	613 > 269	-90	-13	-10
PFTrDA	663 > 619	-100	-5	-10	663 > 169	-100	-24	-10
PFTeDA	713 > 669	-110	-5	-10	713 > 169	-110	-25	-10

*Entrance potential = -10 V
DP: Declustering potential
CE: Collision energy
CXP: Collision cell exit potential

3. Enhancing extraction performance of organophosphorus flame retardants in water samples using Ti-UVM-7 materials

The aim of this work is to develop a method for the extraction and preconcentration of phosphorus flame retardants from water samples by using UVM-7 mesoporous silica materials doped with titanium for the SPE procedure, and GC-MS technique for their later quantitation. The relevant features of the method are established, and the optimal SPE procedure is then applied to the determination of PFRs in real water samples, in comparison with a USEPA reference method.

3.1. Sample treatment and experimental procedure

SPE cartridges were prepared by packing the desired amount of UVM-7 material doped with titanium into an empty propylene cartridge, between two propylene frits. Several parameters were tested in order to achieve the optimum conditions for PFR enrichment. Firstly, the titanium content of the sorbent, as well as the sorbent amount and elution solvent were studied. Once established the optimum cartridges for the retention of the analytes, the solvent volume necessary for their elution, and the possibility of evaporating the elution extract were evaluated. Finally, the breakthrough volume was evaluated by analyzing different volumes of spiked real blank environmental samples under optimized conditions.

After optimization, the recommended procedure was achieved with cartridges containing 200 mg of Ti50-UVM-7 material. Once conditioned with 5 mL of MeOH and 5 mL of ultrapure water, 50 mL of sample were loaded into the cartridge. Then, the cartridge was dried with air for 10 min, and the elution was carried out with 3 mL of ethyl acetate. After the addition of the internal standard, the solvent was evaporated under vacuum at 30 °C until 250 µL and the final extract was injected in the GC-MS in the described conditions.

For the repeatability evaluation, 25-50 mL of several spiked real samples at different levels (3 and 80 µg L^{-1}) were analyzed following this recommended procedure. For the intra-day precision estimation, three replicates were carried out within a day, and for the inter-day precision, three series of three independent extractions were considered. Likewise, the reusability of developed cartridges was assessed by carrying out several extractions in the same conditions with reused cartridges.

Water samples were collected from both irrigation ditches and WWTP from several points in the Valencia (Spain). The bottles were previously cleaned and, after sampling, they were covered with aluminum foil and stored in the darkness at 4 °C until analysis. Before analysis, all samples were filtered in order to remove any particulate matter. Then, 50 mL of each sample were analyzed following the recommended procedure described above. In addition, in order to evaluate the influence of the matrix, a triplicate of each sample type was spiked with PFR solution (40-160 µg L^{-1}) and analyzed through the same procedure.

The same amount of collected water samples was also analyzed by using C18 cartridges for its preconcentration, following the general procedure described by USEPA [299], correcting the matrix effect and possible errors with standard addition calibration or the use of internal standards.

3.2. Results and discussion

3.2.1. Optimization of the SPE procedure

The composition of the sorbent was firstly studied. For this purpose, the described silica UVM-7 materials, either pure or with different amounts of titanium, were tested with cartridges containing 50 mg of each sorbent. In all cases, 10 mL of spiked ultrapure water (1.5 mg L^{-1} of each PFR) were loaded into the conditioned cartridges, and the elution was carried out with 2 mL of ethyl acetate. As can be seen in Figure 66, when blank UVM-7 and Ti-containing materials (with Si/Ti ratios 100 to 5) were compared, a clear effect of the titanium content in PFR retention was observed. The presence of small amounts of Ti centers entails an important increase in the recoveries, especially in the case of TEP and TCEP, with improvements up to 50%. However, when the Si/Ti ratio was reduced to 25 or less, a decrease in the recoveries was observed (mainly in TEP and TCEP as well), being this recovery reduction very remarkable when the highest amount of titanium is introduced (Ti5-UVM-7). Thus, the best recoveries were achieved with Ti50-UVM-7 material, which was selected for the later optimization studies and method development.

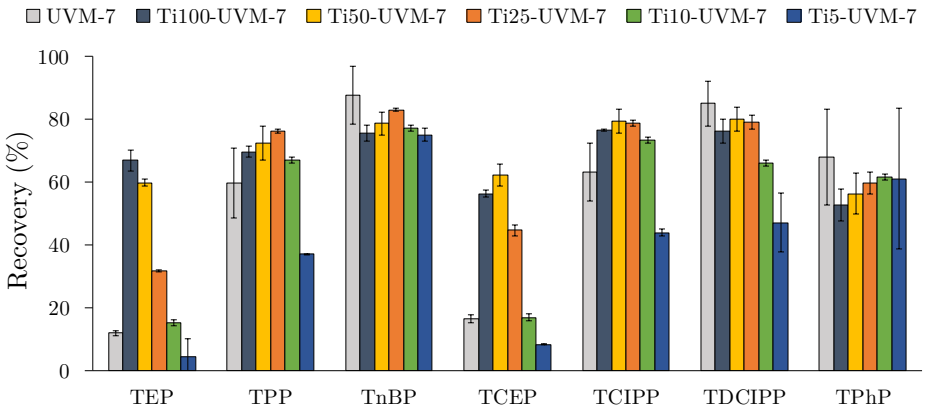

Figure 66. Effect of the amount of titanium introduced in the sorbent on PFRs recoveries. Conditions: 50 mg of each sorbent, 10 mL of spiked ultrapure water (1.5 mg L^{-1}), elution with 2 mL of ethyl acetate.

Probably, this optimum value corresponds to a compromise between enough active Ti sites and the predominance of isolated centers or low nano-sized clusters, in any case still far from resembling rutile or anatase domains. According to UV-Vis and Raman data (Figure 37, 38, and 39), these isolated and well-dispersed active sites must be very similar for the lowest Ti-containing samples (Ti100-UVM-7 and Ti50-UVM7). In both cases, active sites with Ti atoms in tetrahedral coordination seem to be the predominant ones, without leaving aside a relatively low proportion of Ti octahedral sites. As the Ti content increases (samples from Ti25-UVM-7 to Ti5-UVM-7), the potential benefit of a higher proportion of Ti is

strongly reduced due to the growth of Ti clusters and finally with the appearance of anatase nanodomains (Ti5-UVM-7) and the alteration of the UVM-7 structure.

Regarding the influence of the solvent nature, several extractions of spiked ultrapure water (0.4 mg L^{-1}) were carried out using 2 mL of different eluting solvents. The use of n-hexane was firstly discarded since poor recoveries (below 40% in all cases) were obtained for all analytes. This fact is expected since significant non-polar solvents lead to worse extraction efficiencies due to the relative polarity of the PFR [254]. Indeed, better results were achieved with the other solvents, with acceptable results in general (53-102% for ethanol and 60-101% for methanol), except for acetonitrile (with recoveries in the range 38-86%). Even so, best recoveries were obtained using ethyl acetate (84-99%), which was chosen for the method development.

Likewise, cartridges with different amounts of Ti50-UVM-7 material were prepared in order to assess the influence of the sorbent amount. In this case, a real environmental water matrix (from irrigation ditch) was used to consider the influence of the matrix interferences in the analyte retention, and 25 mL of a spiked real matrix (160 µg L^{-1}) were analyzed, using 2 mL of ethyl acetate for the elution step. As shown in Figure 67, poor recoveries were obtained for some analytes (mainly TEP, TCEP, and TCIPP) when 50 mg were used with real matrix samples, thus observing a substantial influence of the matrix. However, better recoveries were achieved when the amount of solid phase was increased, obtaining the best results with 200 and 300 mg of the material. In the case of TDCIPP and TPhP, lower recoveries were achieved with 300 mg, probably due to the insufficient amount of elution solvent, optimized in the next step. Anyway, significant retention was achieved with all tested cartridges for these compounds. Hence, in order to use the minimum but enough amount of phase, cartridges containing 200 mg of Ti50-UVM-7 material were selected.

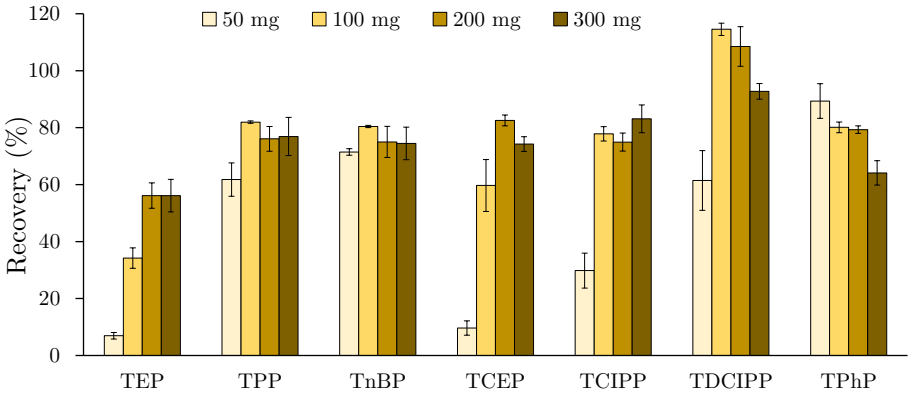

Figure 67. Effect of the sorbent amount (Ti50-UVM-7) on PFRs recoveries. Conditions: 25 mL of spiked irrigation ditch water (160 µg L^{-1}), elution with 2 mL of ethyl acetate.

Also, the elution volume study with volumes from 1 to 4 mL of ethyl acetate showed that the complete desorption of the analytes was achieved when 3 mL were used, thus obtaining recoveries above 80% for all analytes. Likewise, the possibility of evaporating the solvent under vacuum either at 30 or 60 °C was studied. Even though low recoveries of the PFRs were obtained when the solvent evaporation was carried out at 60 °C, no significant loss of any analyte was observed when 30 °C were used, neither with 500 nor 250 µL as final volume. Thus, the possibility of evaporating the extracts until 250 µL was proved, increasing considerably the sensitivity of the method.

Finally, the breakthrough volume was evaluated in order to obtain the maximum enrichment factors for all analytes, by analyzing different volumes of spiked real blank environmental samples in optimized conditions. In this case, no significant variations in extraction yields were observed when sample volumes of 10, 25, and 50 mL were treated, thus allowing this protocol to analyze 50 mL of water samples.

3.2.2. Analytical figures of merit

The linearity and sensitivity of the method were evaluated by analyzing spiked blank real samples (concentrations 0-50 µg L^{-1}) following the recommended procedure. Then, the final extract was injected into the GC-MS system. Limits of detection (LOD) and quantification (LOQ) were estimated as 3 or 10 times the signal-to-noise ratio respectively, and the LOQ was considered as the lower limit of the linear range. As shown in Table 40, LODs in the range 0.019-0.21 µg L^{-1} were achieved for all analytes, although these limits could be improved by using more sophisticated equipment such as GC-MS/MS. Relative standard deviation (RSD) values of the method were also obtained, thus evaluating both intra- and inter-day precision as described. In the first case, RSD values below 11% were achieved for all analytes. However, worse inter-day precision was obtained, with RSDs in the range 2-19%, except in the case of TPP and TDCIPP.

Table 40. Analytical figures of merit of the proposed SPE method combined with the GC-MS system.

Compound	Linearity (µg L^{-1})	Sensitivity (µg L^{-1})		Repeatability, RSD (%)			
				80 µg L^{-1}		3 µg L^{-1}	
		LOD	LOQ	Intra-day	Inter-day	Intra-day	Inter-day
TEP	0.5 - 50	0.14	0.5	7	12	8	5
TPP	0.15 - 50	0.05	0.15	9	22	2	2
TnBP	0.06 - 50	0.019	0.06	3	16	4	4
TCEP	0.3 - 50	0.10	0.3	4	12	8	8
TCIPP	0.4 - 50	0.12	0.4	4	19	3	4
TDCIPP	0.4 - 50	0.10	0.4	7	27	3	24
TPhP	0.7 - 50	0.21	0.7	11	19	9	20

In the same way, the extraction efficiency of the developed method was evaluated by carrying out a triplicate of extractions in several matrices, thus evaluating also the influence of the matrix in PFR retention. As can be seen in Table 41, satisfactory recoveries were achieved with ultrapure water (80-116%), being these recoveries not affected when a complex environmental matrix is used, in the case of irrigation ditch water (80-110%). However, in the case of WWTP water, the matrix effect on the retention of the analytes is more significant (recoveries in the range 65-78%), since a highly complex and dirty matrix is considered, making necessary the use of a standard addition calibration. In any case, the obtained extraction efficiencies, as well as the enrichment factors (calculated according to equation (1)), above 131 in all cases, allowed the determination of PFRs in these matrices through the described method using Ti50-UVM-7 material. A similar experiment was carried out with C18 cartridges following the reference method, and significantly worse recoveries were obtained (Table 41), with recoveries below 45% for TEP, TCEP, and TCIPP, being these results better in the case of TPP, TnBP, TDCIPP, and TPhP.

Furthermore, the reusability of the designed cartridges was also studied repeating the described procedure 3 times with used cartridges, previously washed with 3 mL of ethyl acetate and conditioned as described above. Results showed that no significant variations on the recovery of the analytes were obtained, thus allowing the reuse of the cartridges at least 3 times.

3.2.3. Sample analysis

The developed method was applied to the analysis of several environmental water samples. Specifically, six samples were collected from irrigation ditch (IM1) and WWTP influent channels (WM1-WM5) from several plants of Valencia. In this case, 50 mL of each sample were analyzed through the described SPE protocol and injected into the GC-MS system. Each sample was analyzed in triplicate. The results obtained are summarized in Table 42. As can be seen, TEP, TPP, and TnBP were not detected in any analyzed samples. However, other analytes were detected in WWTP samples, although values below LOQ were obtained for most of them. Quantifiable concentrations were obtained in the case of WM4 and WM5. As observed, the main detected analytes were TCIPP, TDCIPP, and TPhP, with concentrations in the range 0.2-1.5 µg L^{-1}, being these values in accordance with those reported by Lorenzo et al. [264] for WWTP influent channels in València region. An example of a sample chromatogram (spiked and non-spiked) is shown in Figure 68.

Moreover, some positive samples (WM4 and WM5) were also analyzed by a reference method for organic pollutants in water, by using C18 cartridges. In this case, a standard addition calibration was used, since the extraction efficiency with these cartridges was proved to be much lower (see section above). The results are also summarized in Table 42, and statistically comparable concentrations (t-student test with 95% of confidence level) were obtained by using both methods.

Table 41. Extraction efficiencies obtained for each analyte in studied matrices (C18 extraction efficiencies obtained for irrigation ditch matrix).

Compound	Ultrapure water		Irrigation ditch matrix		WWTP matrix		C18 cartridges extraction efficiency (%)
	Extraction efficiency (%)	EF	Extraction efficiency (%)	EF	Extraction efficiency (%)	EF	
TPP	94 ± 12	187	94 ± 8	189	76 ± 10	153	77 ± 4
TnBP	96 ± 11	192	95 ± 3	190	78 ± 6	156	80 ± 20
TCEP	116 ± 10	233	110 ± 5	221	71 ± 7	141	45 ± 8
TCIPP	109 ± 10	218	104 ± 4	208	76 ± 3	153	43 ± 8
TDCIPP	100 ± 16	198	109 ± 8	219	69 ± 11	139	92 ± 7
TPhP	85 ± 8	171	92 ± 10	184	77 ± 10	155	97 ± 11

Table 42. Results obtained (µg L^{-1}) for the determination of PFRs in water samples, using the developed method with Ti50-UVM-7 cartridges, and the reference method with C18 cartridges.

Compound	Ti50-UVM-7						C18	
	IM1	WM1	WM2	WM3	WM4	WM5	WM4	WM5
TEP	<LOD	<LOD	<LOD	<LOD	<LOD	<LOD	<LOD	<LOD
TPP	<LOD	<LOD	<LOD	<LOD	<LOD	<LOD	<LOD	<LOD
TnBP	<LOD	<LOD	<LOD	<LOD	<LOD	<LOD	<LOD	<LOD
TCEP	<LOD	<LOD	<LOQ (0.3)	<LOQ (0.3)	<LOD	<LOD	<LOD	<LOD
TCIPP	<LOD	1.8 ± 0.3	<LOD	0.9 ± 0.3	0.61 ± 0.06	0.6 ± 0.3	0.61 ± 0.19	<LOD
TDCIPP	<LOD	<LOQ (0.3)	<LOQ (0.2)	<LOQ (0.2)	0.38 ± 0.14	<LOD	1.1 ± 0.9	<LOQ (0.3)
TPhP	<LOD	<LOQ (0.7)	<LOQ (0.4)	<LOD	0.9 ± 0.8	1.4 ± 0.5	1.5 ± 1.0	0.90 ± 0.03

Hence, the reported method allows for achieving reliable results for PFR determination in water, being the extraction efficiencies obtained much better than those found with the reference method.

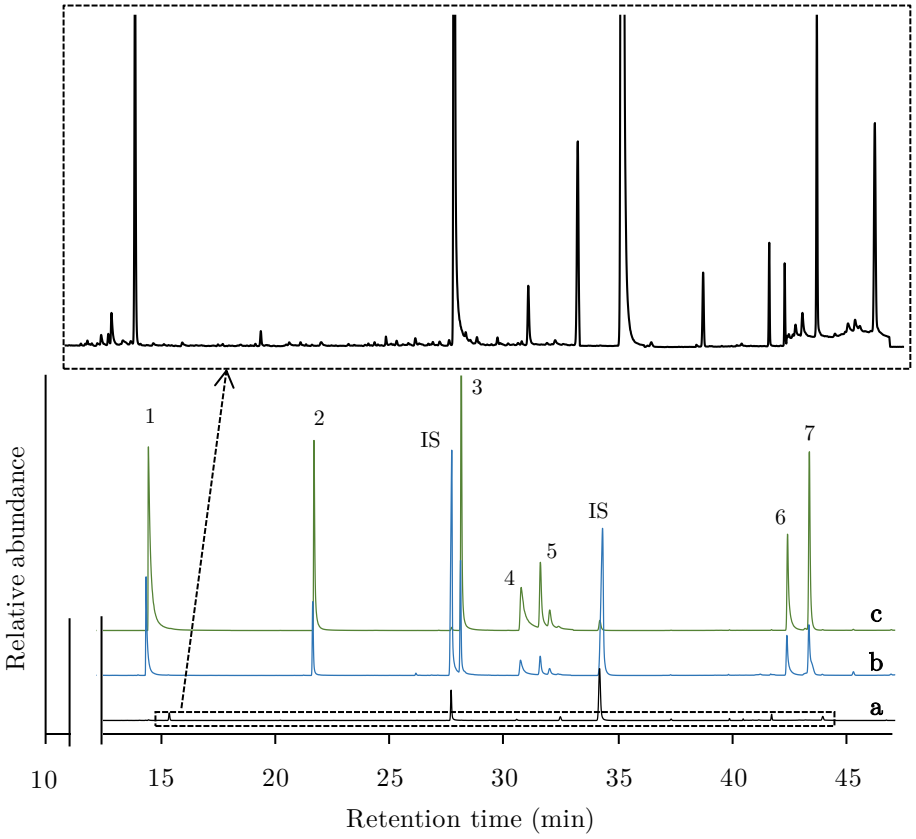

Figure 68. Chromatogram of extracts of a real sample (a) and a spiked real sample with 80 µg L^{-1} (b), and standard solution (16 mg L^{-1}). The chromatogram of the real sample is zoomed in the inset to show the complexity of the cleaned matrix. Target compounds: TEP (1), TPP (2), TnBP (3), TCEP (4), TCIPP (5), TDCIPP (6), TPhP (7).

3.2.4. Comparison with other reported methods

Finally, for the evaluation of the method, some similar reported methods described in the literature for PFR enrichment from water samples have been summarized in Table 43. As can be seen, comparable or better recoveries were achieved with the designed method by using Ti50-UVM-7 sorbent, with minimum recoveries of 65% for complex matrices, being these recoveries >80% in case of simpler samples. It should be noted that higher sample volumes were used in most of these methods, thus entailing better sensitivity (alongside better instrumentation such as MS/MS detector in some cases). However, good enrichment factors have been achieved with the reported method, comparable or better than the other, except in some cases where significantly higher amounts of

Table 43. Comparison of the reported method with other SPE methods for PFR enrichment and detection in water samples.

Samples	Sorbent	LOD (ng L^{-1})	LOQ (ng L^{-1})	Recovery (%)	RSD (%)	EF	Solvents	Analytical technique	Ref.
Surface water, wastewater (50 mL)	Ti-UVM-7 (200 mg)	19-210	60-700	65-110	2-27	131-219	6 mL MeOH, 3 mL EtOAc	GC-MS	This work
Surface water (20 mL)	Oasis HLB (200 mg)	20-50[c]	50-100[c]	48.8-72.5	0.5-5.16	9.8-14.5[b]	9 mL acetone, 3 mL MeOH	UPLC-TQ	[300]
Surface water (200 mL)	Oasis HLB (60 mg)	-[a]	2-6[c]	40-110	2-10	80-220[b]	12 mL ACN	UPLC-TSQ	[301]
Surface water (100 mL)	ENVI-18 (500 mg)	0.3-16[c]	1-35[c]	19.4-90.2	1.5-10.2	19.4-90.2[b]	9.5 mL ACN, 1.5 mL CH_2Cl_2	LC-MS/MS	[302]
Surface water (500-1000 mL)	Serdolith Pad III (3 g)	0.1-4.81[d]	0.29-14.44[d]	29-105	8-32	967-1015[b]	3 mL acetone, 20 mL CH_2Cl_2	GC-MS	[303]
Surface, rain, and wastewater (200 mL)	ENVI-18 (500 mg)	0.3-16[c]	1-35[c]	64.8-113.2	0.7-15.9	129.6-226.4[b]	9.5 mL ACN, 1.5 mL CH_2Cl_2	HPLC-MS/MS	[304]
Wastewater (100 mL)	Oasis HLB (200 mg)	0.3-6[c]	-[a]	42.7-129	0.7-22	42.7-129[b]	12 mL ACN	UPLC-MS/MS	[305]
Wastewater (1000 mL)	Oasis HLB (60 mg) + silica (500 mg)	-[a]	5-10[c]	24.0-105.0	2.1-24.8	240-1031[b]	9 mL EtOAc, 8 mL MeOH	GC-MS	[306]

[a]Not reported.

[b]Not reported. Calculated from reported experimental procedure.

[c]Calculated with LOD = 3 S/N; LOQ = 10 S/N, where S/N is signal-to-noise ratio.

[d]Calculated from the RSD of blanks.

solid-phase were used. In any case, achieved LODs, below 210 ng L^{-1} in all cases are considerably good, taking into account that they are calculated from spiked real matrices, and other different methodologies have been used for their calculation in the extraction methods summarized in the table. Finally, low amounts of more environmentally-friendly solvents have been used in the described method, in comparison with other reported methods, being the method a cleaner, cheaper, and simpler alternative to the determination of PFRs in environmental water samples.

4. Evaluation of iron-doped bimodal mesoporous silica materials as solid-phase extraction sorbents for perfluoroalkyl substances determination in environmental water samples

The aim of this work is to evaluate Fe-UVM-7 materials with different porosity and Fe content for PFASs selective retention, in order to develop an SPE method for their preconcentration and determination in water samples. The later instrumental detection of the analytes is carried out by UHPLC-MS/MS. Once the method features are assessed, the protocol is applied to real water samples in comparison with commercial WAX cartridges, commonly used for PFASs extraction [267].

4.1. Experimental procedure and SPE protocol

For all SPE experiments, cartridges were prepared by packing the desired amount of silica solid-phase (300 mg of Fe50-UVM-7-C_{12} for the recommended procedure) between two polyethylene frits. In all cases, cartridges were conditioned with 5 mL of methanol followed by 5 mL of ultrapure water. After sample loading, cartridges were air-dried for 30 min. Finally, and following the optimized protocol, retained analytes were eluted with 6 mL of methanol. Then, the extracts were preconcentrated by evaporation under a N_2 stream at 60 °C. After the evaporation until 250 µL, the final extract was diluted with 175 µL of methanol and 75 µL of NH_4F 8.3 mM prior to injection in the UHPLC-MS/MS system (final volume of 500 µL).

Water samples were obtained from the irrigation system from several points in the València region. All samples were filtered through a 0.45 µm filter in order to remove any particulate matter and stored at 4 °C until analysis. Before SPE, all samples were adjusted to pH 4.6 with acetate buffer. The samples were analysed through the recommended described protocol. In some cases, samples were spiked with PFASs standard solution (150 ng L^{-1}). Spiked samples were also analyzed by a reference method by using commercial Oasis WAX cartridges (150 mg). In these cases, cartridges were conditioned with 5 mL of NH_4OH 0.1% in methanol, followed by 5 mL of methanol and 5 mL of ultrapure water. The elution procedure was also modified since 3 mL of methanol followed by 3 mL of NH_4OH

0.1% in methanol were used in this case. The subsequent evaporation and concentration step was carried out as described.

The precision, as well as the extraction efficiency of the proposed method, were assessed by analyzing replicates of 100 mL of a spiked real irrigation matrix (150 ng L^{-1} of each analyte) through the recommended procedure. In the case of intra-day precision, three replicates were carried out within a day, while for the inter-day precision, three series of three independent extractions were considered. The sensitivity of the method was also evaluated through the estimation of the limit of detection (LOD) and limit of quantification (LOQ), following the IUPAC recommendations, with a 95% confidence level [203]. The linearity was also studied, considering the LOQ as the lower limit of the linear range.

4.2. Results and discussion

4.2.1. Solid-phase evaluation

Firstly, UVM-7 materials containing several amounts of iron were tested for the adsorption of PFASs. For this purpose, extractions of 10 mL of spiked ultrapure water (1 µg L^{-1}) were performed with cartridges containing 150 mg of each material. As can be seen in Figure 69, an important improvement was observed on most of the analyte recoveries when the iron was introduced in the sorbent, in comparison with the blank UVM-7, as can be seen for the Fe50-UVM-7-C_{16} material, thus confirming the beneficial role of the Fe centers for fluorinated compounds retention. However, it should be noted that more iron introduction did not always imply greater recoveries since an important decrease of the recoveries was observed for the Fe10-UVM-7-C_{16} material.

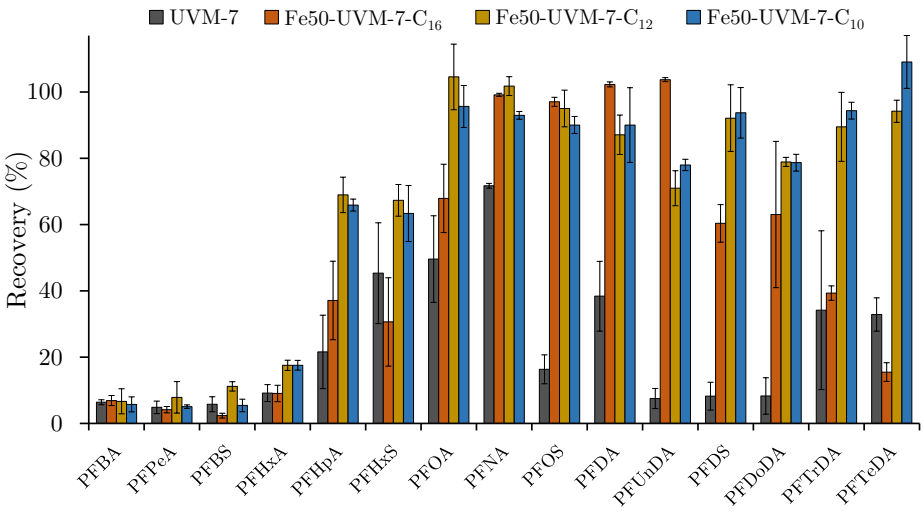

Figure 69. Effect of the sorbent (presence of Fe and pore size) on the recovery of PFASs. Conditions: 150 mg of sorbent, 10 mL of spiked ultrapure water (1 µg L^{-1}), elution 2 mL of methanol.

This behavior can be explained according to characterization observations, since the presence of Fe_2O_3 nanodomains was observed in the high-angle XRD pattern of the Fe10-UVM-7-C_{16} sample and confirmed with the Raman spectroscopy. Therefore, the distribution of Fe atoms along the internal surfaces of the mesopores can be expected to be more irregular. This fact perhaps implies certain heterogeneity in the interaction between the sorbent surface and the analytes (depending on the distribution and nature of the Fe species). Because of that, the molar ratio Si/Fe = 50 was selected as the best option.

Even though the recoveries for some of the analytes (PFNA, PFOS, PFDA, PFUnDA) were around 100%, the extraction performance for other analytes, mainly those with too small or too large size was still unsatisfactory. This could be explained with the characterization data regarding the porous structure of the UVM-7 materials, which mesopore size could not be appropriate for these PFASs. For this reason, other materials with smaller pores were considered, thus using shorter surfactants in the synthesis process, in order to achieve smaller micelles and consequently, smaller pore diameters. As also shown in Figure 69, the assessment of these materials for PFASs retention showed a considerable increase in the retention of several analytes such as PFHpA, PFOA, PFDS, PFTrDA, or PFTeDA when Fe50-UVM-7-C_{12} was used, with recoveries above 60%, although these results were similar for Fe50-UVM-7-C_{10}. Thus, Fe50-UVM-7-C_{12} was chosen as the best solid phase for the method development (since its synthesis is cheaper and easier due to the surfactant amount needed to keep the critical micellar concentration). In this sense, the use of C_{12}TAB supposes a significant reduction in mesopore size (of almost 0.6 nm). In addition, the material does not show the significant presence of Fe_2O_3 nanodomains, which guarantees a homogeneous distribution of Fe along the surface of the mesopores. Both factors cooperate in the optimal capture of the analyte. Also, it should be noted at this point that the adsorption mechanism differs from that operating for commercial adsorbents since the sorbents here reported are expected to capture the PFASs due to the encapsulation of these linear molecules in the mesopores and because of the favorable interaction between their F atoms and the Fe species distributed on the surface of the pore walls. However, unsatisfactory recoveries were obtained for the short-chain analytes, with recoveries below 20% for all tested sorbets. Because of that, this method cannot be applied for these short-chain PFASs, and the method was developed for its application to long-chain PFASs (C_8-C_{14}) extraction from water samples.

4.2.2. Optimization of SPE parameters

Once the solid phase was selected, the loading conditions were studied for selected analytes. First, three extractions of 10 mL of spiked ultrapure water (1.5 µg L^{-1}) were performed at pH 2.7, 4.6, and 6. Although no great differences were observed, the best recoveries were obtained when the acetate buffer was used (pH 4.6), being this condition selected for the method, in order to work at a stable pH range. The loading ionic strength was also tested by adding several amounts of

NaCl to the sample before the SPE. However, in this case, no significant variations were observed among extractions.

The elution step was also evaluated by testing several organic solvents for the selected PFASs elution from the cartridges. Similar extractions of spiked ultrapure water (1.5 µg L^{-1}) were carried out as described, with cartridges containing 150 mg of Fe50-UVM-7-C_{12} and using 3 mL of ethyl acetate, dichloromethane, acetonitrile, and methanol for the elution step. Obtained results showed that the worst recoveries were obtained with dichloromethane (below 40% in almost all cases). Although better results were obtained for acetonitrile and ethyl acetate, the best recoveries were clearly achieved with methanol, being in the range of 79-106%. Thus, methanol was the selected solvent. The possibility of concentrating the final extract by evaporation was also assessed. For this purpose, methanol solutions of the selected PFASs (2 µg L^{-1}) were evaporated at 60 °C with either a vacuum chamber or N_2 stream. No important loss of the analytes was observed with either of the procedures, although better results (variations under 10%) were obtained with nitrogen evaporation, being the selected protocol for analyte preconcentration.

In order to assess the breakthrough volume, several sorbent amounts (between 150 and 300 mg) were tested for the treatment of different volumes of spiked water real matrices, up to 100 mL. In all cases, the total amount of analytes was maintained (15 ng). Obtained results showed that, with 150 mg cartridges, recoveries clearly decreased when sample volume was increased from 10 to 100 mL. However, satisfactory recoveries were obtained for all selected analytes when 300 mg of Fe50-UVM-7-C_{12} were used, even with 100 mL of spiked water. Thus, these cartridges were selected for the method development, allowing us to treat up to 100 mL of water sample with no loss of the analytes.

4.2.3. Method performance

The developed method was evaluated in terms of sensitivity, linearity, and precision. As shown in Table 44, good extraction efficiencies were finally obtained for target PFASs (C_8-C_{14}), with values above 61% for all of them, and close to 100% in the case of PFOS or PFNA. It should be noted that these recoveries are comparable to other methods reported in the literature for PFASs extraction (Table 45), being in some cases better. It should be also mentioned that important differences between extraction efficiencies of different PFASs were detected not only in this study but also in the other methods described, thus being difficult to compare these recoveries. Besides, in some cases, relative recoveries were reported, whilst absolute recoveries are considered in our case, and simpler studies are also reported in some cases with the evaluation of only one analyte. However, the lower recoveries for some analytes make it advisable the application of standard addition calibration, and it was considered for sample analysis henceforth.

Table 44. Analytical figures of merit of the developed SPE-UHPLC-MS/MS method for C_8-C_{14} PFASs extraction from water samples.

Compound	Linearity[a] (µg L^{-1})	Sensitivity (ng L^{-1})		Extraction efficiency (%)	EF	Repeatability RSD (%)	
		LOD	LOQ			Intra-day	Inter-day
PFOA	2 - 50	3.9	12	66 ± 20	132	22	38
PFNA	4 - 50	7.2	22	110 ± 30	212	16	28
PFOS	2 - 50	3.0	9	110 ± 30	212	19	29
PFDA	5 - 50	8.0	24	77 ± 16	154	15	21
PFUnDA	4 - 50	6.8	21	73 ± 15	145	17	21
PFDS	2 - 50	3.5	11	67 ± 14	134	21	21
PFDoDA	4 - 50	6.1	19	75 ± 13	151	13	17
PFTrDA	5 - 50	8.1	25	68 ± 17	136	14	25
PFTeDA	2 - 50	3.5	11	61 ± 14	121	18	23

[a]Referred to final injection solution.

Also, as observed in the tables, these extraction efficiencies lead to enrichment factors (EF, calculated with the expression of equation (1)) in the range of 121-212, being them better than other methods where better recoveries were achieved due to the lower sample volumes and the reduction in the preconcentration. In the same way, satisfactory repeatability was observed, with RSD values below 22% for intra-day precision, and in the range of 17-29% for inter-day precision, except in the case of PFOA, where lower precision between independent days was observed (38%).

The sensitivity of the method was also assessed in terms of LODs and LOQs, as well as the linearity. As shown in Table 44 the developed method allows quantifying the target PFASs in concentrations above 25 ng L^{-1}, with detection limits in the range of 3.0-8.1 ng L^{-1}, and good linearity in the studied range of concentrations. This sensitivity is comparable with some of the methods summarized in Table 45, although in some cases where the used sample volume is higher this sensitivity is not improved with the reported protocol. However, it should be noticed that the methods for the estimation of LODs and LOQs are diverse in all reported works, which makes the sensitivity comparison less reliable.

Finally, the reusability of the cartridges containing the developed material was evaluated by carrying out several consecutive extractions, as previously described, using the same cartridge. In this case, after each use, cartridges were washed with 10 mL of methanol to ensure the elimination of any trace of the analytes and conditioned again as described. Results obtained showed that, after 5 uses of the same cartridge, recovery variations can be attributed to the dispersion of the method and not to a decrease in the extraction efficiency of the material. Thus, the developed cartridges were demonstrated to be reusable up to at least 5 times, which represents an important advantage against other disposable cartridges.

Table 45. Comparison of the proposed method with other reported SPE methods from the literature, for the extraction of C_8-C_{14} PFASs from water samples.

Sample	Sorbent	LOD (ng L^{-1})	LOQ (ng L^{-1})	Recovery (%)	RSD (%)	EF (EF_{max})	Solvents	Det.	Ref.
Well water (100 mL)	Fe-UVM-7-C_{12} (300 mg)	3.0-8.1	9.3-25	61-110	14-29 (38)[a]	121-212 (200)	11 mL MeOH	UPLC-MS/MS	This work
Wastewater (200 mL)	Oasis WAX (60 mg)	0.2-5.8	1.7-11	19-99	2-22	76-396 (400)	8 mL MeOH	HPLC-MS/MS	[262]
Rainwater (200 mL)	Oasis WAX (150 mg)	-[c]	0.02-0.1	97-132	6-15	24-66[b] (25-50)	12 mL MeOH	LC-MS/MS	[290]
Surface and tap water (50 mL)	Oasis WAX (150 mg)	0.3-0.5	1.5-2.5	83-102[d]	0.7-6.2	104-127[b] (125)	15 mL MeOH	LC-MS/MS	[291]
Surface, tap, and wastewater (250 mL-1 L)	Strata-X AW (200 mg) (carbon clean-up)	0.3-3	-[c]	38-104	4-33	380-1040[b] (1000)	26 mL MeOH	LDTD-HRMS	[292]
River, ground, and drinking water (250 mL)	Strata-X AW (200 mg)	-[c]	4-10	(15)[a] 49-103[d]	7-35 (180)[a]	(375)[a] 1225-2575[b] (2500)	15 mL MeOH 1.4 mL DCM 0.6 mL IPA	UHPLC-MS/MS	[293]
Surface and wastewater[e] (200 mL)	Strata-X AW (200 mg) (carbon clean-up)	-[c]	-[c]	98-113	1.8-7.3	1960-2260[b] (2000)	15 mL MTBE 3 mL MeOH	HPLC-MS/MS	[294]
River water (250 mL)	Strata (200 mg)	-[c]	0.01-2	60-92[d]	10-18	600-920[b] (1000)	12 mL MeOH	LC-MS/MS	[295]

Table 45 (*continued*)

Sample	Sorbent	LOD ($ng\ L^{-1}$)	LOQ ($ng\ L^{-1}$)	Recovery (%)	RSD (%)	EF (EF_{max})	Solvents	Det.	Ref.
Surface water[e] (10 mL)	Oasis HLB (225 mg)	0.1	0.5	61-83	3-10	6.1-8.3[b] (10)	7 mL MeOH	LC-MS/MS	[296]
Wastewater (1 L)	Imidazolium-based IL (passive) (30 mg)	0.2-0.3	0.7-1	53.7-110	<13	-[c]	6 mL MeOH	HPLC-MS/MS	[307]
Drinking water (35 mL)	Presep PFC-11 (60 mg)	-[c]	5-25	83.2-112.4	0.1-0.4	58-79[b] (70)	11.5 mL ACN	LC-MS/MS	[308]

[a]Value in brackets refers to a value far out of the range for only one analyte

[b]Not reported. Calculated from experimental reported data

[c]Not reported

[d]Values reported as relative recoveries

[e]Study developed only with C_8 analytes (PFOA and PFOS)

4.2.4. Water analysis

Six water samples were collected from the irrigation system in the region of València and analyzed through the developed method. However, no target PFASs were detected in any of the samples, with values <LOD in all cases. Because of that, two of these samples were spiked with the PFASs solution (150 ng L^{-1}) and analyzed through the developed method, as well as the reference method using Oasis WAX cartridges. As can be seen in Table 46, comparable results were obtained through both methods, and values close to the theoretical ones were achieved. The concordance between both methods was also confirmed with a t-student statistical comparison of means.

Table 46. Obtained concentrations (ng L^{-1}) of target PFASs in the analyzed spiked water samples (spiking level 150 ng L^{-1}).

Compound	M1S		M2S
	Fe50-UVM-7-C_{12}	Oasis WAX	Fe50-UVM-7-C_{12}
PFOA	165 ± 15	150 ± 9	152 ± 5
PFNA	152 ± 15	149 ± 15	150 ± 2
PFOS	161 ± 6	155 ± 15	147 ± 12
PFDA	152 ± 12	151 ± 15	147 ± 3
PFUnDA	147 ± 8	157 ± 10	148 ± 7
PFDS	160 ± 13	141 ± 5	140 ± 14
PFDoDA	138 ± 18	156 ± 8	150 ± 18
PFTrDA	130 ± 20	139 ± 6	138 ± 12
PFTeDA	153 ± 18	164 ± 3	152 ± 8

Hence, the developed method can be properly applied to the determination of selected PFASs (C_8-C_{14}) in real water samples, thus being an alternative for environmental analysis, with good analytical features for these analytes and using a cheap material for the extraction and preconcentration step.

5. Conclusions

In this Chapter, the potential of M-UVM-7 for the retention of environmental organic pollutants has been deeply studied. The modification of these materials, whose favorable effects have been exposed in the last Chapter, has been extended and the effect of their structure on the analyte retention has been studied in a higher grade.

Thus, the modification of the titanium content of the Ti-UVM-7 materials has been demonstrated to play an important role in the retention of organophosphorus compounds, being the obtained results in perfect agreement with the characterization data exposed in Chapter 4. Thus, the compromise between

enough titanium content in the material to interact with P-containing analytes and the presence of isolated tetrahedral titanium centers (in any case still far from resembling TiO_2 nanodomains) have been proved to be the key issue, and it was achieved for the Ti50-UVM-7 material. On the other hand, the presence of iron in the Fe-UVM-7 materials has also proved to play a key role in the retention of fluorinated compounds, thus giving them new selectivity properties, not observed in the last Chapter. Besides, the modulation in the mesopore size exposed in Chapter 4 by using short-tail surfactants, has also proved to affect the retention of these pollutants, being an important tool to adapt UVM-7 materials to the desired target analytes. Hence, with UVM-7 materials containing Ti and Fe, two other SPE methods have been developed in order to extract and determine two families of the most concerning emerging environmental pollutants.

Firstly, the developed method for the extraction of organophosphorus flame retardants has been successfully applied to their determination in real water samples and compared with a reference USEPA method using C18 cartridges. Thus, results have shown that Ti50-UVM-7 material presents good features for PFR enrichment from surface and WWTP water samples, with recoveries much higher than those using the C18 cartridges in the reference method, and above 80% in most of the cases. Also, quantifiable concentrations of some of the target analytes have been measured with this method in real WWTP samples, mainly for TCIPP, TDCIPP, and TPhP. Hence, the reported SPE sorbent is cheap and simple, and showed good extraction efficiencies for PFRs as well as reusability, thus representing a good alternative for PFR determination in water samples.

Likewise, with Fe50-UVM-7-C_{12} material, an analytical method for the determination of PFASs in environmental water samples has been developed, with satisfactory extraction efficiencies in the range of 61-110% for long-chain analytes (C_8-C_{14}). However, poor retentions have been observed for short-chain PFASs with the developed material. Thus, the developed method presents analytical features in general comparable to other similar methods reported in the literature, with good LODs in the range 3.0-8.1 ng L^{-1}. The optimized protocol has been also applied to the analysis of real water samples in comparison with a commercial sorbent. Although no target PFASs were detected in analyzed samples, the analysis of spiked real samples, in comparison to commercial WAX cartridges, confirmed this method as an alternative for target PFASs determination in water samples.

SECTION D

Chapter 7

Characterization of UVM-7 materials with cyclodextrins

1. Introduction

As previously stated in Chapter 1, the ability of cyclodextrins to form host-guest complexes confers them a wide variety of applications, especially with retention purposes. Because of that, and among many other analytical applications, their anchoring to silica matrices has led to many interesting materials in analytical chemistry. However, although their attachment to classical microporous silicas has been widely studied, the combination of CDs with ordered mesoporous silicas such as UVM-7 has not been approached to the same extent [111,164]. Indeed, several applications have been already described with the use of silica xerogels with the modification of cyclodextrins, either embedded or bonded, for the retention and determination of organic pollutants in environmental matrices [17,20,165,166,309]. However, the microporous structure of the xerogels presents several drawbacks regarding their surface area or the suitability of the pore size for the usual volume of organic pollutants, which can be addressed with mesoporous materials with hierarchical porosity such as the here presented.

Thus, as also mentioned, the attachment of organic ligands to the UVM-7 structure has been already considered in previous works for analytical purposes [148,154]. However, the synthesis and characterization of UVM-7 materials containing CDs have not been yet explored, nor its applications to the determination of organic compounds. As explained in Chapter 1, through a modification of the one-pot procedure of the typical synthesis of UVM-7 silicas, the β-CD is expected to be attached to the silica network and be available for the interaction with analytes in retention applications.

2. Characterization of CD-containing porous silica materials

The synthesized hybrid silica β-CD-UVM-7 material was characterized for the first time, thus evaluating the attachment of the CDs and the preservation of the silica structure. Firstly, TEM images were obtained. As shown in Figure 70A, the UVM-7 morphology was preserved with the addition of β-CD by the modification of the one-pot procedure. In fact, the hybrid sample shows a morphology based on aggregates of small primary mesoporous nanoparticles (<40 nm) characteristic of UVM-7 materials. This organization preserves the existence of two hierarchic pore systems: the large pores among nanoparticles and the surfactant-generated intraparticle mesopores (see inset). In comparison, β-CD-Xerogel material, shows the continuous and disordered microporous network characteristic of these materials, as previously stated. Thus, this xerogel morphology was also maintained with the addition of the cyclodextrin. It should be noted that CD-containing xerogels have been widely studied and characterized previously [17,166], and only some data already published are included here for comparative purposes. Likewise, note that some of these data have been already presented in Chapter 4 and repeated here to ease the comparison.

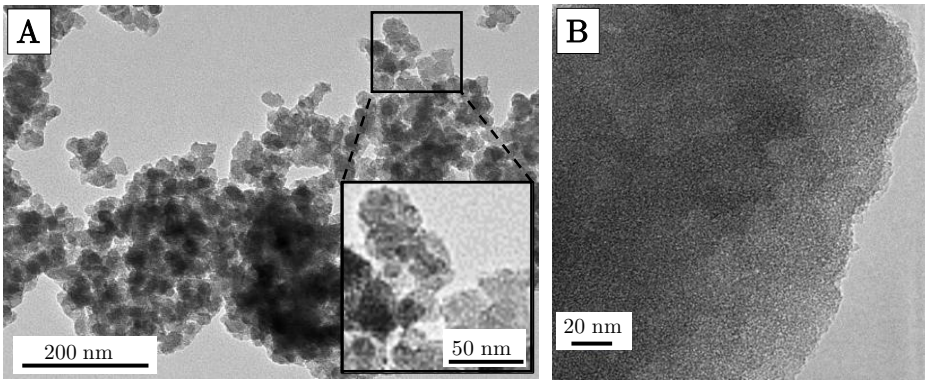

Figure 70. TEM representative images of the β-CD-UVM-7 material (A), with two magnifications, and the β-CD-Xerogel material (B). The UVM-7 image was obtained with a Jeol JEM-1010 instrument and the xerogel micrograph was already published in a previous work [166].

The preservation of the intraparticle mesopore organization typical of UVM-7 silica was confirmed also by XRD (Figure 71). Thereby, the XRD pattern of the hybrid sample shows, in the low-angle domain, an intense peak (2.3° (2θ)) and a shoulder (at ca. 3-4° (2θ)) both characteristics of UVM-7 type silica. These features are consistent with the existence of an intraparticle partially disordered hexagonal mesoporous array, as previously described, in contrast to the completely disordered porous structure of the xerogels at crystalline and pore levels.

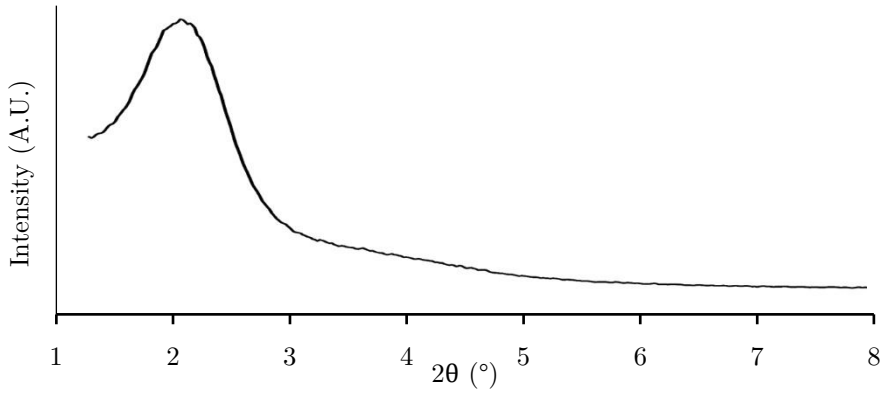

Figure 71. XRD pattern of the β-CD-UVM-7 material obtained from CuKα radiation (Bruker D8 Advance diffractometer).

The porosity of synthesized solids is further illustrated quantitatively through N_2 adsorption-desorption isotherms (Figure 72). The curve of the β-CD-UVM-7 sample shows two adsorption steps. As stated, the first one, due to the filling of the intraparticle mesopores, occurs at intermediate P/P_0 values in the 0.2-0.4 range, as an abrupt increase in the adsorbed volume. The second adsorption step, at P/P_0 values > 0.9, is caused by the filling of the interparticle large voids.

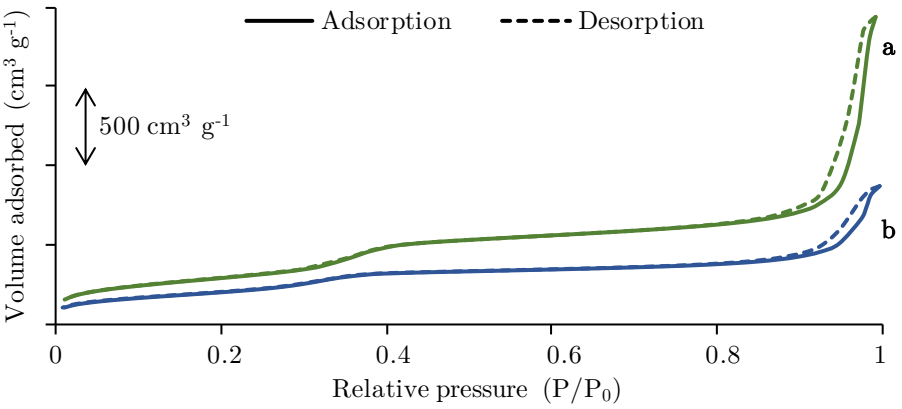

Figure 72. N_2 adsorption-desorption isotherms of the pure UVM-7 (a) and β-CD-UVM-7 (b) materials.

As observed in Table 47, the developed material presents porosity features similar to UVM-7 materials, thus confirming the preservation of the UVM-7 structure, although a significant modification of the BET surface area was observed. However, only a slight modification of the pore size was confirmed, thus maintaining the bimodal mesoporous structure. Thus, despite the modification of the original method and the incorporation of functionalized β-CD, the final β-CD-UVM-7 solid presents high BET surface area and porosity. This large surface area contrast with the lower surface area obtained for β-CD-Xerogel material which is an important drawback for its implementation as sorbent. Also, significantly lower pore size is confirmed in the micro-range, which would entail difficulties for the retention of some analytes depending on its size, in comparison to the bimodal pore system of the synthesized β-CD-UVM-7 material

Table 47. Textural parameters of the synthesized silica materials obtained from N_2 adsorption-desorption isotherms (extracted UVM-7 and β-CD-Xerogel data already presented in Chapter 2 and Chapter 4 respectively).

Material	Surface area (m^2 g^{-1})	Mesopores/Micropores		Macropores	
		Pore size (nm)	Pore volume (cm^3 g^{-1})	Pore size (nm)	Pore volume (cm^3 g^{-1})
UVM-7	1058	2.87	0.99	45.5	1.91
β-CD-UVM-7	738	2.57	0.59	30.09	0.89
β-CD-Xerogel	347	0.63	0.17	-	-

*Surface area estimated according to the BET model. Mesopore sizes and volumes calculated using the BJH method from the adsorption branch of the isotherms
*Porosity data of β-CD-Xerogel was already reported in a previous work [17]

Once the preservation of the silica UVM-7 morphology was proved, the attachment of the β-CD was also studied. Firstly, the CD bonding to the silica was evaluated by NMR. As can be seen in ^{13}C MAS NMR spectra of both modified β-CD-Si and β-CD-UVM-7 material (Figure 73), the representative signals of the cyclodextrin are also present in the silica material after functionalization, except those corresponding to silane groups due to the hydrolysis and condensation processes (peaks 12 and 13). Likewise, the presence of T centers in the case of ^{29}Si MAS NMR, apart from the centers Q^2, Q^3, and Q^4 corresponding to the silica, indicates the presence of the silane group of the modified β-CD in the silica final structure. Moreover, the proportion of the different Q and T sites is Q^4:Q^3:Q^2:T = 56:40:3:1. Also, with this proportion, a relation $Q^4/(Q^3+Q^2)$ of 1.3 was obtained being this value in agreement with the proportion observed for the chemically extracted UVM-7 silica (as presented in Chapter 2), proving also the silica expected structure.

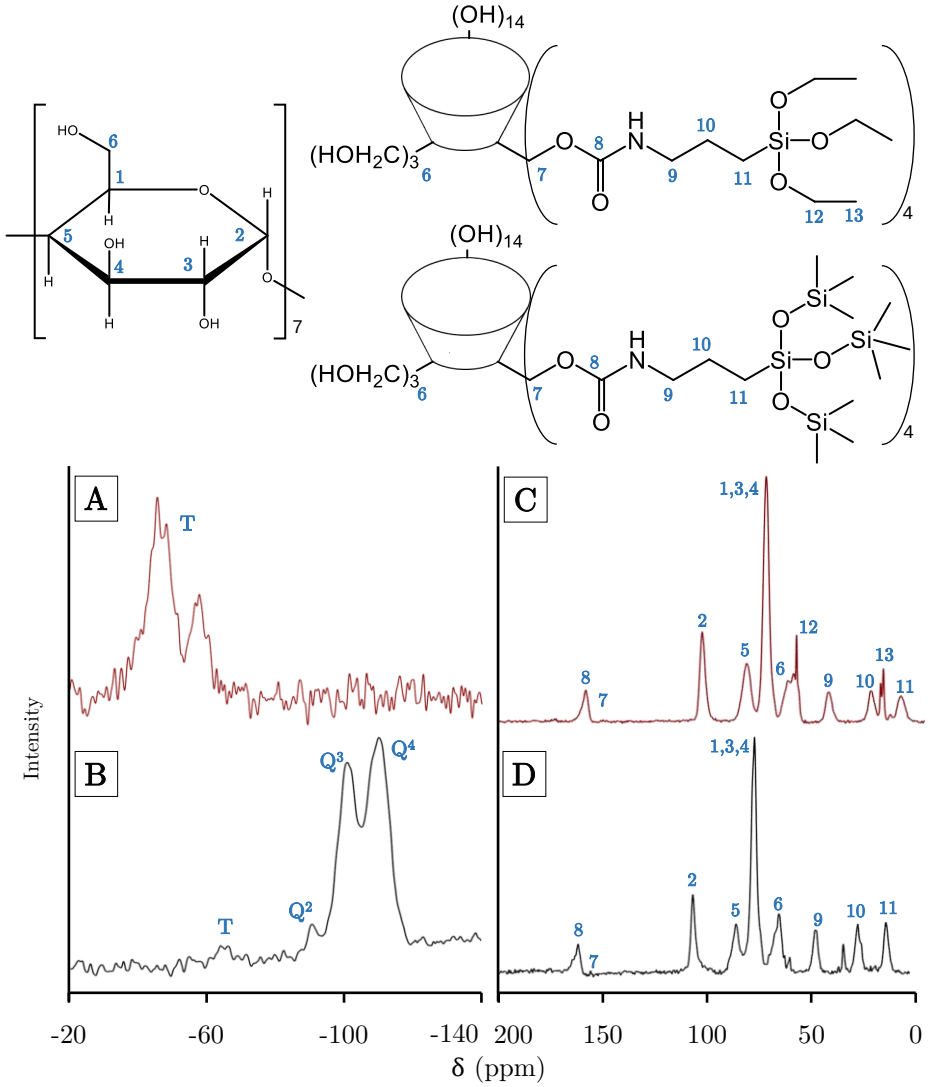

Figure 73. ^{29}Si MAS NMR spectra of modified β-CD-Si precursor (A) and synthesized β-CD-UVM-7 silica (B) showing the presence of T and Q centers in the material; and ^{13}C MAS NMR spectra of β-CD-Si precursor (C) and β-CD-UVM-7 material (D), with their peak identification. Obtained with a Bruker Avance III 400 MHz spectrometer.

The CD amount present in the material was evaluated by CNH and thermogravimetric analysis. Due to the low N content of the modified β-CD molecules, the C content (8.9% wt) provided by the CNH elemental analysis was used as the most reliable data to determine the β-CD amount in our sample. Then, assuming a simplified β-CD_x-SiO_2 chemical formulation, an amount of 0.119 mmol β-CD g^{-1} has been estimated which corresponds to an x value of 0.009. This value is in accordance with NMR data suggesting an approximate (maximum) proportion of T sites of around 1%. Contents on β-CD determined by

thermogravimetric analysis (TGA) are in excellent agreement. The thermogravimetric curve (Figure 74) shows a 19% weight loss (between 93 and 74%) in the 100-500 °C temperature range, which can be attributed to the degradation of β-CD. Weight losses at lower and higher temperatures are associated with solvent removal and condensation of silanol groups, respectively. As expected, the proportion of silanol groups (Q^2 and Q^3) is significant (as seen previously in the NMR spectra), since the C_{16}TAB removal is carried out through ion exchange in an acid medium instead of calcination. Thus, the TGA data allow estimating a proportion of 0.117 mmol β-CD g^{-1}, which corresponds to a concentration of C (wt) = 8.7%.

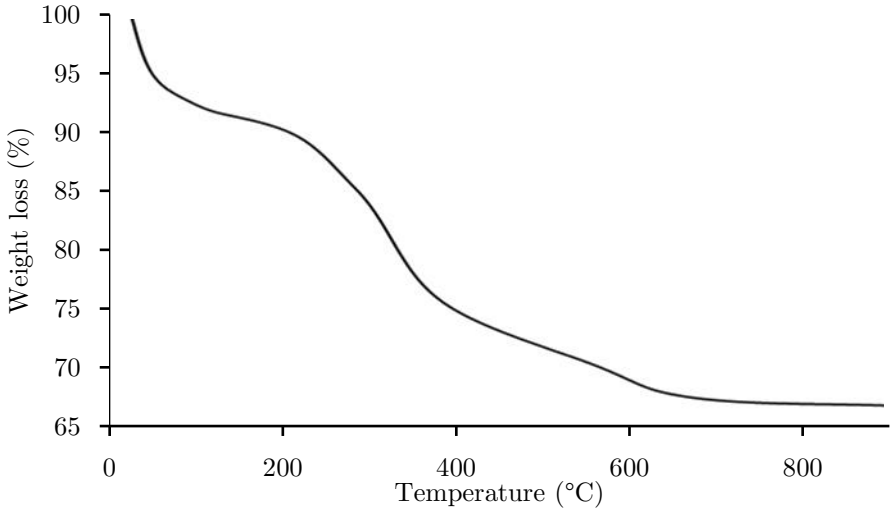

Figure 74. TGA curve of the β-CD-UVM-7 material.

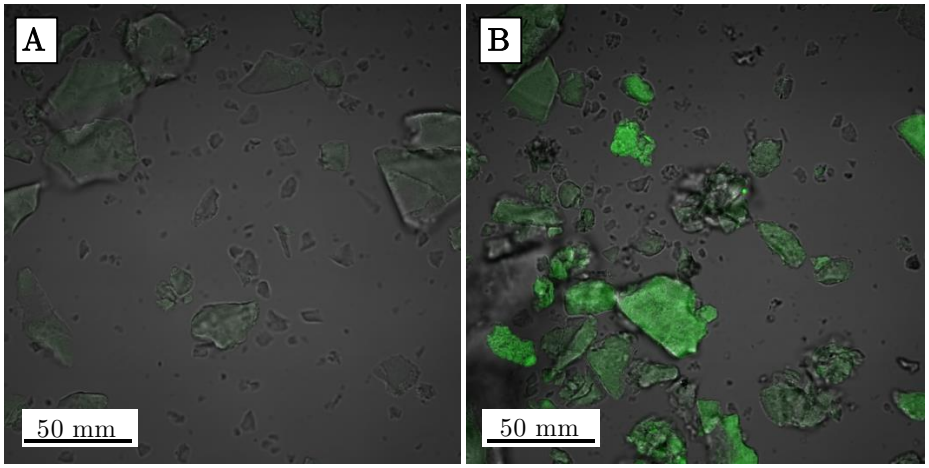

Figure 75. Confocal microscopy images obtained by the fluorescence emission of the inclusion complex formed by the Bodipy-Me and β-CD of the synthesized material (60x magnification lens, water media): blank UVM-7 (A) and synthesized β-CD-UVM-7 materials (B).

In order to evaluate the homogeneity of the CD dispersion in the material, a study with confocal microscopy has been used [310]. For this purpose, cartridges containing 50 mg of both blank and β-CD-containing silica materials were contaminated with 10 mL of a DMF Bodipy-Me solution (1.6 mmol L^{-1}). Then, the material was gently washed with DMF in order to preserve only the Bodipy-Me molecules captured by the cyclodextrin units. These marked materials were analyzed by confocal microscopy, by irradiating the samples with a laser of 488 nm and collecting the intense green emitted fluorescence signal. As can be seen in Figure 75, a good homogeneity was observed in the silica material, observing the green emission in all particles, as opposed to the blank UVM-7 material where the absence of CD was observed.

3. Conclusions

A new material has been synthesized for the first time, by the attachment of β-CD centers to the silica mesoporous support. The resulting material was proved to preserve the UVM-7 typical structure as observed in TEM images, as well as its bimodal porosity, with the presence of aggregated mesoporous nanoparticles that forms a network of large macropores in opposition to the microporous structure of xerogels (Figure 76). The addition of the cyclodextrin has proved to not disturb this structure formation during the synthesis. Moreover, the presence of the CD in the final material was also proved by several techniques in a proportion of approximately 0.117-0.119 mmol β-CD g^{-1}, as well as the homogeneity of the CD through the material.

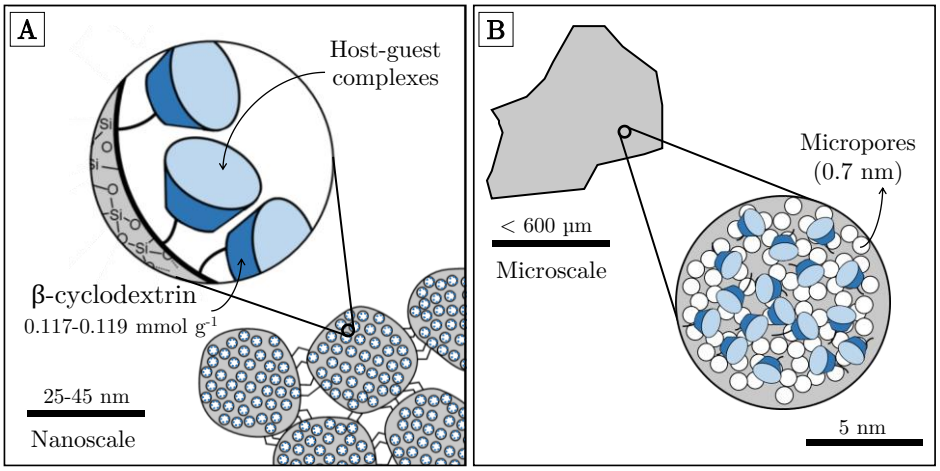

Figure 76. Schematic representation of the characterized structure for β-CD-UVM-7 (A) and β-CD-Xerogel material.

Thus, a β-CD-UVM-7 material was properly synthesized, with the desired structure and the homogeneous attachment of the β-cyclodextrin, which is

expected to be a good sorbent for retention purposes, due to the combination of the excellent features of the UVM-7 solids already discussed, and the ability of β-CD for the retention of organic compounds through the formation of host-guest complexes.

Chapter 8

Functionalization of UVM-7 with cyclodextrins for endocrine-disrupting chemicals extraction and determination in clinical analysis

1. Introduction

The endocrine-disrupting chemicals (EDCs) are a group of natural and synthetic compounds that may interfere in the normal function of the endocrine system in animals and humans when in constant contact with the body for long periods. Since these chemicals are present in a wide variety of everyday-used products such as food, cosmetics, plastic utensils, detergents, or pharmaceuticals, our exposure to them is common, through ingestion, inhalation, or dermal contact. The toxicological effects of these compounds are just beginning to be understood, but several studies have related them to a huge number of disorders and health problems [16,311,312].

Thus, numerous synthetic chemicals have been classified as EDCs in the last decades, including compounds such as bisphenols, parabens, phthalates, or UV-filters. Among them, bisphenol A (BPA) has received special attention in the last decades due to its widespread use in polycarbonate plastics and epoxy resins fabrication, applied as an antioxidant or stabilizer and many studies have shown its potential risk for human health (Figure 77). Likewise, its restriction and regulation has caused the appearance of many derivatives, such as chlorinated

bisphenols, which also present toxicological activity [16,313,314]. On the other hand, parabens are alkyl esters of p-hydroxybenzoic acid (Figure 77) and they are widely used as preservatives due to their lower toxicity and low cost. However, there is growing evidence about their possible adverse effects, giving rise to a tendency to avoid them [315,316].

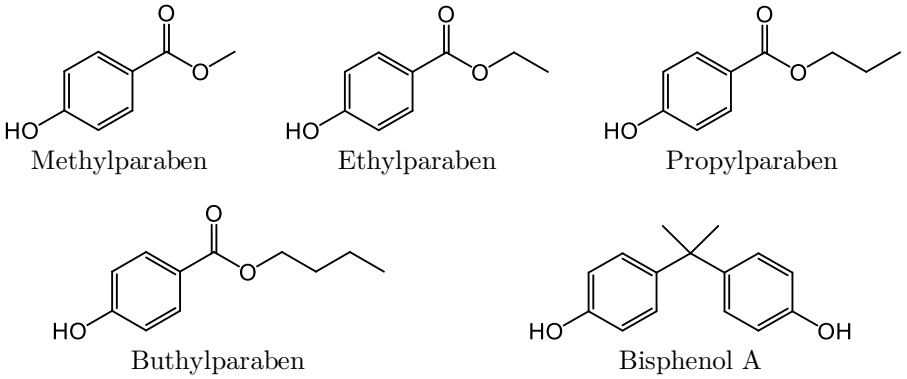

Figure 77. Molecular structures of studied endocrine-disrupting chemicals.

In this sense, and taking into account the toxicity of these chemicals, they have been limited by several institutions. For instance, in the case of the European Union and the United States Food and Drug Administration (US FDA) the parabens concentrations in cosmetic products should not exceed 0.4% for a single paraben and 0.8% for total concentration [317]. Despite these restrictions, the widespread use of these compounds has caused human exposure to them to be still high as has been shown in a wide variety of biomonitoring studies [16,311,317–320]. Although the exposure can be assessed with several analyses such as serum/plasma [321], saliva, hair, or nails, urine has been selected as the most representative matrix sample regarding body burden [16,312,317]. Urine has been widely used for biomonitoring and risk assessment, and there is a large number of studies focused on the determination of EDCs in this matrix. As mentioned, the common exposure to these chemicals drives to detectable levels in almost all urine samples in the range of μg L^{-1}, with concentrations up to the range of mg L^{-1} in some cases for total concentration [16].

Due to the interest of these analyses, several techniques and methods have been developed for parabens and bisphenols determination in urine samples. Although most of them are based on liquid chromatography (LC) [312,320,322–324], other studies have been presented by using gas chromatography (GC) with previous derivatization [325,326], or capillary electrophoresis (CE) [16]. Regarding the detection, several detectors have been used such as UV-Visible and photodiode array (PDA) [323], or fluorescence detector (FLD) [324], but nowadays mass spectrometry detectors (MS and MS/MS) are the most widely used due to their selectivity [16,312,322].

Moreover, because of the complexity of biological samples and the low concentrations present in some of them, extraction techniques are usually required to preconcentrate the analytes and isolate them from the matrix [16]. In this sense, several procedures have been proposed for urine samples [320]. On the one hand, liquid-liquid extraction (LLE) techniques have been widely applied to urine analysis in several determinations. However, since it is a time-consuming technique that often requires large volumes of solvent, miniaturized alternatives have been proposed such as liquid-liquid microextraction (LLME) [325] or dispersive liquid-liquid microextraction (DLLME) [312]. On the other hand, solid-phase extraction techniques (SPE) are very common for EDCs enrichment and clean-up [16,320,322,324], since they are well adapted to multi-residue analysis. In this case, the proper selection of the sorbent material can lead to the quantitative retention of analytes of different classes, with the improvement of the sensitivity and selectivity and low solvent use. Because of that, several sorbents have been proposed in the case of biological samples, mainly the common C18 boned silica, polymeric materials, or more specific sorbents such as immunoaffinity cartridges or molecularly imprinted polymers (MIP) [16].

In this way, cyclodextrins (CD) have been also proposed for parabens retention in some studies. As previously stated in Chapter 1, their truncated-cone shape allows them to form stable host-guest complexes with small organic compounds such as parabens or bisphenols, also thanks to the interaction with the aromatic rings [111,164]. Indeed, the interaction of CDs with parabens has been already studied, thus confirming the formation of the host-guest complexes [327], and several studies have been reported using CDs as active centers for the retention and determination of parabens and bisphenols, either by SPE [328], DLLME [329] or in the development of sensors [330]. In this sense, as previously mentioned, silica materials doped with CDs have been proposed for the extraction of organic pollutants from several matrices [17,165,166], although few studies have combined ordered mesoporous silicas such as the mentioned UVM-7 material with CDs as active centers for the retention [111,164]. Besides, the synthesis procedure of ordered silicas such as UVM-7 allows the introduction of heteroelements such as modified CDs in the structure, thus giving them diverse properties [331–333]. Thus, the described features of the UVM-7 pore network, in combination with CDs, can lead to a proper sorbent for parabens and bisphenols extraction from complex matrices, as discussed in Chapter 7.

2. Materials, reagents, and instrumentation

Methylparaben (MeP), ethylparaben (EtP), propylparaben (PrP), and butylparaben (BuP) solid standards were purchased from Fluka (Buchs, Switzerland), and BPA solid standard was purchased from Sigma-Aldrich (St. Louis, MO, USA). Stock solutions were prepared in methanol (MeOH) from HPLC grade (Labkem, Barcelona, Spain) and stored at -18 °C in darkness. For

SPE procedures, acetic acid (Sigma-Aldrich), sulfuric acid (Merck, Darmstadt, Germany), and NaCl (Scharlab, Barcelona, Spain) were also employed, as well as β-glucuronidase and arylsulfatase solution from *Helix pomatia*, purchased from Roche (Basel, Switzerland). In addition, ultrapure water was obtained from an Adrona purification system (Riga, Latvia). Also, for reference method comparison, ExtraBond C18 commercial cartridges were purchased from Scharlab. Finally, creatinine standard was purchased from Sigma-Aldrich, and picric acid from Panreac AppliChem (Darmstadt, Germany).

For SPE studies, a vacuum pump was used connected to a Vac Elut 20 chamber, as well as a miVac concentrator from SP Scientific (Warminster, PA, USA).

Regarding instrumental determination, a liquid chromatograph QTRAP 6500+ system was used, with a triple quadrupole detector, from Sciex (Framingham, MA, USA). For analyte separation, a mobile phase made of acetonitrile and water with ammonium formate 10 mM was used in a gradient mode (see Table 48) at 0.4 mL min^{-1}. In this case, a Luna Omega polar column (100 x 2.1 mm x 1.6 µm) was used from Phenomenex (Torrance, CA, USA). The mass spectrometer was programmed in negative ionization mode and used parameters for each analyte are summarized in Table 49.

Table 48. Mobile phase gradient for analyte separation in the UHPLC-MS/MS system. Components: water (ammonium formate 10 mM) and acetonitrile.

Time (min)	Acetonitrile (%)
0	10
1	30
2.5	30
4	96
7	95
7.1	10
12	10

Table 49. Detection parameters for UHPLC-MS/MS determination of EDCs.

Compound	Quantifier transition, Q (m/z)	Qualifier transition, q (m/z)
Methylparaben	151 > 92	151 > 136
Ethylparaben	165 > 92	165 > 136
Propylparaben	179 > 92	179 > 136
Butylparaben	193 > 92	193 > 136
Bisphenol A	227 > 133	227 > 212

During optimization, an LC-2000 Plus liquid chromatograph equipped with an FP-2020 Plus Intelligent Fluorescent Detector, a PU-2089 Plus Quaternary Gradient Pump with integrated degasser, and an I/FLC/NetII/ADC interface from Jasco (Madrid, Spain) were also used. In this case, the separation was carried out with a Kromasil C18 column (150 × 4.6 mm, 5 µm particle size) from Análisis Vínicos (Ciudad Real, Spain). An acetonitrile/water mobile phase was used for the separation in isocratic mode (55:45) at 1 mL min^{-1}. The detector was programmed at λ_{ex} = 254 nm and λ_{em} = 310 nm.

3. Use of a novel UVM-7 sorbent modified with β-cyclodextrin for the determination of endocrine-disrupting chemicals in urine samples

The aim of this work is to develop a method for the determination of parabens and bisphenol A in urine samples, by using a UVM-7 material doped with β-CD as SPE sorbent for clean-up and preconcentration purposes. Analytes will be lately quantified by UHPLC-MS/MS. The main features of the analytical method will be assessed, and the developed method will be applied to the analysis of real urine samples.

3.1. Extraction, clean-up procedure, and sample analysis

Urine samples were obtained from 5 healthy volunteers in the range of 20 to 30 years old. The samples were collected by themselves in a 200 mL container asking them to abstain from urinating 2 h before collection. After collection, samples were stored refrigerated and analyzed within the next 48 h. Prior to analysis, urine samples were subjected to enzymatic hydrolysis. Since phenolic compounds are expected to be conjugated with charged species such as glucuronic acid and sulfate in urine excretion [16], samples were hydrolyzed with β-glucuronidase and arylsulfatase. For this purpose, after sample homogenization, an aliquot of 15 mL was split, and the pH was adjusted to 5.5 with diluted acetic acid. After adjusting the sample with 300 µL of acetate buffer, 100 µL of enzyme solution containing both β-glucuronidase and sulfatase were added to each sample. Samples were incubated at 37 °C for 16 hours to ensure the complete hydrolysis [16,311,312].

SPE cartridges were prepared by packing 200 mg of β-CD-UVM-7 sorbent between two polyethylene frits into a 6 mL polypropylene empty cartridge. Cartridges were conditioned with 5 mL of methanol followed by 5 mL of ultrapure water. Before sample loading, and following the optimized procedure, the pH of each urine aliquot was adjusted in the range 2.5-3 with H_2SO_4, and NaCl was added to adjust the conductivity to 150-170 mS cm^{-1}. The hydrolyzed and adjusted aliquot of 15 mL was loaded into the cartridge under vacuum, followed by 5 mL of washing solution (ultrapure water with similar pH and conductivity).

After the washing step, cartridges were air-dried for 10 min, and the analytes were eluted with 3 mL of methanol. The extracts were evaporated at 60 °C under vacuum, reconstituted with 500 µL of methanol, and filtered before UHPLC-MS/MS analysis.

It should be noted that, due to the difficulty of finding human urine exempt from target analytes, synthetic urine was employed in some optimization steps. For this purpose, the synthetic urine was prepared according to the procedure previously described by Bocato et al. [312]. Briefly, to prepare 1 L of synthetic urine, 7.6 g of potassium chloride, 17 g of sodium chloride, 49 g of urea, 2.06 g of citric acid, 0.72 g of ascorbic acid, 2.40 g of potassium phosphate, 2.8 g of creatinine, 1.28 g of sodium hydroxide, 0.94 g of sodium bicarbonate and 560 µL of sulphuric acid were solved in 1 L of ultrapure water, ultrasonicated for 30 min, and stored at 4 °C.

Likewise, for the repeatability and matrix effect evaluation, several aliquots of one sample were spiked (3 µg L^{-1}) and analyzed through the same procedure. Samples were also analyzed through a reference method [334] by using C18 cartridges for the clean-up and preconcentration step. In this case, cartridges were conditioned with 5 mL of methanol and 5 mL of ultrapure water. Then, 5 mL of each sample, previously hydrolyzed as described above, were loaded into the cartridge. After vacuum drying for 10 min, the elution was carried out with 8 mL of methanol, and the extracts were concentrated under vacuum as described.

In order to take into account the differences in urine dilution, urinary creatinine was also determined [311]. For this purpose, the Jaffe method was employed by monitoring the absorbance at 510 nm of the creatinine-alkaline picrate complex in the range of 45 to 180 s [335]. As shown later, total concentrations of parabens and bisphenol A were standardized with the creatinine content of each sample.

3.2. Results and discussion

3.2.1. Optimization of extraction and clean-up parameters

Firstly, non-ordered and hierarchical silica materials containing β-CD were compared. For this purpose, several extractions of 10 mL of spiked ultrapure water (0.3 mg L^{-1}) were carried out with cartridges containing 100 mg of each synthesized material. As can be seen in Figure 78, poor recoveries were obtained with β-CD-Xerogel material (recoveries below 18% in all cases) in comparison with UVM-7 type silica, thus confirming the advantages of the macro-mesoporous structure for the analyte retention. Besides, the key role of β-CD as active centers for analyte retention was proved, since huge differences were observed in the comparison between the modified material and blank silica. These observations are consistent with the characterization studies of the previous chapter, thus confirming the presence and well distribution of the CDs, available for the retention of parabens and BPA. Hence, the advantages of the combination

between β-CD active sites and the highly accessible silica structure have been proved in comparison with xerogel materials where, despite its higher amount of CDs, their accessibility is worse due to their microporous structure. Thus, the material β-CD-UVM-7 was chosen for method development.

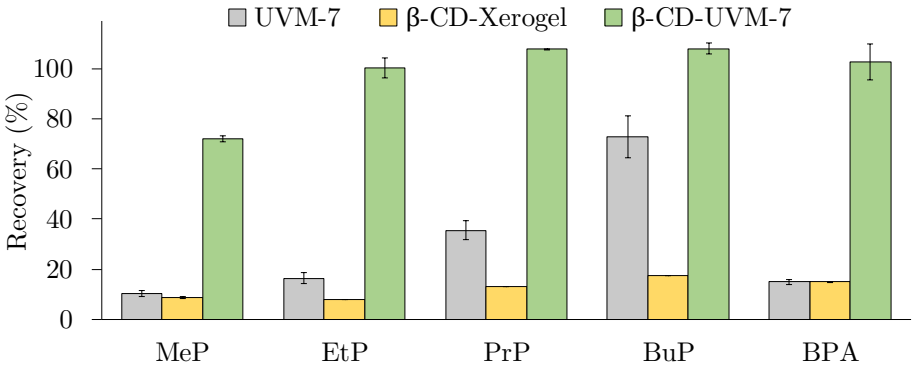

Figure 78. Effect of the type of solid-phase (silica framework and β-CD modification) on the recovery of EDCs. Conditions: 100 mg of solid phase, 10 mL of water spiked with 0.3 mg L^{-1}, elution 3 mL of methanol.

Once the material was selected, retention parameters were studied, namely pH and ionic strength. Firstly, similar extractions were carried out as described above with spiked water samples (60 µg L^{-1}) previously adjusted to pH 2.6, 4.5, and 8.7. After sample loading, cartridges were washed with 5 mL of water at the same pH, and the elution was carried out with 3 mL of methanol. In this case, no important differences were observed in most of the cases, although a slight improvement in the retention was observed at acidic pH (2.6), mainly in the case of MeP and EtP, with recoveries in the range of 52-100% for all analytes.

Likewise, a similar experience was carried out by varying the ionic strength of the sample. In this case, samples with different content of NaCl (0, 1, 2, 3, and 4 M) were considered, as well as the same ionic strength in the washing step. As can be seen in Figure 79, the effect of the ionic strength was clearly proved, mainly in the case of MeP and EtP, with an important improvement on the retentions in the case of high ionic strengths. These observations can be explained due to the salting-out effect, widely studied in host-guest complexes formation. Thus, ionic strength of 4M was selected as the best option for the sample loading as well as the washing step, corresponding to a conductivity of 170 mS cm^{-1}.

The elution step was also studied. Since significative recoveries were already achieved using methanol, and its toxicity is lower than other solvents that may be tested such as acetonitrile, only ethanol and acetone were also explored as alternatives. However, after the elution with 3 mL of each solvent, none of them provide recoveries comparable to methanol (in the range of 37-56% and 53-65% for ethanol and acetone, respectively). Hence, the elution profile was obtained with similar extractions by eluting each 1 mL of methanol separately, up to 6

mL. This study showed that all analytes were quantitatively eluted in the first 3 mL, being the volume selected for the recommended protocol. Moreover, the possibility of preconcentrate the final extract through solvent evaporation was confirmed. For this purpose, 3 mL solutions of the analytes were prepared in methanol. After evaporation under vacuum at 40 and 60 °C, they were reconstituted with 500 µL of methanol. Since no significant loss was observed in none of the cases, the evaporation step was included in the recommended protocol, choosing 60 °C as the best evaporation temperature.

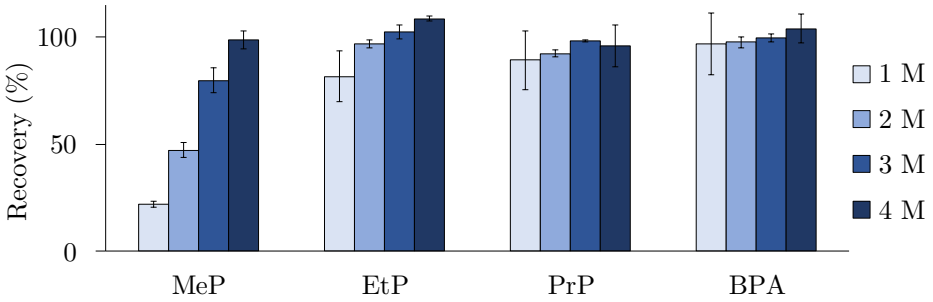

Figure 79. Effect of the loading and washing ionic strength (NaCl content) on the recovery of EDCs. Conditions: 100 mg of β-CD-UVM-7, 10 mL of water spiked with 60 µg L^{-1}, elution 3 mL of methanol.

The breakthrough volume was also studied in comparison with the amount of solid phase. For this purpose, cartridges containing 100 and 200 mg of β-CD-UVM-7 material were prepared. Next, volumes of 10 and 25 mL of spiked synthetic urine (25-60 µg L^{-1}) were treated following the optimized parameters. As observed in Figure 80, when cartridges of 100 mg were used, an increase of sample volume up to 25 mL entailed the partial loss of MeP. However, using 200 mg of sorbent, this decrease was not observed. Thus, cartridges containing 200 mg of β-CD-UVM-7 were selected for the method, thus allowing the treatment of up to 25 mL of sample. The loading capacity was then studied with a set of extractions of synthetic urine samples (25 mL) spiked with concentrations in the range 5-100 µg L^{-1}. After applying the recommended procedure, no variations were observed on the recoveries, thus confirming that designed cartridges can be properly applied to sample analysis in this range of concentrations.

Finally, the reusability of the designed cartridges containing β-CD-UVM-7 was also studied, by carrying out similar consecutive extractions of spiked synthetic urine (60 µg L^{-1}) with the same cartridge following the recommended procedure. After each extraction, cartridges were washed with 10 mL of methanol and conditioned again as described. After 5 uses of the same cartridge, results showed that similar recoveries were obtained, with variations among uses under 6%. Thus, these cartridges can be used at least 5 times with no loss on their extraction efficiency, which represents an important advantage in comparison to other disposable cartridges.

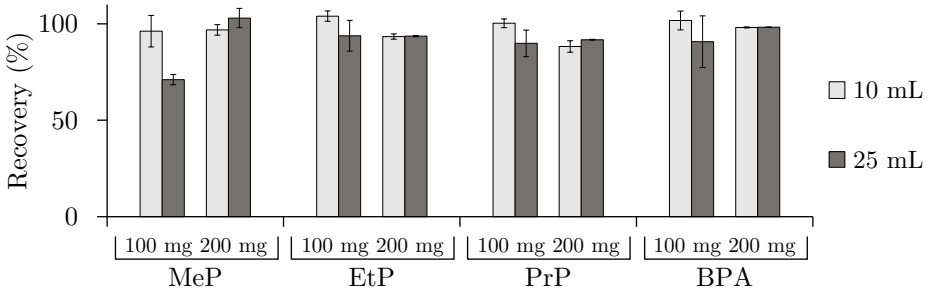

Figure 80. Effect of the sorbent amount (β-CD-UVM-7) and sample volume (spiked synthetic urine 25-60 µg L^{-1}) on the recovery of EDCs.

3.2.2. Analytical figures of merit

The main analytical parameters of the developed method were assessed. The sensitivity was evaluated in terms of limit of detection (LOD) and limit of quantification (LOQ). For this purpose, they were considered as 3 and 10 times the signal-to-noise ratio respectively. Likewise, the linearity was also evaluated with the injection of nine calibration standards, considering the LOQ as the lower limit of the linear range. As shown in Table 50, good linearity and sensitivity were achieved, with LOQs below 0.013 µg L^{-1} for MeP, EtP, and PrP, and 0.18 and 0.19 µg L^{-1} for BuP and BPA respectively. This sensitivity allows determining the target analytes in very low concentrations, being these values much better or, in some cases, similar to those reported in previous methods in the literature, as can be seen in methods summarized in Table 51. It should be noted that this fact represents an important advantage of this method over other reported protocols since it allows to determine the target analytes in very low concentrations in complex urine matrices.

Table 50. Analytical figures of merit of the developed SPE-UHPLC-MS/MS method for the extraction and clean-up of parabens and BPA from urine samples.

Compound	Linearity (µg L^{-1})[a]	Sensitivity (µg L^{-1})		Extraction efficiency (%)	Repeatability RSD (%)	
		LOD	LOQ		Intra-day	Inter-day
Methylparaben	0.4-420	0.004	0.013	96	12	11
Ethylparaben	0.1-420	0.0011	0.004	96	8	16
Propylparaben	0.1-420	0.0008	0.003	107	16	20
Butylparaben	5-420	0.05	0.18	109	13	19
Bisphenol A	6-420	0.06	0.19	107	16	24

[a]Referred to the final extract

Table 51. Comparison of the main analytical parameters of the proposed method with other methods reported in the literature.

Analytes	Sample clean-up	Analytical technique	LOD (µg L^{-1})	LOQ (µg L^{-1})	Recovery (%)	RSD (%)	Ref.
Parabens BPA	SPE (β-CD-UVM-7)	UHPLC- MS/MS	0.0008-0.06	0.004-0.19	96-109	8-24	This work
Parabens BPA	DLLME	LC-MS/MS	0.01-0.08	0.03-0.2	73-111	0.7-11	[312]
Parabens	SPE (Elut-Nexus)	HPLC-MS/MS	-[a]	0.01-0.02	61-89	-[a]	[320]
Parabens	LLE	HPLC-MS/MS	-[a]	0.02-0.2	67.8-78.8	<15	[319]
Parabens	SPE (RP-18)	HPLC-MS/MS	0.10-0.18	0.3-0.6	80-100	5.1-10.6	[322]
BPA	LLME	GC-MS[b]	0.8	1.15	86-110	<10	[325]
Parabens	FPSE[c] (sol-gel CW)	HPLC-PDA	30	100	-[a]	1.2-12.8	[323]
BPA	SPE (ENVI-18)	HPLC-FD	2.7	-[a]	95.9	3.92	[324]

[a]Not reported

[b]Analyte derivatization prior to GC analysis

[c]Fabric phase sorptive extraction

Likewise, the average recoveries of the analytes as well as the repeatability of the method in terms of relative standard deviation (RSD) were also evaluated. To this end, three extractions were carried out within the same day in the case of intra-day RSD and three batches of three independent extractions were considered for inter-day repeatability. In both cases, a spiked urine sample (3 µg L^{-1}) was used, and the extraction and analysis were carried out following the recommended procedure. As can be observed in Table 50, good recoveries were obtained, in the range of 96-109 %, being these recoveries better than those of most of the methods summarized in the comparison table (Table 51). Moreover, RSDs below 16% were obtained for intra-day precision in all cases, although worse precision was observed in the case of inter-day extractions, mainly for PrP, BuP, and BPA, with RSDs below 24%.

3.2.3. Sample analysis

Five samples from different volunteers were analyzed in order to assess the feasibility of the method. For this purpose, the total content (free + conjugated) of parabens and BPA was determined as well as the creatinine content for the result standardization, obtained through the Jaffe method (see Table 52). The obtained concentrations were corrected with the creatinine content of each sample. As observed in the results, both expressed in µg L^{-1} (Table 53) and in terms of µg g_{cr}^{-1} (Table 54), in all analyzed samples were found at least one of the target analytes, being the BPA the most frequently found, with the highest concentrations. These results are consistent with other reported studies, since the presence of parabens, and BPA to a greater extent, in biological human samples is widely proved [311,317–320]. In addition, the analysis of some of the samples through the reference method using C18 cartridges presented similar results, being these values statistically comparable through a t-student test with a confidence level of 95%. Hence, the feasibility and applicability of the reported method have been demonstrated, confirming the designed material as an alternative for the determination of EDCs in urine samples, with all the advantages already described in comparison with other reported methods, such as significantly better sensitivity and better extraction efficiencies above 96%.

Table 52. Creatinine content obtained for each analyzed sample through the Jaffe method.

Compound	Creatinine (mg L^{-1})
Methylparaben	548 ± 4
Ethylparaben	717 ± 15
Propylparaben	1270 ± 20
Butylparaben	553 ± 9
Bisphenol A	610 ± 30

Table 53. Concentrations of parabens and BPA obtained for each sample (n=3) expressed in μg L^{-1}. The values were obtained with the reported method (β-CD-UVM-7 material) and the reference method (C18).

Compound	S1		S2		S3		S4		S5
	β-CD-UVM-7	C18	β-CD-UVM-7	C18	β-CD-UVM-7	C18	β-CD-UVM-7	C18	β-CD-UVM-7
MeP	1.5 ± 0.3	1.56 ± 0.18	<LOD	<LOD	<LOD	<LOD	11.0 ± 1.8	10.5 ± 1.8	2.3 ± 0.3
EtP	<LOD	<LOD	<LOD	<LOD	<LOD	<LOD	<LOD	<LOD	<LOD
PrP	<LOD	<LOD	<LOD	<LOD	<LOD	<LOD	2.26 ± 0.03	2.7 ± 0.3	<LOD
BuP	0.48 ± 0.16	<LOQ	1.9 ± 0.6	1.8 ± 0.5	4.9 ± 0.3	4.9 ± 0.3	5.80 ± 0.19	6.9 ± 1.9	<LOD
BPA	26 ± 5	34 ± 2	49 ± 12	51 ± 3	13 ± 3	12 ± 3	6 ± 3	5.3 ± 0.4	7.5 ± 0.5

Table 54. Concentrations of parabens and BPA obtained for each sample (n=3) corrected with the creatinine content (μg g_{cr}^{-1}). The values were obtained with the reported method (β-CD-UVM-7 material) and the reference method (C18).

Compound	S1		S2		S3		S4		S5
	β-CD-UVM-7	C18	β-CD-UVM-7	C18	β-CD-UVM-7	C18	β-CD-UVM-7	C18	β-CD-UVM-7
MeP	2.7 ± 0.6	2.9 ± 0.3	<LOD	<LOD	<LOD	<LOD	20 ± 3	19 ± 3	3.8 ± 0.4
EtP	<LOD	<LOD	<LOD	<LOD	<LOD	<LOD	<LOD	<LOD	<LOD
PrP	<LOD	<LOD	<LOD	<LOD	<LOD	<LOD	4.10 ± 0.06	4.9 ±0.6	<LOD
BuP	0.9 ± 0.3	<LOD	2.6 ± 0.8	2.5 ± 0.6	3.9 ± 0.3	3.9 ± 02	10.5 ± 0.3	12 ± 4	<LOD
BPA	47 ± 9	62 ± 4	68 ± 17	71 ± 4	11 ± 2	10 ± 3	11 ± 5	10 ± 1	12.4 ± 0.8

*Note that different LODs and LOQs were considered for the reference method (C18) due to the experimental procedure (see Table 55)

Table 55. Sensitivity parameters (μg L^{-1}) of the applied reference method using C18 cartridges.

Compound	LOD	LOQ
Methylparaben	0.012	0.04
Ethylparaben	0.003	0.011
Propylparaben	0.002	0.008
Butylparaben	0.16	0.5
Bisphenol A	0.17	0.6

4. Study of the adsorption ability of the β-CD-UVM-7 sorbent

Several adsorption experiments were carried out to assess the binding ability of the developed β-CD-UVM-7 sorbent, using the BPA as a representative analyte. The kinetic adsorption tests were carried out by adding 20 mg of the sorbent to a 10 mL solution of 20 mg L^{-1} of BPA, and stirring it for different times (1-120 min) at 25 °C. On the other hand, isothermal adsorption experiments were carried out similarly, by stirring 20 mg of the sorbent in 10 mL of solutions with different concentrations (1-150 mg L^{-1}) for 30 min at 25 °C. In both cases, after the adsorption, the solution was filtered to determine the remaining concentration of BPA in the solution. The adsorption amounts were calculated as follows:

$$Q = \frac{(C_0 - C)V}{m} \quad (2)$$

where C_0 and C are the initial and final concentrations, V is the solution volume, and m is the mass of sorbent.

4.1. Kinetic adsorption analysis

The kinetic experiments were carried out at different times in the range of 1-120 min as previously described, and the resulting adsorption curves are shown in Figure 81A. As can be seen, the adsorption was observed to occur almost instantaneously (in the first minute), reaching the plateau in the first 10 minutes, and the complete equilibrium at 20 min. This fact represents an important advantage for the use of this sorbent for an SPE application since the rapid adsorption could play an important role to permit a rapid sample treatment with the designed cartridges. This fast adsorption could be explained owing to the rapid formation of stable host-guest complexes between CDs and the analytes, and thanks to the bimodal mesoporous specific architecture of the UVM-7 silica structure already characterized, which provide the sorbent with great accessibility for the analyte adsorption.

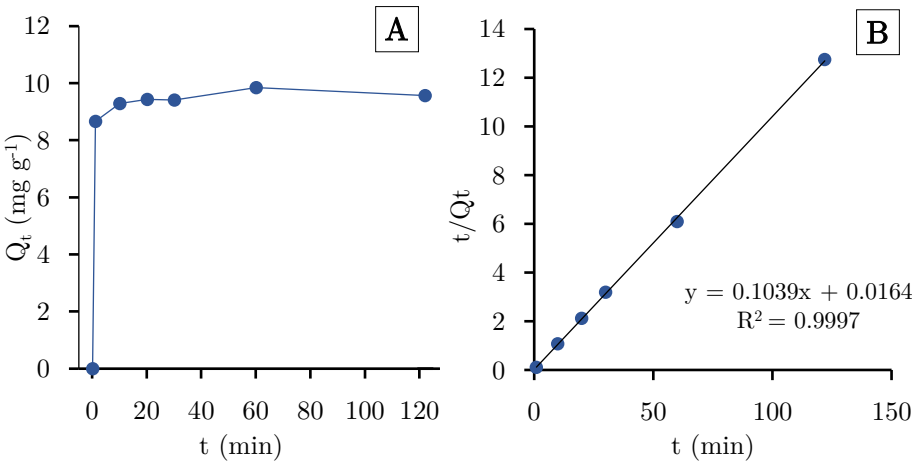

Figure 81. Kinetic adsorption analysis of the β-CD-UVM-7 developed sorbent using BPA as analyte model: kinetic adsorption curve (A) and pseudo-second-order model fitting the obtained values with its linear regression (B).

To further study the mechanism of the adsorption process, pseudo-first-order and pseudo-second-order models were considered, taking into account the following equations:

Pseudo-first-order rate:

$$\mathrm{Ln}\,(Q_e - Q_t) = \mathrm{Ln}Q_{c1} - k_1 t \tag{3}$$

Pseudo-second-order rate:

$$\frac{t}{Q_t} = \frac{1}{k_2 {Q_{c2}}^2} + \frac{t}{Q_{c2}} \tag{4}$$

where Q_e and Q_t are the adsorption capacities at equilibrium and at time t respectively; Q_{c1} and Q_{c2} are the calculated adsorption capacities of the pseudo-first-order and pseudo-second-order models respectively; k_1 and k_2 are the apparent pseudo-first-order and pseudo-second-order rate constants respectively; and t is the adsorption time.

As shown in Figure 81B, the pseudo-second-order rate presents an excellent correlation with the obtained results (R^2 = 0.9997), which implies that the adsorption process of these analytes on the β-CD-UVM-7 material is mainly ruled by this kinetic process. This observation indicates that the adsorption process is mainly attributed to chemical interactions, which is consistent with the nature of the developed sorbent since the retention of the analytes is expected to occur in the β-CD active centers [336–338]. This retention takes place owing to the formation of host-guest complexes, as it has been widely studied for phenolic compounds, and for these analytes specifically [327,339]. As can be observed in Table 56, this finding is consistent with the results obtained for other β-CD-based

sorbents reported in the literature, since the retention mechanism is expected to be also based on the formation of the mentioned host-guest complexes.

Also, from the linear regression equation, a Q_{c2} of 9.62 mg g^{-1}, which is greatly closer to the obtained experimental Q_{eq} (9.84 mg g^{-1}), as well as a kinetic apparent pseudo-second-order constant (k_2) of 0.66 g mg^{-1} min^{-1} were obtained.

Table 56. Comparison of adsorption parameters of the developed sorbent with other β-CD-based sorbents reported in the literature for the adsorption of BPA.

Sorbent	Best kinetic binding model	k_2 (g mg^{-1} min^{-1})	Best adsorption model	Q_{max} (mg g^{-1})	K_L (L mg^{-1})	Ref.
β-CD-UVM-7	Pseudo-second order	0.66	Langmuir	24.43	0.119	This work
CDGO nanosheets	Pseudo-second order	-[a]	Langmuir	23.1	0.237[b]	[340]
TiO_2@ACD @RGO	-[a]	-[a]	Langmuir	24.31	0.014	[341]
β-CDHN	Pseudo-second order	1.54	Langmuir	120.48	0.0483[a]	[337]
CA β-CD	Pseudo-second order	0.00265[b]	Langmuir	83[b]	0.0566[b]	[342]
MP-CDP	Pseudo-second order	0.01394	Langmuir	78.93	0.0891[b]	[343]
P-CDP	Pseudo-second order	1.5	Langmuir	88	0.2475[b]	[344]
β-CDP	Pseudo-second order	0.0566	Langmuir	112.99	0.1328[b]	[336]

[a]Expressed with different units in the original work

[b]Not reported

GO: Graphene oxide; RGO: Reduced GO

ACD: Aspartic acid-β-CD

HN: Hollow nanoparticles

CA β-CD: Citric acid crosslinked β-CD

MP-CDP / P-CDP: Microporous / Porous β-CD polymer

4.2. Isothermal adsorption analysis

On the other hand, the isothermal adsorption was also investigated, by studying the adsorption process at several initial concentrations in the range 1-150 mg L^{-1} as described. As shown in Figure 82A, the adsorption capacity increases with the initial concentration as expected. Moreover, Langmuir and Freundlich models were tested to fit the isothermal obtained experimental data to further investigate the adsorption process. For this purpose, the following equations were used for each model, in order to plot the correspondent values.

Langmuir model:

$$\frac{C_e}{Q_e} = \frac{C_e}{Q_{max}} + \frac{1}{K_L Q_{max}} \quad (5)$$

Freundlich model:

$$LnQ_e = LnK_F + \frac{1}{n} LnC_e \quad (6)$$

where C_e is the equilibrium concentration of the analyte; Q_e and Q_{max} are the equilibrium and maximum adsorption capacities, respectively; K_L is the constant in the Langmuir isothermal adsorption model; and K_F and n are both constants in the Freundlich isothermal adsorption model.

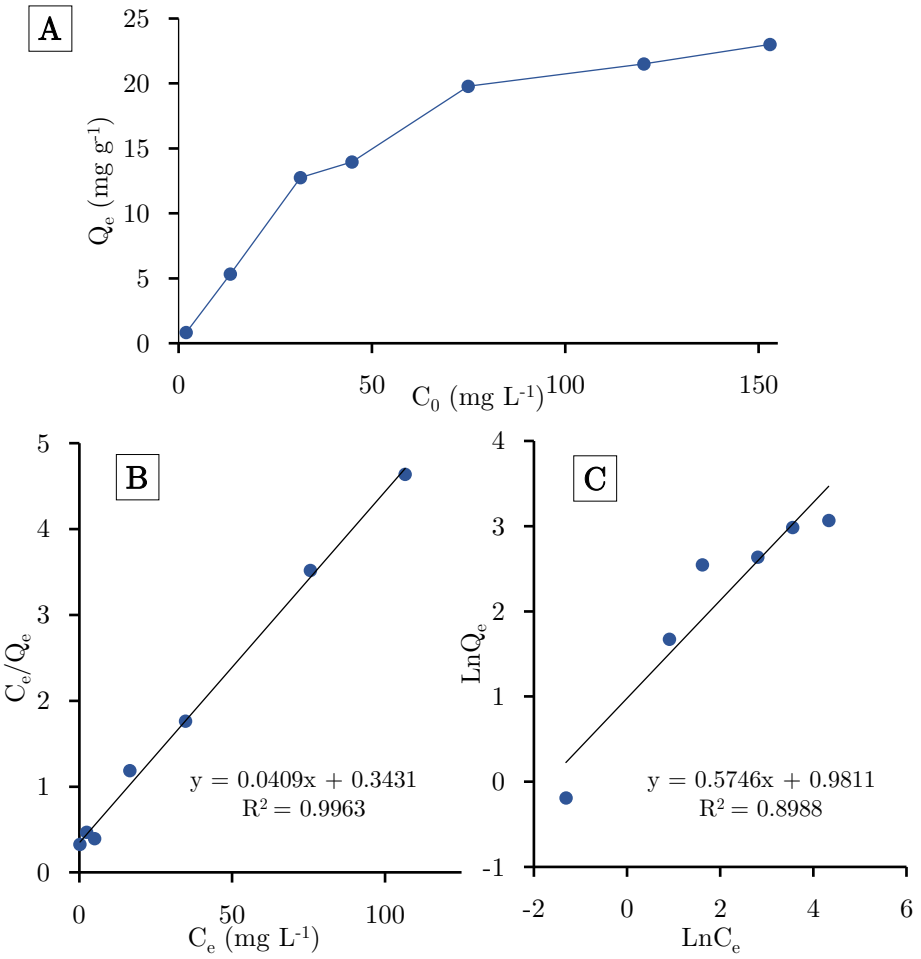

Figure 82. Study of the isothermal adsorption of the β-CD-UVM-7 material using BPA as representative analyte: adsorption isothermal curve (A) and the Langmuir (B) and Freundlich (C) models fitting the obtained values, with the corresponding linear regressions.

As can be seen in Figure 82B and C, the obtained data was clearly better fitted to the Langmuir model, with an R^2 coefficient of 0.9963. This fact could imply the consideration of the adsorption as a monolayer adsorption process in a homogeneous system. Thus, it could be speculated that the great fitting to the Langmuir model responds to an adsorption process that takes place at specific homogeneous sites within the sorbent, with a finite adsorption capacity and a saturation point [336–338]. This model is also in agreement with the sorbent here studied since the adsorption is expected to occur owing to the interaction of the analytes with the β-CD centres, which are expected to have a homogeneous affinity towards the analytes. This observation is also in accordance with other β-CD-based sorbents summarized in Table 56, being all of them well-fitted with the Langmuir adsorption model.

Moreover, from the linear regression obtained from the Langmuir model, the maximum adsorption capacity of the sorbent can be calculated. In this case, the Q_{max} value was estimated as 24.43 mg g^{-1}. Also, the obtained adsorption Langmuir constant was calculated (K_L = 0.119 L mg^{-1}). As observed in Table 56, the obtained maximum adsorption capacity is comparable to many other sorbents previously developed, although it is lower in some cases. However, it should be noted that most of the sorbents summarized in Table 56 are designed for its implementation in remediation applications such as removal or degradation of BPA, in which cases the maximum adsorption plays a key role in the elimination of the maximum amount of pollutant. In our case, the material is designed as an SPE sorbent where lower maximum adsorption capacities are also satisfactory. In any case, it should be highlighted that the obtained maximum adsorption capacity is, by far, enough for the retention of endocrine-disrupting chemicals in the concentrations commonly present in urine samples [16], since it allows the proper treatment of samples with more than 300 mg L^{-1} considering the described experimental parameters. Hence, the adsorption capacity of the developed sorbent, as well as the kinetics of the adsorption of BPA have been demonstrated to be satisfactory for its implementation as SPE sorbent for the extraction of endocrine-disrupting chemicals, as already proved in the previous point.

5. Conclusions

In the present chapter, a novel material has been applied to the clean-up and preconcentration of parabens and BPA in urine samples. The material has been demonstrated to be a mesoporous silica framework type UVM-7, with β-CD active sites bonded to the silica material. Besides, the key role of the CDs in the interaction with analytes has been also proved in comparison to blank UVM-7 material, thus allowing the quantitative retention of these compounds. The advantage of the ordered bimodal pore network was also studied in comparison with disordered xerogel materials, thus highlighting the benefits of the hierarchical porous structure of the designed material.

Thus, a method using the β-CD-UVM-7 material as SPE sorbent has been developed. The main analytical figures of merit stated for the method enhance it as an alternative to other methods reported in the literature, with good sensitivity in terms of LODs (below 0.06 μg L^{-1}) as well as average recoveries above 96%, representing advantages regarding other reported protocols. Indeed, the method has been applied to the analysis of real urine samples in comparison with a reference method, and the results were statistically comparable. The presence of the target analytes in significant concentrations was observed in all samples, and the BPA was the most detected compound, being these observations in agreement with the concentrations usually found in urine samples for these analytes.

Moreover, the adsorption ability of the developed sorbent has been systematically studied in terms of kinetic and isothermal adsorption, being the results in agreement with an adsorption mechanism based on the interaction between CDs and BPA as analyte model, owing to the formation of host-guest complexes. In this sense, the binding kinetics have proved to fit a pseudo-second-order rate, and the isothermal adsorption data have fitted to the Langmuir model, estimating a maximum adsorption capacity of 24.43 mg g^{-1}.

CONCLUSIONS

As **general conclusions** of the present Doctoral Thesis, it should be highlighted the accomplishment in the application of UVM-7 material as sorbents for the retention and extraction of organic hazardous compounds. These materials have been demonstrated to offer great features for their use as air samplers and SPE sorbents in several analytical fields, namely food, environmental and clinical analysis. Thus, the general conclusions of the research are here summarized:

- UVM-7 porous structure has been proved to be crucial in the extraction of aflatoxins from food samples such as tea and milk, with the key role of the pseudo-ordered mesoporous. Owing to the bimodal porosity and the pore size control in the mesoporous range, the quantitative retention of the most common aflatoxins has been achieved.
- Extracted UVM-7 have proved to strongly interact with aflatoxins in comparison to calcined UVM-7 thanks to the greater presence of silanol groups in the silica surface.
- Two analytical methods for the extraction of aflatoxins from tea and milk samples have been successfully developed. Both methods present good analytical parameters with excellent extraction efficiencies. The methods have been applied to the analysis of real food samples and have been demonstrated to be a promising alternative to the expensive commercial immunoaffinity columns.
- The addition of Ti and Fe by co-hydrolysis does not modify the porous structure of the UVM-7 material, except when high amounts of metallic heteroelement are added, where nanodomains of TiO_2 or Fe_2O_3 were observed. This addition has proved to be more homogeneous in the case of the Ti, although a good heteroelement dispersion has been observed in all materials with moderate contents of both Ti and Fe.
- The addition of higher amounts of titanium affects the coordination environment of Ti centers, migrating from the predominance of tetrahedral to octahedral centers, with important effects in their interaction with P-containing analytes.
- The incorporation of Fe to the UVM-7 simultaneously with the modification of the pore size has been achieved for the first time thanks to the use of short-chain surfactants. The materials Fe50-UVM-7-C_{12} and $-C_{10}$ have been demonstrated to preserve de UVM-7 bimodal porosity with a notable reduction in the mesopore size.
- Ti-UVM-7 materials have proved to be more efficient for the retention of organophosphorus compounds in environmental matrices in comparison to Fe-UVM-7. The addition of the Ti by impregnation in the TiO_2-UVM-7 material leads to the formation of large domains of TiO_2, entailing the pore blocking and an important decrease in the analyte recovery. Xerogel materials doped with Ti have also been demonstrated to offer significantly worse results due

to their microporous structure in comparison to the bimodal porosity of UVM-7, and greater difficulties for the homogeneous incorporation of metallic heteroelements.

- The designed air samplers containing Ti25-UVM-7 material have proved to be a great alternative for the sampling of organophosphorus pesticides in occupational risk assessment, with good analytical parameters and quantitative recoveries. These samplers have been successfully applied to real sampling.
- The occupational risk assessment study carried out with the designed samplers has shown that personal protective equipment is needed to work during the application of the pesticide and immediately before it, due to the high pesticide concentrations present in the air.
- Also, with Ti25-UVM-7 material, an SPE method for the extraction of organophosphorus pesticides has been developed, although an important matrix effect has been observed in this case, thus entailing worse analytical parameters. However, the method was successfully applied to the analysis of real samples in comparison to a reference method.
- Better results were observed for the extraction of phosphorus flame retardants, with the development of an SPE method with the Ti50-UVM-7 material. It presents good analytical parameters and satisfactory recoveries in comparison to previous studies. In this case, important concentrations of TCIPP, TDCIPP, and TPhP were detected in the analysis of real samples.
- The addition of Au nanoparticles to the UVM-7 structure by impregnation is clearly favored by the presence of titanium. Au/Ti-UVM-7 materials have been successfully synthesized with a homogeneous dispersion of the Au nanoparticles, and the preservation of the bimodal porous structure of the material.
- Au/Ti50-UVM-7 material has been applied to water analysis and organochlorine pesticide determination, through the design of a sandwich SPE cartridge also with blank UVM-7. With the developed method the simultaneous quantitative extraction of 20 pesticides has been achieved, with good analytical features.
- The interaction of these chlorinated compounds with Au centers has been proved, thus confirming the selectivity offered by Au nanoparticles.
- The presence of iron in the Fe-UVM-7 materials has proved to play a key role in the retention of fluorinated compounds. Besides, the effect of the mesopore size modulation on the retention of these analytes has been also confirmed, which is a suitable tool to adapt these materials to target analytes.
- Fe-UVM-7 materials did not provide satisfactory recoveries for short-chain perfluoroalkyl compounds (C_4-C_8), nor those with larger or smaller mesopore

sizes, being these materials not applicable for the extraction of these compounds.

- For long-chain perfluoroalkyl compounds (C_8-C_{14}), the material Fe50-UVM-7-C_{12} provided good results, and an analytical method for the SPE of PFASs from environmental water samples was developed. The method presented acceptable analytical features in comparison with other reported methods, and its feasibility for the application to the analysis of real samples has been confirmed in comparison with WAX cartridges.
- The attachment of β-CD active centers to the UVM-7 structure has been here presented for the first time. The modification of the one-pot UVM-7 synthesis procedure led to a typical UVM-7 structure with the cyclodextrins bonded to the silica, thus maintaining the bimodal porosity with only a slight decrease on the mesopore size due to the partially blocking.
- This novel material has allowed the development of an SPE method for the extraction and determination of endocrine-disrupting chemicals from urine samples. The method shows good analytical parameters for the extraction of four parabens and bisphenol A in real samples, and important concentrations of these analytes were detected in all analyzed urine samples.
- The adsorption process of the β-CD-UVM-7 material has proved to follow a second-order-rate kinetic binding model, as well as the Langmuir isothermal model, which is in agreement with the adsorption of the analytes owing to the formation of host-guest complexes with CDs available in the material.

Starting from this research and the conclusions exposed above, the following outlook and **future perspectives** can be proposed:

- To apply the developed Ti25-UVM-7 air samplers to high-volume sampling for environmental analysis. Sampler features should be reoptimized as well as some experimental parameters, in order to allow the sampling of huge air volumes and quantify very low concentrations of pesticides in the environmental air.
- To apply these samplers to other organophosphorus compounds such as flame retardants, starting from the good results obtained with these materials for their extraction from water samples.
- To design methods for the determination of pesticide residues in food samples, by using the developed materials containing Ti and Au. Their application to food analysis could be useful regarding pesticide control and vigilance.
- To modify the UVM-7 material with the addition of new metallic heteroelements in order to make it selective for other organic compounds of interest. A wide variety of metals have been demonstrated to be suitable for

their introduction in the UVM-7 structures, which may offer different properties for its use for retention purposes.

- To functionalize the UVM-7 material with other cyclodextrin or host-guest supramolecular organic centers with the aim of making it suitable for the retention of organic compounds with other sizes.

Finally, it must be stated that the present thesis is a great example of the potential of nanomaterials for their application in different areas, as well as the key role they play in current chemistry, and specifically in analytical chemistry. Thus, their great properties as adsorbent materials have led to the development of a large number of analytical techniques, mainly in the sampling, preconcentration, and sample clean-up steps, which are key aspects of the determination of organic hazardous compounds. As has been observed in this work, the versatility of these nanomaterials (and specifically those based on hierarchical porous silica) has given them a highly relevant position in current and future analytical chemistry, since the ongoing development of a wide variety of nanomaterials with specifically tailored properties, allows us to predict their crucial role on the upcoming innovations in analytical chemistry.

BIBLIOGRAPHY

[1] P. Ścigalski, P. Kosobucki, Recent materials developed for dispersive solid phase extraction, Molecules. 25 (2020) 1–26. doi:10.3390/molecules25214869.

[2] Y. Gao, G. Liu, M. Gao, X. Huang, D. Xu, Recent advances and applications of magnetic metal-organic frameworks in adsorption and enrichment removal of food and environmental pollutants, Crit. Rev. Anal. Chem. 50 (2020) 472–484. doi:10.1080/10408347.2019.1653166.

[3] S. Knoll, T. Rösch, C. Huhn, Trends in sample preparation and separation methods for the analysis of very polar and ionic compounds in environmental water and biota samples, Anal. Bioanal. Chem. 412 (2020) 6149–6165. doi:10.1007/s00216-020-02811-5.

[4] Secretariat of the Stockholm Convention - United Nations Environment Programme (UNEP), Stockholm Convention on Persistent Organic Pollutants (POPs). Revised in 2019, (2020) 1–77. http://www.pops.int/TheConvention/Overview/TextoftheConvention/tabid/2232/Default.aspx (accessed January 14, 2022).

[5] M. Lorenzo, J. Campo, Y. Picó, Analytical challenges to determine emerging persistent organic pollutants in aquatic ecosystems, TrAC - Trends Anal. Chem. 103 (2018) 137–155. doi:10.1016/j.trac.2018.04.003.

[6] Z. Zhang, M. Zhou, J. He, T. Shi, S. Zhang, N. Tang, W. Chen, Polychlorinated dibenzo-dioxins and polychlorinated dibenzo-furans exposure and altered lung function: the mediating role of oxidative stress, Environ. Int. 137 (2020) 105521. doi:10.1016/j.envint.2020.105521.

[7] United States Environmental Protection Agency (US EPA), EPA's priority pollutants list, Code of Federal Regulation, Title 40, Part 423, (2012) 653–654.

[8] M. Tankiewicz, J. Fenik, M. Biziuk, Solventless and solvent-minimized sample preparation techniques for determining currently used pesticides in water samples: a review, Talanta. 86 (2011) 8–22. doi:10.1016/j.talanta.2011.08.056.

[9] Secretariat of the Basel Rotterdam and Stockholm Conventions - United Nations Environment Programme (UNEP), Persistent Organic Pollutants Review Committee (POPRC) recommendations for listing chemicals - Chemicals under review, (2022). http://chm.pops.int/Convention/POPsReviewCommittee/Chemicals/tabid/243/Default.aspx (accessed January 14, 2022).

[10] K. Helou, M. Harmouche-Karaki, S. Karake, J.F. Narbonne, A review of organochlorine pesticides and polychlorinated biphenyls in Lebanon: environmental and human contaminants, Chemosphere. 231 (2019) 357–368. doi:10.1016/j.chemosphere.2019.05.109.

[11] Q. Zhang, Y. Yao, Y. Wang, Q. Zhang, Z. Cheng, Y. Li, X. Yang, L. Wang, H. Sun, Plant accumulation and transformation of brominated and organophosphate flame retardants: a review, Environ. Pollut. 288 (2021) 117742.

doi:10.1016/j.envpol.2021.117742.

[12] R.C. Buck, J. Franklin, U. Berger, J.M. Conder, I.T. Cousins, P. de Voogt, A.A. Jensen, K. Kannan, S.A. Mabury, S.P.J. van Leeuwen, Perfluoroalkyl and polyfluoroalkyl substances in the environment: terminology, classification, and origins, Integr. Environ. Assess. Manag. 7 (2011) 513–541. doi:10.1002/ieam.258.

[13] A.J. Ebele, M. Abou-Elwafa Abdallah, S. Harrad, Pharmaceuticals and personal care products (PPCPs) in the freshwater aquatic environment, Emerg. Contam. 3 (2017) 1–16. doi:10.1016/j.emcon.2016.12.004.

[14] D. Montes-Grajales, M. Fennix-Agudelo, W. Miranda-Castro, Occurrence of personal care products as emerging chemicals of concern in water resources: a review, Sci. Total Environ. 595 (2017) 601–614. doi:10.1016/j.scitotenv.2017.03.286.

[15] L. Cizmas, V.K. Sharma, C.M. Gray, T.J. McDonald, Pharmaceuticals and personal care products in waters: occurrence, toxicity, and risk, Environ. Chem. Lett. 13 (2015) 381–394. doi:10.1007/s10311-015-0524-4.

[16] I. Jiménez-Díaz, F. Vela-Soria, R. Rodríguez-Gómez, A. Zafra-Gómez, O. Ballesteros, A. Navalón, Analytical methods for the assessment of endocrine disrupting chemical exposure during human fetal and lactation stages: a review, Anal. Chim. Acta. 892 (2015) 27–48. doi:10.1016/j.aca.2015.08.008.

[17] A. Mauri-Aucejo, P. Amorós, A. Moragues, C. Guillem, C. Belenguer-Sapiña, Comparison of the solid-phase extraction efficiency of a bounded and an included cyclodextrin-silica microporous composite for polycyclic aromatic hydrocarbons determination in water samples, Talanta. 156–157 (2016) 95–103. doi:10.1016/j.talanta.2016.05.011.

[18] H. Liu, S. Ma, X. Zhang, Y. Yu, Application of thermal desorption methods for airborne polycyclic aromatic hydrocarbon measurement: a critical review, Environ. Pollut. 254 (2019) 113018. doi:10.1016/j.envpol.2019.113018.

[19] Y.C. Lin, W.J. Lee, S.J. Chen, G.P. Chang-Chien, P.J. Tsai, Characterization of PAHs exposure in workplace atmospheres of a sinter plant and health-risk assessment for sintering workers, J. Hazard. Mater. 158 (2008) 636–643. doi:10.1016/j.jhazmat.2008.02.006.

[20] A.R. Mauri-Aucejo, P. Ponce-Català, C. Belenguer-Sapiña, P. Amorós, Determination of phenolic compounds in air by using cyclodextrin-silica hybrid microporous composite samplers, Talanta. 134 (2015) 560–567. doi:10.1016/j.talanta.2014.11.057.

[21] S. Król, B. Zabiegała, J. Namieśnik, Monitoring VOCs in atmospheric air I. On-line gas analyzers, TrAC - Trends Anal. Chem. 29 (2010) 1092–1100. doi:10.1016/j.trac.2010.05.007.

[22] Directive 2013/39/EU of the European Parliament and of the Council of 12 August

2013 amending Directives 2000/60/EC and 2008/105/EC as regards priority substances in the field of water policy, Off. J. Eur. Union. L 226 (2013) 1–17.

[23] Directive 2006/118/EC of the European Parliament and of the Council of 12 December 2006 on the protection of groundwater against pollution and deterioration, Off. J. Eur. Union. L 372 (2006) 19–31.

[24] Directive 98/83/EC of 3 November 1998 on the quality of water intended for human consumption, Off. J. Eur. Communities. L 330 (1998) 32–54.

[25] D.J. Hamilton, Á. Ambrus, R.M. Dieterle, A.S. Felsot, C.A. Harris, P.T. Holland, A. Katayama, N. Kurihara, J. Linders, J. Unsworth, S.S. Wong, Regulatory limits for pesticide residues in water (IUPAC technical report), Pure Appl. Chem. 75 (2003) 1123–1155. doi:10.1515/ci.2003.25.6.21.

[26] J. Hanlon, K.S. Galea, S. Verpaele, Review of workplace based aerosol sampler comparison studies, 2004–2020, Int. J. Environ. Res. Public Health. 18 (2021). doi:10.3390/ijerph18136819.

[27] Instituto Nacional de Seguridad y Salud en el Trabajo (INSST), Límites de exposición profesional para agentes químicos en España, (2021) 1–181.

[28] Directive 2008/50/EC of the European Parliament and of the Council of 21 May 2008 on ambient air quality and cleaner air for Europe, Off. J. Eur. Union. L 152 (2008) 1–44.

[29] Directive 2004/107/EC of the European Parliament and of the Council of 15 December 2004 relating to arsenic, cadmium, mercury, nickel and polycyclic aromatic hydrocarbons in ambient air, Off. J. Eur. Union. L 23 (2005) 3–16.

[30] H. Sharifan, M. Bagheri, D. Wang, J.G. Burken, C.P. Higgins, Y. Liang, J. Liu, C.E. Schaefer, J. Blotevogel, Fate and transport of per- and polyfluoroalkyl substances (PFASs) in the vadose zone, Sci. Total Environ. 771 (2021) 145427. doi:10.1016/j.scitotenv.2021.145427.

[31] J.K. Schuster, T. Harner, A. Eng, C. Rauert, K. Su, K.C. Hornbuckle, C.W. Johnson, Tracking POPs in global air from the first 10 years of the GAPS network (2005 to 2014), Environ. Sci. Technol. 55 (2021) 9479–9488. doi:10.1021/acs.est.1c01705.

[32] R. Riaz, R.N. Malik, C.A. de Wit, Soil-air partitioning of semivolatile organic compounds in the Lesser Himalaya region: influence of soil organic matter, atmospheric transport processes and secondary emissions, Environ. Pollut. 291 (2021) 118006. doi:10.1016/j.envpol.2021.118006.

[33] K. Sun, Y. Song, F. He, M. Jing, J. Tang, R. Liu, A review of human and animals exposure to polycyclic aromatic hydrocarbons: health risk and adverse effects, photo-induced toxicity and regulating effect of microplastics, Sci. Total Environ. 773 (2021) 145403. doi:10.1016/j.scitotenv.2021.145403.

[34] J.F. Ayala-Cabrera, F.J. Santos, E. Moyano, Recent advances in analytical

methodologies based on mass spectrometry for the environmental analysis of halogenated organic contaminants, Trends Environ. Anal. Chem. 30 (2021) e00122. doi:10.1016/j.teac.2021.e00122.

[35] T. Rasheed, M. Bilal, F. Nabeel, M. Adeel, H.M.N. Iqbal, Environmentally-related contaminants of high concern: potential sources and analytical modalities for detection, quantification, and treatment, Environ. Int. 122 (2019) 52–66. doi:10.1016/j.envint.2018.11.038.

[36] W. Guo, B. Pan, S. Sakkiah, G. Yavas, W. Ge, W. Zou, W. Tong, H. Hong, Persistent organic pollutants in food: contamination sources, health effects and detection methods, Int. J. Environ. Res. Public Health. 16 (2019) 10–12. doi:10.3390/ijerph16224361.

[37] Joint FAO/WHO Expert Committee on Food Additives, Fifty-seventh report: Evaluation of certain food additives and contaminants, 909 (2002) 1–186.

[38] Joint Meeting on Pesticide Residues (JMPR), Inventory of IPCS and other WHO pesticide evaluations and summary of toxicological evaluations performed by the JMPR through 2009, (2010) 1–56. http://www.who.int/ipcs/publications/jmpr/pesticide_inventory_edition10.pdf.

[39] World Health Organization (WHO) Temporary Adviser Group, Consultation on assessment of the health risk of dioxins; re-evaluation of the tolerable daily intake (TDI): executive summary, Food Addit. Contam. 17 (2000) 223–240.

[40] Comission Regulation (EC) No 1881/2006 of 19 December 2006 setting maximum levels for certain contaminants in foodstuffs, Off. J. Eur. Union. L 364 (2006) 5–24.

[41] European Comission, EU Pesticides database - Pesticide residues, (2022). https://ec.europa.eu/food/plant/pesticides/eu-pesticides-database/mrls/?event=search.pr (accessed January 13, 2022).

[42] J.D.G. McEvoy, Contamination of animal feedingstuffs as a cause of residues in food: a review of regulatory aspects, incidence and control, Anal. Chim. Acta. 473 (2002) 3–26. doi:10.1016/S0003-2670(02)00751-1.

[43] R. Fernández-González, I. Yebra-Pimentel, E. Martínez-Carballo, J. Simal-Gándara, Feed ingredients mainly contributing to polycyclic aromatic hydrocarbon and polychlorinated biphenyl residues, Polycycl. Aromat. Compd. 32 (2012) 280–295. doi:10.1080/10406638.2012.671226.

[44] M.A. Farag, M. Tanios, S. AlKarimy, H. Ibrahim, H.A. Guirguis, Biosensing approaches to detect potential milk contaminants: a comprehensive review, Food Addit. Contam. Part A. 38 (2021) 1169–1192. doi:10.1080/19440049.2021.1914864.

[45] E. Janik, M. Niemcewicz, M. Podogrocki, M. Ceremuga, L. Gorniak, M. Stela, M. Bijak, The existing methods and novel approaches in mycotoxins' detection, Molecules. 26 (2021) 1–19. doi:10.3390/molecules26133981.

[46] A. Alshannaq, J.H. Yu, Occurrence, toxicity, and analysis of major mycotoxins in food, Int. J. Environ. Res. Public Health. 14 (2017) 632–652. doi:10.3390/ijerph14060632.

[47] S.K. Pankaj, H. Shi, K.M. Keener, A review of novel physical and chemical decontamination technologies for aflatoxin in food, Trends Food Sci. Technol. 71 (2018) 73–83. doi:10.1016/j.tifs.2017.11.007.

[48] W.P.P. Liew, S. Mohd-Redzwan, Mycotoxin: its impact on gut health and microbiota, Front. Cell. Infect. Microbiol. 8 (2018) 1–17. doi:10.3389/fcimb.2018.00060.

[49] V. Yusa, M. Millet, C. Coscolla, M. Roca, Analytical methods for human biomonitoring of pesticides. A review, Anal. Chim. Acta. 891 (2015) 15–31. doi:10.1016/j.aca.2015.05.032.

[50] K. Vorkamp, A. Castaño, J.P. Antignac, L.D. Boada, E. Cequier, A. Covaci, M. Esteban López, L.S. Haug, M. Kasper-Sonnenberg, H.M. Koch, O. Pérez Luzardo, A. Osīte, L. Rambaud, M.T. Pinorini, G. Sabbioni, C. Thomsen, Biomarkers, matrices and analytical methods targeting human exposure to chemicals selected for a European human biomonitoring initiative, Environ. Int. 146 (2021) 106082. doi:10.1016/j.envint.2020.106082.

[51] A. Agüera, M.J. Martínez Bueno, A.R. Fernández-Alba, New trends in the analytical determination of emerging contaminants and their transformation products in environmental waters, Environ. Sci. Pollut. Res. 20 (2013) 3496–3515. doi:10.1007/s11356-013-1586-0.

[52] D.C. Harris, Gas chromatography, in: W. H. Freeman and Company (Ed.), Quantitative chemical analysis, Sixth Edition, New York and Basingstoke (USA), 2003: pp. 578–606.

[53] D.C. Harris, High resolution liquid chromatography, in: W. H. Freeman and Company (Ed.), Quantitative chemical analysis, Sixth Edition, New York and Basingstoke (USA), 2003: pp. 607–639.

[54] K. Murtada, Trends in nanomaterial-based solid-phase microextraction with a focus on environmental applications - A review, Trends Environ. Anal. Chem. 25 (2020) e00077. doi:10.1016/j.teac.2019.e00077.

[55] R.E. Majors, Sample preparation fundametals for chormatography, Agilent Technologies, Inc., Canada, 2013.

[56] M. Faraji, Y. Yamini, M. Gholami, Recent advances and trends in applications of solid-phase extraction techniques in food and environmental analysis, Chromatographia. 82 (2019) 1207–1249. doi:10.1007/s10337-019-03726-9.

[57] M. Nasiri, H. Ahmadzadeh, A. Amiri, Sample preparation and extraction methods for pesticides in aquatic environments: a review, TrAC - Trends Anal. Chem. 123 (2020) 115772. doi:10.1016/j.trac.2019.115772.

[58] Z.H. Deng, N. Li, H.L. Jiang, J.M. Lin, R.S. Zhao, Pretreatment techniques and analytical methods for phenolic endocrine disrupting chemicals in food and environmental samples, TrAC - Trends Anal. Chem. 119 (2019) 115592. doi:10.1016/j.trac.2019.07.003.

[59] M. Amoli-Diva, Z. Taherimaslak, M. Allahyari, K. Pourghazi, M.H. Manafi, Application of dispersive liquid-liquid microextraction coupled with vortex-assisted hydrophobic magnetic nanoparticles based solid-phase extraction for determination of aflatoxin M_1 in milk samples by sensitive micelle enhanced spectrofluorimetry, Talanta. 134 (2015) 98–104. doi:10.1016/j.talanta.2014.11.007.

[60] C.L. Arthur, J. Pawliszyn, Solid phase microextraction with thermal desorption using fused silica optical fibers, Anal. Chem. 62 (1990) 2145–2148. doi:10.1021/ac00218a019.

[61] J. Płotka-Wasylka, N. Szczepańska, M. de la Guardia, J. Namieśnik, Miniaturized solid-phase extraction techniques, TrAC - Trends Anal. Chem. 73 (2015) 19–38. doi:10.1016/j.trac.2015.04.026.

[62] A. Andrade-Eiroa, M. Canle, V. Leroy-Cancellieri, V. Cerdà, Solid-phase extraction of organic compounds: a critical review. Part II, TrAC - Trends Anal. Chem. 80 (2016) 655–667. doi:10.1016/j.trac.2015.08.014.

[63] M. Anastassiades, S.J. Lehotay, D. Štajnbaher, F.J. Schenck, Fast and easy multiresidue method employing acetonitrile extraction/partitioning and "dispersive solid-phase extraction" for the determination of pesticide residues in produce, J. AOAC Int. 86 (2003) 412–431. doi:10.1093/jaoac/86.2.412.

[64] R. Perestrelo, P. Silva, P. Porto-Figueira, J.A.M. Pereira, C. Silva, S. Medina, J.S. Câmara, QuEChERS - Fundamentals, relevant improvements, applications and future trends, Anal. Chim. Acta. 1070 (2019) 1–28. doi:10.1016/j.aca.2019.02.036.

[65] V. Yusà, C. Coscollà, W. Mellouki, A. Pastor, M. de la Guardia, Sampling and analysis of pesticides in ambient air, J. Chromatogr. A. 1216 (2009) 2972–2983. doi:10.1016/j.chroma.2009.02.019.

[66] K.C. van Horne, Sorbent extraction technology, Analytichem International (Varian), Habor City, CA (USA), 1985.

[67] H. Dabrowska, Ł. Dabrowski, M. Biziuk, J. Gaca, J. Namieśnik, Solid-phase extraction clean-up of soil and sediment extracts for the determination of various types of pollutants in a single run, J. Chromatogr. A. 1003 (2003) 29–42. doi:10.1016/S0021-9673(03)00849-5.

[68] V. Walker, G.A. Mills, Solid-phase extraction in clinical biochemistry, Ann. Clin. Biochem. 39 (2002) 464–477. doi:10.1258/000456302320314476.

[69] A.R. Fernandez-Alba, A. Agüera, M. Contreras, G. Peñuela, I. Ferrer, D. Barceló, Comparison of various sample handling and analytical procedures for the monitoring of pesticides and metabolites in ground waters, J. Chromatogr. A. 823

(1998) 35–47. doi:10.1016/S0021-9673(98)00439-7.

[70] United States Environmental Protection Agency (US EPA), Method 3535A (SW-846): Solid-phase extraction (SPE). Revision 1, Washington, DC, (2007) 1–24.

[71] United States Environmental Protection Agency (US EPA), Standard operating procedures 1801: Routine analysis of PCBs in water and soil/sediment samples by GC-ECD, Revision 2, Washington, DC, (2006) 1–37.

[72] A. Andrade-Eiroa, M. Canle, V. Leroy-Cancellieri, V. Cerdà, Solid-phase extraction of organic compounds: a critical review (Part I), TrAC - Trends Anal. Chem. 80 (2016) 641–654. doi:10.1016/j.trac.2015.08.015.

[73] A. Azzouz, E. Ballesteros, Combined microwave-assisted extraction and continuous solid-phase extraction prior to gas chromatography-mass spectrometry determination of pharmaceuticals, personal care products and hormones in soils, sediments and sludge, Sci. Total Environ. 419 (2012) 208–215. doi:10.1016/j.scitotenv.2011.12.058.

[74] A. Kouzayha, A. Rahman Rabaa, M. Al Iskandarani, D. Beh, H. Budzinski, F. Jaber, Multiresidue method for determination of 67 pesticides in water samples using solid-phase extraction with centrifugation and gas chromatography-mass spectrometry, Am. J. Anal. Chem. 03 (2012) 257–265. doi:10.4236/ajac.2012.33034.

[75] F. Adachi, A. Yamamoto, K.I. Takakura, R. Kawahara, Occurrence of fluoroquinolones and fluoroquinolone-resistance genes in the aquatic environment, Sci. Total Environ. 444 (2013) 508–514. doi:10.1016/j.scitotenv.2012.11.077.

[76] J. Płotka-Wasylka, M. Marć, N. Szczepańska, J. Namieśnik, New polymeric materials for solid phase extraction, Crit. Rev. Anal. Chem. 47 (2017) 373–383. doi:10.1080/10408347.2017.1298987.

[77] M. Ghani, R.M. Frizzarin, F. Maya, V. Cerdà, In-syringe extraction using dissolvable layered double hydroxide-polymer sponges templated from hierarchically porous coordination polymers, J. Chromatogr. A. 1453 (2016) 1–9. doi:10.1016/j.chroma.2016.05.023.

[78] R. Soltani, A. Shahvar, M. Dinari, M. Saraji, Environmentally-friendly and ultrasonic-assisted preparation of two-dimensional ultrathin Ni/Co-NO_3 layered double hydroxide nanosheet for micro solid-phase extraction of phenolic acids from fruit juices, Ultrason. Sonochem. 40 (2018) 395–401. doi:10.1016/j.ultsonch.2017.07.031.

[79] F.Q. Wang, J. Li, J.F. Wu, G.C. Zhao, Layered double hydroxides as a coating for the determination of phthalate esters in aqueous solution with solid-phase microextraction followed by gas chromatography, Chromatographia. 81 (2018) 799–807. doi:10.1007/s10337-018-3507-3.

[80] N. Manousi, G.A. Zachariadis, E.A. Deliyanni, On the use of metal-organic

frameworks for the extraction of organic compounds from environmental samples, Environ. Sci. Pollut. Res. 28 (2021) 59015–59039. doi:10.1007/s11356-020-07911-4.

[81] B. Hashemi, P. Zohrabi, N. Raza, K.H. Kim, Metal-organic frameworks as advanced sorbents for the extraction and determination of pollutants from environmental, biological, and food media, TrAC - Trends Anal. Chem. 97 (2017) 65–82. doi:10.1016/j.trac.2017.08.015.

[82] P. Rocío-Bautista, V. Pino, J. Pasán, I. López-Hernández, J.H. Ayala, C. Ruiz-Pérez, A.M. Afonso, Insights in the analytical performance of neat metal-organic frameworks in the determination of pollutants of different nature from waters using dispersive miniaturized solid-phase extraction and liquid chromatography, Talanta. 179 (2018) 775–783. doi:10.1016/j.talanta.2017.12.012.

[83] S. Zhang, Z. Du, G. Li, Metal-organic framework-199/graphite oxide hybrid composites coated solid-phase microextraction fibers coupled with gas chromatography for determination of organochlorine pesticides from complicated samples, Talanta. 115 (2013) 32–39. doi:10.1016/j.talanta.2013.04.029.

[84] X. Chen, N. Ding, H. Zang, H. Yeung, R.S. Zhao, C. Cheng, J. Liu, T.W.D. Chan, Fe_3O_4@MOF core-shell magnetic microspheres for magnetic solid-phase extraction of polychlorinated biphenyls from environmental water samples, J. Chromatogr. A. 1304 (2013) 241–245. doi:10.1016/j.chroma.2013.06.053.

[85] Y. Jia, H. Su, Z. Wang, Y.L.E. Wong, X. Chen, M. Wang, T.W.D. Chan, Metal-organic framework@microporous organic network as adsorbent for solid-phase microextraction, Anal. Chem. 88 (2016) 9364–9367. doi:10.1021/acs.analchem.6b03156.

[86] Y. Wang, Y. Tong, X. Xu, L. Zhang, Metal-organic framework-derived three-dimensional porous graphitic octahedron carbon cages-encapsulated copper nanoparticles hybrids as highly efficient enrichment material for simultaneous determination of four fluoroquinolones, J. Chromatogr. A. 1533 (2018) 1–9. doi:10.1016/j.chroma.2017.12.021.

[87] X. Liu, T. Feng, C. Wang, L. Hao, C. Wang, Q. Wu, Z. Wang, A metal-organic framework-derived nanoporous carbon/iron composite for enrichment of endocrine disrupting compounds from fruit juices and milk samples, Anal. Methods. 8 (2016) 3528–3535. doi:10.1039/c6ay00191b.

[88] S. Zhang, Z. Jiao, W. Yao, A simple solvothermal process for fabrication of a metal-organic framework with an iron oxide enclosure for the determination of organophosphorus pesticides in biological samples, J. Chromatogr. A. 1371 (2014) 74–81. doi:10.1016/j.chroma.2014.10.088.

[89] T. Kiljanek, A. Niewiadowska, M. Małysiak, A. Posyniak, Miniaturized multiresidue method for determination of 267 pesticides, their metabolites and polychlorinated biphenyls in low mass beebread samples by liquid and gas

chromatography coupled with tandem mass spectrometry, Talanta. 235 (2021) 122721. doi:10.1016/j.talanta.2021.122721.

[90] Z.A. Temerdashev, E.A. Vinitskaya, V. V. Milevskaya, M.A. Statkus, Preconcentration of phenolic compounds on carbon sorbents and their chromatographic determination in aqueous extracts of medicinal plants, J. Anal. Chem. 76 (2021) 296–305. doi:10.1134/S106193482103014X.

[91] N.I. Hill, J. Becanova, R. Lohmann, A sensitive method for the detection of legacy and emerging per- and polyfluorinated alkyl substances (PFAS) in dairy milk, Anal. Bioanal. Chem. 414 (2022) 1235–1243. doi:10.1007/s00216-021-03575-2.

[92] N.N. Naing, S.F.Y. Li, H.K. Lee, Evaluation of graphene-based sorbent in the determination of polar environmental contaminants in water by micro-solid phase extraction-high performance liquid chromatography, J. Chromatogr. A. 1427 (2016) 29–36. doi:10.1016/j.chroma.2015.12.012.

[93] A. Mehdinia, N. Khodaee, A. Jabbari, Fabrication of graphene/Fe_3O_4@polythiophene nanocomposite and its application in the magnetic solid-phase extraction of polycyclic aromatic hydrocarbons from environmental water samples, Anal. Chim. Acta. 868 (2015) 1–9. doi:10.1016/j.aca.2014.12.022.

[94] A. Mehdinia, S. Rouhani, S. Mozaffari, Microwave-assisted synthesis of reduced graphene oxide decorated with magnetite and gold nanoparticles, and its application to solid-phase extraction of organochlorine pesticides, Microchim. Acta. 183 (2016) 1177–1185. doi:10.1007/s00604-015-1691-5.

[95] K. Jiang, Q. Huang, K. Fan, L. Wu, D. Nie, W. Guo, Y. Wu, Z. Han, Reduced graphene oxide and gold nanoparticle composite-based solid-phase extraction coupled with ultra-high-performance liquid chromatography-tandem mass spectrometry for the determination of 9 mycotoxins in milk, Food Chem. 264 (2018) 218–225. doi:10.1016/j.foodchem.2018.05.041.

[96] S. Mahpishanian, H. Sereshti, Three-dimensional graphene aerogel-supported iron oxide nanoparticles as an efficient adsorbent for magnetic solid phase extraction of organophosphorus pesticide residues in fruit juices followed by gas chromatographic determination, J. Chromatogr. A. 1443 (2016) 43–53. doi:10.1016/j.chroma.2016.03.046.

[97] H.L. Jiang, Y.L. Lin, N. Li, Z.W. Wang, M. Liu, R.S. Zhao, J.M. Lin, Application of magnetic N-doped carbon nanotubes in solid-phase extraction of trace bisphenols from fruit juices, Food Chem. 269 (2018) 413–418. doi:10.1016/j.foodchem.2018.07.032.

[98] D. Zacs, I. Rozentale, I. Reinholds, V. Bartkevics, Multi-walled carbon nanotubes as effective sorbents for rapid analysis of polycyclic aromatic hydrocarbons in edible oils using dispersive solid-phase extraction (d-SPE) and gas chromatography—tandem mass spectrometry (GC-MS/MS), Food Anal. Methods. 11 (2018) 2508–2517. doi:10.1007/s12161-018-1240-z.

[99] A. Jakubus, K. Godlewska, M. Gromelski, K. Jagiello, T. Puzyn, P. Stepnowski, M. Paszkiewicz, The possibility to use multi-walled carbon nanotubes as a sorbent for dispersive solid phase extraction of selected pharmaceuticals and their metabolites: effect of extraction condition, Microchem. J. 146 (2019) 1113–1125. doi:10.1016/j.microc.2019.02.051.

[100] M. Azizi-Lalabadi, H. Hashemi, J. Feng, S.M. Jafari, Carbon nanomaterials against pathogens; the antimicrobial activity of carbon nanotubes, graphene/graphene oxide, fullerenes, and their nanocomposites, Adv. Colloid Interface Sci. 284 (2020) 102250. doi:10.1016/j.cis.2020.102250.

[101] H. Liu, Y. Luan, A. Lu, B. Li, M. Yang, J. Wang, An oligosorbent-based aptamer affinity column for selective extraction of aflatoxin B_2 prior to HPLC with fluorometric detection, Microchim. Acta. 185 (2018) 71. doi:10.1007/s00604-017-2591-7.

[102] V. Pichon, F. Brothier, A. Combès, Aptamer-based-sorbents for sample treatment - a review, Anal. Bioanal. Chem. 407 (2015) 681–698. doi:10.1007/s00216-014-8129-5.

[103] S. Lin, N. Gan, J. Zhang, L. Qiao, Y. Chen, Y. Cao, Aptamer-functionalized stir bar sorptive extraction coupled with gas chromatography-mass spectrometry for selective enrichment and determination of polychlorinated biphenyls in fish samples, Talanta. 149 (2016) 266–274. doi:10.1016/j.talanta.2015.11.062.

[104] M. Khodadadi, A. Malekpour, M.A. Mehrgardi, Aptamer functionalized magnetic nanoparticles for effective extraction of ultratrace amounts of aflatoxin M_1 prior its determination by HPLC, J. Chromatogr. A. 1564 (2018) 85–93. doi:10.1016/j.chroma.2018.06.022.

[105] M.N.H. Rozaini, N. Yahaya, B. Saad, S. Kamaruzaman, N.S.M. Hanapi, Rapid ultrasound assisted emulsification micro-solid phase extraction based on molecularly imprinted polymer for HPLC-DAD determination of bisphenol A in aqueous matrices, Talanta. 171 (2017) 242–249. doi:10.1016/j.talanta.2017.05.006.

[106] J. Li, R. Dong, X. Wang, H. Xiong, S. Xu, D. Shen, X. Song, L. Chen, One-pot synthesis of magnetic molecularly imprinted microspheres by RAFT precipitation polymerization for the fast and selective removal of 17β-estradiol, RSC Adv. 5 (2015) 10611–10618. doi:10.1039/c4ra11177j.

[107] W. Lu, W. Ming, X. Zhang, L. Chen, Molecularly imprinted polymers for dispersive solid-phase extraction of phenolic compounds in aqueous samples coupled with capillary electrophoresis, Electrophoresis. 37 (2016) 2487–2495. doi:10.1002/elps.201600119.

[108] J. He, L. Song, S. Chen, Y. Li, H. Wei, D. Zhao, K. Gu, S. Zhang, Novel restricted access materials combined to molecularly imprinted polymers for selective solid-phase extraction of organophosphorus pesticides from honey, Food Chem. 187 (2015) 331–337. doi:10.1016/j.foodchem.2015.04.069.

[109] Y.P. Song, L. Zhang, G.N. Wang, J.X. Liu, J. Liu, J.P. Wang, Dual-dummy-template molecularly imprinted polymer combining ultra performance liquid chromatography for determination of fluoroquinolones and sulfonamides in pork and chicken muscle, Food Control. 82 (2017) 233–242. doi:10.1016/j.foodcont.2017.07.002.

[110] W. Huang, P. Wang, P. Jiang, X. Dong, S. Lin, Preparation and application of a restricted access material with hybrid poly(glycerol mono-methacrylate) and cross-linked bovine serum albumin as hydrophilic out layers for directly on-line high performance liquid chromatography analysis of enrofloxacin a, J. Chromatogr. A. 1573 (2018) 59–65. doi:10.1016/j.chroma.2018.08.067.

[111] C. Belenguer-Sapiña, E. Pellicer-Castell, A.R. Mauri-Aucejo, E.F. Simó-Alfonso, P. Amorós, Cyclodextrins as a key piece in nanostructured materials: quantitation and remediation of pollutants, Nanomaterials. 11 (2021) 1–28. doi:10.3390/nano11010007.

[112] A. Walcarius, M.M. Collinson, Analytical chemistry with silica sol-gels: traditional routes to new materials for chemical analysis, Annu. Rev. Anal. Chem. 2 (2009) 121–143. doi:10.1146/annurev-anchem-060908-155139.

[113] C.T. Kresge, M.E. Leonowicz, W.J. Roth, J.C. Vartuli, J.S. Beck, Ordered mesoporous molecular sieves synthesized by a liquid-crystal template mechanism, Nature. 359 (1992) 710. http://dx.doi.org/10.1038/359710a0.

[114] N. Casado, D. Pérez-Quintanilla, S. Morante-Zarcero, I. Sierra, Current development and applications of ordered mesoporous silicas and other sol–gel silica-based materials in food sample preparation for xenobiotics analysis, Trends Anal. Chem. 88 (2017) 167–184. doi:10.1016/j.trac.2017.01.001.

[115] S. Cabrera, J. El Haskouri, C. Guillem, J. Latorre, A. Beltrán-Porter, D. Beltrán-Porter, M.D. Marcos, P. Amorós, Generalised syntheses of ordered mesoporous oxides: the atrane route, Solid State Sci. 2 (2000) 405–420. doi:10.1016/S1293-2558(00)00152-7.

[116] J. El Haskouri, J.M. Morales, D. Ortiz de Zárate, L. Ferna, J. Latorre, C. Guillem, A. Beltrán, D. Beltrán, P. Amorós, Nanoparticulated silicas with bimodal porosity: chemical control of the pore sizes, Inorg. Chem. 47 (2008) 8267–8277. doi:10.1021/ic800893a.

[117] J.L. Armstrong, R.A. Fenske, M.G. Yost, M. Tchong-French, J. Yu, Comparison of polyurethane foam and XAD-2 sampling matrices to measure airborne organophosphorus pesticides and their oxygen analogs in an agricultural community, Chemosphere. 92 (2013) 451–457. doi:10.1016/j.chemosphere.2013.01.109.

[118] National Institute for Occupational Safety and Health (NIOSH), Manual of Analythical Methods (Fourth Edition). Method 5600: Organophosphorus pesticides, (1994) 1–20.

[119] National Institute for Occupational Safety and Health (NIOSH), Manual of Analythical Methods (Fourth Edition). Method 2546: Cresol (all isomers) and phenol, (1994) 1–4.

[120] United States Environmental Protection Agency (US EPA), Compendium of methods for the determination of toxic organic compounds in ambeint air. Method TO-17: Determination of volatile organic compounds in ambient air using active sampling onto sorbent tubes, (1999) 1–49.

[121] United States Environmental Protection Agency (US EPA), Compendium of methods for the determination of air pollutants in indoor air. Method IP -1B: Solid adsorbent tubes, (1990) 1–85.

[122] X. Zhang, A. Saini, C. Hao, T. Harner, Passive air sampling and nontargeted analysis for screening POP-like chemicals in the atmosphere: opportunities and challenges, TrAC - Trends Anal. Chem. 132 (2020) 116052. doi:10.1016/j.trac.2020.116052.

[123] J. Lexén, M. Bernander, I. Cotgreave, P.L. Andersson, Assessing exposure of semi-volatile organic compounds (SVOCs) in car cabins: current understanding and future challenges in developing a standardized methodology, Environ. Int. 157 (2021) 106847. doi:10.1016/j.envint.2021.106847.

[124] United States Environmental Protection Agency (US EPA), Compendium of methods for the determination of toxic organic compounds in ambeint air. Method TO-10A: Determination of pesticides and polychlorinated biphenyls in ambient air using low volume polyurethane foam (PUF) sampling followed by gas chromatographic multi-detector detection (GC/MD), (1999) 1–33.

[125] R.K. Iler, The chemistry of silica, John Wiley & Sons, Inc., New York (USA), 1979.

[126] W. Stöber, A. Fink, E. Bohn, Controlled growth of monodisperse silica spheres in the micron size range, J. Colloid Interface Sci. 26 (1968) 62–69. doi:10.1109/ICOSP.2006.345929.

[127] L.L. Hench, J.K. West, The sol-gel process, Chem. Rev. 90 (1990) 33–72.

[128] T.M. Wu, G.R. Wu, H.M. Kao, J.L. Wang, Using mesoporous silica MCM-41 for in-line enrichment of atmospheric volatile organic compounds, J. Chromatogr. A. 1105 (2006) 168–175. doi:10.1016/j.chroma.2005.09.030.

[129] M. Lashgari, H.K. Lee, Determination of perfluorinated carboxylic acids in fish fillet by micro-solid phase extraction, followed by liquid chromatography-triple quadrupole mass spectrometry, J. Chromatogr. A. 1369 (2014) 26–32. doi:10.1016/j.chroma.2014.09.082.

[130] M. Lashgari, C. Basheer, H. Kee Lee, Application of surfactant-templated ordered mesoporous material as sorbent in micro-solid phase extraction followed by liquid chromatography-triple quadrupole mass spectrometry for determination of

perfluorinated carboxylic acids in aqueous media, Talanta. 141 (2015) 200–206. doi:10.1016/j.talanta.2015.03.049.

[131] M. Lashgari, H.K. Lee, Micro-solid phase extraction of perfluorinated carboxylic acids from human plasma, J. Chromatogr. A. 1432 (2016) 7–16. doi:10.1016/j.chroma.2016.01.005.

[132] A.S. Barreto, A. Aquino, S.C.S. Silva, M.E. De Mesquita, M.J. Calhorda, M.S. Saraiva, S. Navickiene, A novel application of mesoporous silica material for extraction of pesticides, Mater. Lett. 65 (2011) 1357–1359. doi:10.1016/j.matlet.2011.01.082.

[133] L. Kharbouche, M.D. Gil García, A. Lozano, H. Hamaizi, M. Martínez Galera, Determination of personal care products in water using UHPLC–MS after solid phase extraction with mesoporous silica-based MCM-41 functionalized with cyanopropyl groups, J. Sep. Sci. 43 (2020) 2142–2153. doi:10.1002/jssc.201901148.

[134] Y. Shuang, T. Zhang, L. Li, Preparation of a stilbene diamido-bridged bis(β-cyclodextrin)-bonded chiral stationary phase for enantioseparations of drugs and pesticides by high performance liquid chromatography, J. Chromatogr. A. 1614 (2020) 460702. doi:10.1016/j.chroma.2019.460702.

[135] C. Hofmann, A. Duerkop, A.J. Baeumner, Nanocontainers for analytical applications, Angew. Chemie Int. Ed. 58 (2019) 12840–12860. doi:10.1002/anie.201811821.

[136] N. Casado, D. Pérez-Quintanilla, S. Morante-Zarcero, I. Sierra, Bi-functionalized mesostructured silicas as reversed-phase/strong anion-exchange sorbents. Application to extraction of polyphenols prior to their quantitation by UHPLC with ion-trap mass spectrometry detection, Microchim. Acta. 186 (2019) 164. doi:10.1007/s00604-019-3267-2.

[137] L. Zhao, H. Qin, R. Wu, H. Zou, Recent advances of mesoporous materials in sample preparation, J. Chromatogr. A. 1228 (2012) 193–204. doi:10.1016/j.chroma.2011.09.051.

[138] J.S. Beck, J.C. Vartuli, W.J. Roth, M.E. Leonowicz, C.T. Kresge, K.D. Schmitt, C.T.-W. Chu, D.H. Olson, E.W. Sheppard, S.B. McCullen, J.B. Higgins, J.L. Schlenker, A new family of mesoporous molecular sieves prepared with liquid crystal templates, J. Am. Chem. Soc. 114 (1992) 10834–10843. doi:10.1021/ja00053a020.

[139] P.J. Amorós del Toro, A. Beltrán Porter, D. Beltrán Porter, A.B. Descalzo López, J. El Haskouri, C. Guillem Villar, J. Latorre Saborit, M.D. Marcos Martínez, G. Rodríguez-López, Patent ES2228195B1 - New porous oxides ordered with bimodal pore system: preparation, conforming procedure and its uses, 2001.

[140] M.M. Trandafir, A. Moragues, P. Amorós, V.I. Parvulescu, Selective hydrogenation of nitroderivatives over Au/TiO_2/UVM-7 composite catalyst, Catal. Today. 355 (2020) 893–902. doi:10.1016/j.cattod.2019.02.053.

[141] A. Moragues, F. Neaţu, V.I. Pârvulescu, M.D. Marcos, P. Amorós, V. Michelet, Heterogeneous gold catalyst: synthesis, characterization, and application in 1,4-addition of boronic acids to enones, ACS Catal. 5 (2015) 5060–5067. doi:10.1021/acscatal.5b01207.

[142] V.I. Pârvulescu, S.M. Coman, N. Candu, J. El Haskouri, D. Beltrán, P. Amorós, Synthesis, characterization and catalytic behavior of SnTf/MCM-41 and SnTf/UVM-7 as new green catalysts for etherification reactions, J. Mater. Sci. 44 (2009) 6693–6700. doi:10.1007/s10853-009-3599-0.

[143] P. Burguete, A. Beltrán, C. Guillem, J. Latorre, F. Pérez-Pla, D. Beltrán, P. Amorós, Pore length effect on drug uptake and delivery by mesoporous silicas, Chempluschem. 77 (2012) 817–831. doi:10.1002/cplu.201200099.

[144] É. Pérez-Esteve, M. Ruiz-Rico, C. De La Torre, L.A. Villaescusa, F. Sancenón, M.D. Marcos, P. Amorós, R. Martínez-Máñez, J.M. Barat, Encapsulation of folic acid in different silica porous supports: a comparative study, Food Chem. 196 (2016) 66–75. doi:10.1016/j.foodchem.2015.09.017.

[145] J. El Haskouri, D. Ortiz de Zárate, C. Guillem, J. Latorre, M. Caldés, A. Beltrán, D. Beltrán, A.B. Descalzo, G. Rodríguez-López, R. Martínez-Máñez, M.D. Marcos, P. Amorós, Silica-based powders and monoliths with bimodal pore systems., Chem. Commun. (2002) 330–331. doi:10.1039/b110883b.

[146] J. El Haskouri, D. Ortiz de Zaráte, F. Pérez-Pla, A. Cervilla, C. Guillem, J. Latorre, M.D. Marcos, A. Beltrán, D. Beltrán, P. Amorós, Improving epoxide production using Ti-UVM-7 porous nanosized catalysts, New J. Chem. 26 (2002) 1093–1095. doi:10.1039/b205856c.

[147] A. Moragues, B. Puértolas, Á. Mayoral, R. Arenal, A.B. Hungría, S. Murcia-Mascarós, S.H. Taylor, B. Solsona, T. García, P. Amorós, Understanding the role of Ti-rich domains in the stabilization of gold nanoparticles on mesoporous silica-based catalysts, J. Catal. 360 (2018) 187–200. doi:10.1016/j.jcat.2018.02.003.

[148] S. Muñoz-Pina, J. V. Ros-Lis, Á. Argüelles, R. Martínez-Máñez, A. Andrés, Influence of the functionalisation of mesoporous silica material UVM-7 on polyphenol oxidase enzyme capture and enzymatic browning, Food Chem. 310 (2020) 125741. doi:10.1016/j.foodchem.2019.125741.

[149] D. Ortiz de Zárate, L. Fernández, A. Beltrán, C. Guillem, J. Latorre, D. Beltrán, P. Amorós, Expanding the atrane route: generalized surfactant-free synthesis of mesoporous nanoparticulated xerogels, Solid State Sci. 10 (2008) 587–601. doi:10.1016/j.solidstatesciences.2007.10.014.

[150] H. Shirkhanloo, S. Davari Ahranjani, A lead analysis based on amine functionalized bimodal mesoporous silica nanoparticles in human biological samples by ultrasound assisted-ionic liquid trap-micro solid phase extraction, J. Pharm. Biomed. Anal. 157 (2018) 1–9. doi:10.1016/j.jpba.2018.05.004.

[151] H. Shirkhanloo, M. Ghazaghi, A. Rashidi, A. Vahid, Arsenic speciation based on

amine-functionalized bimodal mesoporous silica nanoparticles by ultrasound assisted-dispersive solid-liquid multiple phase microextraction, Microchem. J. 130 (2017) 137–146. doi:10.1016/j.microc.2016.08.013.

[152] H. Shirkhanloo, M. Falahnejad, H. Zavvar Mousavi, On-line ultrasound-assisted dispersive micro-solid-phase extraction based on amino bimodal mesoporous silica nanoparticles for the preconcentration and determination of cadmium in human biological samples, Biol. Trace Elem. Res. 171 (2016) 472–481. doi:10.1007/s12011-015-0538-6.

[153] H. Shirkhanloo, A. Khaligh, F. Golbabaei, Z. Sadeghi, A. Vahid, A. Rashidi, On-line micro column preconcentration system based on amino bimodal mesoporous silica nanoparticles as a novel adsorbent for removal and speciation of chromium (III, VI) in environmental samples, J. Environ. Heal. Sci. Eng. 13 (2015) 1–12. doi:10.1186/s40201-015-0205-z.

[154] H. Shirkhanloo, M. Falahnejad, H. Zavvar Mousavi, Mesoporous silica nanoparticles as an adsorbent for preconcentration and determination of trace amount of nickel in environmental samples by atom trap flame atomic absorption spectrometry, J. Appl. Spectrosc. 82 (2016) 1072–1077. doi:10.1007/s10812-016-0231-3.

[155] Y. Salinas, J. V. Ros-Lis, J.L. Vivancos, R. Martínez-Máñez, S. Aucejo, N. Herranz, I. Lorente, E. Garcia, A chromogenic sensor array for boiled marinated turkey freshness monitoring, Sensors Actuators B Chem. 190 (2014) 326–333. doi:10.1016/j.snb.2013.08.075.

[156] Y. Salinas, J. V. Ros-Lis, J.L. Vivancos, R. Martínez-Máñez, M.D. Marcos, S. Aucejo, N. Herranz, I. Lorente, Monitoring of chicken meat freshness by means of a colorimetric sensor array, Analyst. 137 (2012) 3635–3643. doi:10.1039/c2an35211g.

[157] Y. Salinas, J. V. Ros-Lis, J.L. Vivancos, R. Martínez-Máñez, M.D. Marcos, S. Aucejo, N. Herranz, I. Lorente, E. Garcia, A novel colorimetric sensor array for monitoring fresh pork sausages spoilage, Food Control. 35 (2014) 166–176. doi:10.1016/j.foodcont.2013.06.043.

[158] A.B. Descalzo, K. Rurack, H. Weisshoff, R. Martínez-Máñez, M.D. Marcos, P. Amorós, K. Hoffmann, J. Soto, Rational design of a chromo- and fluorogenic hybrid chemosensor material for the detection of long-chain carboxylates, J. Am. Chem. Soc. 127 (2005) 184–200. doi:10.1021/ja045683n.

[159] M. Comes, E. Aznar, M. Moragues, M.D. Marcos, R. Martínez-Máñez, F. Sancenón, J. Soto, L.A. Villaescusa, L. Gil, P. Amorós, Mesoporous hybrid materials containing nanoscopic “binding pockets” for colorimetric anion signaling in water by using displacement assays, Chem. Eur. J. 15 (2009) 9024–9033. doi:10.1002/chem.200900890.

[160] M. Comes, M.D. Marcos, R. Martínez-Máñez, F. Sancenón, L.A. Villaescusa, A.

Graefe, G.J. Mohr, Hybrid functionalised mesoporous silica-polymer composites for enhanced analyte monitoring using optical sensors, J. Mater. Chem. 18 (2008) 5815–5823. doi:10.1039/b810992c.

[161] H. Martínez Pérez-Cejuela, I. Ten-Doménech, J. El Haskouri, P. Amorós, E.F. Simó-Alfonso, J.M. Herrero-Martínez, Solid-phase extraction of phospholipids using mesoporous silica nanoparticles: application to human milk samples, Anal. Bioanal. Chem. 410 (2018) 4847–4854. doi:10.1007/s00216-018-1121-8.

[162] A. Weller, E.J. Carrasco-Correa, C. Belenguer-Sapiña, A. Mauri-Aucejo, P. Amorós, J.M. Herrero-Martínez, Organo-silica hybrid capillary monolithic column with mesoporous silica particles for separation of small aromatic molecules, Microchim. Acta. 184 (2017) 3799–3808. doi:10.1007/s00604-017-2404-z.

[163] M. Pérez-Cabero, F.A. Esteve-Turrillas, D. Beltrán, P. Amorós, Hierarchical porous carbon with designed pore architecture and study of its adsorptive properties, Solid State Sci. 12 (2010) 15–25. doi:10.1016/j.solidstatesciences.2009.09.017.

[164] A. Gentili, Cyclodextrin-based sorbents for solid phase extraction, J. Chromatogr. A. 1609 (2020) 460654. doi:10.1016/j.chroma.2019.460654.

[165] C. Belenguer-Sapiña, E. Pellicer-Castell, P. Amorós, E.F. Simó-Alfonso, A.R. Mauri-Aucejo, A new proposal for the determination of polychlorinated biphenyls in environmental water by using host-guest adsorption, Sci. Total Environ. 724 (2020) 138266. doi:10.1016/j.scitotenv.2020.138266.

[166] C. Belenguer-Sapiña, E. Pellicer-Castell, J. El Haskouri, C. Guillem, E.F. Simó-Alfonso, P. Amorós, A. Mauri-Aucejo, Design, characterization and comparison of materials based on β and γ cyclodextrin covalently connected to microporous silica for environmental analysis, J. Chromatogr. A. 1563 (2018) 10–19. doi:10.1016/j.chroma.2018.05.070.

[167] V.S. Narkhede, A. De Toni, V. V. Narkhede, M. Guraya, J.W. Niemantsverdriet, M.W.E. van den Berg, W. Grünert, H. Gies, Au/TiO_2 catalysts encapsulated in the mesopores of siliceous MCM-48 - Reproducible synthesis, structural characterization and activity for CO oxidation, Microporous Mesoporous Mater. 118 (2009) 52–60. doi:10.1016/j.micromeso.2008.08.037.

[168] S.T. Mahmud, L.D. Wilson, Synthesis and characterization of surface-modified mesoporous silica materials with β-cyclodextrin, Cogent Chem. 2 (2016) 1–19. doi:10.1080/23312009.2015.1132984.

[169] L. Xie, M. Chen, Y. Ying, Development of methods for determination of aflatoxins, Crit. Rev. Food Sci. Nutr. 56 (2016) 2642–2664. doi:10.1080/10408398.2014.907234.

[170] Agencia Española de Seguridad Alimentaria y Nutrición (AESAN), Informe del Comité Científico de la AESAN en relación al efecto sobre la población española de la derogación de la normativa nacional sobre límite màximos permitidos para

las aflatoxinas B_1, B_2, G_1 y G_2 en alimentos, Revista del Comité Científico. 14 (2011) 27–42.

[171] V. Pagkali, P.S. Petrou, E. Makarona, J. Peters, W. Haasnoot, G. Jobst, I. Moser, K. Gajos, A. Budkowski, A. Economou, K. Misakos, I. Raptis, S.E. Kakabakos, Simultaneous determination of aflatoxin B_1, fumonisin B_1 and deoxynivalenol in beer samples with a label-free monolithically integrated optoelectronic biosensor, J. Hazard. Mater. 359 (2018) 445–453. doi:10.1016/j.jhazmat.2018.07.080.

[172] L.-J. Du, C. Chu, E. Warner, Q.-Y. Wang, Y.-H. Hu, K.-J. Chai, J. Cao, L.-Q. Peng, Y.-B. Chen, J. Yang, Q.-D. Zhang, Rapid microwave-assisted dispersive micro-solid phase extraction of mycotoxins in food using zirconia nanoparticles, J. Chromatogr. A. 1561 (2018) 1–12. doi:10.1016/j.chroma.2018.05.031.

[173] X. Pascari, A.J. Ramos, S. Marín, V. Sanchís, Mycotoxins and beer. Impact of beer production process on mycotoxin contamination. A review, Food Res. Int. 103 (2018) 121–129. doi:10.1016/j.foodres.2017.07.038.

[174] A.O. Okaru, K.O. Abuga, I.O. Kibwage, T. Hausler, B. Luy, T. Kuballa, J. Rehm, D.W. Lachenmeier, Aflatoxin contamination in unrecorded beers from Kenya - A health risk beyond ethanol, Food Control. 79 (2017) 344–348. doi:10.1016/j.foodcont.2017.04.006.

[175] Z. Pouretedal, M. Mazaheri, Aflatoxins in black tea in Iran, Food Addit. Contam. Part B. 6 (2013) 127–129. doi:10.1080/19393210.2013.764551.

[176] G. Martínez-Domínguez, R. Romero-González, A. Garrido Frenich, Multi-class methodology to determine pesticides and mycotoxins in green tea and royal jelly supplements by liquid chromatography coupled to Orbitrap high resolution mass spectrometry, Food Chem. 197 (2016) 907–915. doi:10.1016/j.foodchem.2015.11.070.

[177] F. Ma, R. Chen, P. Li, Q. Zhang, W. Zhang, X. Hu, Preparation of an immunoaffinity column with amino-silica gel microparticles and its application in sample cleanup for aflatoxin detection in agri-products, Molecules. 18 (2013) 2222–2235. doi:10.3390/molecules18022222.

[178] S. Sun, K. Yao, S. Zhao, P. Zheng, S. Wang, Y. Zeng, D. Liang, Y. Ke, H. Jiang, Determination of aflatoxin and zearalenone analogs in edible and medicinal herbs using a group-specific immunoaffinity column coupled to ultra-high-performance liquid chromatography with tandem mass spectrometry, J. Chromatogr. B. 1092 (2018) 228–236. doi:10.1016/j.jchromb.2018.06.012.

[179] B. Bi, J. Bao, G. Xi, Y. Xu, L. Zhang, Determination of multiple mycotoxin residues in Panax ginseng using simultaneous UPLC-ESI-MS/MS, J. Food Saf. 38 (2018) 1–7. doi:10.1111/jfs.12458.

[180] A. Saha, N.A. Gajbhiye, B.B. Basak, P. Manivel, High-performance liquid chromatography tandem mass spectrometry for simultaneous detection of aflatoxins B_1, B_2, G_1 and G_2 in Indian medicinal herbs using QuEChERS-based

extraction procedure, Int. J. Environ. Anal. Chem. 98 (2018) 622–643. doi:10.1080/03067319.2018.1485902.

[181] M. Ventura, A. Gómez, I. Anaya, J. Díaz, F. Broto, M. Agut, L. Comellas, Determination of aflatoxins B_1, G_1, B_2 and G_2 in medicinal herbs by liquid chromatography–tandem mass spectrometry, J. Chromatogr. A. 1048 (2004) 25–29. doi:10.1016/j.chroma.2004.07.033.

[182] Real Decreto 475/1988 de 13 de mayo por el que se establecen los límites máximos permitidos de las aflatoxinas B1, B2, G1 y G2, en alimentos para consumo humano, Boletín Oficial del Estado. 121 (1988) 15329.

[183] World Health Organization International Agency for Research on Cancer (WHO IARC), Monographs on the evaluation of carcinogenic risks to humans. Volume 82: Some traditional herbal medicines, some mycotoxins, naphtalene and styrene, (2002) 1–557. http://monographs.iarc.fr/ENG/Monographs/vol83/mono83-1.pdf.

[184] M. Busman, J.R. Bobell, C.M. Maragos, Determination of the aflatoxin M_1 (AFM_1) from milk by direct analysis in real time - mass spectrometry (DART-MS), Food Control. 47 (2015) 592–598. doi:10.1016/j.foodcont.2014.08.003.

[185] L. Campone, A.L. Piccinelli, R. Celano, I. Pagano, M. Russo, L. Rastrelli, Rapid and automated analysis of aflatoxin M_1 in milk and dairy products by online solid phase extraction coupled to ultra-high-pressure-liquid-chromatography tandem mass spectrometry, J. Chromatogr. A. 1428 (2016) 212–219. doi:10.1016/j.chroma.2015.10.094.

[186] A. Prandini, G. Tansini, S. Sigolo, L. Filippi, M. Laporta, G. Piva, On the occurrence of aflatoxin M_1 in milk and dairy products, Food Chem. Toxicol. 47 (2009) 984–991. doi:10.1016/j.fct.2007.10.005.

[187] L. Campone, A.L. Piccinelli, R. Celano, M. Russo, L. Rastrelli, Rapid analysis of aflatoxin M_1 in milk using dispersive liquid-liquid microextraction coupled with ultrahigh pressure liquid chromatography tandem mass spectrometry, Anal. Bioanal. Chem. 405 (2013) 8645–8652. doi:10.1007/s00216-013-7277-3.

[188] R. Romero-González, A. Garrido Frenich, J.L. Martínez Vidal, O.D. Prestes, S.L. Grio, Simultaneous determination of pesticides, biopesticides and mycotoxins in organic products applying a quick, easy, cheap, effective, rugged and safe extraction procedure and ultra-high performance liquid chromatography-tandem mass spectrometry, J. Chromatogr. A. 1218 (2011) 1477–1485. doi:10.1016/j.chroma.2011.01.034.

[189] M. Muscarella, S. Lo Magro, C. Palermo, D. Centonze, Validation according to European Commission Decision 2002/657/EC of a confirmatory method for aflatoxin M_1 in milk based on immunoaffinity columns and high performance liquid chromatography with fluorescence detection, Anal. Chim. Acta. 594 (2007) 257–264. doi:10.1016/j.aca.2007.05.029.

[190] J. Stroka, E. Ankalm, U. Jörissen, J. Gilbert, Immunoaffinity column cleanup with

liquid chromatography using post-column bromination for determination of aflatoxins in peanut butter, pistachio paste, fig paste, and paprika powder: collaborative study, J. AOAC Int. 83 (2000) 320–340.

[191] Y. Nonaka, K. Saito, N. Hanioka, S. Narimatsu, H. Kataoka, Determination of aflatoxins in food samples by automated on-line in-tube solid-phase microextraction coupled with liquid chromatography-mass spectrometry, J. Chromatogr. A. 1216 (2009) 4416–4422. doi:10.1016/j.chroma.2009.03.035.

[192] M. Quinto, G. Spadaccino, C. Palermo, D. Centonze, Determination of aflatoxins in cereal flours by solid-phase microextraction coupled with liquid chromatography and post-column photochemical derivatization-fluorescence detection, J. Chromatogr. A. 1216 (2009) 8636–8641. doi:10.1016/j.chroma.2009.10.031.

[193] M. Manoochehri, A.A. Asgharinezhad, M. Safaei, Determination of aflatoxin M_1 in milk powder by ultrasonic-assisted extraction and dispersive solid-phase clean-up, J. Chromatogr. Sci. 53 (2015) 1000–1006. doi:10.1093/chromsci/bmu131.

[194] A.C. Manetta, L. Di Giuseppe, M. Giammarco, I. Fusaro, A. Simonella, A. Gramenzi, A. Formigoni, High-performance liquid chromatography with post-column derivatisation and fluorescence detection for sensitive determination of aflatoxin M_1 in milk and cheese, J. Chromatogr. A. 1083 (2005) 219–222. doi:10.1016/j.chroma.2005.06.039.

[195] Y. Wang, X. Liu, C. Xiao, Z. Wang, J. Wang, H. Xiao, L. Cui, Q. Xiang, T. Yue, HPLC determination of aflatoxin M1 in liquid milk and milk powder using solid phase extraction on OASIS HLB, Food Control. 28 (2012) 131–134. doi:10.1016/j.foodcont.2012.04.037.

[196] C. Wu, J. He, Y. Li, N. Chen, Z. Huang, L. You, L. He, S. Zhang, Solid-phase extraction of aflatoxins using a nanosorbent consisting of a magnetized nanoporous carbon core coated with a molecularly imprinted polymer, Microchim. Acta. 185 (2018) 515. doi:10.1007/s00604-018-3051-8.

[197] S. Wei, Y. Liu, Z. Yan, L. Liu, Molecularly imprinted solid phase extraction coupled to high performance liquid chromatography for determination of aflatoxin M_1 and B_1 in foods and feeds, RSC Adv. 5 (2015) 20951–20960. doi:10.1039/c4ra16784h.

[198] W.K. Li, H.X. Zhang, Y.P. Shi, Simultaneous determination of aflatoxin B_1 and zearalenone by magnetic nanoparticle filled amino-modified multi-walled carbon nanotubes, Anal. Methods. 10 (2018) 3353–3363. doi:10.1039/c8ay00815a.

[199] Z. Durmus, B. Zengin Kurt, I. Gazioğlu, E. Sevgi, C. Kizilarslan Hancer, Spectrofluorimetric determination of aflatoxin B_1 in winter herbal teas via magnetic solid phase extraction method by using metal–organic framework (MOF) hybrid structures anchored with magnetic nanoparticles, Appl. Organomet. Chem. 34 (2020) 2–11. doi:10.1002/aoc.5375.

[200] S. Alilou, M. Amirzehni, P.A. Eslami, A simple fluorometric method for rapid

screening of aflatoxins after their extraction by magnetic MOF-808/graphene oxide composite and their discrimination by HPLC, Talanta. 235 (2021) 122709. doi:10.1016/j.talanta.2021.122709.

[201] K.G. Espenschied, E. Barrey, M. Ye, Quantifying picogram concentrations of aflatoxin M_1 in liquid milk using SPE cleanup and LC/MS analysis, Sigma-Aldrich Report. 331.1 - Food and Beverage Analysis (2014) 5–7.

[202] J.J. Karnes, E.A. Gobrogge, R.A. Walker, I. Benjamin, Unusual structure and dynamics at silica/methanol and silica/ethanol interfaces - A molecular dynamics and nonlinear optical study, J. Phys. Chem. B. 120 (2016) 1569–1578. doi:10.1021/acs.jpcb.5b07777.

[203] A.C. Olivieri, N.M. Faber, J. Ferré, R. Boqué, J.H. Kalivas, H. Mark, Uncertainty estimation and figures of merit for multivariate calibration (IUPAC Technical Report), Pure Appl. Chem. 78 (2006) 633–661. doi:10.1351/pac200678030633.

[204] D.C. Harris, Statistics, in: W. H. Freeman and Company (Ed.), Quantitative chemical analysis, Sixth Edition, New York and Basingstoke (USA), 2007: pp. 61–79.

[205] X. Wang, P. Li, Rapid screening of mycotoxins in liquid milk and milk powder by automated size-exclusion SPE-UPLC-MS/MS and quantification of matrix effects over the whole chromatographic run, Food Chem. 173 (2015) 897–904. doi:10.1016/j.foodchem.2014.10.056.

[206] W.D. Cornell, P. Cieplak, C.I. Bayly, I.R. Gould, K.M. Merz, D.M. Ferguson, D.C. Spellmeyer, T. Fox, J.W. Caldwell, P.A. Kollman, A second generation force field for the simulation of proteins, nucleic acids, and organic molecules, J. Am. Chem. Soc. 117 (1995) 5179–5197. doi:10.1021/ja00124a002.

[207] A.-R. Allouche, Software news and updates. Gabedit - Graphical user interface for computational chemistry softwares, J. Comput. Chem. 32 (2008) 174–182. doi:10.1002/jcc.21600.

[208] N. Pijarn, A. Jaroenworaluck, W. Sunsaneeyametha, R. Stevens, Synthesis and characterization of nanosized-silica gels formed under controlled conditions, Powder Technol. 203 (2010) 462–468. doi:10.1016/j.powtec.2010.06.007.

[209] J. El Haskouri, S. Cabrera, M. Gutierrez, A. Beltrán-Porter, D. Beltrán-Porter, M.D. Marcos, P. Amorós, Very high titanium content mesoporous silicas, Chem. Commun. (2001) 309–310. doi:10.1039/b008810m.

[210] A.M. Taiwo, A review of environmental and health effects of organochlorine pesticide residues in Africa, Chemosphere. 220 (2019) 1126–1140. doi:10.1016/j.chemosphere.2019.01.001.

[211] S. Mostafalou, M. Abdollahi, Pesticides: an update of human exposure and toxicity, Arch. Toxicol. 91 (2017) 549–599. doi:10.1007/s00204-016-1849-x.

[212] P. Montuori, E. De Rosa, P. Sarnacchiaro, F. Di Duca, D.P. Provvisiero, A.

Nardone, M. Triassi, Polychlorinated biphenyls and organochlorine pesticides in water and sediment from Volturno River, Southern Italy: occurrence, distribution and risk assessment, Environ. Sci. Eur. 32 (2020) 123. doi:10.1186/s12302-020-00408-4.

[213] M.V. Russo, P. Avino, G. Cinelli, I. Notardonato, Sampling of organophosphorus pesticides at trace levels in the atmosphere using XAD-2 adsorbent and analysis by gas chromatography coupled with nitrogen-phosphorus and ion-trap mass spectrometry detectors, Anal. Bioanal. Chem. 404 (2012) 1517–1527. doi:10.1007/s00216-012-6205-2.

[214] A. Serrano-Medina, A. Ugalde-Lizárraga, M.S. Bojorquez-Cuevas, J. Garnica-Ruiz, M.A. González-Corral, A. García-Ledezma, G. Pineda-García, J.M. Cornejo-Bravo, Neuropsychiatric disorders in farmers associated with organophosphorus pesticide exposure in a rural village of northwest méxico, Int. J. Environ. Res. Public Health. 16 (2019) 689. doi:10.3390/ijerph16050689.

[215] Regulation (EC) No 1107/2009 of the European Parliament and of the Council of 21 October 2009 concerning the placing of plant protection products on the market and repealing Council Directives 79/117/EEC and 91/414/EEC, Off. J. Eur. Union. L 309 (2009) 1–50.

[216] C. Coscollà, V. Yusà, M.I. Beser, A. Pastor, Multi-residue analysis of 30 currently used pesticides in fine airborne particulate matter (PM 2.5) by microwave-assisted extraction and liquid chromatography-tandem mass spectrometry, J. Chromatogr. A. 1216 (2009) 8817–8827. doi:10.1016/j.chroma.2009.10.040.

[217] C. Garcerá, E. Moltó, P. Chueca, Spray pesticide applications in Mediterranean citrus orchards: canopy deposition and off-target losses, Sci. Total Environ. 599–600 (2017) 1344–1362. doi:10.1016/j.scitotenv.2017.05.029.

[218] Instituto Nacional de Seguridad e Higiene en el Trabajo (INSHT), Guia técnica para la evaluación y prevención de los riesgos relacionados con los agentes químicos presentes en los lugares de trabajo, (2013) 1–168.

[219] Dow Agrosciences Iberica S.A., Ficha de datos de seguridad de acuerdo con el Reglamento (UE) no 2015/830. Reldan™ E Insecticide, (2015) 1–19.

[220] A. Mojiri, J.L. Zhou, B. Robinson, A. Ohashi, N. Ozaki, T. Kindaichi, H. Farraji, M. Vakili, Pesticides in aquatic environments and their removal by adsorption methods, Chemosphere. 253 (2020) 126646. doi:10.1016/j.chemosphere.2020.126646.

[221] United States Environmental Protection Agency (US EPA), Method 8081B (SW-846): Organochlorine pesticides by gas chromatography. Revison 2, Washington, DC, (2007) 1–57.

[222] M. Lyytikäinen, J.V.K. Kukkonen, M.J. Lydy, Analysis of pesticides in water and sediment under different storage conditions using gas chromatography, Arch. Environ. Contam. Toxicol. 44 (2003) 437–444. doi:10.1007/s00244-002-2168-1.

[223] A. Gutiérrez-Serpa, P. Rocío-Bautista, V. Pino, F. Jiménez-Moreno, A.I. Jiménez-Abizanda, Gold nanoparticles based solid-phase microextraction coatings for determining organochlorine pesticides in aqueous environmental samples, J. Sep. Sci. 40 (2017) 2009–2021. doi:10.1002/jssc.201700046.

[224] J.P. Pérez-Trujillo, S. Frías, M.J. Sánchez, J.E. Conde, M.A. Rodríguez-Delgado, Determination of organochlorine pesticides by gas chromatography with solid-phase microextraction, Chromatographia. 56 (2002) 191–197.

[225] J. Kawahara, R. Horikoshi, T. Yamaguchi, K. Kumagai, Y. Yanagisawa, Air pollution and young children's inhalation exposure to organophosphorus pesticide in an agricultural community in Japan, Environ. Int. 31 (2005) 1123–1132. doi:10.1016/j.envint.2005.04.001.

[226] E.R. Kennedy, M.T. Abell, J. Reynolds, D. Wickman, A sampling and analytical method for the simultaneous determination of multiple organophosphorus pesticides in air, Am. Ind. Hyg. Assoc. J. 55 (1994) 1172–1177. doi:10.1080/15428119491018259.

[227] A. Abdi Hassan, M. Sajid, H. Al Ghafly, K. Alhooshani, Ionic liquid-based membrane-protected micro-solid-phase extraction of organochlorine pesticides in environmental water samples, Microchem. J. 158 (2020) 105295. doi:10.1016/j.microc.2020.105295.

[228] Z. Huang, H.K. Lee, Micro-solid-phase extraction of organochlorine pesticides using porous metal-organic framework MIL-101 as sorbent, J. Chromatogr. A. 1401 (2015) 9–16. doi:10.1016/j.chroma.2015.04.052.

[229] M.M. Nascimento, G.O. da Rocha, J.B. de Andrade, Customized dispersive micro-solid-phase extraction device combined with micro-desorption for the simultaneous determination of 39 multiclass pesticides in environmental water samples, J. Chromatogr. A. 1639 (2021) 461781. doi:10.1016/j.chroma.2020.461781.

[230] V. Yusà, C. Coscollà, M. Millet, New screening approach for risk assessment of pesticides in ambient air, Atmos. Environ. 96 (2014) 322–330. doi:10.1016/j.atmosenv.2014.07.047.

[231] C. Coscollà, A. Yahyaoui, P. Colin, C. Robin, L. Martinon, S. Val, A. Baeza-Squiban, A. Mellouki, V. Yusà, Particle size distributions of currently used pesticides in a rural atmosphere of France, Atmos. Environ. 81 (2013) 32–38. doi:10.1016/j.atmosenv.2013.08.057.

[232] D. Barceló, Environmental Protection Agency and other methods for the determination of priority pesticides and their transformation products in water, J. Chromatogr. A. 643 (1993) 117–143. doi:10.1016/0021-9673(93)80546-K.

[233] L. Pelit, T.N. Dizdaş, Preparation and application of a polythiophene solid-phase microextraction fiber for the determination of endocrine-disruptor pesticides in well waters, J. Sep. Sci. 36 (2013) 3234–3241. doi:10.1002/jssc.201300633.

[234] X. Jiang, M. Wu, W. Wu, J. Cheng, H. Zhou, M. Cheng, A novel dispersive micro-solid phase extraction method combined with gas chromatography for analysis of organochlorine pesticides in aqueous samples, Anal. Methods. 6 (2014) 9712–9717. doi:10.1039/c4ay02302a.

[235] M.R. Hadjmohammadi, M. Peyrovi, P. Biparva, Comparison of C18 silica and multi-walled carbon nanotubes as the adsorbents for the solid-phase extraction of chlorpyrifos and phosalone in water samples using HPLC, J. Sep. Sci. 33 (2010) 1044–1051. doi:10.1002/jssc.200900494.

[236] M.E. Báez, M. Rodríguez, O. Lastra, P. Contreras, Solid phase extraction of organophosphorus, triazine, and triazole-derived pesticides from water samples. A critical study, J. High Resolut. Chromatogr. 20 (1997) 591–596. doi:10.1002/jhrc.1240201105.

[237] Z. Cheng, F. Dong, J. Xu, X. Liu, X. Wu, Z. Chen, X. Pan, Y. Zheng, Atmospheric pressure gas chromatography quadrupole-time-of-flight mass spectrometry for simultaneous determination of fifteen organochlorine pesticides in soil and water, J. Chromatogr. A. 1435 (2016) 115–124. doi:10.1016/j.chroma.2016.01.025.

[238] X. Gao, M. Pan, G. Fang, W. Jing, S. He, S. Wang, An ionic liquid modified dummy molecularly imprinted polymer as a solid-phase extraction material for the simultaneous determination of nine organochlorine pesticides in environmental and food samples, Anal. Methods. 5 (2013) 6128–6134. doi:10.1039/c3ay41083h.

[239] C.R.M. Vigna, L.S.R. Morais, C.H. Collins, I.C.S.F. Jardim, Poly(methyloctylsiloxane) immobilized on silica as a sorbent for solid-phase extraction of some pesticides, J. Chromatogr. A. 1114 (2006) 211–215. doi:10.1016/j.chroma.2006.03.034.

[240] W.A. Wan Ibrahim, K.V. Veloo, M.M. Sanagi, Novel sol-gel hybrid methyltrimethoxysilane-tetraethoxysilane as solid phase extraction sorbent for organophosphorus pesticides, J. Chromatogr. A. 1229 (2012) 55–62. doi:10.1016/j.chroma.2012.01.022.

[241] Z. Soutoudehnia Korrani, W.A. Wan Ibrahim, H. Rashidi Nodeh, H.Y. Aboul-Enein, M.M. Sanagi, Simultaneous preconcentration of polar and non-polar organophosphorus pesticides from water samples by using a new sorbent based on mesoporous silica, J. Sep. Sci. 39 (2016) 1144–1151. doi:10.1002/jssc.201500896.

[242] R. Mahmoud, S.A. Moaty, F. Mohamed, A. Farghali, Comparative study of single and multiple pollutants system using Ti-Fe chitosan LDH adsorbent with high performance in wastewater treatment, J. Chem. Eng. Data. 62 (2017) 3703–3722. doi:10.1021/acs.jced.7b00453.

[243] J. Lu, D. Liu, J. Hao, G. Zhang, B. Lu, Phosphate removal from aqueous solutions by a nano-structured Fe-Ti bimetal oxide sorbent, Chem. Eng. Res. Des. 93 (2015) 652–661. doi:10.1016/j.cherd.2014.05.001.

[244] N. Shams, H.N. Lim, R. Hajian, N.A. Yusof, J. Abdullah, Y. Sulaiman, I. Ibrahim,

N.M. Huang, A. Pandikumar, A promising electrochemical sensor based on Au nanoparticles decorated reduced graphene oxide for selective detection of herbicide diuron in natural waters, J. Appl. Electrochem. 46 (2016) 655–666. doi:10.1007/s10800-016-0950-4.

[245] X. Liu, W.J. Li, L. Li, Y. Yang, L.G. Mao, Z. Peng, A label-free electrochemical immunosensor based on gold nanoparticles for direct detection of atrazine, Sensors Actuators B Chem. 191 (2014) 408–414. doi:10.1016/j.snb.2013.10.033.

[246] Agencia Española de Normalización y Certificación (AENOR), Norma UNE-EN 1079:2009 - Exposición en le lugar de trabajo. Procedimiento de medida de gases y vapores que utilizan muestreadores por aspiración. Requisitos y métodos de ensayo, (2010) 1–43.

[247] F.A. Esteve-Turrillas, A. Pastor, M. de la Guardia, Evaluation of working air quality by using semipermeable membrane devices. Analysis of organophosphorus pesticides, Anal. Chim. Acta. 626 (2008) 21–27. doi:10.1016/j.aca.2008.07.039.

[248] N.I. Rousis, R. Bade, L. Bijlsma, E. Zuccato, J. V. Sancho, F. Hernandez, S. Castiglioni, Monitoring a large number of pesticides and transformation products in water samples from Spain and Italy, Environ. Res. 156 (2017) 31–38. doi:10.1016/j.envres.2017.03.013.

[249] Q. Han, Z. Wang, J. Xia, L. Xia, S. Chen, X. Zhang, M. Ding, Graphene as an efficient sorbent for the SPE of organochlorine pesticides in water samples coupled with GC-MS, J. Sep. Sci. 36 (2013) 3586–3591. doi:10.1002/jssc.201300373.

[250] G. Fang, W. Chen, Y. Yao, J. Wang, J. Qin, S. Wang, Multi-residue determination of organophosphorus and organochlorine pesticides in environmental samples using solid-phase extraction with cigarette filter followed by gas chromatography-mass spectrometry, J. Sep. Sci. 35 (2012) 534–540. doi:10.1002/jssc.201100870.

[251] S. Ozcan, A. Tor, M.E. Aydin, Application of magnetic nanoparticles to residue analysis of organochlorine pesticides in water samples by GC/MS, J. AOAC Int. 95 (2012) 1343–1349. doi:10.5740/jaoacint.SGE_Ozcan.

[252] H. Lange, B.H. Juárez, A. Carl, M. Richter, N.G. Bastús, H. Weller, C. Thomsen, R. Von Klitzing, A. Knorr, Tunable plasmon coupling in distance-controlled gold nanoparticles, Langmuir. 28 (2012) 8862–8866. doi:10.1021/la3001575.

[253] D.E. Mustafa, T. Yang, Z. Xuan, S. Chen, H. Tu, A. Zhang, Surface plasmon coupling effect of gold nanoparticles with different shape and size on conventional surface plasmon resonance signal, Plasmonics. 5 (2010) 221–231. doi:10.1007/s11468-010-9141-z.

[254] I. van der Veen, J. de Boer, Phosphorus flame retardants: properties, production, environmental occurrence, toxicity and analysis., Chemosphere. 88 (2012) 1119–53. doi:10.1016/j.chemosphere.2012.03.067.

[255] I. Pantelaki, D. Voutsa, Organophosphate flame retardants (OPFRs): a review on

analytical methods and occurrence in wastewater and aquatic environment, Sci. Total Environ. 649 (2019) 247–263. doi:10.1016/j.scitotenv.2018.08.286.

[256] A. Marklund, B. Andersson, P. Haglund, Organophosphorus flame retardants and plasticizers in Swedish sewage treatment plants, Environ. Sci. Technol. 39 (2005) 7423–7429. doi:10.1021/es051013l.

[257] H. Wolschke, R. Sühring, R. Massei, J. Tang, R. Ebinghaus, Regional variations of organophosphorus flame retardants - Fingerprint of large river basin estuaries/deltas in Europe compared with China, Environ. Pollut. 236 (2018) 391–395. doi:10.1016/j.envpol.2018.01.061.

[258] T. Reemtsma, M. García-López, I. Rodríguez, J.B. Quintana, R. Rodil, Organophosphorus flame retardants and plasticizers in water and air I. Occurrence and fate, TrAC - Trends Anal. Chem. 27 (2008) 727–737. doi:10.1016/j.trac.2008.07.002.

[259] G.L. Wei, D.Q. Li, M.N. Zhuo, Y.S. Liao, Z.Y. Xie, T.L. Guo, J.J. Li, S.Y. Zhang, Z.Q. Liang, Organophosphorus flame retardants and plasticizers: sources, occurrence, toxicity and human exposure, Environ. Pollut. 196 (2015) 29–46. doi:10.1016/j.envpol.2014.09.012.

[260] C. Bach, V. Boiteux, J. Hemard, A. Colin, C. Rosin, J.F. Munoz, X. Dauchy, Simultaneous determination of perfluoroalkyl iodides, perfluoroalkane sulfonamides, fluorotelomer alcohols, fluorotelomer iodides and fluorotelomer acrylates and methacrylates in water and sediments using solid-phase microextraction-gas chromatography/mass spectrometry, J. Chromatogr. A. 1448 (2016) 98–106. doi:10.1016/j.chroma.2016.04.025.

[261] Z. Wang, I.T. Cousins, M. Scheringer, R.C. Buck, K. Hungerbühler, Global emission inventories for C_4-C_{14} perfluoroalkyl carboxylic acid (PFCA) homologues from 1951 to 2030, part I: production and emissions from quantifiable sources, Environ. Int. 70 (2014) 62–75. doi:10.1016/j.envint.2014.04.013.

[262] C. Gremmel, T. Frömel, T.P. Knepper, HPLC–MS/MS methods for the determination of 52 perfluoroalkyl and polyfluoroalkyl substances in aqueous samples, Anal. Bioanal. Chem. 409 (2017) 1643–1655. doi:10.1007/s00216-016-0110-z.

[263] S. Bull, K. Burnett, K. Vassaux, L. Ashdown, T. Brown, L. Rushton, Extensive literature search and provision of summaries of studies related to the oral toxicity of perfluoroalkylated substances (PFASs), their precursors and potential replacements in experimental animals and humans, EFSA Support. Publ. EN-572 11 (2014) 245. doi:10.2903/sp.efsa.2014.en-572.

[264] M. Lorenzo, J. Campo, M. Morales Suárez-Varela, Y. Picó, Occurrence, distribution and behavior of emerging persistent organic pollutants (POPs) in a Mediterranean wetland protected area, Sci. Total Environ. 646 (2019) 1009–1020. doi:10.1016/j.scitotenv.2018.07.304.

[265] United States Environmental Protection Agency (US EPA), Fact sheet: 2010/2015 PFOA Stewardship Program, (2006). https://www.epa.gov/assessing-and-managing-chemicals-under-tsca/fact-sheet-20102015-pfoa-stewardship-program (accessed January 14, 2022).

[266] Directive 2008/105/EC of the European Parliament and of the Council of 16 December 2008 on environmental quality standards in the field of water policy, amending and subsequently repealing Council Directives 82/176/EEC, 83/513/EEC, 84/156/EEC, 84/491/EEC, 86/280/EEC and amending Directive 2000/60/EC of the European Parliament and of the Council, Off. J. Eur. Union. L 348 (2008) 84–97.

[267] H. Joerss, C. Apel, R. Ebinghaus, Emerging per- and polyfluoroalkyl substances (PFASs) in surface water and sediment of the North and Baltic Seas, Sci. Total Environ. 686 (2019) 360–369. doi:10.1016/j.scitotenv.2019.05.363.

[268] European Chemicals Agency (ECHA), Candidate list of substances of very high concern for authorisation, (2022). https://echa.europa.eu/es/candidate-list-table (accessed January 14, 2022).

[269] Y. Pico, C. Blasco, M. Farré, D. Barceló, Occurrence of perfluorinated compounds in water and sediment of L'Albufera Natural Park (València, Spain), Environ. Sci. Pollut. Res. 19 (2012) 946–957. doi:10.1007/s11356-011-0560-y.

[270] E. Pignotti, G. Casas, M. Llorca, A. Tellbüscher, D. Almeida, E. Dinelli, M. Farré, D. Barceló, Seasonal variations in the occurrence of perfluoroalkyl substances in water, sediment and fish samples from Ebro Delta (Catalonia, Spain), Sci. Total Environ. 607–608 (2017) 933–943. doi:10.1016/j.scitotenv.2017.07.025.

[271] S.P. Lenka, M. Kah, L.P. Padhye, A review of the occurrence, transformation, and removal of poly- and perfluoroalkyl substances (PFAS) in wastewater treatment plants, Water Res. 199 (2021) 117187. doi:10.1016/j.watres.2021.117187.

[272] B. Xu, S. Liu, J.L. Zhou, C. Zheng, J. Weifeng, B. Chen, T. Zhang, W. Qiu, PFAS and their substitutes in groundwater: occurrence, transformation and remediation, J. Hazard. Mater. 412 (2021) 125159. doi:10.1016/j.jhazmat.2021.125159.

[273] J.C. Baluyot, E.M. Reyes, M.C. Velarde, Per- and polyfluoroalkyl substances (PFAS) as contaminants of emerging concern in Asia's freshwater resources, Environ. Res. 197 (2021) 111122. doi:10.1016/j.envres.2021.111122.

[274] U.J. Kim, K. Kannan, Occurrence and distribution of organophosphate flame retardants/plasticizers in surface waters, tap water, and rainwater: implications for human exposure, Environ. Sci. Technol. 52 (2018) 5625–5633. doi:10.1021/acs.est.8b00727.

[275] U.J. Kim, J.K. Oh, K. Kannan, Occurrence, removal, and environmental emission of organophosphate flame retardants/plasticizers in a wastewater treatment plant in New York State, Environ. Sci. Technol. 51 (2017) 7872–7880. doi:10.1021/acs.est.7b02035.

[276] S. Lai, Z. Xie, T. Song, J. Tang, Y. Zhang, W. Mi, J. Peng, Y. Zhao, S. Zou, R. Ebinghaus, Occurrence and dry deposition of organophosphate esters in atmospheric particles over the northern South China Sea, Chemosphere. 127 (2015) 195. doi:10.1016/j.chemosphere.2015.02.015.

[277] H. Joerss, Z. Xie, C.C. Wagner, W.J. Von Appen, E.M. Sunderland, R. Ebinghaus, Transport of legacy perfluoroalkyl substances and the replacement compound HFPO-DA through the Atlantic gateway to the Arctic ocean - Is the Arctic a sink or a source?, Environ. Sci. Technol. 54 (2020) 9958–9967. doi:10.1021/acs.est.0c00228.

[278] Z. Wang, Z. Xie, W. Mi, A. Möller, H. Wolschke, R. Ebinghaus, Neutral poly/perfluoroalkyl substances in air from the Atlantic to the Southern ocean and in Antarctic snow, Environ. Sci. Technol. 49 (2015) 7770–7775. doi:10.1021/acs.est.5b00920.

[279] T. Portolés, L.E. Rosales, J. V. Sancho, F.J. Santos, E. Moyano, Gas chromatography-tandem mass spectrometry with atmospheric pressure chemical ionization for fluorotelomer alcohols and perfluorinated sulfonamides determination, J. Chromatogr. A. 1413 (2015) 107–116. doi:10.1016/j.chroma.2015.08.016.

[280] M. Monteleone, A. Naccarato, G. Sindona, A. Tagarelli, A rapid and sensitive assay of perfluorocarboxylic acids in aqueous matrices by headspace solid phase microextraction-gas chromatography-triple quadrupole mass spectrometry, J. Chromatogr. A. 1251 (2012) 160–168. doi:10.1016/j.chroma.2012.06.033.

[281] U. Berger, M.A. Kaiser, A. Kärrman, J.L. Barber, S.P.J. van Leeuwen, Recent developments in trace analysis of poly- and perfluoroalkyl substances, Anal. Bioanal. Chem. 400 (2011) 1625–1635. doi:10.1007/s00216-011-4823-8.

[282] T. Jin, J. Cheng, C. Cai, M. Cheng, S. Wu, H. Zhou, Graphene oxide based sol-gel stainless steel fiber for the headspace solid-phase microextraction of organophosphate ester flame retardants in water samples, J. Chromatogr. A. 1457 (2016) 1–6. doi:10.1016/j.chroma.2016.06.038.

[283] J. Andresen, K. Bester, Elimination of organophosphate ester flame retardants and plasticizers in drinking water purification, Water Res. 40 (2006) 621–629. doi:10.1016/j.watres.2005.11.022.

[284] H. Wolschke, R. Sühring, Z. Xie, R. Ebinghaus, Organophosphorus flame retardants and plasticizers in the aquatic environment: a case study of the Elbe River, Germany, Environ. Pollut. 206 (2015) 488–493. doi:10.1016/j.envpol.2015.08.002.

[285] Y. Wang, H. Sun, H. Zhu, Y. Yao, H. Chen, C. Ren, F. Wu, K. Kannan, Occurrence and distribution of organophosphate flame retardants (OPFRs) in soil and outdoor settled dust from a multi-waste recycling area in China, Sci. Total Environ. 625 (2018) 1056–1064. doi:10.1016/j.scitotenv.2018.01.013.

[286] C. González-Barreiro, E. Martínez-Carballo, A. Sitka, S. Scharf, O. Gans, Method optimization for determination of selected perfluorinated alkylated substances in water samples, Anal. Bioanal. Chem. 386 (2006) 2123–2132. doi:10.1007/s00216-006-0902-7.

[287] S.P.J. van Leeuwen, J. de Boer, Extraction and clean-up strategies for the analysis of poly- and perfluoroalkyl substances in environmental and human matrices, J. Chromatogr. A. 1153 (2007) 172–185. doi:10.1016/j.chroma.2007.02.069.

[288] J.B. Quintana, R. Rodil, T. Reemtsma, M. García-López, I. Rodríguez, Organophosphorus flame retardants and plasticizers in water and air II. Analytical methodology, TrAC - Trends Anal. Chem. 27 (2008) 904–915. doi:10.1016/j.trac.2008.08.004.

[289] J. Pawliszyn, H.L. Lord, Handbook of sample preparation, John Wiley & Sons, Inc., Hoboken, NJ, USA, 2010. doi:10.1002/9780813823621.

[290] S. Taniyasu, K. Kannan, L.W.Y. Yeung, K.Y. Kwok, P.K.S. Lam, N. Yamashita, Analysis of trifluoroacetic acid and other short-chain perfluorinated acids (C_2-C_4) in precipitation by liquid chromatography-tandem mass spectrometry: comparison to patterns of long-chain perfluorinated acids (C_5-C_{18}), Anal. Chim. Acta. 619 (2008) 221–230. doi:10.1016/j.aca.2008.04.064.

[291] J. Janda, K. Nödler, H.J. Brauch, C. Zwiener, F.T. Lange, Robust trace analysis of polar (C_2-C_8) perfluorinated carboxylic acids by liquid chromatography-tandem mass spectrometry: method development and application to surface water, groundwater and drinking water, Environ. Sci. Pollut. Res. 26 (2019) 7326–7336. doi:10.1007/s11356-018-1731-x.

[292] G. Munoz, S. Vo Duy, H. Budzinski, P. Labadie, J. Liu, S. Sauvé, Quantitative analysis of poly- and perfluoroalkyl compounds in water matrices using high resolution mass spectrometry: optimization for a laser diode thermal desorption method, Anal. Chim. Acta. 881 (2015) 98–106. doi:10.1016/j.aca.2015.04.015.

[293] V. Boiteux, C. Bach, V. Sagres, J. Hemard, A. Colin, C. Rosin, J.F. Munoz, X. Dauchy, Analysis of 29 per- and polyfluorinated compounds in water, sediment, soil and sludge by liquid chromatography–tandem mass spectrometry, Int. J. Environ. Anal. Chem. 96 (2016) 705–728. doi:10.1080/03067319.2016.1196683.

[294] D. Zacs, V. Bartkevics, Trace determination of perfluorooctane sulfonate and perfluorooctanoic acid in environmental samples (surface water, wastewater, biota, sediments, and sewage sludge) using liquid chromatography – Orbitrap mass spectrometry, J. Chromatogr. A. 1473 (2016) 109–121. doi:10.1016/j.chroma.2016.10.060.

[295] J. Campo, F. Pérez, A. Masiá, Y. Picó, M. la Farré, D. Barceló, Perfluoroalkyl substance contamination of the Llobregat River ecosystem (Mediterranean area, NE Spain), Sci. Total Environ. 503–504 (2015) 48–57. doi:10.1016/j.scitotenv.2014.05.094.

[296] Y. Liu, J. Bao, X.M. Hu, G.L. Lu, W.J. Yu, Z.H. Meng, Optimization of extraction methods for the analysis of PFOA and PFOS in the salty matrices during the wastewater treatment, Microchem. J. 155 (2020) 104673. doi:10.1016/j.microc.2020.104673.

[297] S. Rayne, K. Forest, Perfluoroalkyl sulfonic and carboxylic acids: a critical review of physicochemical properties, levels and patterns in waters and wastewaters, and treatment methods, J. Environ. Sci. Heal. Part A. 44 (2009) 1145–1199. doi:10.1080/10934520903139811.

[298] R.L. Johnson, A.J. Anschutz, J.M. Smolen, M.F. Simcik, R.L. Penn, The adsorption of perfluorooctane sulfonate onto sand, clay, and iron oxide surfaces, J. Chem. Eng. Data. 52 (2007) 1165–1170.

[299] United States Environmental Protection Agency (US EPA), Method 525.2: Determination of organic compounds in drinking water by liquid-solid extraction and capillary column gas chromatography/mass spectrometry. Revision 2. Cincinnati, OH, (1995) 1–60.

[300] C. Yang, Y. Li, D. Zha, G. Lu, Q. Sun, D. Wu, A passive sampling method for assessing the occurrence and risk of organophosphate flame retardants in aquatic environments, Chemosphere. 167 (2017) 1–9. doi:10.1016/j.chemosphere.2016.09.141.

[301] X. Wang, J. Liu, Y. Yin, Development of an ultra-high-performance liquid chromatography-tandem mass spectrometry method for high throughput determination of organophosphorus flame retardants in environmental water, J. Chromatogr. A. 1218 (2011) 6705–6711. doi:10.1016/j.chroma.2011.07.067.

[302] L. Gao, Y. Shi, W. Li, W. Ren, J. Liu, Y. Cai, Determination of organophosphate esters in water samples by mixed-mode liquid chromatography and tandem mass spectrometry, J. Sep. Sci. 38 (2015) 2193–2200. doi:10.1002/jssc.201500213.

[303] U.E. Bollmann, A. Möller, Z. Xie, R. Ebinghaus, J.W. Einax, Occurrence and fate of organophosphorus flame retardants and plasticizers in coastal and marine surface waters, Water Res. 46 (2012) 531–538. doi:10.1016/j.watres.2011.11.028.

[304] Y. Shi, L. Gao, W. Li, Y. Wang, J. Liu, Y. Cai, Occurrence, distribution and seasonal variation of organophosphate flame retardants and plasticizers in urban surface water in Beijing, China, Environ. Pollut. 209 (2016) 1–10. doi:10.1016/j.envpol.2015.11.008.

[305] K. Liang, F. Shi, J. Liu, Occurrence and distribution of oligomeric organophosphorus flame retardants in different treatment stages of a sewage treatment plant, Environ. Pollut. 232 (2018) 229–235. doi:10.1016/j.envpol.2017.09.036.

[306] I. Rodríguez, F. Calvo, J.B. Quintana, E. Rubí, R. Rodil, R. Cela, Suitability of solid-phase microextraction for the determination of organophosphate flame retardants and plasticizers in water samples, J. Chromatogr. A. 1108 (2006) 158–

165. doi:10.1016/j.chroma.2006.01.008.

[307] L. Wang, X. Gong, R. Wang, Z. Gan, Y. Lu, H. Sun, Application of an immobilized ionic liquid for the passive sampling of perfluorinated substances in water, J. Chromatogr. A. 1515 (2017) 45–53. doi:10.1016/j.chroma.2017.08.001.

[308] Y. Igarashi, M. Takahashi, T. Tsutsumi, K. Inoue, H. Akiyama, Monitoring analysis of perfluoroalkyl substances and F-53B in bottled water, tea and juice samples by LC-MS/MS, Chem. Pharm. Bull. 69 (2021) 286–290. doi:10.1248/cpb.c20-00888.

[309] S. Soler-Seguí, C. Belenguer-Sapiña, P. Amorós, A. Mauri-Aucejo, Evaluation of a cylodextrin-silica hybrid microporous composite for the solid-phase extraction of polycyclic aromatic hydrocarbons, Anal. Sci. 32 (2016) 659–665. doi:10.2116/analsci.32.659.

[310] C. Belenguer-Sapiña, E. Pellicer-Castell, C. Vila, E.F. Simó-Alfonso, P. Amorós, A.R. Mauri-Aucejo, A poly(glycidyl-co-ethylene dimethacrylate) nanohybrid modified with β -cyclodextrin as a sorbent for solid-phase extraction of phenolic compounds, Microchim. Acta. 186 (2019) 1–11. doi:10.1007/s00604-019-3739-4.

[311] M. Guth, T. Pollock, M. Fisher, T.E. Arbuckle, M.F. Bouchard, Concentrations of urinary parabens and reproductive hormones in girls 6–17 years living in Canada, Int. J. Hyg. Environ. Health. 231 (2021) 113633. doi:10.1016/j.ijheh.2020.113633.

[312] M.Z. Bocato, C.A. Cesila, B.F. Lataro, A.R.M. de Oliveira, A.D. Campíglia, F. Barbosa, A fast-multiclass method for the determination of 21 endocrine disruptors in human urine by using vortex-assisted dispersive liquid-liquid microextraction (VADLLME) and LC-MS/MS, Environ. Res. 189 (2020) 109883. doi:10.1016/j.envres.2020.109883.

[313] T.P. van der Meer, M. van Faassen, A.P. van Beek, H. Snieder, I.P. Kema, B.H.R. Wolffenbuttel, J. V. van Vliet-Ostaptchouk, Exposure to endocrine disrupting chemicals in the dutch general population is associated with adiposity-related traits, Sci. Rep. 10 (2020) 1–10. doi:10.1038/s41598-020-66284-3.

[314] T.P. van der Meer, M. van Faassen, H. Frederiksen, A.P. van Beek, B.H.R. Wolffenbuttel, I.P. Kema, J. V. van Vliet-Ostaptchouk, Development and interlaboratory validation of two fast UPLC-MS-MS methods determining urinary bisphenols, parabens and phthalates, J. Anal. Toxicol. 43 (2019) 452–464. doi:10.1093/jat/bkz027.

[315] J.R. Rochester, Bisphenol A and human health: a review of the literature, Reprod. Toxicol. 42 (2013) 132–155. doi:10.1016/j.reprotox.2013.08.008.

[316] P.D. Darbre, P.W. Harvey, Paraben esters: review of recent studies of endocrine toxicity, absorption, esterase and human exposure, and discussion of potential human health risks, J. Appl. Toxicol. 28 (2008) 561–578. doi:10.1002/jat.1358.

[317] K. Nowak, W. Ratajczak-Wrona, M. Górska, E. Jabłońska, Parabens and their effects on the endocrine system, Mol. Cell. Endocrinol. 474 (2018) 238–251. doi:10.1016/j.mce.2018.03.014.

[318] R. Huang, Z. Liu, H. Yin, Z. Dang, P. Wu, N. Zhu, Z. Lin, Bisphenol A concentrations in human urine, human intakes across six continents, and annual trends of average intakes in adult and child populations worldwide: a thorough literature review, Sci. Total Environ. 626 (2018) 971–981. doi:10.1016/j.scitotenv.2018.01.144.

[319] L. Wang, Y. Wu, W. Zhang, K. Kannan, Characteristic profiles of urinary p-hydroxybenzoic acid and its esters (parabens) in children and adults from the United States and China, Environ. Sci. Technol. 47 (2013) 2069–2076. doi:10.1021/es304659r.

[320] W.L. Ma, L. Wang, Y. Guo, L.Y. Liu, H. Qi, N.Z. Zhu, C.J. Gao, Y.F. Li, K. Kannan, Urinary concentrations of parabens in Chinese young adults: implications for human exposure, Arch. Environ. Contam. Toxicol. 65 (2013) 611–618. doi:10.1007/s00244-013-9924-2.

[321] Y. Wang, G. Li, Q. Zhu, C. Liao, A multi-residue method for determination of 36 endocrine disrupting chemicals in human serum with a simple extraction procedure in combination of UPLC-MS/MS analysis, Talanta. 205 (2019) 120144. doi:10.1016/j.talanta.2019.120144.

[322] X. Ye, Z. Kuklenyik, A.M. Bishop, L.L. Needham, A.M. Calafat, Quantification of the urinary concentrations of parabens in humans by on-line solid phase extraction-high performance liquid chromatography-isotope dilution tandem mass spectrometry, J. Chromatogr. B. 844 (2006) 53–59. doi:10.1016/j.jchromb.2006.06.037.

[323] A. Tartaglia, A. Kabir, S. Ulusoy, E. Sperandio, S. Piccolantonio, H.I. Ulusoy, K.G. Furton, M. Locatelli, FPSE-HPLC-PDA analysis of seven paraben residues in human whole blood, plasma, and urine, J. Chromatogr. B. 1125 (2019) 121707. doi:10.1016/j.jchromb.2019.06.034.

[324] L. Mao, C. Sun, H. Zhang, Y. Li, D. Wu, Determination of environmental estrogens in human urine by high performance liquid chromatography after fluorescent derivatization with p-nitrobenzoyl chloride, Anal. Chim. Acta. 522 (2004) 241–246. doi:10.1016/j.aca.2004.04.071.

[325] N.Y. Polovkov, J.E. Starkova, R.S. Borisov, A simple, inexpensive, non-enzymatic microwave-assisted method for determining bisphenol-A in urine in the form of trimethylsilyl derivative by GC/MS with single quadrupole, J. Pharm. Biomed. Anal. 188 (2020) 113417. doi:10.1016/j.jpba.2020.113417.

[326] A. Azzouz, A.J. Rascón, E. Ballesteros, Simultaneous determination of parabens, alkylphenols, phenylphenols, bisphenol A and triclosan in human urine, blood and breast milk by continuous solid-phase extraction and gas chromatography-mass

spectrometry, J. Pharm. Biomed. Anal. 119 (2016) 16–26. doi:10.1016/j.jpba.2015.11.024.

[327] A.R.S. Couto, S. Aguiar, A. Ryzhakov, K.L. Larsen, T. Loftsson, Interaction of native cyclodextrins and their hydroxypropylated derivatives with parabens in aqueous solutions. Part 1: evaluation of inclusion complexes, J. Incl. Phenom. Macrocycl. Chem. 93 (2019) 309–321. doi:10.1007/s10847-018-00876-5.

[328] Y. Li, P. Lu, J. Cheng, Q. Wang, C. He, Simultaneous solid-phase extraction and determination of three bisphenols in water samples and orange juice by a porous β-cyclodextrin polymer, Food Anal. Methods. 11 (2018) 1476–1484. doi:10.1007/s12161-017-1131-8.

[329] Y. Xu, L. Wei, X. Chen, J. Zhao, Y. Wang, Application of the liquid–liquid dispersed microextraction based on phase transition behavior of temperature sensitive polymer to rapidly detect 5 BPs in food packaging, Food Chem. 347 (2021) 128960. doi:10.1016/j.foodchem.2020.128960.

[330] J. Bae, Y. Hwang, S.H. Park, S.J. Park, J. Lee, H.J. Kim, A. Jang, S. Park, O.S. Kwon, An elaborate sensor system based on conducting polymer-oligosaccharides in hydrogel and the formation of inclusion complexes, J. Ind. Eng. Chem. 90 (2020) 266–273. doi:10.1016/j.jiec.2020.07.023.

[331] I.M. Trofymchuk, N. Roik, L. Belyakova, Sol-gel synthesis of ordered β-cyclodextrin-containing silicas, Nanoscale Res. Lett. 11 (2016). doi:10.1186/s11671-016-1380-2.

[332] Z. Nan, X. Xue, W. Hou, X. Yan, S. Han, Fabrication of MCM-41 mesoporous silica through the self-assembly supermolecule of β-CD and CTAB, J. Solid State Chem. 180 (2007) 780–784. doi:10.1016/j.jssc.2006.11.011.

[333] S.M. Alahmadi, S. Mohamad, M.J. Maah, Organic-inorganic hybrid materials based on mesoporous silica MCM-41 with β-cyclodextrin and its applications, Asian J. Chem. 26 (2014) 4323–4329.

[334] S. Lu, S. Gong, S. Ma, X. Zeng, Z. Yu, G. Sheng, J. Fu, Determination of parabens in human urine by liquid chromatography coupled with electrospray ionization tandem mass spectrometry, Anal. Methods. 6 (2014) 5566–5572. doi:10.1039/c3ay42063a.

[335] M. Llobat-Estellés, A. Sevillano-Cabeza, P. Campíns-Falcó, Kinetic and chemometric studies of the determination of creatinine using the Jaffé reaction: Part I. Kinetics of the reaction: analytical conclusions, Analyst. 114 (1989) 597–602. doi:10.1039/AN9891400597.

[336] Z. Wang, P. Zhang, F. Hu, Y. Zhao, L. Zhu, A crosslinked β-cyclodextrin polymer used for rapid removal of a broad-spectrum of organic micropollutants from water, Carbohydr. Polym. 177 (2017) 224–231. doi:10.1016/j.carbpol.2017.08.059.

[337] Y. Liu, M. Liu, J. Jia, D. Wu, T. Gao, X. Wang, J. Yu, F. Li, β-cyclodextrin-

based hollow nanoparticles with excellent adsorption performance towards organic and inorganic pollutants, Nanoscale. 11 (2019) 18653–18661. doi:10.1039/c9nr07342f.

[338] M. Md Yusoff, N. Yahaya, N. Md Saleh, M. Raoov, A study on the removal of propyl, butyl, and benzyl parabens: via newly synthesised ionic liquid loaded magnetically confined polymeric mesoporous adsorbent, RSC Adv. 8 (2018) 25617–25635. doi:10.1039/c8ra03408g.

[339] G. Crini, M. Morcellet, Synthesis and applications of adsorbents containing cyclodextrins, J. Sep. Sci. 25 (2002) 789–813. doi:10.1002/1615-9314(20020901)25:13<789::AID-JSSC789>3.0.CO;2-J.

[340] Z.H. Chen, Z. Liu, J.Q. Hu, Q.W. Cai, X.Y. Li, W. Wang, Y. Faraj, X.J. Ju, R. Xie, L.Y. Chu, β-cyclodextrin-modified graphene oxide membranes with large adsorption capacity and high flux for efficient removal of bisphenol A from water, J. Memb. Sci. 595 (2020) 117510. doi:10.1016/j.memsci.2019.117510.

[341] G. Wang, J. Dai, Q. Luo, N. Deng, Photocatalytic degradation of bisphenol A by TiO_2@aspartic acid-β-cyclodextrin@reduced graphene oxide, Sep. Purif. Technol. 254 (2021) 117574. doi:10.1016/j.seppur.2020.117574.

[342] W. Huang, Y. Hu, Y. Li, Y. Zhou, D. Niu, Z. Lei, Z. Zhang, Citric acid-crosslinked β-cyclodextrin for simultaneous removal of bisphenol A, methylene blue and copper: the roles of cavity and surface functional groups, J. Taiwan Inst. Chem. Eng. 82 (2018) 189–197. doi:10.1016/j.jtice.2017.11.021.

[343] Y. Li, P. Lu, J. Cheng, X. Zhu, W. Guo, L. Liu, Q. Wang, C. He, S. Liu, Novel microporous β-cyclodextrin polymer as sorbent for solid-phase extraction of bisphenols in water samples and orange juice, Talanta. 187 (2018) 207–215. doi:10.1016/j.talanta.2018.05.030.

[344] A. Alsbaiee, B.J. Smith, L. Xiao, Y. Ling, D.E. Helbling, W.R. Dichtel, Rapid removal of organic micropollutants from water by a porous β-cyclodextrin polymer, Nature. 529 (2016) 190–194. doi:10.1038/nature16185.

ANNEX I

List of figures

Introducció

Chapter 1

Chapter 2

Chapter 3

Chapter 4

Chapter 5

Chapter 6

Chapter 7

Chapter 8

ANNEX II

List of tables

Introducció

Chapter 2

Chapter 3

Chapter 4

Chapter 5

Chapter 6

Chapter 7

Chapter 8

ANNEX III

Publications derived from the PhD Thesis

Study of silica-structured materials as sorbents for organophosphorus pesticides determination in environmental water samples

Enric Pellicer-Castell, Carolina Belenguer-Sapiña, Pedro Amorós, Jamal El Haskouri, José Manuel Herrero-Martínez, Adela Mauri-Aucejo

Talanta 189 (2018) 560–567 (IF: 4.916, Q1)

https://doi.org/10.1016/j.talanta.2018.07.044

Abstract

A novel sorbent based on a UVM-7 mesoporous silica doped with Ti has been synthesized and used for solid-phase extraction of several organophosphorus pesticides in environmental water samples followed by gas chromatography coupled to a nitrogen-phosphorus selective detector. Thus, mesoporous silica materials doped with Ti and Fe as well as immobilized cyclodextrin silica-based supports were prepared and morphologically characterized by several techniques such as transmission electronic microscopy, nitrogen adsorption-desorption and X-ray diffraction. These sorbents were comparatively evaluated, and Ti25-UVM-7 material was selected as the best solid phase. After optimization of extraction parameters such as amount of solid-phase, type and volume of eluent, pH and ionic strength and breakthrough volume, recoveries between 81% and 104.5% were achieved, with RSD values below 7.8% and 12% for intra-day and inter-day repeatability respectively. Moreover, limits of quantification in the range 0.5–4.4 μg L^{-1} were achieved for all target compounds using mass spectrometry detector. In addition, the developed method was applied for analysis of real water samples and it was validated with commercial C18 cartridges. Matrix effect was demonstrated in complex environmental matrices and the good reusability of synthesized material was also proved.

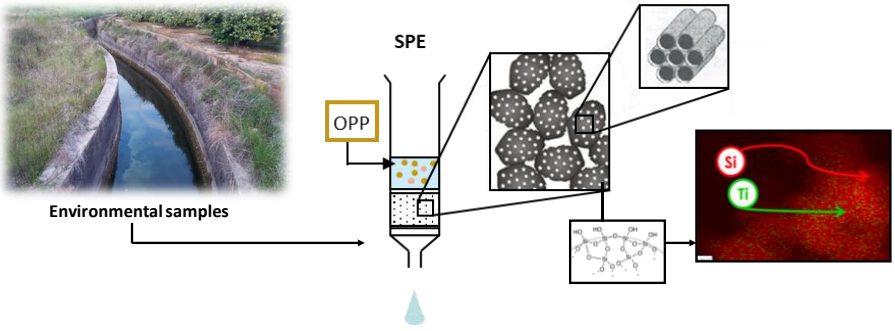

Extraction of aflatoxins by using mesoporous silica (type UVM-7), and their quantitation by HPLC-MS

Enric Pellicer-Castell, Carolina Belenguer-Sapiña, Jamal El Haskouri, José Manuel Herrero-Martínez, Vicent J. Borràs, Pedro Amorós, Adela R. Mauri-Aucejo

Microchimica Acta 186 (2019) 792 (IF: 6.232, Q1)

https://doi.org/10.1007/s00604-019-3958-8

Abstract

A solid-phase extraction procedure has been developed by using a sorbent derived from UVM-7 mesoporous silica. The sorbent was applied to the extraction of aflatoxins B_1, B_2, G_1 and G_2 from tea samples followed by HPLC with mass spectrometric detection. The sorbent was characterized by transmission electron microscopy, nuclear magnetic resonance, X-ray diffraction and nitrogen adsorption-desorption. UVM-7 is found to be the best solid phase. The amount of solid-phase, type and volume of eluent, pH value and ionic strength and breakthrough volume were optimized. Following the recommended procedure, recoveries between 96.0 and 98.2% were achieved, with RSD values of <5.1%, and the limits of detection are in the range from 0.14 to 0.7 μg kg^{-1}. The material is reusable. The method was applied to the analysis of real tea samples. A low matrix effect is found, and recoveries are >88%. The results were compared with those obtained by immunoaffinity columns as a reference method. Only low concentrations of aflatoxin G_2 were found in some samples, and results obtained with both methods are shown to be statistically sound and comparable.

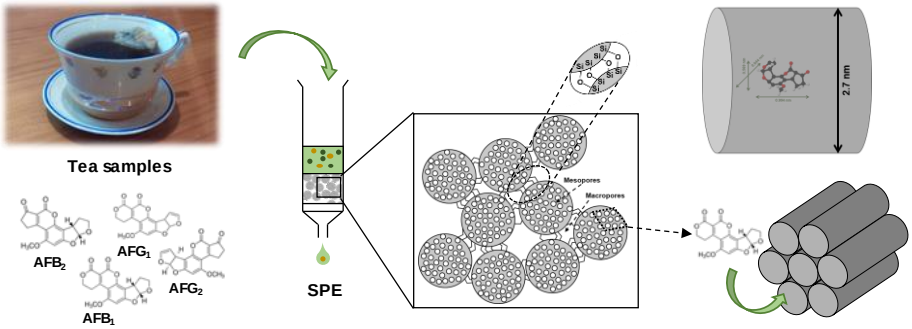

Comparison of silica-based materials for organophosphorus pesticides sampling and occupational risk assessment

Enric Pellicer-Castell, Carolina Belenguer-Sapiña, Pedro Amorós, Jamal El Haskouri, José Manuel Herrero-Martínez, Adela R. Mauri-Aucejo

Analytica Chimica Acta 1110 (2020) 26-34 (IF: 6.558, Q1)

https://doi.org/10.1016/j.aca.2020.03.008

Abstract

A novel air sampler has been designed containing a sorbent based on UVM-7 mesoporous silica doped with Ti. The sorbent has been applied for the determination of organophosphorus pesticides in occu- pational air, followed by gas chromatography with mass spectrometry detection. Thus, several silica materials with different structures (mesoporous UVM-7 and microporous xerogels) were synthesized, and modified with the addition of Ti and Fe. The structure of these materials was proved by transmission electronic microscopy, energy-dispersive X-ray, X-ray diffraction, nitrogen adsorption-desorption and UV-Vis and Raman spectroscopy. The potential of these materials for the retention of pesticides was evaluated and Ti25-UVM-7 was selected as the best solid phase for analyte sorption. Then, several sampling parameters were optimized and analytical features such as breakthrough volume were determined. Using the designed samplers, quantitative retentions were achieved with recoveries in the range 93-107% for all analytes except for diazinon (82%). RSD values below 13% were obtained. Likewise, the sensitivity of the method was studied, and limits of quantification below 0.5 mg m^{-3} were obtained for all pesticides. The reusability of the material was also proved. The developed procedure has been applied to the air sampling and occupational risk assessment, during and after methyl-chlorpyrifos application in orange plantations. High concentrations and exposure rates above the limit value for ensure safe work conditions were obtained. At the same time, the air was sampled with XAD-2 samplers as a reference method, and results obtained with both devices were statistically comparable.

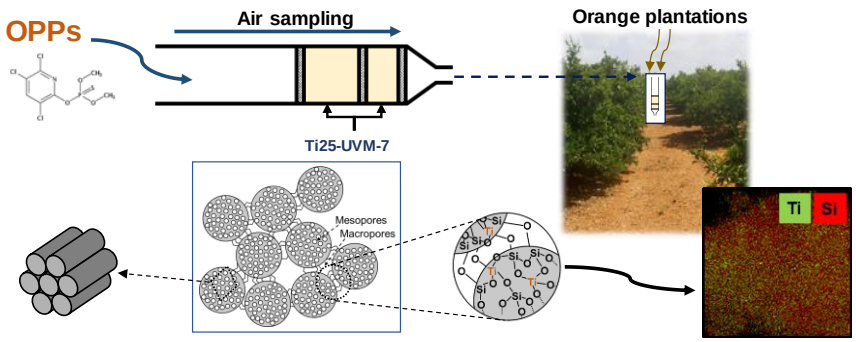

Bimodal porous silica nanomaterials as sorbents for an efficient and inexpensive determination of aflatoxin M_1 in milk and dairy products

Enric Pellicer-Castell, Carolina Belenguer-Sapiña, Pedro Amorós, José Manuel Herrero-Martínez, Adela R. Mauri-Aucejo

Food Chemistry 333 (2020) 127421 (IF: 7.514, Q1)

https://doi.org/10.1016/j.foodchem.2020.127421

Abstract

An extraction procedure was developed for the determination of aflatoxin M_1 in milk and dairy products. A sorbent based on UVM-7 mesoporous silica was used as solid phase for the sample clean-up, and the analyte determination was carried out by HPLC coupled to a fluorescence detector. The material architecture was characterized by transmission electronic microscopy, X-ray diffraction, ^{29}Si NMR and nitrogen adsorption-des- orption. After the optimization of extraction parameters, the influence of the matrix has been evaluated, ob- taining recoveries in the range 78–105% for whole and skimmed milk and yogurt matrix. The reusability of the material was also proved. The sensitivity of the method was also evaluated, and a LOQ (0.015 μg kg^{-1}) below the European legislation limit was obtained. The procedure was successfully applied for the determination of aflatoxin M_1 in real samples. The results were compared with those obtained with a reference method, being the results statistically comparable.

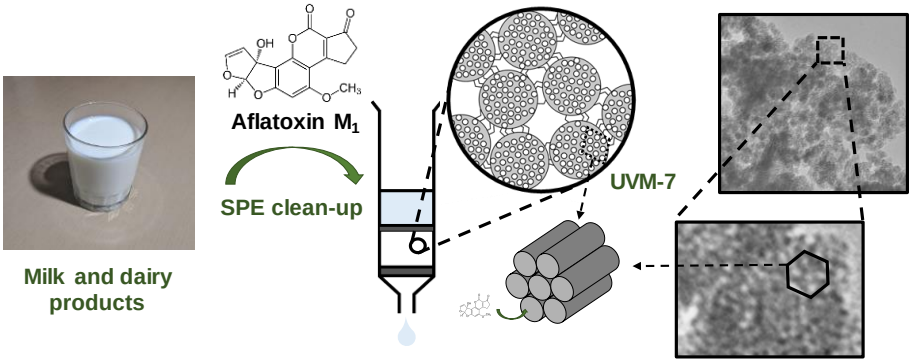

Enhancing extraction performance of organophosphorus flame retardants in water samples using titanium hierarchical porous silica materials as sorbents

Enric Pellicer-Castell, Carolina Belenguer-Sapiña, Pedro Amorós, Jamal El Haskouri, José Manuel Herrero-Martínez, Adela R. Mauri-Aucejo

Journal of Chromatography A 1639 (2021) 461938 (IF, 2020: 4.759, Q1)

https://doi.org/10.1016/j.chroma.2021.461938 0021-9673

Abstract

A sorbent for the extraction of organophosphorus flame retardants has been proposed, based on UVM-7 (University of Valencia Materials) mesoporous silica doped with titanium. Designed cartridges have been applied to the extraction and preconcentration of flame retardants in water samples, followed by gas chromatography coupled to a mass spectrometry detector. Firstly, UVM-7 materials with different con- tents of titanium were synthesized and characterized by several techniques, thus confirming the proper mesoporous architecture. The potential of these materials was assessed in comparison with their mor- phological properties, resulting Ti50-UVM-7 the best solid phase. Several extraction parameters were also optimized. Analytical parameters were also evaluated, and limits of detection from 0.019 to 0.21 ng mL^{-1} were obtained, as well as intra-day relative standard deviation below 11% for all analytes. Extraction efficiencies above 80% in water samples were achieved. The reusability of the material was also proved. Finally, the designed protocol was applied for the analysis of real water samples, and quantifiable concentrations of tris(2-chloroisopropyl) phosphate (TCIPP), tris(1,3-dichloro-2-propyl) phosphate (TDCIPP) and triphenyl phosphate (TPhP) were obtained in some samples. The method was compared with a United States Environmental Protection Agency general method with C18 cartridges.

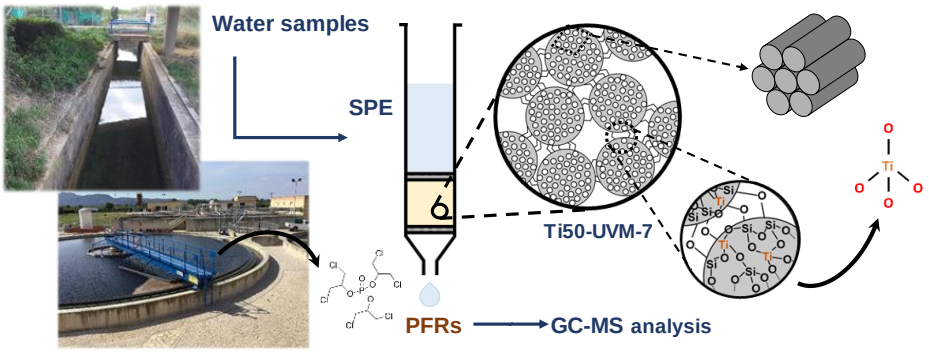

Mesoporous silica sorbent with gold nanoparticles for solid-phase extraction of organochlorine pesticides in water samples

Enric Pellicer-Castell, Carolina Belenguer-Sapiña, Pedro Amorós, Jamal El Haskouri, José Manuel Herrero-Martínez, Adela R. Mauri-Aucejo

Journal of Chromatography A 1662 (2022) 462729 (IF, 2020: 4.759, Q1)

https://doi.org/10.1016/j.chroma.2021.462729

Abstract

In this work, a novel sorbent, based on UVM-7 mesoporous silica doped with Au, has been proposed for organochlorine pesticides extraction. Cartridges containing this material have been applied to the preconcentration of 20 pesticides from water samples, through a solid-phase extraction (SPE) protocol, with their later determination by gas chromatography with an electron capture detector. First, UVM-7 materials were properly characterized by X-ray diffraction, N_2 adsorption-desorption, electron microscopy techniques, and UV-Vis spectroscopy, thus confirming their structure and Au incorporation. After optimization of main extraction parameters, recoveries in the range of 80–110% were obtained for most of the analytes, with enrichment factors comprised between 275 and 430. The obtained sensitivity was comparable with other reported methods, with limits of quantification in the range of 0.3-20 ng L^{-1} , thus allowing the determination of these compounds according to European legislation. The developed method has been successfully applied to the analysis of real spiked samples in comparison with a reference method, thus being this sorbent an alternative for organochlorine pesticide enrichment, through a simple, reusable, cheap, and environmentally friendly SPE procedure.

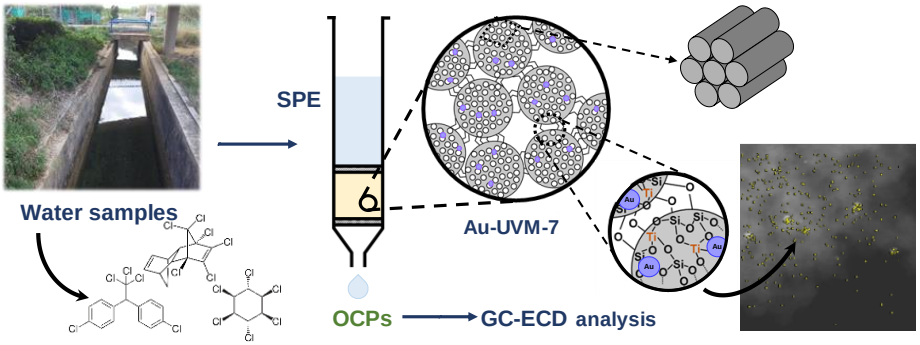

A β-cyclodextrin sorbent based on hierarchical mesoporous silica for the determination of endocrine-disrupting chemicals in urine samples

Enric Pellicer-Castell, Carolina Belenguer-Sapiña, Pedro Amorós, Jamal El Haskouri, José Manuel Herrero-Martínez, Adela R. Mauri-Aucejo

Journal of Chromatography A 1671 (2022) 463007 (IF, 2020: 4.759, Q1)

https://doi.org/10.1016/j.chroma.2022.463007

Abstract

In the present work, a method for the determination of parabens and bisphenol A in urine samples has been developed. For this purpose, a novel hierarchical mesoporous silica doped with β-cyclodextrin was developed and used as a sorbent for preconcentration and clean-up step, before analyte determination by liquid chromatography coupled to mass spectrometry detector. Disordered silica materials were also synthesized for comparison purposes. All materials were characterized by electron microscopy, X-ray diffraction, porosimetry, nuclear magnetic resonance, thermogravimetric analysis, elemental CNH analysis, and confocal microscopy, and the attachment of cyclodextrins has been proved as well as their uniform distribution in the resulting material. After the optimization of several protocol parameters, good analytical features were achieved, including recoveries in the range of 96-109% for all analytes, as well as relative standard deviations between 8 and 24%. Also, limits of quantification in the range of 0.003-0.19 μg L^{-1} were obtained in all cases. The developed method was applied to the determination of parabens and bisphenol A in real urine samples in comparison with a reference method using C18 cartridges, including the correction with creatinine content. Target analytes were detected in all analysed samples, with being BPA the most detected compound.

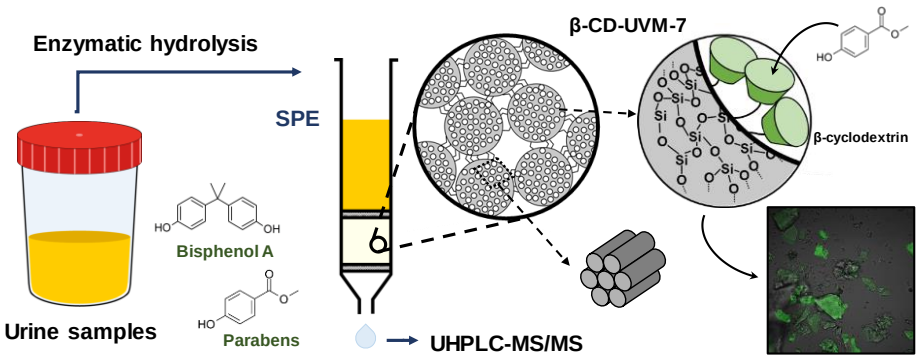

Iron-doped bimodal mesoporous silica materials as sorbents for solid-phase extraction of perfluoroalkyl substances in environmental water samples

Enric Pellicer-Castell, Carolina Belenguer-Sapiña, Jamal El Haskouri, Pedro Amorós, José Manuel Herrero-Martínez, Adela R. Mauri-Aucejo

Nanomaterials 12 (2022) 1441 (IF, 2020: 5.076, Q1)

https://doi.org/10.3390/nano12091441

Abstract

In this work, sorbents based on UVM-7 mesoporous silica doped with Fe have been synthesized and applied to solid-phase extraction of perfluoroalkyl substances from environmental water samples. These emerging pollutants were then determined by liquid chromatography coupled with a mass spectrometry detector. Thus, Fe-UVM-7 mesoporous silica materials with different contents of iron, as well as different pore sizes (by using alkyltrimethilamonium bromide surfactants with different organic tail lengths) were synthesized, and their structure was confirmed for the first time by transmission electron microscopy, nitrogen adsorption-desorption, and X-ray diffraction, and Raman spectroscopy. After comparison, Fe50-UVM-7-C_{12} was selected as the best material for analyte retention, and several extraction parameters were optimized regarding the loading and elution step. Once the method has been developed and applied to real matrices, extraction efficiencies in the range 61-110 % were obtained for analytes with C_8-C_{14} chain length, both perfluoroalkyl carboxylates, and perfluoroalkyl sulfonates. Likewise, limits of detection in the range 3.0-8.1 ng L^{-1} were obtained for all target analytes. In the analysis of real well-water samples, no target compounds were detected. Spiked samples were analyzed in comparison to Oasis WAX cartridges, and statistically comparable results were achieved.

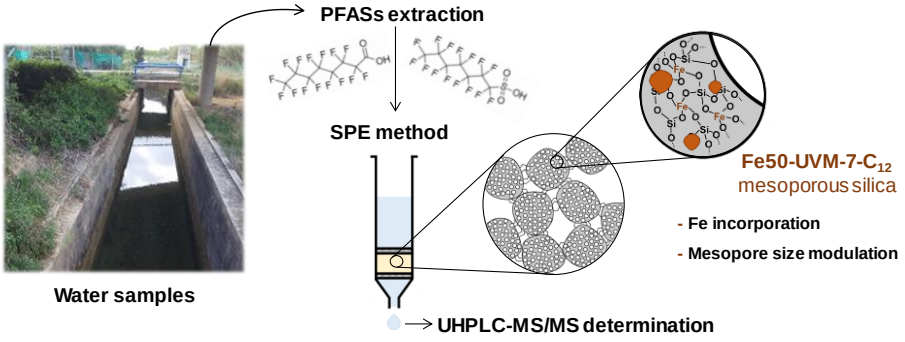

ANNEX IV

Other publications and contributions

During the realization of this thesis, the author has also participated in the following **publications** in scientific journals:

- C Belenguer-Sapiña, E Pellicer-Castell, J El Haskouri, C Guillem, EF Simó-Alfonso, P Amorós, A Mauri-Aucejo (2018). **Design, characterization and comparison of materials based on β and γ cyclodextrin covalently connected to microporous silica for environmental analysis**. *Journal of Chromatography A* 1563, 10-19.
- C Belenguer-Sapiña, E Pellicer-Castell, C Vila, EF Simó-Alfonso, P Amorós, AR Mauri-Aucejo (2019). **A poly (glycidyl-co-ethylene dimethacrylate) nanohybrid modified with β-cyclodextrin as a sorbent for solid-phase extraction of phenolic compounds**. *Microchimica Acta* 186 (9), 1-11.
- C Belenguer-Sapiña, E Pellicer-Castell, P Amorós, EF Simó-Alfonso, AR Mauri-Aucejo (2020). **A new proposal for the determination of polychlorinated biphenyls in environmental water by using host-guest adsorption**. *Science of The Total Environment* 724, 138266.
- C Belenguer-Sapiña, E Pellicer-Castell, AR Mauri-Aucejo, EF Simó-Alfonso, P Amorós (2021). **Cyclodextrins as a key piece in nanostructured materials: quantitation and remediation of pollutants**. *Nanomaterials* 11 (1), 7.
- C Belenguer-Sapiña, E Pellicer-Castell, SP Chali, BJ Ravoo, P Amorós, EF Simó-Alfonso, AR Mauri-Aucejo (2021). **Host-guest interactions for extracting antibiotics with a γ-cyclodextrin poly (glycidyl-co-ethylene dimethacrylate) hybrid sorbent**. *Talanta* 232, 122478.
- C Belenguer-Sapiña, R Sáez-Hernández, E Pellicer-Castell, S Armenta, AR Mauri-Aucejo (2022). **Simultaneous determination of third-generation synthetic cannabinoids in oral fluids using cyclodextrin-silica porous sorbents**. *Microchemical Journal* 172, 106915.
- C Belenguer-Sapiña, E Pellicer-Castell, J El Haskouri, EF Simó-Alfonso, P Amorós, AR Mauri-Aucejo (2022). **Assessment of migrating endocrine-disrupting chemicals in bottled acidic juice using type UVM-7 mesoporous silica modified with cyclodextrin**. *Food Chemistry* 380, 132207.
- C Belenguer-Sapiña, E Pellicer-Castell, J El Haskouri, EF Simó-Alfonso, P Amorós, AR Mauri-Aucejo (2022). **A type UVM-7 mesoporous silica with γ-cyclodextrin for the isolation of three veterinary antibiotics (ofloxacin, norfloxacin, and ciprofloxacin) from different fat-rate milk samples**. *Journal of Food Composition and Analysis 109, 104463.*

Furthermore, the research carried out by the autor, derived from this PhD Thesis as well as from other collaborations, has led to the following contributions in scientific congresses and meetings:

XVI Reunión Científica de la Sociedad de Cromatografía y Técnicas Afines SECyTA 2016, Sevilla, 02-04 of November 2016

- **Poster P-ENV-30**. Study of silica-structured materials for organophosphorus pesticide sampling and determination. C Belenguer-Sapiña, E Pellicer-Castell, A Mauri-Aucejo, P Amorós.

15th Instrumental Analysis Conference, Barcelona, 03-05 of October 2017

- **Poster P-78**. Study of the cyclodextrin-based materials advantages for pesticides analysis in water samples. A Mauri-Aucejo, P Amorós, C Belenguer-Sapiña, E Pellicer-Castell.
- **Poster P-79.** Use of cyclodextrin-silica composites in the sample treatment step for environmental analysis. C Belenguer-Sapiña, E Pellicer-Castell, P Amorós, J El Haskouri, E Simó-Alfonso, A Mauri-Aucejo.
- **Poster P-80**. Comparison of titanium-based materials for organophosphorus pesticides determination in environmental samples. E Pellicer-Castell, C Belenguer-Sapiña, P Amorós, J El Haskouri, JM Herrero-Martínez, A Mauri-Aucejo.

2nd Workshop Advances in Separation Techniques (CLECEM), Valencia, 23-24 of November 2017

- **Oral Communication OC-5.** Application of mesoporous silica materials in environmental analysis. E Pellicer-Castell, C Belenguer-Sapiña, P Amorós, J El Haskouri, JM Herrero-Martínez, A Mauri-Aucejo.
- **Oral Communication OC-6.** New uses of old-known molecules such as cyclodextrin in analytical chemistry. C Belenguer-Sapiña, E Pellicer-Castell, A Mauri-Aucejo, P Amorós, E Simó-Alfonso.

XVIII Reunión de la SECyTA, Granada, 02-04 of October 2018

- **Poster P-SP-01.** Determination of phenolic compounds in tea by using cyclodextrin-methacrylate hybrid monolithic materials. C Belenguer-Sapiña, E Pellicer-Castell, A Mauri-Aucejo, P Amorós, EF Simó-Alfonso, C Vila.
- **Poster P-SP-02.** Synthesis of ground polymeric sorbents with cyclodextrin nanoparticles for analytical applications. A Mauri-Aucejo, E Pellicer-Castell, C Belenguer-Sapiña, P Amorós, EF Simó-Alfonso, C Vila.
- **Poster P-SP-04.** Extraction and determination of aflatoxins in food samples by using a novel mesoporous silica-based sorbent. E Pellicer-Castell, C Belenguer-Sapiña, N Puertes-Espadas, A Mauri-Aucejo, P Amorós.

3rd Workshop Advances in Separation Techniques (CLECEM), Valencia, 22-23 of November 2018

- **Oral Communication OC-3.** Analysis of phenolic compounds in tea samples by using host-guest chemistry in hybrid methacrylate polymeric sorbents. C Belenguer-Sapiña, E Pellicer-Castell, EF Simó-Alfonso, A Mauri-Aucejo, P Amorós.
- **Oral Communication OC-5.** Recent advances in the application of mesoporous silica materials in food and environmental analysis. E Pellicer-Castell, C Belenguer-Sapiña, P Amorós, JM Herrero-Martínez, A Mauri-Aucejo.

1st Workshop Young Researchers in Chemistry (University of Valencia), Valencia, 06-07 of June 2019

- **Oral Communication OC-9.** Use of silica porous materials as solid phase for aflatoxin extraction and determination in tea samples. E Pellicer-Castell, C Belenguer-Sapiña, A Mauri-Aucejo, P Amorós, J El Haskouri, JM Herrero-Martínez.
- **Oral Communication OC-17.** Cyclodextrins as a versatile tool through their application in Analytical Chemistry. C Belenguer-Sapiña, E Pellicer-Castell, AR Mauri-Aucejo, P Amorós, EF Simó-Alfonso.
- **Poster P-20.** Preconcentration of polychlorinated biphenyls in water samples by using new types of materials containing cyclodextrin. C Belenguer-Sapiña, E Pellicer-Castell, AR Mauri-Aucejo, P Amorós, EF Simó-Alfonso.
- **Poster P-21.** Application of mesoporous silica materials in food and environmental analysis. E Pellicer-Castell, C Belenguer-Sapiña, A Mauri-Aucejo, P Amorós, JM Herrero-Martínez.

48th International Symposium of High-Performance Liquid Phase Separations and Related Techniques, Milan, 16-20 of June 2019

- **Poster P-242**. Cyclodextrins and their application in environmental analysis: variables affecting host-guest interaction with different types of analytes. C Belenguer-Sapiña, E Pellicer-Castell, EF Simó-Alfonso, P Amorós, A Mauri-Aucejo.
- **Poster P-244.** Determination of aflatoxins in medicinal herbs by using mesoporous silica-structured materials for its preconcentration. E Pellicer-Castell, C Belenguer-Sapiña, A Mauri-Aucejo, P Amorós, JM Herrero-Martínez.

Jornada de valorización de un nuevo procedimiento de síntesis asistida por microondas de sílice porosa (University of Valencia), Valencia, 15 of December 2020

- **Invited Oral Communication**. Aplicaciones de los materiales mesoporosos en analítica. C Belenguer-Sapiña, E Pellicer-Castell.

XXIII International Symposium on Advances in Extraction Technologies (ExTech), Alacant, 03 of June-02 of July 2021

- **Poster P-98.** Determination of polychlorinated biphenyls in water samples by using cyclodextrin-silica materials. C Belenguer-Sapiña, E Pellicer-Castell, P Amorós, EF Simó-Alfonso, AR Mauri-Aucejo.
- **Poster P-99**. Extracting antibiotics from water with a cyclodextrin-modified poly(glycidyl-co-ethylene dimethacrylate) hybrid sorbent. C Belenguer-Sapiña, E Pellicer-Castell, SP Chali, BJ Ravoo, P Amorós, EF Simó-Alfonso, AR Mauri-Aucejo.
- **Poster P-101.** Use of mesoporous silica material with gold nanoparticles as sorbent for organochlorine pesticides preconcentration from water samples. E Pellicer-Castell, C Belenguer-Sapiña, A Mauri-Aucejo, JM Herrero-Martínez, P Amorós, J El Haskouri.
- **Poster P-102.** Determination of endocrine disrupting chemicals in urine using a hybrid cyclodextrin mesoporous silica material as sorbent. E Pellicer-Castell, C Belenguer-Sapiña, A Mauri-Aucejo, JM Herrero-Martínez, P Amorós, J El Haskouri.
- **Poster P-172**. A cyclodextrin-silica composite as a sorbent for the extraction of synthetic cannabinoids from saliva. A Mauri-Aucejo, C Belenguer-Sapiña, E Pellicer-Castell, R Sáez-Hernández, S Armenta.
- **Poster P-173**. Extraction of organophosphorus flame retardants in water samples using titanium hierarchical porous silica materials as sorbents. A Mauri-Aucejo, E Pellicer-Castell, C Belenguer-Sapiña, , JM Herrero-Martínez, P Amorós, J El Haskouri.


VM • ALEXANDER PP VI